

**MATHEMATICAL MODELING AND SIMULATION OF APOPTOSIS AND NITRIC
OXIDE EFFECTS**

by

Elife Zerrin Bagci

B.S., Bogazici University, 1997

M.S., Bogazici University, 2001

Submitted to the Graduate Faculty of
School of Medicine in partial fulfillment
of the requirements for the degree of
Doctor of Philosophy

University of Pittsburgh

2007

UNIVERSITY OF PITTSBURGH

SCHOOL OF MEDICINE

This dissertation was presented

by

Elife Zerrin Bagci

It was defended on

March 1, 2007

and approved by

Takis Benos, Ph.D., Assistant Professor, Department of Computational Biology

Timothy R. Billiar, M.D., Professor, Department of Surgery

G. Bard Ermentrout, Ph.D., Professor, Department of Mathematics

Guillermo Romero, Ph.D., Associate Professor, Department of Pharmacology

Yoram Vodovotz, Ph.D., Associate Professor, Department of Surgery

Dissertation Advisor: Ivet Bahar, Ph.D., Professor, Department of Computational Biology

Copyright © by Elife Zerrin Bagci

2007

**MATHEMATICAL MODELING AND SIMULATION OF APOPTOSIS
AND NITRIC OXIDE EFFECTS**

Elife Zerrin Bagci, PhD

University of Pittsburgh, 2007

Apoptosis, or programmed cell death, is a process of crucial importance for maintaining a homeostatic balance between cell proliferation and death. In the present study a new mathematical model is presented that draws attention to the possible occurrence of bistability in mitochondria-dependent apoptotic pathways, as well as a transition from bistable to monostable behavior -either apoptotic or cytoprotective, under well-defined conditions. Bistability is proposed to be conferred by positive feedback loops that enhance caspase-3 activation pathways through mitochondria and by kinetic cooperativity in the formation of an apoptosome complex. It essentially ensures that cells will not die in the presence of relatively small pro-apoptotic effects, but will undergo apoptosis when perturbing conditions or levels of pro-apoptotic agents exceed certain threshold values. The passage from bistable to monostable cytoprotective behavior i.e., resistance to apoptosis, may be induced by decreasing the levels of Bax, a pro-apoptotic enzyme, in agreement with experimental observations; while the opposite passage to a pro-apoptotic monostable state may be triggered by a change in the levels of mitochondrial permeability transition pore complexes (PTPCs). Further computations shed light on the origins of the experimentally observed dichotomous effects of nitric oxide (NO), demonstrating that the

relative concentrations of anti- and pro-apoptotic reactive NO species, and the interplay of glutathione, dominate the cell fate at long times (of the order of hours). Transient apoptotic effects may be observed in the presence of high levels of intracellular non-heme iron, the duration of which may reach up to hours, despite the eventual convergence to an anti-apoptotic state. The computational results thus point to the importance of the precise timing of NO production and external stimulation in determining the eventual pro- or anti-apoptotic role of NO. The same mathematical model (network of interactions) applied with different model parameters to different cell types demonstrates that cells with high levels of intracellular non-heme iron are resistant to apoptosis while those subjected to high levels of superoxide undergo pathological death, consistent with experimental observations.

TABLE OF CONTENTS

ACKNOWLEDGMENTS	XVIII
1.0 INTRODUCTION.....	1
1.1 COMPUTATIONAL CELLULAR DYNAMICS.....	1
1.1.1 Quantitative modeling as a tool for improving our understanding of the dynamics of cellular processes	1
1.1.2 Focus of the present thesis: Modeling apoptosis and its regulation by mitochondria-dependent pathways:.....	2
1.2 APOPTOSIS.....	3
1.2.1 Apoptosis is important for healthy functioning of the organism.....	3
1.2.2 Caspases are enzymes playing a major role in initiating and executing apoptotic responses	4
1.2.3 Apoptotic pathways	4
1.2.4 Experimental studies point to mechanisms of regulating apoptosis	9
1.2.5 Regulation of apoptosis.....	10
1.2.6 Positive feedback loops in apoptotic pathways	11
1.2.7 Dysregulation of apoptosis and associated pathological conditions.....	12
1.3 NITRIC OXIDE EFFECTS ON APOPTOSIS.....	13
1.3.1 Nitric oxide dependent pathways	13

1.3.2	Coupling NO-dependent pathways to apoptotic pathways.....	16
1.4	APOPTOSIS MODELS	17
1.4.1	Bistable models.....	19
1.4.2	Models with a switch from cell survival to cell death.....	19
1.4.3	Stochastic simulations.....	20
1.4.4	What is missing in existing models, and what is our goal?	20
2.0	EMERGENCE OF BISTABILITY IN MATHEMATICAL MODELS FOR APOPTOSIS.....	22
2.1	SIMPLIFIED MODEL FOR MITOCHONDRIA-DEPENDENT APOPTOSIS WITH KINETIC COOPERATIVITY (MODEL 2-A).....	22
2.2	SIMPLIFIED MODEL FOR MITOCHONDRIA-DEPENDENT APOPTOSIS WITHOUT KINETIC COOPERATIVITY (MODEL 2-B).....	25
2.3	COMPARISON OF THE TWO SIMPLIFIED MODELS: ROLE OF KINETIC COOPERATIVITY IN IMPARTING BISTABILITY	26
2.3.1	Rate equations for the two models	26
2.3.2	Calculation of the corresponding phase planes.....	27
2.3.3	Interpretation of nullclines and assessment of the role of kinetic cooperativity	29
2.4	PASSAGE BETWEEN MONOSTABLE AND BISTABLE RESPONSES. 30	
2.4.1	Introduction to the theorem by Craciun et al. (2006).....	30
2.4.2	Positive feedback loop with (Model 2-A) and without (Model 2-B) kinetic cooperativity.....	34

2.4.3	Positive feedback loop with inhibition (Model 2-C)	35
2.4.4	Model without an explicit positive feedback loop (Model 2-D)	37
2.5	BISTABILITY IN BIOCHEMICAL REACTION NETWORKS	38
3.0	MATHEMATICAL MODELING OF MITOCHONDRIAL APOPTOTIC PATHWAYS	40
3.1	REGULATION OF APOPTOSIS.....	41
3.2	MODEL AND METHODS	42
3.2.1	Kinetic model for mitochondria-dependent apoptotic pathways (Model 3)	42
3.2.2	Adoption of simple mass-action kinetics.....	53
3.2.3	Approximations in model parameters	55
3.3	COOPERATIVITY IN APOPTOSOME FORMATION CAUSES BISTABILITY IN THE MITOCHONDRIA-DEPENDENT MODEL OF APOPTOSIS	56
3.4	BIOLOGICAL SIGNIFICANCE OF BISTABILITY. ROLES OF BAX, BCL-2, AND MPTP IN PATHOLOGICAL APOPTOSIS	59
3.4.1	Bax degradation and expression rates can determine the transition between bistable and monostable responses.....	59
3.4.2	Bcl-2 modulates the effect of Bax	62
3.4.3	Effect of MPTP on the detailed mitochondria-dependent apoptosis model	64
3.5	ROBUSTNESS OF COOPERATIVE APOPTOSOME FORMATION AS A MECHANISM THAT IMPARTS BISTABILITY.....	66

3.6	COMPARISON WITH EXPERIMENTS.....	67
3.6.1	Inhibition of Bax degradation induces apoptosis in Bcl-2 overexpressing cells	67
3.6.2	Simulating the effect of Silymarin on apoptosis.....	68
3.7	SUGGESTED EXPERIMENT TO REVEAL THE MECHANISM OF CASPASE-3 ACTIVATION.....	71
4.0	COMPETING EFFECTS OF NITRIC OXIDE IN REGULATING APOPTOSIS: INSIGHTS FROM COMPUTATIONAL MODELING.....	72
4.1	NITRIC OXIDE EFFECTS ON APOPTOSIS.....	73
4.2	MODELS.....	75
4.2.1	Generation of NO-related oxidative and nitrosative species ONOO⁻, N₂O₃, and FeL_nNO (Model 4-A).	75
4.2.2	Effects of NO-related reactions on apoptotic pathways (Model 4-B).....	81
4.3	RESULTS AND DISCUSSION.....	84
4.3.1	Delay in apoptosis induction (Model 3).....	84
4.3.2	Nitric oxide associated network (Model 4-A).	85
4.3.3	Anti-apoptotic and pro-apoptotic effects of NO (Model 4-B).	87
5.0	CONCLUSION.....	98
5.1	INSIGHTS ON APOPTOSIS FROM MATHEMATICAL MODELING AND SIMULATIONS AND RELEVANT EXPERIMENTAL DATA	98
5.2	SUMMARY OF NO EFFECTS ON APOPTOSIS, AND RELEVANT EXPERIMENTAL DATA	100
5.3	LIMITATIONS AND FUTURE DIRECTIONS	102

APPENDIX A	104
BIBLIOGRAPHY	233

LIST OF TABLES

Table 1. The set of differential rate equations adopted in Model 3	50
Table 2. The parameters used in Model 3.....	52
Table 3. Reactions included in Model 4-A	77
Table 4. Rate equations for Model 4-A	79
Table 5. Equilibrium levels and initial concentrations used in Model 4-A	81
Table 6. Reactions bridging between Models 3 to 4-A	82
Table 7. Modified differential equations from either Model 3 or 4-A.....	83

LIST OF FIGURES

Figure 1. Mitochondria-dependent apoptotic pathways. The dotted box includes the interactions considered in Model 3 ((Bagci et al., 2006) and chapter 3 of this thesis). Solid arrows indicate chemical reactions or upregulation; those terminated by a bar indicate inhibition or downregulation; and dashed arrows indicate subcellular translocation. The components of the model are procaspase-8 (pro8), procaspase-3 (pro3), procaspase-9 (pro9), caspase-8 (casp8), caspase-9 (casp9), , caspase-3 (casp3), IAP (inhibitor of apoptosis), cytochrome *c* (cyt *c*), apoptotic protease activating factor 1 (Apaf-1), the heptameric apoptosome complex (apop), the mitochondrial permeability transition pore complex (PTPC), p53, Bcl-2, Bax, Bid, truncated Bid (tBid)..... 8

Figure 2. NO-related reactions used in Model 4-A. The following compounds are included: ONOO⁻ (peroxynitrite), GPX (glutathione peroxidase), O₂⁻ (superoxide), GSH (glutathione), GSNO (nitrosoglutathione), GSSG (glutathione disulfide), CcOX (cytochrome *c* oxidase), SOD (superoxide dismutase), FeL_n (non-heme iron compounds), FeL_nNO (non-heme iron nitrosyl compounds), NADPH (reduced form of nicotinamide adenine dinucleotide phosphate), NADP⁺ (oxidized form of nicotinamide adenine dinucleotide phosphate). The references for the reactions and their rate constants are presented in Table 3. The orange colored compounds interfere with apoptotic pathways (See Table 6). The purple colored compounds comprise the GSH module that

modulates the concentrations of orange colored compounds. Green color is used for NO, the key molecule in the reaction network..... 18

Figure 3. Schematic representations of Models 2-A and B in respective panels A and B. The symbol \emptyset refers to degraded compounds. The symbol μ refers to degradation rate constant and Ω refers to the rate of formation of the species indicated by the subscript..... 24

Figure 4. Time evolution of casp3 concentration in response to pro-apoptotic stimuli that causes [casp3] to be 0.001 μ M at time = 0. The curve is calculated using Model 2-A and parameters presented in Section 2.1. Caspase-3 is activated to nanomolar values in about 10 minutes in accordance with single cell experiments (Tyas et al., 2000). 25

Figure 5. Nullclines for Models 2-A and 2-B in respective panels A and B. The filled circles indicate stable fixed points and open circles indicate the unstable fixed points. The inset in panel A shows the unstable fixed point and the stable manifold in red that separates the cell survival and death regions. The arrows in panel A denote the trajectories for the time evolutions of [casp3] and [cyt *c*]. The solid curves on panels A and B are the [casp3] nullclines and the dashed curves are the [cyt *c*] nullclines. Panel A depicts two stable fixed points hence Model 2-A is bistable as opposed to Model 2-B that has one stable fixed point. 28

Figure 6. Species-reaction graph for the example presented in the study by Craciun et al. (2006) in Figure 2. 31

Figure 7. Species-reaction graphs for Models 2-A and 2-B in respective panels A and B. The difference between panels A and B is is that all cycles in panel B are 1-cycles as opposed to one of the cycles in panel A which consists an arc with a label 2. The label 2 indicates that the stoichiometric constant of species cyt *c* is 2 in the associated reaction ($2\text{cyt } c \rightarrow \text{casp3}$). A *c*-pair

consists of two arcs from a given reaction box to two species that are either reactants or products in the reaction. Each c-pair is shown by a different color. 36

Figure 8. Species-reaction graph for Model 2-C. The orange c-pair is split between two even cycles. c-pair consists of two arcs from the reaction box to two species that are either reactants or products in the reaction. Each c-pair is shown by a different color..... 37

Figure 9. Species-reaction graph for model 2-D. Each c-pair is shown by different colors..... 39

Figure 10. Time evolution of caspase-3 in response to minor changes in initial caspase-8 concentration $[\text{casp8}]_0$. (A) *cell survival* when $[\text{casp8}]_0$ is small ($10^{-5} \mu\text{M}$), indicated by the decrease in the caspase-3 concentration (initially $10^{-5} \mu\text{M}$) to zero at steady state. The abscissa is shown in logarithmic scale to display the time evolution of caspase-3 more clearly; (B) *apoptosis*, implied by the increase in caspase-3 concentration to a high value ($4.5 \times 10^{-3} \mu\text{M}$) at steady state despite the same initial value of caspase-3 as in panel A, when $[\text{casp8}]_0$ is higher ($10^{-4} \mu\text{M}$); (C) *monostable apoptosis*, in the absence of cooperativity ($p = 1$) using the same initial concentrations of caspase-3 and caspase-8 as in panel A. Here caspase-3 concentration reaches a high value ($6 \times 10^{-3} \mu\text{M}$) at long times indicative of apoptotic response. Note that the ordinate scales are different in the panels. 58

Figure 11. Effect of Bax degradation rate (μ_{Bax}) on cell fate. Calculations are performed using Model 3. (A) Bifurcation diagram for casp3 concentration with the bifurcation parameter μ_{Bax} along the abscissa. Limit point for saddle-node bifurcation is $\mu_{\text{Bax}} = 0.11 \text{ s}^{-1}$. Below this limit point, there are three steady states, two of which are stable and one unstable; and above the limit point, there is only one stable state, cell survival. The arrows indicate the equilibrium concentrations reached when starting from any point in the diagram; (B) The high initial concentration of caspase-3 ($0.1 \mu\text{M}$) decreases to zero when μ_{Bax} is in the monostable cell

survival region (0.2 s^{-1}) despite the high $[\text{casp8}]_0$ value; (C) Bifurcation diagram for casp3 with the bifurcation parameter $\Omega^{\circ}_{\text{Bax}}$. Limit point for saddle-node bifurcation is $\Omega^{\circ}_{\text{Bax}} = 6.03 \times 10^{-6} \mu\text{M} / \text{s}$. The stable cell survival line ($[\text{casp3}]_o = 0$) is not shown because the y-axis is logarithmic.

..... 61

Figure 12. Effects of Bcl-2 expression rate on cell behavior in response to changes in Bax levels. Calculations are performed using Model 3. (A) Effect on the bifurcation diagram for μ_{Bax} ; (B) Effect on the bifurcation diagram for $\Omega^{\circ}_{\text{Bax}}$ 63

Figure 13. Bifurcation diagram as a function of the concentration of mitochondrial permeability transition pore complex [PTPC]. The limit points for saddle-node bifurcation are at $[\text{PTPC}] = 2.3 \times 10^{-4} \mu\text{M}$ and $9.0 \times 10^{-4} \mu\text{M}$ 65

Figure 14. Time evolution of (A) $\text{cyt } c$; (B) caspase-3 levels with (open circles) and without (filled circles) inhibition of Bax degradation. Inhibition of Bax degradation induces an accumulation in $\text{cyt } c$ and caspase-3 levels. Calculations are performed using Model 3..... 68

Figure 15. Comparison of the experimental and theoretical changes in casp3 , Bax, Bcl-2 and $\text{cyt } c$ concentrations in response the relative changes in $[\text{p53}]$ (that are induced by changes in the flavanoid silymarin concentrations). Panel A displays the caspase-3 levels corresponding to each selected $[\text{p53}]$ computed by present simulations using Model 3. Panels B-D display the results from computations (solid bars) and those from experiments (crisscrossed bars) for each choice of relative $[\text{p53}]$ shown in panel A..... 70

Figure 16. Time evolution of $[\text{casp3}]$ predicted by the bistable Model 3 in response to different strengths of apoptotic stimuli, A) in a cell subjected to a weak EC apoptotic signal (reflected by the low concentration $[\text{casp8}]_o$); B) in a cell that is subjected to a stronger EC pro-apoptotic signal. Caspase-3 is activated at 60 minutes; C) in a cell that is subjected to a stronger EC pro-

apoptotic signal than one in panel B. Caspase-3 is activated at 30 minutes. Panels A and B illustrate two opposite effects induced by different initial concentrations of caspase-8. The threshold concentration $[\text{caps8}]_0$ required for the switch from anti-apoptotic to pro-apoptotic response is calculated to be $8.35 \times 10^{-5} \mu\text{M}$. Panels B and C illustrate the shift in the onset time of apoptosis depending on $[\text{caps8}]_0$. D) Dependence of apoptotic response time on the initial caspase-8 concentration. The ordinate is the onset time of caspase-3 activation, and the abscissa is the initial concentration of caspase-8 in excess of the threshold concentration required for the initiation of apoptosis (evidenced by increase in $[\text{casp3}]$, see panels B-C). The onset time of caspase-3 activation exhibits a logarithmic decrease with $\Delta[\text{casp8}]_0$ ($[\text{casp8}]_0 - 8.35 \times 10^{-5} \mu\text{M}$). 86

Figure 17. Time evolution of A) GSH, B) N_2O_3 , C) FeL_nNO , and D) ONOO^- concentrations predicted by Model 4-A. N_2O_3 and FeL_nNO increase to high concentrations by a switch-like mechanism induced by a decrease in $[\text{GSH}]$ due to conversion of GSH to GSNO and subsequently to GSSG. $[\text{ONOO}^-]$ does not follow a similar switch-like increase in its concentration. Solid curve is for $[\text{GSH}]_0 = 10^4 \mu\text{M}$, dotted curve for $[\text{GSH}]_0 = 10^3 \mu\text{M}$, and dashed curve with diamonds for $[\text{GSH}]_0 = 10^2 \mu\text{M}$. The response is thus sharper and earlier in the presence of lower initial concentrations of GSH. 88

Figure 18. Time evolution of $[\text{GSH}]$ and $[\text{casp3}]$ predicted by Model 4-B in the presence of N_2O_3 effects. Here, in order to visualize the effect of N_2O_3 exclusively, the reaction (4-XXII) in Table 6 is included in the model while those involving FeL_nNO and ONOO^- (reactions (4-XX, 4-XXIII-XXV) are not, assuming FeL_n concentration and rate of formation of superoxide to be zero. The solid curves depict the time evolution of $[\text{casp3}]$, and dotted curves refer to $[\text{GSH}]$. The three rows of panels are the counterparts of those in Figure 15A-C, with the different columns

referring to different initial concentrations of GSH: A-C) $[GSH]_0 = 10^3 \mu M$; D-F) $[GSH]_0 = 10^2 \mu M$; G-I) $[GSH]_0 = 0 \mu M$ 90

Figure 19. Time evolution of $[GSH]$ and $[casp3]$ predicted by Model 4-B in the presence of N_2O_3 and FeL_nNO . N_2O_3 is present in the model ($[O_2]$ is non-zero) as well as FeL_nNO ($[FeL_n]$ is non-zero). Each column is a counterpart of Figure 15A-C with different initial concentrations of GSH. A-C) $[GSH]_0 = 10^4 \mu M$; D-F) $[GSH]_0 = 10^3 \mu M$. Solid curve shows the time evolution of $[casp3]$, and dotted curve that of $[GSH]$ 92

Figure 20. Time evolutions of $[GSH]$ and $[casp3]$ predicted by Model 4-B in the presence of N_2O_3 , FeL_nNO and $ONOO^-$. The initial concentration of PTPC is $0.01 \mu M$. Each column is a counterpart of Figure 15A-C and has a different initial concentration for GSH. A-C) $[GSH]_0 = 10^4 \mu M$; D-F) $[GSH]_0 = 10^3 \mu M$. Solid curve is for time evolution of $[casp3]$, and dashed curve for time evolution of $[GSH]$. Caspase-3 concentrations at long times are $2.4 \times 10^{-4} \mu M$ and $2.5 \times 10^{-8} \mu M$ for panels A-C and D-F, respectively. 95

Figure 21. Time evolutions of $[GSH]$ and $[casp3]$ predicted by Model 4-B in the absence of N_2O_3 , FeL_nNO and presence of $ONOO^-$. The initial concentration of PTPC is $0.0001 \mu M$. A-C) $[GSH]_0 = 10^4 \mu M$; D-F) $[GSH]_0 = 10^2 \mu M$. Solid and dashed curves refer to the time evolutions of $[casp3]$ and $[GSH]$, respectively..... 97

ACKNOWLEDGMENTS

I would like to thank people who made this thesis possible. The list is long, people who gave me academic help and emotional support, people I know personally or do not, people with us or passed away.

First, I acknowledge my parents, Mahpup Bagci and Ziver Bagci who gave birth to me and raised me. They always loved me and I am sure they will always love me no matter what I do. I thank you for everything you did for me, including your support while I was working on this thesis. I love you.

My sister, Bilge is very special for me. She has such a beautiful heart. I love you, sister, and I thank you for everything you did for me.

I want to thank Dr. Bedamati Das. She helped me a lot when I first came to USA when I left my parents for the first time in my life. You are a very special person, Beda, I think you have unmeasurable amount of IQ and EQ. ☺

Alper Acar is my oldest friend and he always had confidence in me, even when I did not have much. He helped me so many times. You are a wonderful friend Alper, thank you for everything.

I thank Chris Myers for everything he did for me.

I thank my best friend Clara Myers for her emotional support and wonderful friendship. I love you, Clara.

I thank my advisor Dr. Ivet Bahar for her support and academic guidance in my research experience in my Master's and Ph.D. Thank you Dr. Bahar, for supporting me to be a scientist. That is very special for me.

I thank Dr. Bard Ermentrout for his support and academic guidance in my research in this thesis. It was a lot of fun to work with you, Bard. I miss your barbeque parties, you are a great cook.

I thank my other thesis committee members, Dr. Takis Benos, Dr. Timothy R. Billiar, Dr. Yoram Vodovotz and Dr. Romero Guillermo for their support and academic guidance.

I thank Dr. Stephen L. Phillips and Cindy Duffy. You were always so helpful and supportive in my Ph.D. study. I love you.

I thank my therapists Michelle Sabino and Diane Dolata. They were not just working with me; they were putting their heart out next to mine. You are wonderful, ladies.

I have two more wonderful ladies to thank, Nancy Linderman and Sandra Yates. You are two of the loveliest and the most intelligent persons I met in my life. I love you.

I thank James Clossin and Dr. Judy Wieber for their friendship and help during my Ph.D. study.

I thank Dr. Basak Isin, Alpay Temiz, Dr. Lee-Wei Yang, Dr. Betul Unlusu, Dr. Chakra Chennubhotla, Zheng Yang, Dr. Indira Shrivastava and Dr. Dror Tobi for their friendship and help during my Ph.D. study.

I thank the owners of Istanbul Grille for their delicious and nutritious food they had that gave me the energy to finish this thesis.

I thank members of Dr. John Tyson's lab for their friendship while I was correcting this thesis.

I thank Veronica Ivanova for her lovely friendship that she honored me with while writing this thesis. I miss you Veronica.

I thank Mustafa Kemal Atatürk for founding Turkey, making the wonderful education I got in Turkey possible and his trust in and encouragement for Turkish people, and women especially, to dream and to be whoever they want that helped me fulfill many of my dreams. Rest in peace, dear Atatürk.

The last but definitely not the least, I thank all the musicians of whose music I listened to during my studies. They are countless, but the ones I listened to the most are Turkish folk and traditional music musicians, Beethoven, Chaikowsky and Teoman. The musician I discovered the latest, Nick Cave, is amazing. He is in his forties and I just discovered tens of his songs that each one I listen to hundreds of times and he has hundreds of more songs to discover! He made me so much in love with music similar to what I felt for science when I was thirteen. I thank you, Mr. Nick Cave, for your heart that you shared through your music. Can I sing with you someday? ☺

I almost forgot one other person to thank, me. ☺ I spent little time on activities other than writing this thesis. I did not read books, watch movies as much as I wanted to and discover more musicians like Nick Cave during writing this thesis. From now on, I will. ☺

NOMENCLATURE

Abbreviations:

8-OH-dG:	8-hydroxy-deoxyguanosine
ANT:	adenine nucleotide translocase
Apaf-1:	apoptotic protease activating factor 1
apop:	apoptosome
BAR:	bifunctional apoptosis regulator
casp3:	caspase-3
casp8:	caspase-8
cGMP:	cyclic guanosine monophosphate
CcOX:	cytochrome <i>c</i> oxidase
CyP-D:	cyclophilin-D
cyt <i>c</i> :	cytochrome <i>c</i>
cyt <i>c</i> _{mito} :	mitochondrial cytochrome <i>c</i>
dG:	deoxyguanosine
DISC:	death inducing signaling complex
FADD:	Fas-Associated Death Domain proteins
FasL:	Fas ligand
FeL _n :	non-heme iron
FeL _n NO:	non-heme iron-nitrosyl complexes
GPX:	glutathione peroxidase
GSH:	glutathione
GSNO:	nitrosoglutathione

GSSG:	glutathione disulfide
IAP:	inhibitor of apoptosis
ICAD:	inhibitor of caspase-activated DNase
LLnV:	N-carbobenzoxy-L-leucyl-norvalinal
MPTPs:	mitochondrial permeability transition pores
NADP ⁺ :	oxidized form of nicotinamide adenine dinucleotide phosphate
NADPH:	reduced form of nicotinamide adenine dinucleotide phosphate
NO:	nitric oxide
O ₂ ⁻ :	superoxide
ONOO ⁻ :	peroxynitrite
sGC:	soluble guanylate cyclase
PCD:	programmed cell death
proc3:	procaspase-3
proc8:	procaspase-8
proc9:	procaspase-9
PTPC:	mitochondrial permeability transition pore complex
SOD:	superoxide dismutase
SR graph:	species reaction graph
tBid:	truncated Bid
TNF:	tumor necrosis factor
TRAIL:	tumor necrosis-related apoptosis-inducing ligand
VDAC:	voltage-dependent anion channel

List of parameters

k_1 :	rate constant of reaction 2-I
k_2 :	rate constant of reaction 2-II
μ_{c3} :	degradation rate of casp3
μ_{cc} :	degradation rate of cyt c
μ_{ccm} :	degradation rate of cyt c_{mito}
Ω_{ccm} :	rate of formation of cyt c_{mito}
k_1^f :	rate constant of the forward reaction 2-III
k_1^r :	rate constant of the reverse reaction 2-III
k_2^f :	rate constant of the forward reaction 2-IV
k_2^r :	rate constant of the reverse reaction 2-IV
k_3^f :	rate constant of the forward reaction 2-V
k_3^r :	rate constant of the reverse reaction 2-V
k_4^f :	rate constant of the forward reaction 2-VI
k_4^r :	rate constant of the reverse reaction 2-VI
F_i :	rate of production of species i in the reaction network presented in section 2.4.1
ξ_i :	rate of degradation of species i in the reaction network presented in section 2.4.1

1.0 INTRODUCTION

1.1 COMPUTATIONAL CELLULAR DYNAMICS

1.1.1 Quantitative modeling as a tool for improving our understanding of the dynamics of cellular processes

Mathematical models of biochemical processes and computer simulations of molecular events at the cellular scale can increase our insight into the molecular basis of microphysiological processes in cellular systems. The models constructed using available biological data can, not only reproduce experiments, but also give insights into the spatial and temporal dynamics of cellular processes. This type of modeling is described as computational cellular dynamics (Kitano, 2006; Kholodenko, 2006). The other important use of computational models is their efficient generation of data compared to experiments. Experiments usually require time consuming treatments whereas computational models can be readily modified and simulated. Also, the measurement of the concentration and activities of the components in the biochemical system may require difficult techniques whereas a range of quantities can be easily screened to search for optimal parameters. Therefore, realistic models that incorporate experimental data are expected to become increasingly important for rapid generation of testable hypotheses and predicting the effects of various experimental settings such as the depletion or supply of one or

more of components in the system. The predictions of the models that are of interest in the healthy and pathological functioning of organisms can then be validated by experiments, and experiments can provide, in return, insights for model improvement and parameter optimization (Kitano, 2002).

1.1.2 Focus of the present thesis: Modeling apoptosis and its regulation by mitochondria-dependent pathways:

Apoptosis is a highly regulated form of cell death. There have been considerable efforts for mathematical modeling of apoptotic regulation in response to various stimuli (Aldridge et al., 2006; Bagci et al., 2006; Bentele et al., 2004; Eissing et al., 2004; Legewie et al., 2006; Rehm et al., 2006; Siehs et al., 2002; Stucki and Simon, 2005). In particular, NO has been widely recognized to be an important modulator of apoptosis although the origin and mechanisms of its proapoptotic and antiapoptotic effects are still to be clarified.

The first aim in the present thesis is to construct a new model and perform a quantitative analysis of the corresponding reaction kinetics for improving our understanding of the regulation of apoptotic response, with particular focus on mitochondria-dependent apoptosis. In the present thesis, the term ‘reaction’ is used in a broad sense, to refer to both chemical reactions and physical interactions (e.g. binding, multimerization, dissociation or disassembly). The second aim is to construct a mathematical model for describing the dynamics of NO pathways. Finally, the third aim will be the integration of the two models, so as to explain the dichotomous effects of NO with the help of a deterministic model that couples NO chemistry to apoptotic pathways.

1.2 APOPTOSIS

1.2.1 Apoptosis is important for healthy functioning of the organism

The biochemical mechanism of apoptosis, a form of programmed cell death (PCD), is an area of extensive study because of the importance of maintaining the homeostatic balance in response to pro- or anti-apoptotic stimuli (Sanfilippo and Blaho, 2003). The balance between cell proliferation and apoptosis is crucial for the healthy functioning of organisms. About 10^{10} cells die in a day in each individual, which counters the number of new cells that are generated through mitosis. This corresponds to the whole body weight in one year (Reed, 2002).

Apoptosis is a highly regulated form of cell death, unlike necrosis that is an uncontrolled and undesirable cell death. During development, apoptosis is involved in sculpting the body, shaping the organs, and carving out the fingers and the toes. Apoptosis is also necessary for eliminating pathogen-invaded cells and cells with severely damaged DNA. In apoptosis, the cells die individually (Tyas et al., 2000); however in necrosis, groups of cells are simultaneously affected (King, 2000; Weinberg, 2006). During apoptosis, the volume of the cells decrease and they are packaged into small apoptotic bodies that are consumed by neighboring cells. During necrosis, on the other hand, the volume of the cells increases and cells die by lysis without clearance of the remains of the cells as in apoptosis. Hence, necrosis usually gives rise to inflammation while apoptosis does not. Mitochondria functions are normal at the initiation of apoptosis, whereas they are aberrant in necrosis (King, 2000).

1.2.2 Caspases are enzymes playing a major role in initiating and executing apoptotic responses

Caspases are a structurally related group of cysteine proteases, essential for apoptosis. They possess a crucial cysteine residue that specifically cleaves peptide bonds after aspartate residues, hence their nomenclature: cysteine-dependent **asp**artate-specific protease. They are normally inactive (as pro-caspases) and require proteolytic processing for activity, which can be achieved by other activated caspases, or by the formation of large protein complexes known as the DISC (death inducing signalling complex) and the apoptosome (see below). Pro-apoptotic stimuli usually activate *initiator* caspases, e.g., caspases-8 and -9. These caspases in turn activate the *executioner* caspases e.g, caspases-3 and -7. Executioner caspases cause morphological changes in the cells by cleaving many proteins. These changes indicate that the cell is undergoing apoptosis.

1.2.3 Apoptotic pathways

Apoptotic responses are triggered and propagated by two different mechanisms, referred to as *extrinsic* and *intrinsic* apoptotic pathways.

In the case of extrinsic pathways, apoptosis is initiated by extracellular signals. Death ligands such as Fas ligand (FasL), tumor necrosis factor (TNF) or tumor necrosis-related apoptosis-inducing ligand (TRAIL), usually induce the oligomerization of the associated TNF-Receptors (TNF-Rs), followed by the recruitment of adaptor proteins - Fas-Associated Death Domain proteins (FADD), to the cytoplasmic portions of the receptors (Nagata, 1997). The resulting Death Inducing Signaling Complex (DISC) recruits multiple procaspases-8 molecules

that mutually cleave and activate one another through induced proximity (Figure 1). In Type I cells, activation of caspase-8 (casp8) in large quantities leads to the activation of other caspases, including the executioner caspase-3 (casp3) that ultimately leads to apoptosis. In Type II cells, the amount of casp8 generated at the DISC is small, and the activation cascade does not propagate directly, but is, instead, amplified via the mitochondria (Figure 1). The biochemical pathways presented in Figure 1 will be discussed in more detail in Chapter 3 and used in Model 3 for our computational study of apoptosis.

Apoptosis can also be triggered intracellularly. This pathway is called intrinsic or mitochondrial apoptotic pathway. Intrinsic apoptotic pathways can be activated by excessive amounts of calcium within the cell, excessive amounts of oxidants, DNA-damaging agents, and other agents that disrupt the microtubules that are key components of the cytoskeleton and the mitotic spindle (Weinberg, 2006).

1.2.3.1. Bcl-2 family members in mitochondrial apoptotic pathways

The mitochondrial apoptotic pathway observed in Type II cells is largely mediated through Bcl-2 family proteins. This family includes both pro-apoptotic proteins such as Bid, Bax, Bak, and BNIP3 that promote mitochondrial permeability, and anti-apoptotic members such as Bcl-2 and Bcl-xL that inhibit their effects, or inhibit the mitochondrial release of cytochrome *c* (cyt *c*) (Antonsson et al., 1997). The pro-apoptotic and anti-apoptotic Bcl-2 family member proteins inhibit a number of proteins. Anti-apoptotic Bcl-2, Bcl-xL, Bcl-w, Mcl-1 and A1 inhibit pro-apoptotic Bax and Bak. As another layer of regulation, pro-apoptotic Bad inhibits Bcl-2, Bcl-xL and Bcl-w and pro-apoptotic Noxa inhibits Mcl-1 and A1. Bim, Puma and tBid inhibits Bcl-2, Bcl-xL, Bcl-w, Mcl-1 and A1 (Weinberg, 2006).

The mitochondrial apoptotic pathway is initiated by the cleavage of Bid by casp8. The translocation of the truncated Bid (tBid) to the mitochondria induces the oligomerization of Bax along with the formation of a channel on the mitochondria membrane. Pro-apoptotic molecules such as cyt *c* and Smac/DIABLO are released to the cytoplasm through these channels (Yin et al., 1999). The relative levels of pro- and anti-apoptotic Bcl-2 family proteins determine whether the cyt *c* in mitochondria will be released or not (Weinberg, 2006). The balance between them is delicate. The experiments presented by Bouillet et al (2001) demonstrate that the kidney tissue from a Bcl-2 double knockout mouse exhibits excessive apoptosis as opposed to the tissue from a wild type mouse which is healthy. However, this deleterious effect is abolished in a Bcl-2 $-/-$ and Bim $+/-$ (Bim is a pro-apoptotic Bcl-2 family protein) mouse.

1.2.3.2. Mechanism of cytochrome *c* release from the mitochondria

The mechanisms of cyt *c* release from mitochondria are highly diverse and controversial (Newmeyer and Ferguson-Miller, 2003; Nakagawa et al., 2005). We assume here that cyt *c* is released by two independent mechanisms:

(i) formation of Bax channels as described above

(ii) formation/activation of mitochondrial permeability transition pores (MPTPs) (Green and Kroemer, 2004; Halestrap and Brenner, 2003) irrespective of Bax channel formation.

An enzyme known as adenine nucleotide translocase (ANT) forms the inner membrane channel of MPTP. Binding of cyclophilin-D (CyP-D) to ANT facilitates a conformational change converting the ANT from a specific transporter to a non-specific pore that releases cyt *c* and Smac/DIABLO to the cytoplasm. A voltage-dependent anion channel (VDAC) binds to the outer

face of the ANT, and together VDAC, ANT and CyP-D represent the minimal set of proteins that assemble to form the MPTP (Halestrap and Brenner, 2003).

Another important component of apoptosis regulation network is the tumor suppressor protein p53. This protein simultaneously suppresses transcriptional level of Bcl-2 and activates Bax. Cyt *c* leakage supports the formation of an apoptosome complex by binding to apoptotic protease activating factor-1 (Apaf-1) that activates the caspase-9 (casp9) molecules (upon cleavage of the bound zymogen procaspases-9). The activated casp9 molecules in turn activate casp3 molecules (Vodovotz et al., 2004). Caspase-3 cleaves ICAD (inhibitor of caspase activated DNase), leading to DNA degradation or fragmentation (Enari et al., 1998), while the inhibitor of apoptosis (IAP) inhibits both casp3 and casp9 activities (Figure 1). Smac/DIABLO released from mitochondria together with cyt *c* binds to IAPs and dissociates them from caspases, abolishing their inhibitory effect on caspases. Hence, mitochondria have two pro-apoptotic effects, activation of casp9 and casp3 molecules, along with inhibition of the caspase inhibitors IAPs.

Apoptosis is followed by packaging of cell fragments and their removal by phagocytosis. Hence, apoptosis is a “silent” form of cell death as opposed to necrosis that causes inflammation (Salvesen, 2002).

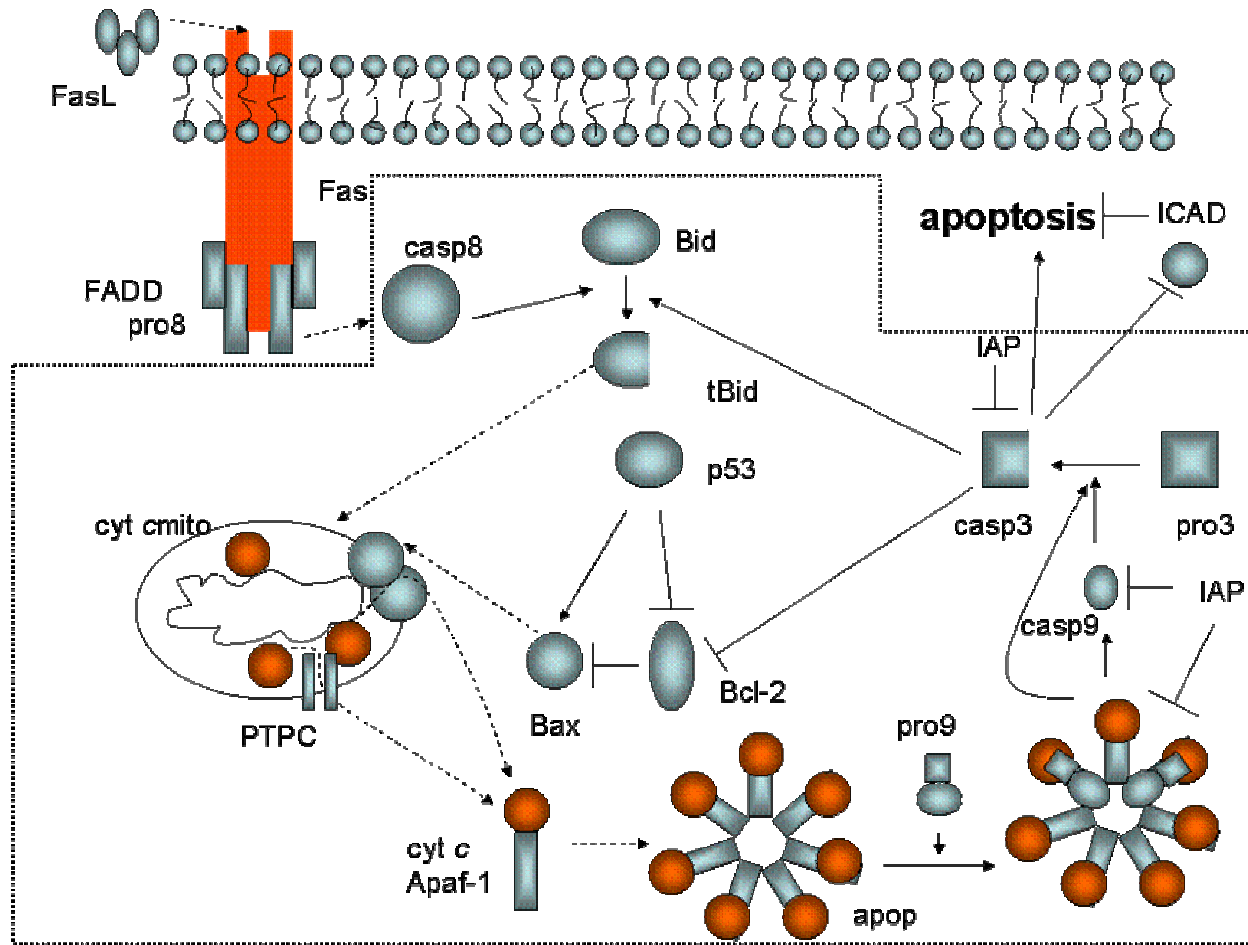


Figure 1. Mitochondria-dependent apoptotic pathways. The dotted box includes the interactions considered in Model 3 ((Bagci et al., 2006) and chapter 3 of this thesis). Solid arrows indicate chemical reactions or upregulation; those terminated by a bar indicate inhibition or downregulation; and dashed arrows indicate subcellular translocation. The components of the model are procaspase-8 (pro8), procaspase-3 (pro3), procaspase-9 (pro9), caspase-8 (casp8), caspase-9 (casp9), caspase-3 (casp3), IAP (inhibitor of apoptosis), cytochrome *c* (cyt *c*), apoptotic protease activating factor 1 (Apaf-1), the heptameric apoptosome complex (apop), the mitochondrial permeability transition pore complex (PTPC), p53, Bcl-2, Bax, Bid, truncated Bid (tBid).

All caspases are synthesized as inactive enzymes (zymogens), which are activated by proteolysis. The initiator caspases-8 and -9 are suggested to be activating themselves after being recruited to protein complexes where they exist in high concentrations. This is called *induced proximity* hypothesis (Salvesen and Dixit, 1999). The executioner procaspases, on the other hand, are activated through their cleavage by initiator caspases. Executioner caspases cleave “death substrates” that cause morphological transformations of cells into small apoptotic bodies. Examples of death substrates are lamins, inhibitor of caspase-activated DNase (ICAD) and cytoskeletal proteins such as actin and plectin. Lamins are at the inner surface of the nuclear membrane and their cleavage is involved in chromatin condensation and nuclear shrinkage seen in apoptosis. The cleavage of ICAD results in the dissociation of caspase-activated DNase that fragments the chromosomal DNA. Cleavage of cytoskeletal proteins results in the dissociation of the cytoskeleton, the formation of blebs that protrude from the cell membrane and the formation of apoptotic bodies that are cleared by the neighboring cells (Weinberg, 2006).

1.2.4 Experimental studies point to mechanisms of regulating apoptosis

A recent study by Nair and co-workers (Nair et al., 2004) invites attention to the occurrence of a bifurcation into two states, favoring either cell death or cell survival, upon examination of a population of cells undergoing oxidative stress. Essentially, each cell is observed to activate either homeostatic or apoptotic signals early after hydrogen peroxide (H₂O₂) exposure; eventually, the stimuli that activate pro-apoptotic signals cause a given cell to succumb to PCD in accord with an all-or-none activation of the caspase cascade (Rehm et al., 2002). The remaining cells, which undergo activation of the ERK signaling pathway at an early stage of oxidative stress, exhibit cytoprotective responses. The observed bistable behavior, or the choice

of individual cells between these two competing and mutually exclusive responses is suggested to be a stochastic process (Nair et al., 2004), the origin and mechanism of which is still to be elucidated. A recent study (Bentele et al., 2004), on the other hand, points to the occurrence of a transition from cell survival to cell death provided that the stimuli exceed some threshold values. In this case, the cells exhibit essentially a transition between two monostable regimes, rather than two states possibly coexisting under certain combination of stimuli as observed by Nair et al. (2004).

In view of these different viewpoints, and knowing that bistability is a functional feature in many cellular networks (Angeli et al., 2004; Ferrell and Xiong, 2001; Ferrell, 2002; Ozbudak et al., 2004; Xiong and Ferrell, 2003), we aim here at exploring if and how a mathematical model of apoptosis can explain the occurrence of a bistable response. Of particular interest is also to assess the conditions necessary for a transition from bistable to monostable behavior that may be related to dysregulation of apoptosis.

1.2.5 Regulation of apoptosis

Apoptosis is highly regulated and should occur only in cells of which death will benefit the organism. So cell survival state should be resistant to apoptotic signals. For example only the cells infected should be killed by cytotoxic T lymphocytes or natural killer (NK) cells that induce death receptor Fas (Weinberg, 2006). A few death ligands from the killer cells can diffuse to the cells that are healthy and close to the target cell. These cells should be resistant to small apoptotic stimulus they receive. Additionally, the cells do not apoptose with a small DNA damage. If the DNA damage is not severe, it is repaired by DNA repair mechanisms and the cell does not apoptose. On the other hand, the cell should not be very resistant to apoptotic stimuli

because, in this case, apoptosis would be impossible. This would suggest two possibilities for regulation of apoptosis: bistability (Bagci et al., 2006; Eissing et al., 2004; Legewie et al., 2006) and monostable cell survival with transient executioner caspase activation (Bagci et al., 2007).

1.2.6 Positive feedback loops in apoptotic pathways

Positive feedback loops amplify a weak signal to a strong response. The positive feedback loops in mitochondria-dependent apoptotic pathways amplify the weak pro-apoptotic signal to an apoptotic response. Positive feedback loops can also play a role for emergence of bistability in systems that have ultrasensitivities such as kinetic cooperativity (Bagci et al., 2006) and inhibition (Eissing et al., 2004). The effect of positive feedback loops in bistability has recently been demonstrated by Craciun et al. (2006). The following positive feedback loops are considered in mathematical models that are bistable (Bagci et al., 2006; Eissing et al., 2004; Legewie et al. 2006) and those included in the models that have a switch-like behavior (Aldridge et al., 2006; Bentele et al.; 2004):

- Activation of casp3 by casp8 that, in return, activates casp3. This feedback loop is considered in the models of Aldridge et al. (2006) and Eissing et al. (2004).
- Caspase-3 upregulates itself through two positive feedback loops involving cleavage of Bid and Bcl-2 (Bagci et al., 2006). These feedback loops are illustrated in Figure 1.
- Caspase-3 activates caspase-2 that in return activates more casp3 by cleaving Bid. This feedback loop is considered in the model of Bentele et al. (2004).
- Activation of casp3 by casp9 that, itself, activates casp3. This feedback is considered in the model of Legewie et al. (2006).

1.2.7 Dysregulation of apoptosis and associated pathological conditions

Dysregulation of apoptotic signalling may play a primary or secondary role in various diseases: insufficient apoptosis leads to cancer (cell accumulation, resistance to therapy), autoimmunity (failure to eliminate autoreactive lymphocytes), persistent infections (failure to remove infected cells), etc., whereas excessive apoptosis contributes to neurodegeneration (Alzheimer's disease, Parkinson's disease, Huntington's disease, amyotrophic lateral sclerosis), autoimmunity (uncontrolled apoptosis induction in specific organs), AIDS (depletion of T lymphocytes), and ischaemia (stroke, myocardial infarction) (Reed, 2002).

Most or possibly all kinds of cancer cells inactivate key components of the apoptosis-inducing machinery. They inhibit apoptosis by decreasing levels or activities of important pro-apoptotic proteins, e.g., FADD, casp8, p53, casp9, and Bax. Conversely, they upregulate certain anti-apoptotic proteins, e.g., IAPs and Bcl-2 (Weinberg, 2006).

Pathologies such as ischemia and neurodegenerative diseases involve excessive apoptosis. After ischemia, increased intracellular calcium and reactive oxygen species trigger mitochondrial permeability, which causes cell loss in cardiac infarction and cerebral stroke. Mitochondrial permeability transition and death of neurons are observed in neurodegenerative diseases (Green and Kroemer, 2004).

1.3 NITRIC OXIDE EFFECTS ON APOPTOSIS

1.3.1 Nitric oxide dependent pathways

Nitric oxide (NO) is a lipophilic and highly diffusible molecule whose effects on cell survival and death are highly complex. The effect of NO depends on its concentration and its form within the cell. The complexity of NO effects arises from the ability of NO to react with many molecules such as *reactive oxygen species*, metal ions and proteins. These reactions may promote apoptosis in one cell type while having an anti-apoptotic effect in another cell type (Kim et al., 2001). Furthermore, the concentration of NO can determine the fate of a specific type of cell; NO can protect against apoptosis in physiological concentrations, but can be toxic at higher concentrations (Kim et al., 1999). Those observations can be explained by *direct* and *indirect* effects of NO. The direct effects of NO are exerted by NO itself. The indirect effects are mediated through reactive nitric oxide species formed by the reactions of NO with reactive oxygen species metal ions and proteins (Kim et al., 2001; Wink et al., 1999; Wink et al., 1994).

1.3.1.1. Direct effects of NO on apoptotic responses

One important direct effect of NO is its reaction with soluble guanylate cyclase (sGC) to produce anti-apoptotic cyclic guanosine monophosphate (cGMP) (Kim et al., 2001b; Kim et al., 1997) using GTP (Cary et al., 2005), following the reaction scheme



Synthesis of cGMP has several regulatory/anti-inflammatory effects like regulation of vascular tone, inhibition of platelet aggregation, and leukocyte-endothelial cell interactions (Grisham et al., 1999). cGMP can have both pro- and anti-apoptotic effects depending on which chemical reactions it will go through in the cell .

NO can also react with non-heme iron (FeL_n) to form iron-nitrosyl complexes (FeL_nNO) (Kim et al., 2000).

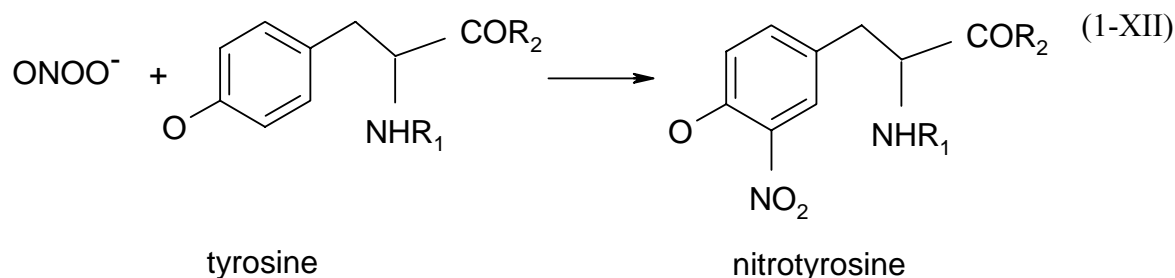


Here L denotes any ligand other than heme. Iron-nitrosyl complexes (FeL_nNO) inhibit caspases by nitrosation of these enzymes, and thus they have anti-apoptotic effect (see reaction (1-VII))

The third direct effect of NO is its oxygenation reaction. The end product of NO reaction with oxygen is N_2O_3



(iii) nitration of tyrosine to form nitrotyrosine succeeding the formation of ONOO⁻ through the reaction of NO with the superoxide (O₂⁻), (Beckman and Koppenol, 1996; Huie and Padmaja, 1993)



(iv) nitrosation of thiol groups in caspases by N₂O₃ (Wink et al., 1994),



leading again to inactivation of caspases, i.e. an anti-apoptotic effect.

1.3.2 Coupling NO-dependent pathways to apoptotic pathways

As can be clearly seen from the set of effects summarized above, NO has dichotomous effects on apoptosis. Whether it acts as a cytoprotective or a cytotoxic agent is most likely to be determined by NO and O₂⁻ levels, GSH and non-heme iron content (Hon et al., 2002) of the particular cell. For example S-nitrosation of caspases is an important anti-apoptotic effect of NO (Li et al., 1997) especially in cells with high non-heme iron content (Kim et al., 2000). This cytoprotective effect involves the above listed reactions 1-IV, 1-VII and 1-XIII). On the other hand, another important effect of NO is mediated by its reaction with O₂⁻ to form peroxynitrite (ONOO⁻), as described above. Peroxynitrite is implicated in apoptosis (Vodovotz et al., 2004). These suggest

that the effects of NO are largely determined by the different pathways or series of reactions it can trigger, and a sensitive balance, or competition between these counter effects. Our aim is to understand the conditions leading to the dominance of one or the other effect, first, and then to couple those pathways/reactions to apoptotic pathways so as to improve our understanding of the modulation of apoptosis by NO. The network for NO related reactions are presented in Figure 2. More details on the particular reactions and parameters shown in the figure will be presented in Chapter 4.

1.4 APOPTOSIS MODELS

Fussenegger et al. (2000) pioneered the mathematical modeling of apoptotic pathways that include both receptor-induced (extrinsic) and mitochondria-dependent (intrinsic) pathways. However, their model invariably progresses towards apoptosis, containing no anti-apoptotic mechanisms for cells. More recent models (Bentele et al., 2004; Eissing et al., 2004; Siehs et al., 2002; Stucki and Simon, 2005) point to the requirement of a homeostatic balance between the two responses, manifested by a bistable behavior (cell survival and cell death as two stable states) or a switch from one response (cell survival) to another (cell death) under well-defined conditions.

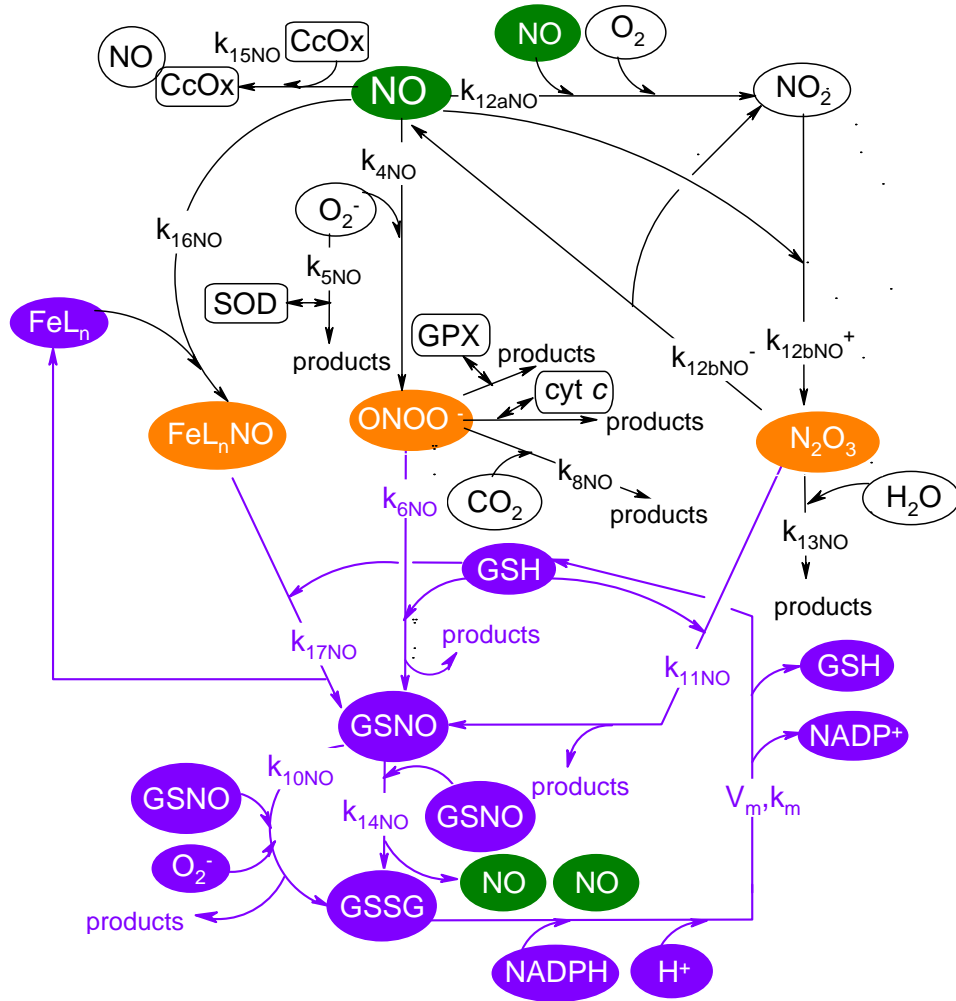


Figure 2. NO-related reactions used in Model 4-A. The following compounds are included: ONOO⁻ (peroxynitrite), GPX (glutathione peroxidase), O₂⁻ (superoxide), GSH (glutathione), GSNO (nitrosoglutathione), GSSG (glutathione disulfide), CcOX (cytochrome *c* oxidase), SOD (superoxide dismutase), FeL_n (non-heme iron compounds), FeL_nNO (non-heme iron nitrosyl compounds), NADPH (reduced form of nicotinamide adenine dinucleotide phosphate), NADP⁺ (oxidized form of nicotinamide adenine dinucleotide phosphate). The references for the reactions and their rate constants are presented in Table 3. The orange colored compounds interfere with apoptotic pathways (See Table 6). The purple colored compounds comprise the GSH module that modulates the concentrations of orange colored compounds. Green color is used for NO, the key molecule in the reaction network.

1.4.1 Bistable models

An insightful first study has been performed by Eissing et al. (2004) for receptor-induced apoptosis of Type I cells. Bistability was shown therein to result from the interplay between caspase-3 activation and the inhibitors of apoptosis (IAP and bifunctional apoptosis regulator (BAR)). In the basic model that includes only IAP, bistability was possible for a narrow range of parameters that are far from the values reported in the literature due to a balance between caspase-3 activation and inhibition solely due to IAP. However, the bistability was shown therein to be possible for a wider range of parameters close to the values reported in literature by further inhibition by BAR. Eissing et al. (2004) also showed computationally that apoptosis which takes about 10 minutes in single cells (Tyas et al., 2000; Rehm et al., 2002) seems to take longer in a culture of cells. .

Legewie et al. (2006) showed that inhibition of casp3 and casp9 by inhibitors results in an implicit feedback loop and bistability. They also showed how cell-specific protein expression determines qualitative features of casp3 activation, such as gradual versus all-or-none apoptosis and reversible versus irreversible response.

1.4.2 Models with a switch from cell survival to cell death

The switch model proposed by Bentele et al. (2004) is not bistable and suggests a transition from cell survival to cell death provided that the stimuli exceed some threshold values. With regard to apoptotic pathways, Bentele et al. (2004) included both extrinsic and intrinsic pathways. They have performed a systematical analysis not only to determine the parameters from experiments, but also to assess the most important interactions by a rigorous sensitivity analysis.

The model proposed by Stucki and Simon (2005) focuses on the regulation of caspase-3 activation and degradation only. Their model predicts an allosteric activation of the caspase-3 degradation by the IAP–caspase-3 complex, which is represented by a Hill function with a Hill coefficient greater than unity. They predict that a caspase-3 concentration greater than a threshold value triggers downstream apoptotic events and eventually cell death.

1.4.3 Stochastic simulations

Siehs et al. (2002) focused on the interactions of Bcl-2 family members and consequent cyt *c* release. In terms of the method of approach, Siehs et al. (2002) simulated the time evolution of Bcl-2 family molecules using discrete time and space variables in a lattice molecular automaton. Their model predicts that the Bcl-2 family proteins such as Bcl-2, Bax and Bak form a diffusion-driven molecular switch that dampens apoptosis induction. This controls the apoptosis cascade under noisy, apoptosis inducing conditions. This study thus differs from those described above, in that the stochastic character of cell cycle regulation has been incorporated by discrete time and space variables.

1.4.4 What is missing in existing models, and what is our goal?

The model by Eissing et al (2004) addresses an important issue that model by Fussenegger et al. (2000) did not include. The cell survival state is bistable in model by Eissing et al. (2004) However, their model does not refer to mitochondrial apoptotic pathways. The model by Legewie et al. also has a stable cell survival state, however the authors concentrate on only a portion of the mitochondrial apoptotic pathways. Bentele et al. (2004), incorporated a switch into

their model, however it seems more appropriate to have a switch mechanism that is not defined *a-priori* but emerges as an output. Again, the models by Stucki and Simon (2005) and Siehs et al. (2002) concentrated only on a particular portion of the mitochondrial apoptotic pathways.

Our first goal is to study mitochondria-dependent apoptotic pathways that incorporate mitochondrial activation (through Bid truncation and permeability pore (PTPC) opening at the mitochondria), mitochondrial cytochrome *c* release, apoptosome complex formation, and caspase-9 and caspase-3 activations. Our second goal is to ensure that the model predicts cell survival in the presence of minimal pro-apoptotic signals, while a robust bistable response occurs under a broad range of conditions. Our final goal is to shed light into the origins of the experimentally observed dichotomous effects of NO on apoptosis in different types of cells.

2.0 EMERGENCE OF BISTABILITY IN MATHEMATICAL MODELS FOR APOPTOSIS

In this chapter, we show how bistability emerges as a natural consequence of the competition between counter effects and how kinetic cooperativity may play a crucial role in imparting bistability. We present the results from several mathematical models for apoptosis in literature (Bagci et al., 2006; Eissing et al., 2004; Legewie et al., 2006) to provide an overview of different hypotheses and perspectives, how they deviate, and in which ways they complement each other.

2.1 SIMPLIFIED MODEL FOR MITOCHONDRIA-DEPENDENT APOPTOSIS WITH KINETIC COOPERATIVITY (MODEL 2-A)

First, we consider a simplified model (Figure 3A) for apoptosis with three components that have essentially the same network features as the detailed model (Model 3 in Chapter 3 and (Bagci et al., 2006)). This model has been shown to yield a number of qualitative results comparable to those obtained with the more detailed model shown in Figure 1. The common features of the detailed and simplified models are 1) positive feedback loop for casp3, 2) *kinetic cooperativity* (Bagci et al., 2006) in one of the steps in the positive feedback loop, 3) formation of cyt *c* in mitochondria, and 4) degradation of all components (Bagci et al., 2006).

The kinetic scheme adopted for the simplified mitochondria-dependent (intrinsic) apoptotic pathways with kinetic cooperativity is presented in Figure 3A. The diagram notations proposed by Kitano et al. (2005) are used in Figure 3. According to these notations, mRNAs are shown by parallelograms, proteins by smoothed rectangles, translations by dashed arrows, reactions by arrows, degraded compounds by \emptyset . The individual steps in this model essentially represent/approximate the combinations of several interactions that are explicitly considered in the detailed model (Model 3 in Chapter 3 and (Bagci et al., 2006)). Mainly, the first step is a combination of the set of reactions/interactions that involve apoptosome formation and casp3 activation.



The corresponding rate constant is k_1 . This step requires a *kinetic cooperativity* (Bagci et al., 2006) because the stoichiometric coefficient of $\text{cyt } c$ is greater than unity. The second step completes the positive feedback loop where casp3 induces the release of mitochondrial $\text{cyt } c$ ($\text{cyt } c_{\text{mito}}$) to the cytosol which, in turn, promotes an increase in the concentration of casp3.



The corresponding rate constant is designated as k_2 .

The differential rate equations associated with the kinetic scheme displayed in Figure 3A are

$$d[\text{casp3}]/dt = k_1[\text{cyt } c]^2 - \mu_{c3}[\text{casp3}] \quad (2-1)$$

$$d[\text{cyt } c]/dt = -2k_1[\text{cyt } c]^2 + k_2[\text{casp3}][\text{cyt } c_{\text{mito}}] - \mu_{cc}[\text{cyt } c] \quad (2-2)$$

$$d[\text{cyt } c_{\text{mito}}]/dt = \Omega_{\text{ccm}} - k_2[\text{casp3}][\text{cyt } c_{\text{mito}}] - \mu_{\text{ccm}}[\text{cyt } c_{\text{mito}}] \quad (2-3)$$

Here μ_{cc} , μ_{casp3} and μ_{ccm} refer to the degradation rates of the respective compounds (cyt *c*, caspase-3 and mitochondrial cyt *c*), and Ω_{ccm} is the rate of production (de novo synthesis) of mitochondria cyt *c*. Note that the term $-k_2[casp3][cyt\ c_{mito}]$ is not included in eq (2-1) as casp3 serves therein as a catalyst only, i.e. it does not enter the reaction (as also indicated by the diagonal arrow that restores its concentration in Figure 3).

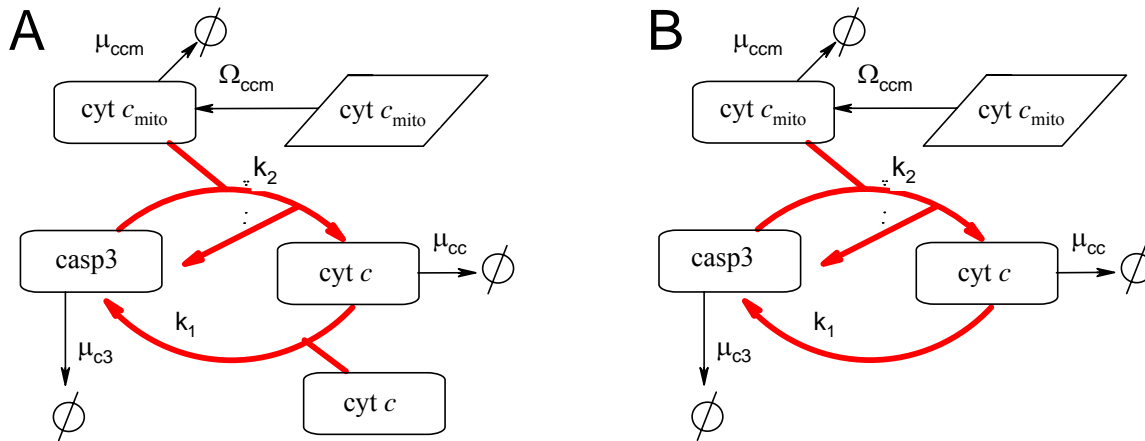


Figure 3. Schematic representations of Models 2-A and B in respective panels A and B. The symbol \emptyset refers to degraded compounds. The symbol μ refers to degradation rate constant and Ω refers to the rate of formation of the species indicated by the subscript..

We use a constant rate of formation of cyt c_{mito} and constant degradation rates for cyt c_{mito} , cyt *c* and casp3 with values comparable to those adopted in our study (Model 3 in Chapter 3 and (Bagci et al., 2006)). These values ($\Omega_{ccm} = 0.0003 \mu\text{M/s}$, $\mu_{c3} = \mu_{cc} = \mu_{ccm} = 0.006 \text{ s}^{-1}$) ensure that the apoptotic steady state concentration of casp3 is nanomolar. The rate constants are assigned the values of $k_1 = 2 \mu\text{M}^{-1}\text{s}^{-1}$, $k_2 = 2 \mu\text{M}^{-1}\text{s}^{-1}$ that ensure activation of casp3 in about 10 minutes (Tyas et al., 2000), as illustrated in Figure 4. The initial casp3 concentration, $[casp3]_0$, of $0.001 \mu\text{M}$ evolves to $0.018 \mu\text{M}$ in about 10 minutes. The initial concentrations of cyt *c* and cyt

c_{mito} are taken as zero in the simulations (The same results as in Figure 4 are obtained by assuming a non-zero initial concentration of cyt c_{mito}).

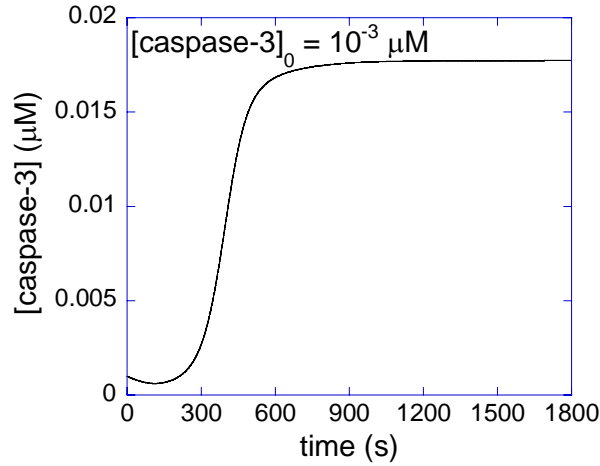


Figure 4. Time evolution of casp3 concentration in response to pro-apoptotic stimuli that causes $[\text{casp3}]$ to be $0.001 \mu\text{M}$ at time = 0. The curve is calculated using Model 2-A and parameters presented in Section 2.1. Caspase-3 is activated to nanomolar values in about 10 minutes in accordance with single cell experiments (Tyas et al., 2000).

2.2 SIMPLIFIED MODEL FOR MITOCHONDRIA-DEPENDENT APOPTOSIS WITHOUT KINETIC COOPERATIVITY (MODEL 2-B)

A schematic description of the simplified mitochondria-dependent apoptotic pathways without kinetic cooperativity is presented in Figure 3B. The major difference is the absence of a second cyt c molecule that contributes to the reaction with rate constant k_1 (compare the lower right portions of the two panels A and B). Therefore, the stoichiometric coefficient of cyt c is assigned a value of unity, which eliminates kinetic cooperativity. The associated differential rate equations become

$$d[\text{casp3}]/dt = k_1[\text{cyt } c] - \mu_{c3}[\text{casp3}] \quad (2-4)$$

$$d[\text{cyt } c]/dt = -k_1[\text{cyt } c] + k_2[\text{casp3}][\text{cyt } c_{\text{mito}}] - \mu_{cc}[\text{cyt } c] \quad (2-5)$$

$$d[\text{cyt } c_{\text{mito}}]/dt = \Omega_{\text{ccm}} - k_2[\text{casp3}][\text{cyt } c_{\text{mito}}] - \mu_{\text{ccm}}[\text{cyt } c_{\text{mito}}] \quad (2-6)$$

2.3 COMPARISON OF THE TWO SIMPLIFIED MODELS: ROLE OF KINETIC COOPERATIVITY IN IMPARTING BISTABILITY

2.3.1 Rate equations for the two models

For calculation purposes, we reduce the 3-dimensional models A and B (composed of three components) to 2-dimensions upon assuming steady state conditions for $\text{cyt } c_{\text{mito}}$, i.e. equating $d[\text{cyt } c_{\text{mito}}]/dt$ to zero, and substituting the identity

$$[\text{cyt } c_{\text{mito}}] = \Omega_{\text{ccm}} / (k_2[\text{casp3}] + \mu_{\text{ccm}}) \quad (2-7)$$

for $[\text{cyt } c_{\text{mito}}]$ using eq 2-3. The rate of change in $\text{cyt } c$ concentration then becomes

$$d[\text{cyt } c]/dt = -k_1[\text{cyt } c]^2 + k_2 \Omega_{\text{ccm}}[\text{casp3}]/(k_2[\text{casp3}] + \mu_{\text{ccm}}) - \mu_{cc}[\text{cyt } c] \quad (2-8)$$

in model 2-A and,

$$d[\text{cyt } c]/dt = -k_1[\text{cyt } c] + k_2 \Omega_{\text{ccm}}[\text{casp3}]/(k_2[\text{casp3}] + \mu_{\text{ccm}}) - \mu_{cc}[\text{cyt } c] \quad (2-9)$$

in Model 2-B, using the respective equations 2-2 and 2-5.

2.3.2 Calculation of the corresponding phase planes

Our goal is to obtain the phase planes for the two systems, as a function of the two variables, [cyt *c*] and [casp3]. To this aim, we plot the nullclines corresponding to each component, i.e. the loci of concentration pairs that maintain the concentration of each component fixed such that:

$$d[\text{casp3}]/dt = 0 \quad (2-10)$$

$$d[\text{cyt } c]/dt = 0 \quad (2-11)$$

Therefore, [casp3] and [cyt *c*] nullclines are obtained by equating the respective equations 2-1 and 2-8 to zero in model A, and 2-4 and 2-9 in model B, which yield

$$[\text{casp3}] = \frac{k_1[\text{cyt } c]^2}{\mu_{c3}} \quad (2-12)$$

and

$$[\text{casp3}] = \frac{2k_1\mu_{ccm}[\text{cyt } c]^2 + \mu_{cc}\mu_{ccm}[\text{cyt } c]}{k_2\Omega_{ccm} - 2k_1k_2[\text{cyt } c]^2 - k_2\mu_{cc}[\text{cyt } c]} \quad (2-13)$$

for model 2-A, and

$$[\text{casp3}] = \frac{k_1[\text{cyt } c]}{\mu_{c3}} \quad (2-14)$$

$$[\text{casp3}] = \frac{[\text{cyt } c](k_1\mu_{ccm} + \mu_{cc}\mu_{ccm})}{k_2\Omega_{ccm} - k_1k_2[\text{cyt } c] - k_2\mu_{cc}[\text{cyt } c]} \quad (2-15)$$

for model 2-B. The results are shown in Figure 5, panels A and B for the respective models. We observe that the two nullclines in panel A intersect at three points (fixed points), two of them being stable (at [cyt *c*, casp3] = [0,0] and [0.007, 0.018] μM) and the third unstable (at [cyt *c*, casp3] = [0.0002, 1.4x10⁻⁵] μM). The inset in panel A enlarge the portion of the nullcline that displays this unstable point, which cannot be discerned in the main figure. Model 2-B, on the

other hand, exhibits one unstable ($[\text{cyt } c, \text{casp3}] = [0,0] \mu\text{M}$) and one stable ($[\text{cyt } c, \text{casp3}] = [0.0001, 0.0468] \mu\text{M}$) fixed point. Fixed point is the locus of the concentrations of casp3 and cyt c where the initial concentrations of the two components evolve to.

The fixed points of Model 2-A could be obtained by equating the equations for the nullclines for casp3 and cyt c (2-12 and 2-13, respectively). The resulting polynomial is third order, hence there are three fixed points two of which are bistable. If the order of the reaction 2-1 in Model 2-A was larger than 2 ($n = 3, 4, \dots$), the polynomial would be of the order of $2n-1$. Therefore bistability is expected for $n \geq 3$.

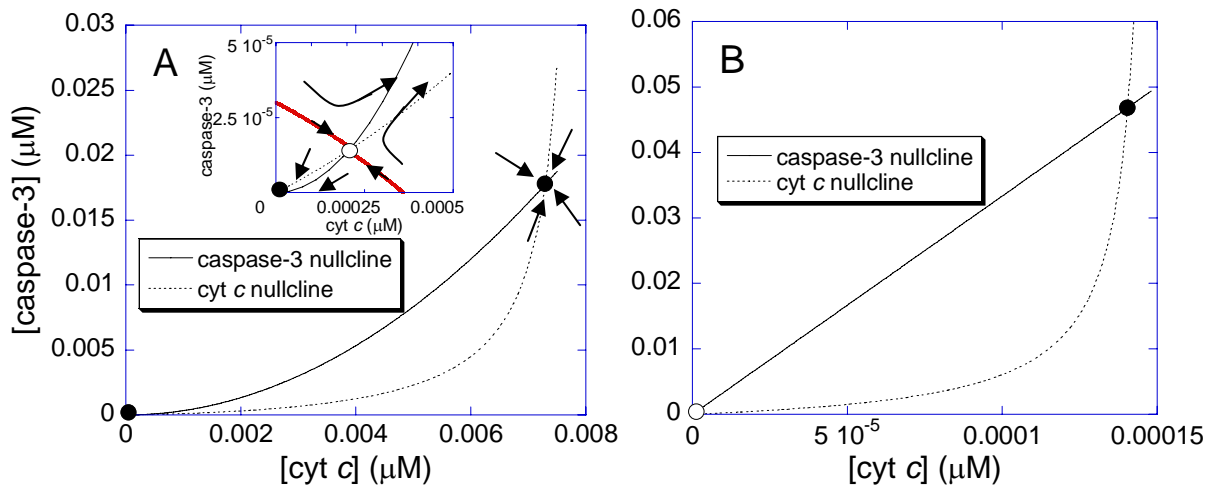


Figure 5. Nullclines for Models 2-A and 2-B in respective panels A and B. The filled circles indicate stable fixed points and open circles indicate the unstable fixed points. The inset in panel A shows the unstable fixed point and the stable manifold in red that separates the cell survival and death regions. The arrows in panel A denote the trajectories for the time evolutions of $[\text{casp3}]$ and $[\text{cyt } c]$. The solid curves on panels A and B are the $[\text{casp3}]$ nullclines and the dashed curves are the $[\text{cyt } c]$ nullclines. Panel A depicts two stable fixed points hence Model 2-A is bistable as opposed to Model 2-B that has one stable fixed point.

2.3.3 Interpretation of nullclines and assessment of the role of kinetic cooperativity

The stable fixed points act as attractors, such that any perturbation in their neighborhood drives the system back to the original fixed point. Thus, in Model 2-A, an initial casp3 and cyt *c* concentration to the lower left of the red line in inset of Figure 5A results in zero steady-state casp3 concentration while an initial casp3 and cyt *c* concentration to the upper right of the red line results in high steady-state [casp3] regime, thus inducing an anti- or pro-apoptotic behavior, respectively. Hence the model is bistable, either cell survival or cell death being induced depending on the original casp3 concentration. The unstable fixed point and the other repelling points on the red line in Figure 5A inset which is called the stable *manifold* can be viewed as cell fate decision points.

Model 2-B has only one stable fixed point with high casp3 concentration. The other fixed point with zero casp3 concentration is an unstable fixed point. Model 2-B is therefore monostable with two fixed points for all combinations of parameters as can be proved by equating Eq.s 11 and 12 to find fixed points. One fixed point is at the origin and the other one is a point with non-zero concentrations of the components.

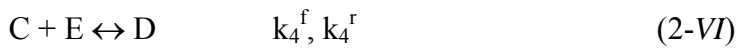
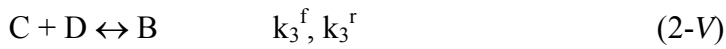
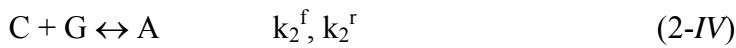
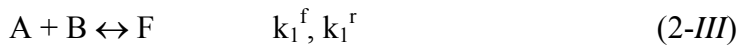
The monostable Model 2-B does not involve kinetic cooperativity, in contrast to Model 2-A that involves kinetic cooperativity and is bistable. Model 2-B cannot be adopted for modeling apoptotic response because it predicts that even a minimal apoptotic stimulus would result in high casp3 concentration that will lead to apoptosis in the fluctuating environment of cells. On the other hand, healthy functioning of cells requires the initiation of apoptosis under well-defined conditions, rather than minimal exposure to triggering events. The comparative analysis here suggests that kinetic cooperativity may be an important mechanism in regulation of apoptotic response and imparting a bistable response.

2.4 PASSAGE BETWEEN MONOSTABLE AND BISTABLE RESPONSES

Craciun et al. (2006) recently presented a theorem that distinguishes between reaction networks that might support bistable behavior and those that cannot. First we introduce their theorem with an example presented in Figure 2 in the study by Craciun et al. (2006) and then apply it to the bistable models for apoptosis reported in the literature (Bagci et al., 2006; Eissing et al., 2004; Legewie et al., 2006).

2.4.1 Introduction to the theorem by Craciun et al. (2006)

Terminology used in the theorem is illustrated by the example presented in Figure 2 that is in the study by Craciun et al. (2006). The reactions and rate equations for the species are:



where the superscript f denotes forward reaction and r denotes reverse reaction.

$$d[A]/dt = F_A - \xi_A[A] - k_1^f[A][B] + k_1^r[F] + k_2^f[C][G] - k_2^r[A] \quad (2-16)$$

$$d[B]/dt = F_B - \xi_B[B] - k_1^f[A][B] + k_1^r[F] + k_3^f[C][D] - k_3^r[B] \quad (2-17)$$

$$d[C]/dt = F_C - \xi_C[C] - k_2^f[C][G] + k_2^r[A] - k_3^f[C][D] + k_3^r[B] - k_4^f[C][E] + k_4^r[D] \quad (2-18)$$

$$d[D]/dt = F_D - \xi_D[D] - k_3^f[C][D] + k_3^r[B] + k_4^f[C][E] - k_4^r[D] \quad (2-19)$$

$$d[E]/dt = F_E - \xi_E[E] - k_4^f[C][E] + k_4^r[D] \quad (2-20)$$

$$d[F]/dt = F_F - \xi_F[F] + k_1^f[A][B] - k_1^r[F] \quad (2-21)$$

$$d[G]/dt = F_G - \xi_G[G] - k_2^f[C][G] + k_2^r[A] \quad (2-22)$$

The species-reaction (SR) graph of the above network is presented in Figure 6.

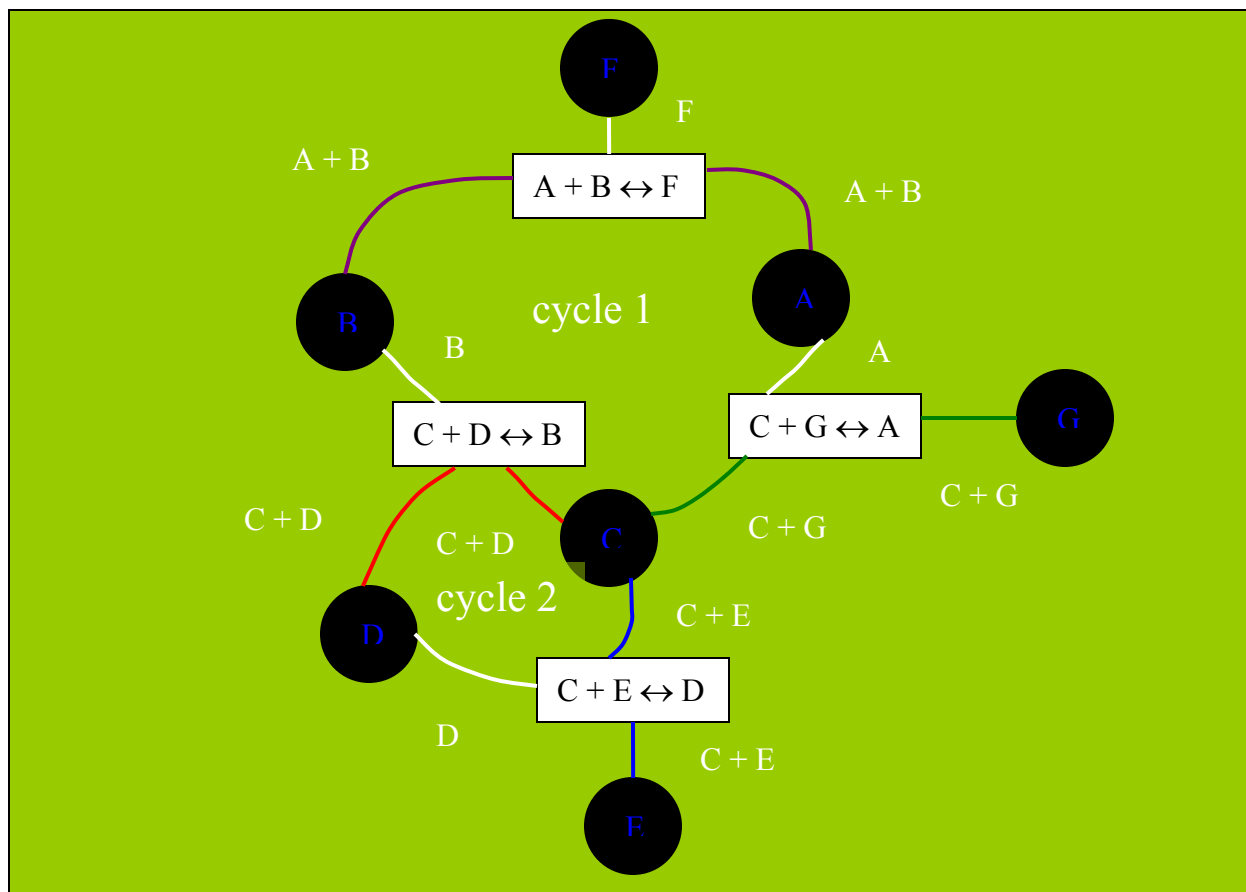


Figure 6. Species-reaction graph for the example presented in the study by Craciun et al. (2006) in Figure 2.

- In the graph, *species* (A, B, C, D, E, F, G) are shown with a circular symbol.
- *Reactions* are shown in the boxes. Reversible reactions are also shown in one box. There are four reversible reactions hence four reaction boxes in Figure 6.

- *Complexes* are one or two species that are either at the left or the right of the reaction arrows. They are shown with white letters in the SR graph (Figure 6). There are eight complexes in the figure. Note that the complexes with only one species (A, B, D and F) are presented once in the figure, whereas the complexes with two species (A+B, C + D, C+E, C+G) are presented twice.
- The *arcs* are drawn between a species circle and a reaction box in which the species appears. The arcs are labeled with the complex in which the species appears. If a species appears in both complexes of a reaction as in $A + B \leftrightarrow 2A$, then two arcs are drawn between the reaction box and the species A, each labeled by one of the two different complexes (A+B and 2A).
- *Complex pair (c-pair)* is a pair of arcs adjacent to the same reaction box which carry the same complex label. The two arcs in a c-pair are drawn in the same color. White arcs are drawn from a single species complex to a reaction box and two white arcs *do not* constitute a c-pair. There are four c-pairs in Figure 6 because there are four complexes with two species in the reactions (A+B, C+G, C+D, C+E). The purple c-pair is for the complex A+B, the green c-pair is for the complex C+G, the red c-pair is for the complex C+D, and the blue c-pair is for the complex C+E.
- *Cycle* is a closed path in which no arc or vertex is traversed twice. There are three cycles in the Figure 6, cycle 1, 2 and unlabeled outer cycle, traversing species A-C-D-B-A.

- There are three kinds of cycles, *1-cycles*, *odd-cycles* and *even-cycles*. These classifications are not mutually exclusive. A cycle can be both odd cycle and 1-cycle or both even-cycle and 1-cycle. Odd-cycles have odd number of c-pairs and even-cycles have even number of c-pairs or no c-pairs. 1-cycles consist of only arcs labeled with species that have stoichiometric coefficients of 1. All three cycles are both 1-cycles and odd cycles in Figure 6.
- Two cycles split a c-pair if one of the arcs is contained in just one of the cycles and both of the arcs are contained within the other cycle, or one of the arcs is contained in one of the cycles and the other arc is within the other cycle. In Figure 6, cycles 1 and 2 split the red (C+D) c-pair: Both red arcs are among the arcs of the two cycles, but cycle 1 contains only one of the red (C+D) arcs. The large outer cycle and cycle 1 also split the red c-pair, as do the outer cycle and cycle 2.

After presenting the terminology, we quote the theorem from the study by Craciun et al. (2006):

“Consider a reaction network for which the SR graph has both of the following properties.

- (i) Each cycle in the graph is a 1-cycle, an odd cycle, or both.
- (ii) No c-pair is split by two even-cycles.

For such a reaction network, the corresponding mass-action differential equations can not admit more than one positive steady state, no matter what (positive) values the rate constants, effluent coefficients, or species supply rates take.”

The assumptions of constant supply rate of substrates, diffusion (or degradation) of substrates and products by a first order reaction rate, and constant amounts of enzymes within the cell, i.e., no supply and removal of the enzymes, are made in the theorem.

It should be noted that when conditions (i) and/or (ii) are not satisfied, the theorem gives no information on whether the network is monostable or bistable.

The theorem also concludes that when there are no cycles in the SR graph, the corresponding ordinary differential equations can not give rise to more than one positive equilibrium.

2.4.2 Positive feedback loop with (Model 2-A) and without (Model 2-B) kinetic cooperativity

Model 2-A is converted to an SR graph in Figure 7A (the white arcs are shown with gray arcs in this SR graph because the background is white in this SR graph). The theorem tells that the model can be bistable. The reason is that it violates both conditions (i) and (ii) in the theorem. It violates condition (i) as opposed to Model 2-B (Figure 7B) that violates only condition (ii). There are 3 cycles in both Figures 7A and B. The SR graph in Figure 7A has one cycle that does not satisfy condition (i), because the outer large cycle is neither a 1-cycle (the coefficient of 2 in cyt c gray arc) nor an odd cycle (because it is an even cycle with zero c-pairs). The SR graph in Figure 7B, on the other hand, obeys the condition (i) because all three cycles in the graph are 1-cycles. The SR graph in Figure 7A violates condition (ii) because the even cycles cycle 1 and outer cycle split the red c-pair. Similarly, the SR graph in Figure 7B violates condition (ii). The theorem is not conclusive for the mono/bistability of both Model 2-A and B. Both can be monostable and bistable for a range of parameter values. We know from previous discussion that

Model 2-B is monostable. Violation of condition (i) in Model 2-A as opposed to Model 2-B makes it bistable (see Figure 5).

2.4.3 Positive feedback loop with inhibition (Model 2-C)

The basic model by Eissing et al. (2004) is used in constructing the SR graph displayed in Figure 8. The model essentially contains a feedback loop (casp8 reaction with proc3 produces casp3, which in turn reacts with proc8 to produce casp8; see the cycle on the left) and takes into consideration the inhibition of casp3 by IAP via formation of a complex casp3.IAP following the reaction scheme



where IAP_{deg} is degraded IAP.

This graph obeys the first condition of the theorem because all cycles are 1-cycles (Figure 8). However, it does not obey the second condition of the theorem because the orange c-pair is split by two even cycles. First even cycle is traversed by species casp8, the left orange arc, $\text{casp8} + \text{proc3} \rightarrow \text{casp8} + \text{casp3}$ reaction box, the lower red arc, species casp8. The second even cycle is traversed by species casp8, the lower red arc, $\text{casp8} + \text{proc3} \rightarrow \text{casp8} + \text{casp3}$ reaction box, the right orange arc, species casp3, the upper green arc, $\text{casp3} + \text{proc8} \rightarrow \text{casp3} + \text{casp8}$ reaction box, the left black arc, species casp8. In this case, the theorem is silent, i.e., the theorem cannot

indicate if the model can be bistable for some values of parameters. However, Eissing et al. (2004) showed that this reaction network is bistable for a range of parameter values.

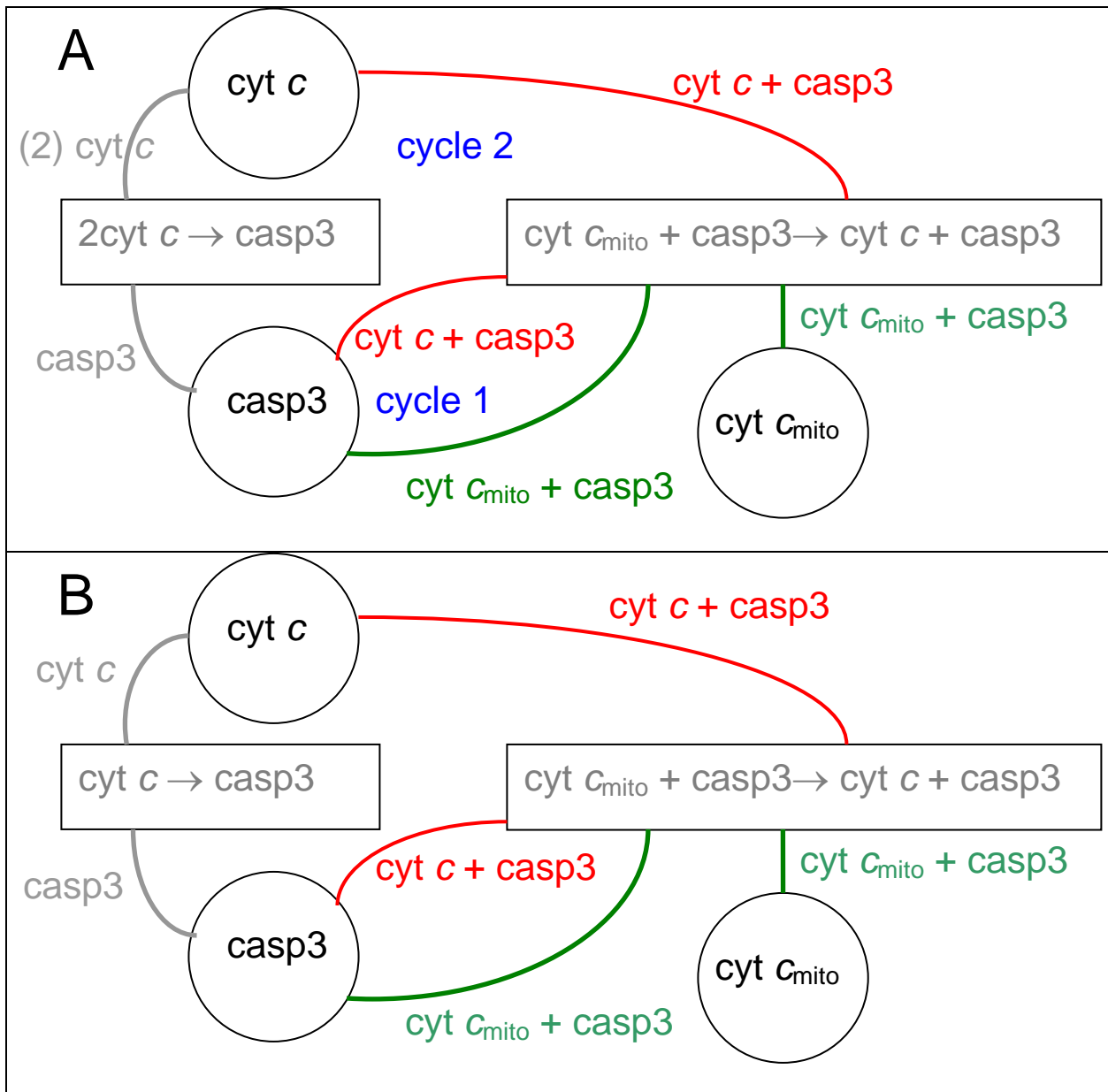


Figure 7. Species-reaction graphs for Models 2-A and 2-B in respective panels A and B. The difference between panels A and B is that all cycles in panel B are 1-cycles as opposed to one of the cycles in panel A which consists of an arc with a label 2. The label 2 indicates that the stoichiometric constant of species $\text{cyt } c$ is 2 in the associated reaction ($2\text{cyt } c \rightarrow \text{casp3}$). A c-pair consists of two arcs from a given reaction box to two species that are either reactants or products in the reaction. Each c-pair is shown by a different color.

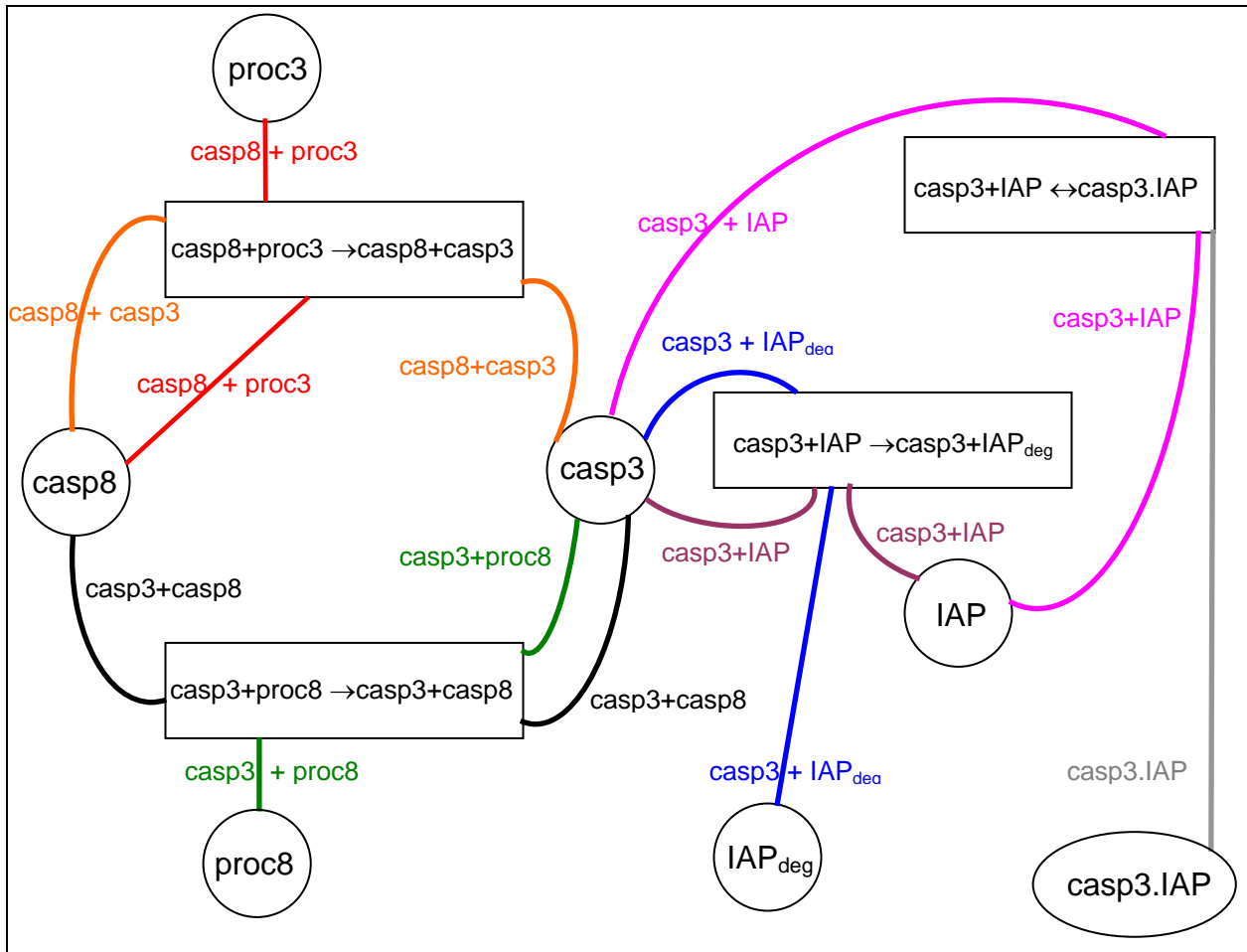


Figure 8. Species-reaction graph for Model 2-C. The orange c-pair is split between two even cycles. c-pair consists of two arcs from the reaction box to two species that are either reactants or products in the reaction. Each c-pair is shown by a different color.

2.4.4 Model without an explicit positive feedback loop (Model 2-D)

Legewie et al. (2006) showed that a reaction network without an explicit positive feedback can also manifest bistability. The example they used was the activation of casp3 by casp9 and the inhibition of IAP without a positive feedback from casp3 to casp9. The corresponding set of reactions are





We display the SR graph for this model in Figure 9 and show that the network does not obey the second condition of the theorem because the red c-pair is split by two even-cycles. Craciun et al. (2006) reported that this network is indeed bistable for some set of parameter values (Table 1, entry 4).

2.5 BISTABILITY IN BIOCHEMICAL REACTION NETWORKS

The analysis in this chapter shows that reaction networks (chemical or biochemical) do not necessarily require an explicit feedback loop to manifest bistability ((Legewie et al. 2006) and Model 2-D). However, explicit positive feedbacks can predispose the reaction networks for bistability ((Bagci et al., 2006) and Model 2-A; (Eissing et al., 2005) and Model 2-C). We also see that inhibitory reactions may also induce bistability ((Eissing et al., 2005) and Model 2-C; (Legewie et al. 2006) and Model 2-D). The analysis also shows that kinetic cooperativity can be an alternative mechanism for imparting bistability ((Bagci et al., 2006) and Model 2-A).

The theorem by Craciun et al. (2006) shows that the reaction networks should have unusual properties for imparting bistability, a feature that is not often encountered in non-biological processes, e.g., in chemical engineering. Some properties leading to bistability, were presented in this chapter, such as kinetic cooperativity, explicit and implicit positive feedback loops and inhibitory reactions. Those features are common to a large majority of biochemical

reaction networks suggesting that bistability is a common regulatory mechanism in biochemical pathways.

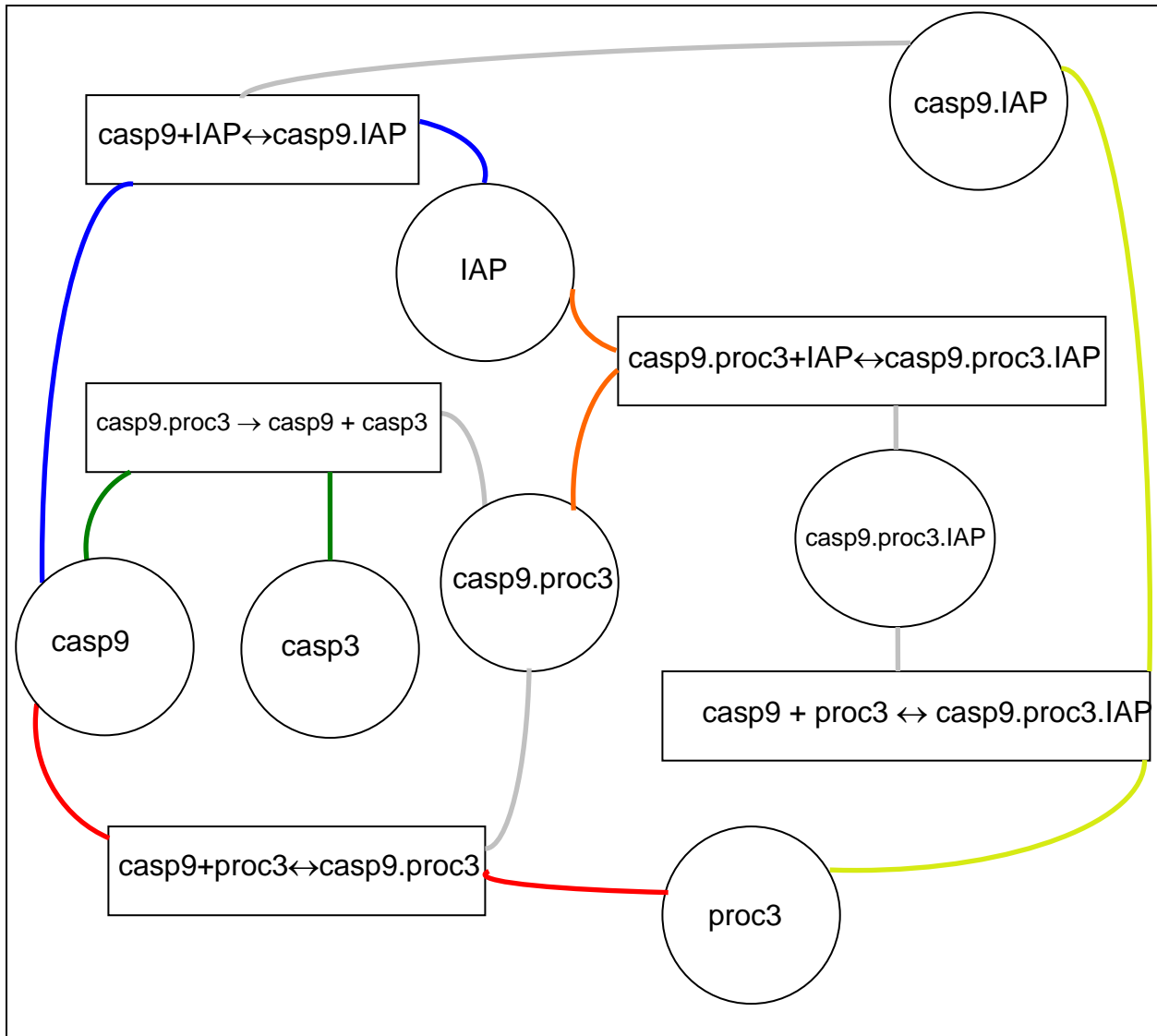


Figure 9. Species-reaction graph for model 2-D. Each c-pair is shown by different colors.

3.0 MATHEMATICAL MODELING OF MITOCHONDRIAL APOPTOTIC PATHWAYS

Work discussed in this chapter is published in *Biophys. J.*, **2006**, *90(5)*, 1546-1559. We propose a mathematical model for mitochondria-dependent apoptosis, in which kinetic cooperativity in the formation of the apoptosome is a key element ensuring bistability. We examine the role of Bax and Bcl-2 synthesis and degradation rates, as well as the number of MPTPs, on the cell response to apoptotic stimuli. Our analysis suggests that cooperative apoptosome formation is a mechanism for inducing bistability, more robust than other mechanisms, such as inhibition of casp3 by IAP. Simulations predict a pathological state in which cells will exhibit a monostable cell survival if the Bax degradation rate is above a threshold value, or if the Bax expression rate is below a threshold value. Resistance of cells to apoptosis in chemotherapy is an example of a pathological state exhibiting monostable cell survival. Otherwise, the outcome is either cell death or survival depending on the initial casp3 levels. We show that high expression rates of Bcl-2 can counteract the effects of Bax. Our simulations also demonstrate a monostable apoptotic response that is pathological if the number of MPTPs exceeds a threshold value. The present study supports our view, based on mathematical modeling, that cooperativity in apoptosome formation may be critically important for determining the healthy responses to apoptotic stimuli. Furthermore, the analysis sheds light into the roles of Bax and Bcl-2 and MPTP vis-à-vis apoptosome formation.

3.1 REGULATION OF APOPTOSIS

The biochemical mechanism of apoptosis is an area of extensive study because the balance between cell proliferation and apoptosis is crucial for the healthy functioning of organisms. Dysregulation of apoptosis is implicated in many degenerative and autoimmune diseases, including cancer, acquired immune deficiency syndrome, neurodegenerative disorders, and viral and bacterial infections (Fadeel et al., 1999). Knowing that bistability is a functional feature in many cellular networks (Angeli et al., 2004; Ferrell and Xiong, 2001; Ferrell, 2002; Ozbudak et al., 2004; Xiong and Ferrell, 2003), it is important to develop a mathematical model of apoptosis that can potentially explain how a bistable response can emerge. Of particular interest is to assess the conditions necessary for a transition from bistable to monostable behavior.

Our model demonstrates the possible occurrence of bistability in mitochondria-dependent pathways under certain conditions (see below), as well as a transition from bistable to monostable behavior -either apoptotic or cytoprotective, beyond threshold concentrations of particular components. Bistability is imparted by *kinetic cooperativity* in the formation of a heptameric complex by Apaf-1 and cyt *c* molecules (apoptosome), following the release of cyt *c* from the mitochondria. The term kinetic cooperativity refers to an effective reaction order larger than unity, and in the present model the formation of the heptameric apoptosome complex is the reaction exhibiting this behavior. The cooperativity (Hill, 1985) in the formation of the apoptosome complex is a feature that has not been included in previous mathematical models (Bentele et al., 2004; Eissing et al., 2004; Fussenegger et al., 2000; Siehs et al., 2002) and it is of interest to explore the potential role of such a cooperativity on the cell fate predicted.

In the following sections of the chapter, we will present the results obtained for the response of the cell to changes in the accessible levels of two members of the Bcl-2 family, Bax

and Bcl-2, as well as the numbers of MPTPs. Our analysis indicates that monostable cell survival is induced if the expression (or degradation) rate of Bax is lower (or higher) than a particular threshold, in qualitative agreement with other studies (Oltvai et al., 1993). We will also show that high numbers of MPTPs may have a role in pathological cell death (excessive apoptosis) (Green and Kroemer, 2004). Parameter space searches using both reduced and detailed mitochondria-dependent apoptosis models suggest that cooperativity in apoptosome formation is a plausible mechanism to ensure bistability in response to apoptotic stimuli. The loss of bistability manifested by monostable cell survival or cell death implicates Bax, Bcl-2 and MPTP in pathologies like cancer and neurodegenerative disorders.

3.2 MODEL AND METHODS

3.2.1 Kinetic model for mitochondria-dependent apoptotic pathways (Model 3)

3.2.1.1. Overview

A schematic description of the mitochondria-dependent (intrinsic) apoptotic pathways included in our model is given in Figure 1. This model is referred to as Model 3. The involved reactions/interactions are summarized below, along with the corresponding rate constants (k_i) and fluxes (J_i). There are a total of 32 compounds involved in our model, and a set of 31 rate equations controlling their chemical and physical interactions. The total number of parameters in the model is 102, comprised of 41 rate constants, 26 fluxes, 8 production rates, 17 degradation rates, 10 known initial concentrations. The sets of reactions controlling the kinetics of these intrinsic pathways are described in the next section, and explicit expressions for the differential

rate equations and the values of the parameters adopted in the calculations are presented in the Tables 1 and 2, respectively.

3.2.1.2. Description of the sequence of reactions and corresponding parameters

Model 3 (Figure 1) consists of the eleven groups of reactions described below.

(1) *Cleavage of Bid by caspase-8*. The cleavage of Bid to truncated Bid (tBid) by casp8 (Luo et al., 1998) is described by the following reactions, rate constants and fluxes



Upon cleavage, Bid is activated to induce the release of cytochrome *c* from the mitochondria, which will be described below.

(2) *Cooperative formation of an apoptosome complex*. The apoptosome complex (apop) is a multimeric assembly of seven Apaf-1 and seven cyt *c* molecules (Acehan et al., 2002; Jiang and Wang, 2004). To include in our model the cooperative nature of apoptosome formation, we adopt the reactions



with the reaction rate of $7k_{1b}^+[\text{cyt } c \cdot \text{Apaf-1}]^p$ for the second reaction, such that (see Table 1)

$$d[\text{cyt } c \cdot \text{Apaf-1}]/dt = J_1 - 7J_{1b} \quad (3-1)$$

where

$$J_1 = k_1^+[\text{cyt } c][\text{Apaf-1}] - k_1^-[\text{cyt } c \cdot \text{Apaf-1}] \quad (3-2)$$

$$J_{1b} = k_{1b}^+[\text{cyt } c \cdot \text{Apaf-1}]^p - k_{1b}^-[\text{apop}] \quad (3-3)$$

A reaction order (p) higher than unity for the apoptosome complex entails a *kinetic cooperativity* conducive to bistability, as will be shown in the results from calculations. For illustrative purposes, we show below a kinetic mechanism that results in an effective reaction order of $p = 4$

Consider the formation of a heptamer by the following series of reactions



Assuming pre-equilibrium for the fast reactions (3-V) and (3-VI), we obtain, after equating the forward (superscript f) and reverse (superscript b, for backward) reaction rates in these steps to each other, the following identities

$$k_{3V}^f[A]^2 = k_{3V}^b[A_2] \quad (3-4)$$

$$k_{3VI}^f[A_2][A] = k_{3VI}^b[A_3] \quad (3-5)$$

The rate equation for A_4 formation

$$d[A_4]/dt = k_{3VII}[A_3][A] \quad (3-6)$$

becomes after substituting equations 3-4 and 3-5,

$$d[A_4] = \frac{k_{3VI}^f [A_2][A]^2}{k_{3VI}^b} \quad (3-7a)$$

$$\Rightarrow d[A_4] = \frac{k_{3VI}^f k_{3V}^f [A]^4}{k_{3V} k_{3VI}^b} \quad (3-7b)$$

Given that the last three reactions of the series (3-VIII) – (3-X), are fast, reaction (3-VII) controls the rate of formation of A_7 such that $d[A_4]/dt \sim [A]^4$. This type of dependence on the concentration of the monomers is assumed in our model, i.e. $p = 4$ in eq (3-3), where $[A]$ is replaced by $[cyt\ c \cdot Apaf-1]$.

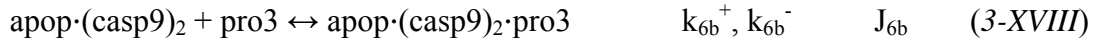
(3) *Initiator caspase-9 activation* involves five reactions; the binding of the procaspase-9 (pro9) to the apoptosome complex, followed by the binding of a second pro9 to form the complex $apop \cdot (pro9)_2$ and the cleavage of the bound procaspases to yield the holoenzyme $apop \cdot (casp9)_2$, the dissociation of which finally leads to caspases-9 (Fussenegger et al., 2000; Rodriguez and Lazebnik, 1999), i.e.



(4) *Activation of caspase-3 by caspase-9* is described by two reactions, the complexation of casp9 with the pro3, and the following cleavage of pro3 to yield the executioner casp3 molecule (Fussenegger et al., 2000), i.e.



(5) *Another mechanism of activation of caspase-3* is the complexation of holoenzyme $\text{apop}\cdot(\text{casp9})_2$ with the zymogen pro3, followed by the cleavage of pro3 to yield casp3 (Riedl et al., 2005; Rodriguez and Lazebnik, 1999), i.e.



(6) *Inhibition of caspase-9 and -3 by IAPs.* IAP inhibits both casp9 (Shiozaki et al., 2003) and casp3 molecules following the reactions (Fussenegger et al., 2000):



(7) *Cleavage of Bid by caspase-3.* In addition to caspase-8 that initiates the cleavage of Bid, casp3 produced downstream also truncates Bid to tBid in Type II cells (Luo et al., 1998; Slee et al., 2000). The corresponding reactions are



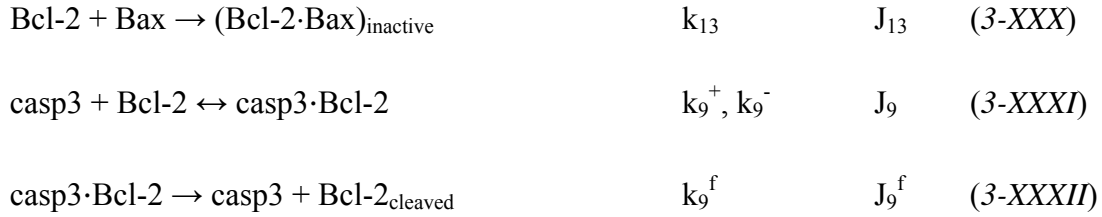
The activation of Bid by casp3 completes the first of two positive feedback loops present in our model. The second is due to the cleavage of the inhibitory protein Bcl-2 by casp3 (see item 9 below). Upon cleavage, Bcl-2 can no longer inhibit the channel-opening activity of Bax (Antonsson et al., 1997). Therefore, casp3 indirectly enhances the formation of channels for proapoptotic cyt *c* release.

(8) *Cyt c release from mitochondria to cytoplasm.* In the model proposed by Fussenegger and co-workers (Fussenegger et al., 2000), cyt *c* is released when the concentration of casp3 relative to that of Bcl-2 exceeds a threshold value. Here, we adopt a different mechanism based on experimental observations (Lutter et al., 2001; Wei et al., 2001; Wolter et al., 1997; Yi et al., 2003), summarized by the following sequence of events



Accordingly, tBid translocates to the mitochondria (k_{11}), forms a complex with Bax (k_{12a}) to initiate Bax oligomerization and channel (Bax_2) formation (k_{12b}). Cyt *c* is then released through the channel (k_{14}).

(9) *Inhibition of Bax by Bcl-2, and cleavage (inactivation) of Bcl-2 by caspase-3.* The cleavage of anti-apoptotic Bcl-2 by casp3 (Kim et al., 1998), which otherwise would inhibit Bax, is described by



(10) *p53 regulation of Bax and Bcl-2 synthesis.* p53 upregulates the synthesis of Bax and downregulates that of Bcl-2 (Karpinich et al., 2002; Weller, 1998). Joers et al. (2004) observed that although p53 levels increase in all cells subject to DNA damage, only in some cells is the transcriptional activity of p53 switched on, whereas in the remainder it is switched off. To account for this switch-like response of p53 to DNA damage, the following expressions are used for the rates of formation of Bax and Bcl-2

$$\Omega_{\text{Bcl-2}} = \Omega_{\text{Bcl-2}}^0 [\text{p53}]^4_{\text{thresh}} / ([\text{p53}]^4 + [\text{p53}]^4_{\text{thresh}}) \quad (3-8)$$

$$\Omega_{\text{Bax}} = \Omega_{\text{Bax}}^0 (1 + [\text{p53}]^4 / ([\text{p53}]^4 + [\text{p53}]^4_{\text{thresh}})) \quad (3-9)$$

The above two expressions closely approximate the qualitative switch-like activity of p53. The adoption of continuous functions as opposed to discrete threshold values permits us to perform a bifurcation analysis using the AUTO package. Note that these two equations represent the only expressions different from simple mass-action kinetics adopted in this text. The expression (3-8) originates from the assumption that Bcl-2 is expressed with a rate of $\Omega_{\text{Bcl-2}}^0$ when $[\text{p53}] = 0$, however, the expression rate $\Omega_{\text{Bcl-2}}$ approaches zero when $[\text{p53}] \gg [\text{p53}]_{\text{thresh}}$. Hence, there is a switch for Bcl-2 expression rate dependant on $[\text{p53}]$ value. The exponent 4 is

chosen in the expression as opposed to a lower integer value to approximate a sharp switching function, i.e., step function. Expression (3-9) is adopted by similar arguments. We explored the effect of using other numbers for the exponents and we will discuss the results in Section 3.6.2.

(11) *Synthesis and degradation reactions.* In addition to the above sets of reactions, the model includes the synthesis and degradation of a number of components. The proteins being synthesized (and corresponding synthesis rates) are Apaf-1 ($\Omega_{\text{Apaf-1}}$), IAP (Ω_{IAP}), pro3 (Ω_{pro3}), pro9 (Ω_{pro9}), Bid (Ω_{Bid}), Bcl-2 (Ω_{Bcl2}), Bax (Ω_{Bax}), and cyt c_{mito} (Ω_{cytmit}). Recent studies show that many molecules involved in apoptotic pathways are regulated by the ubiquitin-proteasome pathway (Yang and Yu, 2003). A first order degradation kinetics with a uniform rate constant of μ is adopted here for casp8, casp9, casp3, pro9, pro3, Apaf-1, IAP, Bcl-2, Bid, tBid, tBid_{mito}, Bax, Bax₂, tBid:Bax cyt c and cyt c_{mito} . The initial concentrations of all compounds are zero, except for pro3 and pro9, Apaf-1, Bid, Bax, Bcl-2, IAP and cyt c_{mito} that are all taken as 0.004 μM since the concentrations of proteins are usually in the nanomolar range (Chen et al., 2000), unless otherwise stated or varied. Initial concentrations of casp8 and casp3 are indicated for each simulation.

Table 1. The set of differential rate equations adopted in Model 3

$d[\text{Apaf-1}]/dt = -J_1 + J_{\text{Apaf-1}}$	$d[\text{apop} \cdot (\text{casp9})_2 \cdot \text{pro3}]/dt = J_{6b} - J_{6b}^f$
$d[\text{cyt } c \cdot \text{Apaf-1}]/dt = J_1 - 7J_{1b}$	$d[\text{casp3}]/dt = J_6^f + J_{6b}^f - J_7 - J_8 + J_8^f - J_9 + J_9^f + J_{\text{casp3}}$
$d[\text{apop}]/dt = J_{1b} - J_2 + J_{4b}$	$d[\text{casp8}]/dt = -J_0 + J_0^f + J_{\text{casp8}}$
$d[\text{apop} \cdot \text{pro9}]/dt = J_2 - J_3$	$d[\text{Bid}]/dt = -J_0 - J_8 + J_{\text{Bid}}$
$d[\text{apop} \cdot (\text{pro9})_2]/dt = J_3 - J_3^f$	$d[\text{casp8} \cdot \text{Bid}]/dt = J_0 - J_0^f$
$d[\text{apop} \cdot (\text{casp9})_2]/dt = J_3^f - J_4 - J_{5c} - J_{6b} + J_{6b}^f$	$d[\text{Bcl-2}]/dt = -J_9 - J_{13} + J_{\text{Bcl2}}$
$d[\text{apop} \cdot \text{casp9}]/dt = J_4 - J_{4b} - J_{5b}$	$d[\text{casp3} \cdot \text{Bid}]/dt = J_8 - J_8^f$
$d[\text{casp9}]/dt = J_4 - J_{4b} - J_5 - J_6 + J_6^f + J_{\text{casp9}}$	$d[\text{casp3} \cdot \text{Bcl-2}]/dt = J_9 - J_9^f$
$d[\text{pro9}]/dt = -J_2 - J_3 + J_{\text{pro9}}$	$d[\text{Bax}]/dt = -J_{12a} - J_{12b} - J_{13} + J_{\text{Bax}}$
$d[\text{IAP}]/dt = -J_5 - J_{5b} - J_{5c} - J_7 + J_{\text{IAP}}$	$d[\text{tBid}]/dt = J_0 + J_8^f - J_{11} + J_{12b} + J_{\text{tBid}}$
$d[\text{casp9} \cdot \text{IAP}]/dt = J_5$	$d[\text{tBid} \cdot \text{Bax}]/dt = J_{12a} - J_{12b} + J_{\text{tBidBax}}$
$d[\text{apop} \cdot \text{casp9} \cdot \text{IAP}]/dt = J_{5b}$	$d[\text{cyt } c_{\text{mito}}]/dt = -J_{14} + J_{\text{cytmit}}$
$d[\text{apop} \cdot (\text{casp9})_2 \cdot \text{IAP}]/dt = J_{5c}$	$d[\text{Bax}_2]/dt = J_{12b} + J_{\text{Bax2}}$
$d[\text{casp3} \cdot \text{IAP}]/dt = J_7$	$d[\text{tBid}_{\text{mito}}]/dt = J_{11} - J_{12a} + J_{\text{tBidmit}}$
$d[\text{pro3}]/dt = -J_6 - J_{6b} + J_{\text{pro3}}$	$d[\text{cyt } c]/dt = J_{14} - J_1 + J_{\text{cytc}}$
$d[\text{casp9} \cdot \text{pro3}]/dt = J_6 - J_6^f$	

with

$J_0' = k_0^+ [\text{casp8}][\text{Bid}] - k_0^- [\text{casp8} \cdot \text{Bid}]$	$J_{\text{Apaf-1}} = \Omega_{\text{Apaf-1}} - \mu[\text{Apaf-1}]$
$J_0^f = k_0^f [\text{casp8} \cdot \text{Bid}]$	$J_{\text{IAP}} = \Omega_{\text{IAP}} - \mu[\text{IAP}]$
$J_1 = k_1^+ [\text{cyt } c][\text{Apaf-1}] - k_1^- [\text{cyt } c \cdot \text{Apaf-1}]$	$J_{\text{pro3}} = \Omega_{\text{pro3}} - \mu[\text{pro3}]$
$J_{1b} = k_{1b}^+ [\text{cyt } c \cdot \text{Apaf-1}]^p - k_{1b}^- [\text{apop}]$	$J_{\text{pro9}} = \Omega_{\text{pro9}} - \mu[\text{pro9}]$

$J_2 = k_2^+[\text{apop}][\text{pro9}] - k_2^-[\text{apop}\cdot\text{pro9}]$	$J_{\text{Bid}} = \Omega_{\text{Bid}} - \mu[\text{Bid}]$
$J_3 = k_3^+[\text{apop}\cdot\text{pro9}][\text{pro9}] - k_3[\text{apop}\cdot(\text{pro9})_2]$	$J_{\text{Bcl2}} = \Omega_{\text{Bcl2}} - \mu_{\text{Bcl2}}[\text{Bcl-2}]$
$J_3^f = k_3^f[\text{apop}\cdot(\text{pro9})_2]$	$J_{\text{Bax}} = \Omega_{\text{Bax}} - \mu_{\text{Bax}}[\text{Bax}]$
$J_4 = k_4^+[\text{apop}\cdot(\text{casp9})_2] - k_4^-[\text{apop}\cdot\text{casp9}][\text{casp9}]$	$J_{\text{cytmit}} = \Omega_{\text{cytmit}} - \mu[\text{cyt } c_{\text{mito}}]$
$J_{4b} = k_{4b}^+[\text{apop}\cdot\text{casp9}] - k_{4b}^-[\text{apop}][\text{casp9}]$	$J_{\text{casp9}} = -\mu[\text{casp9}]$
$J_5 = k_5^+[\text{casp9}][\text{IAP}] - k_5^-[\text{casp9}\cdot\text{IAP}]$	$J_{\text{casp3}} = -\mu[\text{casp3}]$
$J_{5b} = k_{5b}^+[\text{apop}\cdot\text{casp9}][\text{IAP}] - k_{5b}^-[\text{apop}\cdot\text{casp9}\cdot\text{IAP}]$	$J_{\text{tBid}} = -\mu[\text{tBid}]$
$J_{5c} = k_{5c}^+[\text{apop}\cdot(\text{casp9})_2][\text{IAP}] - k_{5c}^-[\text{apop}\cdot(\text{casp9})_2\cdot\text{IAP}]$	$J_{11} = k_{11}[\text{tBid}]$
$J_6 = k_6^+[\text{casp9}][\text{pro3}] - k_6^-[\text{casp9}\cdot\text{pro3}]$	$J_6^f = k_6^f[\text{casp9}\cdot\text{pro3}]$
$J_9 = k_9^+[\text{casp3}][\text{Bcl2}] - k_9^-[\text{casp3}\cdot\text{Bcl2}]$	$J_{12a} = k_{12a}[\text{tBid}_{\text{mito}}][\text{Bax}]$
$J_{6b} = k_{6b}^+[\text{apop}\cdot(\text{casp9})_2][\text{pro3}] - k_{6b}^-[\text{apop}\cdot(\text{casp9})_2\cdot\text{pro3}]$	$J_{12b} = k_{12b}[\text{tBid}\cdot\text{Bax}][\text{Bax}]$
$J_{6b}^f = k_{6b}^f[\text{apop}\cdot(\text{casp9})_2\cdot\text{pro3}]$	$J_{14} = k_{14}[\text{Bax}_2][\text{cyt } c_{\text{mito}}]$
$J_7 = k_7^+[\text{casp3}][\text{IAP}] - k_7^-[\text{casp3}\cdot\text{IAP}]$	$J_9^f = k_9^f[\text{casp3}\cdot\text{Bcl2}]$
$J_8 = k_8^+[\text{casp3}][\text{Bid}] - k_8^-[\text{casp3}\cdot\text{Bid}]$	$J_8^f = k_8^f[\text{casp3}\cdot\text{Bid}]$
$J_{13} = k_{13}[\text{Bcl2}][\text{Bax}] \quad \text{and} \quad J_{14} = k_{14}[\text{Bax}_2][\text{cyt } c_{\text{mito}}]$	$J_8^f = k_8^f[\text{casp3}\cdot\text{Bid}]$

Table 2. The parameters used in Model 3*

Rate constants		Other parameters
$k_0^+ = 10 \mu\text{M}^{-1}\text{s}^{-1}$	$k_0^- = 0.5 \text{ s}^{-1}$	$p = 4$
$k_0^f = 0.1 \text{ s}^{-1}$	$k_1^+ = 5 \mu\text{M}^{-1}\text{s}^{-1}$	$[\text{p53}_{\text{thresh}}] = 0.004 \mu\text{M}$
$k_1^- = 0.5 \text{ s}^{-1}$	$k_{1b}^+ = 5 \times 10^4 \mu\text{M}^{-3}\text{s}^{-1}$	$\mu = 0.006 \text{ s}^{-1}$
$k_{1b}^- = 0.5 \text{ s}^{-1}$	$k_2^+ = 10 \mu\text{M}^{-1}\text{s}^{-1}$	$\Omega_{\text{Apaf-1}} = 3 \times 10^{-4} \mu\text{M/s}$
$k_2^- = 0.5 \text{ s}^{-1}$	$k_3^+ = 10 \mu\text{M}^{-1}\text{s}^{-1}$	$\Omega_{\text{IAP}} = 3 \times 10^{-5} \mu\text{M/s}$
$k_3^- = 0.5 \text{ s}^{-1}$	$k_3^f = 0.1 \text{ s}^{-1}$	$\Omega_{\text{pro3}} = 3 \times 10^{-4} \mu\text{M/s}$
$k_4^+ = 5 \mu\text{M}^{-1}\text{s}^{-1}$	$k_4^- = 0.5 \text{ s}^{-1}$	$\Omega_{\text{pro9}} = 3 \times 10^{-4} \mu\text{M/s}$
$k_{4b}^+ = 5 \mu\text{M}^{-1}\text{s}^{-1}$	$k_{4b}^- = 0.5 \text{ s}^{-1}$	$\Omega_{\text{Bid}} = 3 \times 10^{-5} \mu\text{M/s}$
$k_5^+ = 5 \mu\text{M}^{-1}\text{s}^{-1}$	$k_5^- = 0.0035 \text{ s}^{-1}$	$\Omega_{\text{Bcl2}}^0 = 8 \times 10^{-5} \mu\text{M/s}$
$k_{5b}^+ = 5 \mu\text{M}^{-1}\text{s}^{-1}$	$k_{5b}^- = 0.0035 \text{ s}^{-1}$	$\Omega_{\text{Bax}}^0 = 3 \times 10^{-5} \mu\text{M/s}$
$k_{5c}^+ = 5 \mu\text{M}^{-1}\text{s}^{-1}$	$k_{5c}^- = 0.0035 \text{ s}^{-1}$	$\Omega_{\text{cytmit}} = 3 \times 10^{-4} \mu\text{M/s}$
$k_6^+ = 10 \mu\text{M}^{-1}\text{s}^{-1}$	$k_6^- = 0.5 \text{ s}^{-1}$	$[\text{p53}] = 0.0066 \mu\text{M}$
$k_6^f = 0.001 \text{ s}^{-1}$	$k_{6b}^+ = 10 \mu\text{M}^{-1}\text{s}^{-1}$	
$k_{6b}^- = 0.5 \text{ s}^{-1}$	$k_{6b}^f = 0.1 \text{ s}^{-1}$	
$k_7^+ = 5 \mu\text{M}^{-1}\text{s}^{-1}$	$k_7^- = 0.0035 \text{ s}^{-1}$	
$k_8^+ = 10 \mu\text{M}^{-1}\text{s}^{-1}$	$k_8^- = 0.5 \text{ s}^{-1}$	
$k_8^f = 0.1 \text{ s}^{-1}$	$k_9^+ = 10 \mu\text{M}^{-1}\text{s}^{-1}$	
$k_9^- = 0.5 \text{ s}^{-1}$	$k_9^f = 0.1 \text{ s}^{-1}$	
$k_{11} = 10 \text{ s}^{-1}$	$k_{12a} = 10 \mu\text{M}^{-1}\text{s}^{-1}$	
$k_{12b} = 10 \mu\text{M}^{-1}\text{s}^{-1}$	$k_{13} = 10 \mu\text{M}^{-1}\text{s}^{-1}$	

$k_{14} = 10 \mu\text{M}^{-1}\text{s}^{-1}$		
---	--	--

* All rate constants, except for k_7^- , k_5^- , k_{5b}^- , k_{5c}^- , k_{1b}^+ , k_{11} , k_{12a} , k_{12b} , k_{13} , k_{14} , $[p53_{\text{thresh}}]$ are set up to within one order of magnitude difference with respect to those used by Asthagiri and Lauffenburger (2001) in their simulations of mitogen-activated protein kinase (MAPK) pathways. The ratio of k_7^+ to k_7^- ensures an equilibrium constant of 0.7 nM (Deveraux et al., 1997), as well as those used for defining k_5^- , k_{5b}^- and k_{5c}^- . The values of k_{1b}^+ , k_{11} , k_{12a} , k_{12b} , k_{13} , k_{14} , $[p53_{\text{thresh}}]$ are suitably set to achieve fluxes comparable to other compounds' fluxes. k_6^f is assigned a value smaller than k_{6b}^f because of experimental observations by Riedl et al. (2005). The degradation constant of all species is assigned as 0.006 s^{-1} unless specified otherwise in the text. This value is within the range of parameters used for degradation rate constants adopted by Chen et al. (2000) The rates of synthesis are within the range of values used by Chen et al. (2000).

3.2.2 Adoption of simple mass-action kinetics

Model 3 contains 31 components, including the different forms of the same molecule (e.g. Bid and tBid) and the same protein in different subcellular environments (e.g. *cyt c* in the cytosol and in the mitochondria). As presented above, all interactions (chemical or physical) are treated as chemical reactions, and their time-evolution is described by classical chemical reaction kinetics.

We do not have conservation of the enzyme and thus do not use Michaelis-Menten (MM) simplifications for our reactions. We use the standard mass action models from which MM kinetics is derived when the total enzyme concentration is constant. In all of our reactants, we maintain a small source as well as degradation for the enzyme, such that the total enzyme concentration is not conserved until steady state conditions are reached. This provides robustness to the model which a simple conservation model lacks. In the absence of the source and degradation, and by the assumption of steady state conditions for particular products, the kinetics reduces to MM kinetics. In the present approach, the equations for the concentrations of enzyme, $[E]$, and for the enzyme-substrate concentration, $[ES]$, obey the general form

$$d[E]/dt = \sum_i J_i + J_{\text{source}} - J_{\text{decay}} \quad (3-10)$$

$$d[ES]/dt = - \sum_i J_i \quad (3-11)$$

where J is the contribution from the reactions in which they participate, and the latter two terms refer to their production and degradation rates, so that there is no longer conservation of the total enzyme and the MM assumption is violated.

In the case of MM kinetics, on the other hand, the set of reactions and equations would be



where P is the product, k^f is the rate constant of forward reaction and k^b is the rate constant of reverse reaction in (3-XXXIII) and k_{cat} is the rate constant for catalytic reaction in (3-XXXIV).

The differential rate equations for the enzyme and enzyme-substrate complex read in this case

$$d[E]/dt = \sum_i J_i = - k^f[E][S] + k^b[ES] + k_{cat}[ES] \quad (3-12)$$

$$d[ES]/dt = - \sum_i J_i = k^f[E][S] - k^b[ES] - k_{cat}[ES] \quad (3-13)$$

The total concentration of enzyme (in isolated and complexed form) is constant over time and equal to

$$[E] + [ES] = E_T \quad (3-14)$$

as follows from Eqs 3-12 and 3-13 that lead to the identity

$$d[E]/dt + d[ES]/dt = 0 \quad (3-15)$$

In the reaction cascade, enzyme and substrate first form the enzyme-substrate complex with a rapid and reversible step with no chemical changes taking place. The enzyme and substrate are held together by noncovalent interactions. The chemical conversion of substrate to product takes

place in second step with a rate constant k_{cat} in reaction (3-XXXIV). Assuming pre-equilibrium for the fast reactions in (3-XXXIII),

$$k^f[E][S] = k^b[ES] \quad (3-16)$$

$$[E][S]/[ES] = k^b/k^f = K_M \quad (3-17)$$

where K_M is Michaelis constant.

The rate of production of P is

$$v \equiv d[P]/dt = k_{cat}[ES] \quad (3-18)$$

Inserting Eq. (3-14) into Eq. (3-17) to eliminate [E] and rearranging, we obtain

$$[ES] = [E]_T[S] / (K_M + [S]) \quad (3-19)$$

which, upon substitution in eq 3-18 leads to the so-called Michaelis-Menten equation (Fersht, 2002)

$$v = [E]_T[S]k_{cat} / (K_M + [S]) \quad (3-20)$$

3.2.3 Approximations in model parameters

The model parameters are listed in Table 2. Most of them have been assigned values within an order of magnitude of those used in previous studies (Asthagiri and Lauffenburger, 2001; Chen et al., 2000). These parameters, corresponding to MAP kinase pathways, were adopted in view of the lack of experimental data on the rate parameters of the above listed reactions, and experimental data have been incorporated when available (see Table 2 footnote). With these choices of parameters, it will be shown that the model exhibits resistance to caspase-3 activation when p53 level is low and bistability to apoptotic stimuli when p53 level is high in agreement with experiments (44). In view of the lack of precise quantitative information on most parameters, the present results should be viewed as qualitative, rather than quantitative. The

coefficient p was chosen to be 4. Smaller values were also observed to lead to bistability, although the associated threshold concentrations of caspase-3 were unrealistically low (e.g., 0.004 molecules per cell for $p = 3$ and 3.2×10^{-6} molecules per cell for $p = 2$). The simulations and bifurcation analysis have been performed using the software XPPAUT (<http://www.math.pitt.edu/~bard/xpp/xpp.html>) developed by Professor Bard Ermentrout at the University of Pittsburgh, Department of Mathematics (Ermentrout, 2002).

3.3 COOPERATIVITY IN APOPTOSOME FORMATION CAUSES BISTABILITY IN THE MITOCHONDRIA-DEPENDENT MODEL OF APOPTOSIS

Any stimulus that produces casp8 may initiate mitochondria-dependent apoptotic interactions (Figure 1). Caspase-8 truncates Bid to tBid, which results in the activation of casp3 by a cascade of reactions following the translocation of tBid to the mitochondria. The activation of casp3 gives rise to two positive feedback loops that amplify the response to the initial triggering effect of casp8. Our model does not include the pathways upstream of casp8 activation. We assume that a transient pro-apoptotic stimulation results in the production of casp8 in proportion to the exposure of the cell to death signal ligands. Here the coefficient p involved in the formation of apoptosome is taken as $p = 4$. The upper limit $p = 7$ can not be adopted because in this case, the model is not bistable but monostable cell survival where casp3 is not activated even for very high apoptotic stimulus. Although p might be as large as seven for a fully cooperative formation of a heptameric structure, a value of four was observed to be sufficient to ensure bistability, while lower p values would necessitate unrealistic (picomolar) concentrations of casp3 to ensure a bistable response.

Figure 10 panels *A* and *B* illustrate two opposite behaviors observed in response to small changes in pro-apoptotic stimuli (represented here by the initial casp8 concentration $[\text{casp8}]_0$) provided that the apoptotic pathways involve a cooperative step. When $[\text{casp8}]_0$ is relatively low, $[\text{casp8}]_0 = 10^{-5} \mu\text{M}$, for example, cell survival is observed as a monostable response (Figure 10A) using the differential rate equations and parameters listed in the respective Tables 1 and 2. Cell survival is manifested therein by a decrease in the concentration of casp3 to negligibly small values. On the other hand, the opposite behavior, i.e. monostable PCD, is induced (Figure 10B) if the pro-apoptotic stimulus exceeds a threshold level (see below). The concentration of casp3 is shown to increase in this case by two orders of magnitude, to $4.5 \times 10^{-3} \mu\text{M}$, from the same initial concentration ($10^{-5} \mu\text{M}$) as in Figure 10A. The only different input for generating the result displayed in panel B as compared to panel A is the increase (from $10^{-5} \mu\text{M}$ to $10^{-4} \mu\text{M}$) in the initial concentration of $[\text{casp8}]_0$.

We note that the model is not restricted to apoptosis caused by extracellular stimuli exclusively. The PCD in panel B was verified to also occur with a zero initial casp8 concentration and non-zero initial casp3 concentration (e.g. $[\text{casp3}]_0 = 5 \times 10^{-4} \mu\text{M}$, which eventually leads to $[\text{casp3}] = 4.8 \times 10^{-3} \mu\text{M}$ - data not shown). Therefore, apoptosis may be equally driven by intrinsic pro-apoptotic stimuli that induce casp3 activation. In our analysis, casp3 steady state concentrations of the order of nanomolar were accepted to be indicative of apoptosis, whereas cell survival would refer to vanishingly small concentrations.

Finally, in the absence of cooperativity ($p = 1$), the same initial conditions for caspase-8 and caspase-3 that led to cell survival in Figure 10A, are now observed to induce apoptosis, as implied by the high concentrations ($6 \times 10^{-3} \mu\text{M}$) caspase-3 reaches at steady state (Figure 10C). This is an example of pathological cell death rather than a normal response to small apoptotic

stimuli (cell survival/protection). The system does not exhibit a bistable behavior in response to variations in $[\text{casp8}]_0$. Instead, apoptosis is the only stable state, despite the low original concentration of casp8.

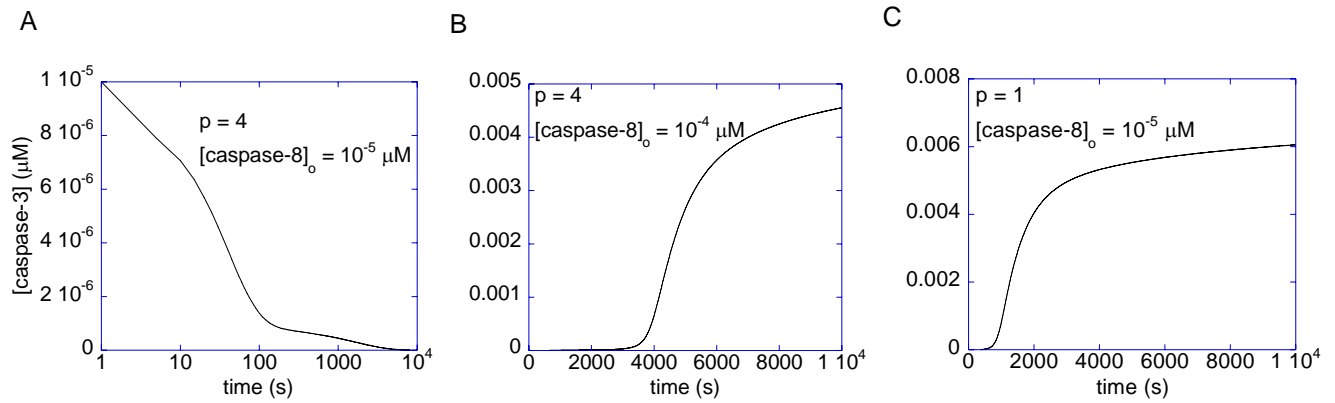


Figure 10. Time evolution of caspase-3 in response to minor changes in initial caspase-8 concentration $[\text{casp8}]_0$. (A) *cell survival* when $[\text{casp8}]_0$ is small (10^{-5} μM), indicated by the decrease in the caspase-3 concentration (initially 10^{-5} μM) to zero at steady state. The abscissa is shown in logarithmic scale to display the time evolution of caspase-3 more clearly; (B) *apoptosis*, implied by the increase in caspase-3 concentration to a high value (4.5×10^{-3} μM) at steady state despite the same initial value of caspase-3 as in panel A, when $[\text{casp8}]_0$ is higher (10^{-4} μM); (C) *monostable apoptosis*, in the absence of cooperativity ($p = 1$) using the same initial concentrations of caspase-3 and caspase-8 as in panel A. Here caspase-3 concentration reaches a high value (6×10^{-3} μM) at long times indicative of apoptotic response. Note that the ordinate scales are different in the panels.

Taken together, these results suggest that the cooperativity in apoptosome formation, might be a mechanism in cells to ensure healthy functioning of cells to apoptotic stimuli, instead of invariably leading to apoptosis in response to minimal stimulation.

3.4 BIOLOGICAL SIGNIFICANCE OF BISTABILITY. ROLES OF BAX, BCL-2, AND MPTP IN PATHOLOGICAL APOPTOSIS

3.4.1 Bax degradation and expression rates can determine the transition between bistable and monostable responses

Apoptosis can be controlled by the degradation rate of pro-apoptotic proteins such as Bax (Li and Dou, 2000). We examined if our mathematical model confirms this behavior. Figure 11A depicts the bifurcation diagram as a function of the degradation rate (μ_{Bax}) of Bax and the initial concentration of casp3. The limit point for saddle-node bifurcation is found as $\mu_{\text{Bax}} = 0.11 \text{ s}^{-1}$ using the parameters listed in Table 2. Below this limit point, there exist three steady states, two of which are stable and one unstable. Therefore, the system is bistable in this regime and the response may be either apoptosis or cell survival depending on the combination of the original caspase-3 concentration and Bax degradation rate. Conversely, above the limit point, there is only one stable state (cell survival), i.e. the system is monostable due to the depletion of pro-apoptotic Bax.

The arrows in Figure 11A, indicate the direction of evolution of casp3 levels, starting from any region of the diagram (i.e. any combination of the two parameters). The solid curve represents the *stable* apoptosis loci achieved with casp3 concentrations above the dotted curve, and the lower solid line represents the stable cell survival state, characterized by zero casp3 concentration. The dashed curve represents the loci of *unstable* steady-state leading to either cell death or cell survival, upon slight perturbation. It also defines the threshold concentration of apoptotic stimuli $[\text{casp3}]_0$ to trigger apoptosis as a function of the degradation rate of Bax. In the

monostable regime, even very high initial casp3 concentrations decay to zero. Therefore, when the rate of degradation of Bax is higher than the limit point, apoptosis cannot occur.

Figure 11B illustrates the time evolution towards monostable cell survival. With $\mu_{\text{Bax}} = 0.2 \text{ s}^{-1}$ (higher than the limit point), the concentration of casp3 decays from $[\text{casp3}]_0 = 0.1 \text{ }\mu\text{M}$ to zero, even when $[\text{casp8}]_0$ is also high ($0.1 \text{ }\mu\text{M}$). Notably, our results are in accord with those of Li and Dou, who demonstrated that elevated Bax degradation is a survival mechanism in human cancer cells (Li and Dou, 2000).

Figure 11C is the bifurcation diagram for rate of formation of Bax. The limit point for the saddle-node bifurcation is $\Omega_{\text{Bax}}^0 = 6.03 \times 10^{-6} \text{ }\mu\text{M/s}$. Above this point, a bistable behavior is predicted in response to pro-apoptotic stimuli. For $\Omega_{\text{Bax}}^0 < 6.03 \times 10^{-6} \text{ }\mu\text{M/s}$, on the other hand, the response is monostable cell survival, even in the presence of high apoptotic stimuli. This result is consistent with observations of decreased Bax expression in human breast cancers (Schorr et al., 1999).

The present model thus predicts that cells will exhibit a monostable cell survival response to apoptotic stimuli if the degradation rate of Bax is above some threshold value or if the expression rate of Bax is below some threshold value (shown in the respective panels A and C of Figure 11). In this monostable regime, the casp3 concentration always diminishes to zero because there is not a sufficiently high concentration of Bax to open up channels on mitochondrial membrane for releasing cyt *c*. The net result is that the activation rate of casp3 becomes lower than its degradation rate, eventually leading to vanishingly low concentrations of casp3. In the bistable regime, on the other hand, a dichotomous response favoring either cell survival (vanishingly small casp3 concentration) or programmed cell death (casp3 above nanomolar concentration) is elicited, depending on the original casp3 concentrations. Overall, the

model predicts that there exists a critical point at which the amount of Bax leads to monostable cell survival that might be associated with the onset of cancer in living cells.

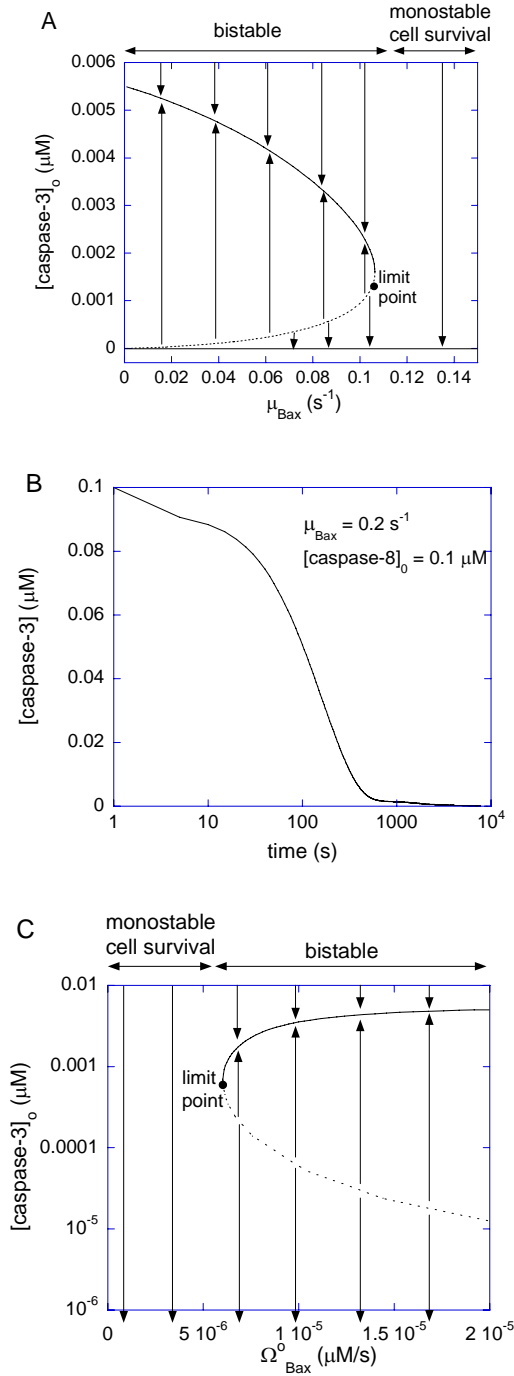


Figure 11. Effect of Bax degradation rate (μ_{Bax}) on cell fate. Calculations are performed using Model 3. (A) Bifurcation diagram for casp3 concentration with the bifurcation parameter μ_{Bax} along the abscissa. Limit point for saddle-node bifurcation is $\mu_{Bax} = 0.11 \text{ s}^{-1}$. Below this limit point, there are three steady states, two of which are stable and one unstable; and above the limit point, there is only one stable state, cell survival. The arrows indicate the equilibrium concentrations reached when starting from any point in the diagram; (B) The high initial concentration of caspase-3 (0.1 μM) decreases to zero when μ_{Bax} is in the monostable cell survival region (0.2 s^{-1}) despite the high [casp8]₀ value; (C) Bifurcation diagram for casp3 with the bifurcation parameter Ω_{Bax}^0 . Limit point for saddle-node bifurcation is $\Omega_{Bax}^0 = 6.03 \times 10^{-6} \text{ μM /s}$. The stable cell survival line ([casp3]₀ = 0) is not shown because the y-axis is logarithmic.

3.4.2 Bcl-2 modulates the effect of Bax

Bcl-2 is the classical, anti-apoptotic member of the Bcl-2 family. Danial and Korsmeyer state in their review (Danial and Korsmeyer, 2004) that the ratio of Bcl-2 to Bax constitutes a rheostat that sets the threshold of susceptibility to apoptosis for the mitochondria-dependent pathway. Accordingly, we tested if our mathematical model would demonstrate a counteracting role of Bcl-2 vis-à-vis the effects of Bax. We illustrate the effect of Bcl-2 on the pro-apoptotic effects of Bax in Figure 12A. The series of curves in this figure represent the bifurcation diagrams as a function of the degradation rate of Bax for different expression rates of Bcl-2. Figure 12B displays the results as a function of the synthesis rate of Bax. Therefore, Figure 12A and Figure 12B are the counterparts of the respective Figure 11A and Figure 11C obtained for different rates of formation of Bcl-2.

The increase in the rate of formation of Bcl-2, $\Omega_{\text{Bcl-2}}^{\circ}$, is observed to have several effects (Figure 12A). First, the limit point for the saddle-node bifurcation decreased to lower Bax degradation rates, i.e. cell survival becomes even more prominent. When $\Omega_{\text{Bcl-2}}^{\circ} = 8 \times 10^{-5} \mu\text{M/s}$, the limit point was $\mu_{\text{Bax}} = 0.11 \text{ s}^{-1}$ (Figure 11A). This result is included in Figure 12A for comparative purposes. The limit point decreased to $\mu_{\text{Bax}} = 0.085 \text{ s}^{-1}$ for $\Omega_{\text{Bcl-2}}^{\circ} = 3.2 \times 10^{-4} \mu\text{M/s}$, and to $\mu_{\text{Bax}} = 0.042 \text{ s}^{-1}$ for $\Omega_{\text{Bcl-2}}^{\circ} = 8 \times 10^{-4} \mu\text{M/s}$. Hence, the bistable cell survival region, which may possibly give rise to apoptosis becomes narrower, while the monostable cell survival region becomes broader, when Bcl-2 is over-expressed. This result is consistent with the observation that Bcl-2 is over-expressed in many types of tumors that exhibit low rates of apoptosis (Reed, 1999). Second, the threshold concentration of casp3 for undergoing apoptosis with a given Bax degradation rate μ_{Bax} , tends to increase with increase in Bcl-2 expression rate, as indicated by the

vertical shifting of the dashed portions of the curves in Figure 12A. This result implies that larger or more potent pro-apoptotic stimuli are needed for PCD when Bcl-2 expression levels are relatively high. Third, the apoptotic concentration of casp3 for given degradation rates of Bax (i.e. the solid portions of the bifurcation curves) are lowered with increasing Bcl-2 expression rates.

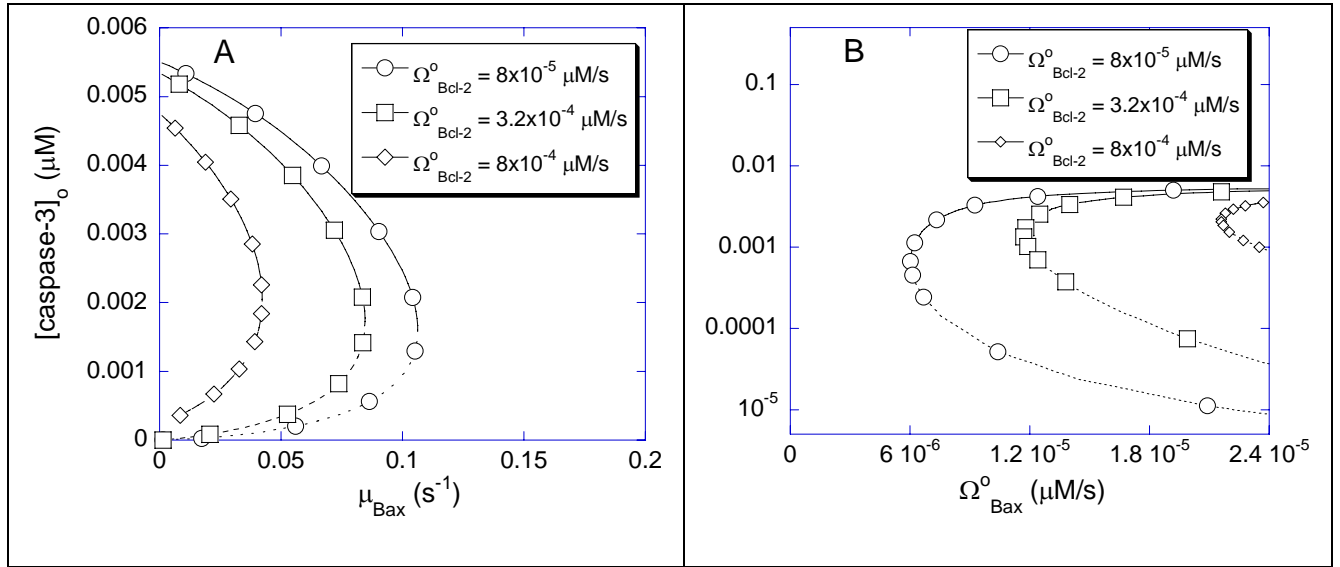


Figure 12. Effects of Bcl-2 expression rate on cell behavior in response to changes in Bax levels. Calculations are performed using Model 3. (A) Effect on the bifurcation diagram for μ_{Bax} ; (B) Effect on the bifurcation diagram for Ω_{Bax}^o .

In Figure 12B, we observe the equilibrium caspase-3 concentrations as a function of Bax expression rate, Ω_{Bax}^o , again for various rates of formation of Bcl-2, Ω_{Bcl-2}^o : First, the limit point for the saddle-node bifurcation shifts to higher Ω_{Bax}^o values with increasing Ω_{Bcl-2}^o . The limit point of $\Omega_{Bax}^o = 6.03 \times 10^{-6} \mu M/s$ (also shown in Figure 11C) is shifted to $1.17 \times 10^{-5} \mu M/s$, and then to $2.16 \times 10^{-5} \mu M/s$ as Ω_{Bcl-2}^o increases from $8 \times 10^{-5} \mu M/s$ to $3.2 \times 10^{-4} \mu M/s$, and then to $8 \times 10^{-4} \mu M/s$. Hence, the bistable region becomes narrower and the monostable cell survival region,

broader, when Bcl-2 expression levels increase. Second, the threshold $[\text{casp3}]_0$ for entering apoptosis shift to higher values in the bistable regions. Third, the steady-state concentrations of casp3 in the case of apoptosis slightly shift to lower values, similarly to their counterparts in Figure 12A.

These results suggest that the pro-apoptotic effect of a low rate of Bax degradation or high rate of Bax expression can be counteracted by high rate of Bcl-2 expression. This behavior is in line with the known interaction of these proteins (Danial and Korsmeyer, 2004). High Bcl-2 oncogene expression has been shown to sensitize the cells to cancer. Conversely, down-regulation of Bcl-2 can sensitize melanoma cells to apoptosis (Chawla-Sarkar et al., 2004; Zangemeister-Wittke et al., 2000). In a broader sense, the relative production and degradation rates of Bax and Bcl-2 determine whether the cell will survive or undergo apoptosis (Danial and Korsmeyer, 2004), consistent with our analysis.

3.4.3 Effect of MPTP on the detailed mitochondria-dependent apoptosis model

The mechanisms of cyt *c* release from mitochondria are highly diverse and controversial (Newmeyer and Ferguson-Miller, 2003; Nakagawa et al., 2005). In Model 3, we assume that cyt *c* release is closely dependent on the formation/activation of MPTPs (Green and Kroemer, 2004; Halestrap and Brenner, 2003) irrespective of Bax channel formation on mitochondria. The non-specific MPTP involved in cyt *c* release is proposed to be a complex formed by the proteins VDAC-ANT-CyP-D (Halestrap and Brenner, 2003). We will denote this non-specific pore by PTPC here. The release of cyt *c* from the non-specific pore, $\text{cyt } c_{\text{mito}} + \text{PTPC} \rightarrow \text{cyt } c$ is included in the model to account for this dependence.

The bifurcation diagram in Figure 13 illustrates the effect of PTPC level on the steady state concentration of caspase-3. In these calculations, the p53 concentration was assigned a relatively low value ($0.0022 \mu\text{M}$) so that the response to apoptotic stimulus (here $[\text{casp3}]_0$) would be monostable cell survival in the absence of PTPC. At low levels of PTPC ($< 2.3 \times 10^{-4} \mu\text{M}$), the system exhibits a monostable cell survival. At intermediate PTPC levels ($2.3 \times 10^{-4} \mu\text{M} < [\text{PTPC}] < 9.0 \times 10^{-4} \mu\text{M}$), a bistable behavior is observed, in accord with the healthy functioning of cells. At PTPC levels above the limit point of $9.0 \times 10^{-4} \mu\text{M}$, apoptosis is induced, which may be pathological in some cases (Green and Kroemer, 2004).

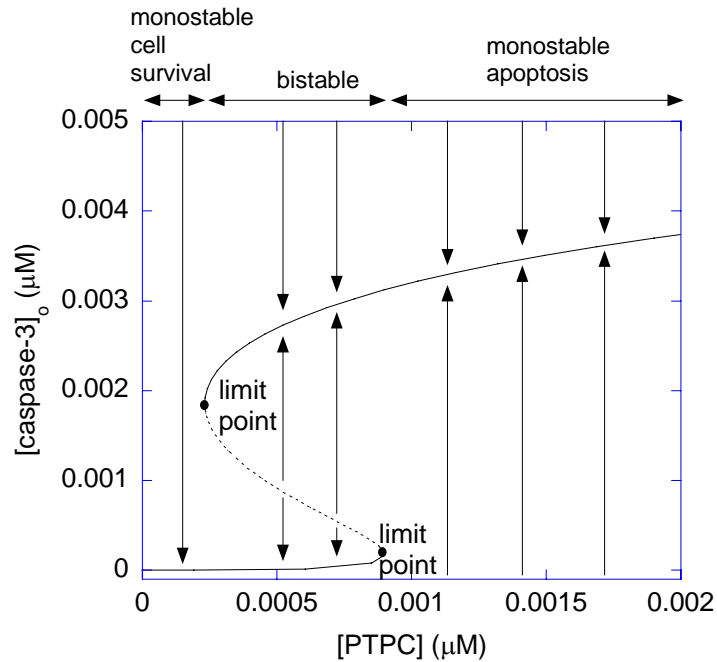


Figure 13. Bifurcation diagram as a function of the concentration of mitochondrial permeability transition pore complex $[\text{PTPC}]$. The limit points for saddle-node bifurcation are at $[\text{PTPC}] = 2.3 \times 10^{-4} \mu\text{M}$ and $9.0 \times 10^{-4} \mu\text{M}$.

3.5 ROBUSTNESS OF COOPERATIVE APOPTOSOME FORMATION AS A MECHANISM THAT IMPARTS BISTABILITY

Inhibition of caspases (Eissing et al., 2004) was proposed previously as a mechanism that can lead to bistability. We compared the robustness of two different mechanisms in inducing bistability: inhibition of casp3 by IAP and cooperative formation of apoptosome. To this aim, we organized the parameters into 13 groups and varied them within an order of magnitude, which led to $2^{13} = 8192$ parameter sets. In the absence of cooperativity (i.e. when the coefficient p was set equal to unity), none of the 8192 simulations led to a bistable response to apoptotic stimuli despite the IAP inhibition of casp3. In the presence of cooperativity, or when p was assigned the respective values of 2 and 3, we observed that 320 and 736 of the runs resulted in a bistable response, supporting the importance of cooperative apoptosome formation for inducing bistability over a wide range of parameters.

Eissing et al. (2007) recently studied simplified models that include kinetic cooperativity, zero-order ultrasensitivity or inhibitors. Using the previously described measures for robustness in bistable systems (Ma and Iglesias, 2002; Eissing et al., 2005), they find that theoretically all three model structures are robust in terms of bistability. In all cases, the bistability and its robustness depend on the right combination of parameters. That may explain why our choice of parameters resulted in different findings than theirs. What happens *in vivo* is probably a combination of these mechanisms to secure a tight switch (Manoharan et al., 2006).

3.6 COMPARISON WITH EXPERIMENTS

3.6.1 Inhibition of Bax degradation induces apoptosis in Bcl-2 overexpressing cells

Li and Dou (2000) studied the effect of a proteasome inhibitor, N-carbobenzoxy-L-leucyl-norvalinal (LLnV), on Bcl-2 overexpressing Jurkat T-cells that are protected from apoptosis. LLnV was shown to induce caspase-mediated apoptosis after *cyt c* release. It was also shown that LLnV inhibited Bax degradation in a cell-free assay. These findings are consistent with a role for the ubiquitin-proteasome pathway in regulating key players in the apoptotic cascade (Yang and Yu, 2003).

In order to test this conjecture, we carried out the following simulations. First, we examined the response of Bcl-2-overexpressing cells to apoptotic stimuli in the absence of a proteasome inhibitor. We assigned the values of $\mu_{\text{Bax}} = 0.1 \text{ s}^{-1}$ and $\Omega_{\text{Bcl-2}}^{\circ} = 3.2 \times 10^{-4} \text{ } \mu\text{M/s}$, which result in monostable cell survival as the Bax degradation rate is higher than the limit point (0.085 s^{-1}) (See Figure 12A). The curve with the filled circles in Figure 14A and B displays the time evolution of *cyt c* and caspase-3, respectively, under these conditions. Both curves show the depression of apoptotic molecules to negligibly low concentrations, suggesting the occurrence of monostable cell survival under these conditions. Second, we simulated the time evolution of the same Bcl-2-overexpressing cells in the presence of a proteasome inhibitor, by linearly decreasing μ_{Bax} to 0.04 s^{-1} in 1200 seconds, and maintaining this rate constant thereafter. The initial concentrations for both *caspl* and *pro3* were assigned to be $0.1 \text{ } \mu\text{M}$. This simulation resulted in an increase in *cyt c* release and an increase in *caspl* level (curves with open circles in panels A and B of Figure 14). The qualitative agreement between simulations and experiments suggests

that the onset of cancer may be associated with a Bax degradation rate higher than a certain threshold value (the limit point in the bifurcation diagram shown in Figure 12A).

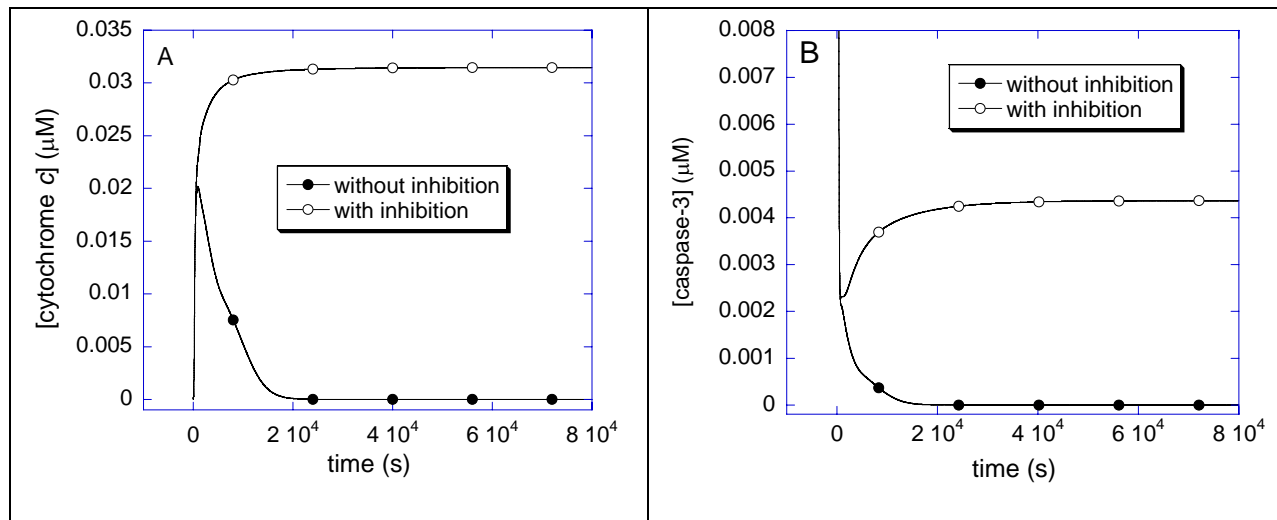


Figure 14. Time evolution of (A) cyt *c*; (B) caspase-3 levels with (open circles) and without (filled circles) inhibition of Bax degradation. Inhibition of Bax degradation induces an accumulation in cyt *c* and caspase-3 levels. Calculations are performed using Model 3.

3.6.2 Simulating the effect of Silymarin on apoptosis

In an experimental study by Katiyar et al. (2005), it was shown that silymarin, a plant flavonoid that is known to inhibit skin carcinogenesis in mice, induced casp3 activation in JB6 C141 cells (preneoplastic epidermal keratinocytes). The concentration of silymarin was shown therein to be correlated with p53 concentrations, suggesting that silymarin acts via increasing the p53 levels.

In order to explore if our model could explain/interpret the experimental data collected by Katiyar et al., we performed a mathematical analysis of the effect of changes in p53. We varied p53 concentration from a low value (0.0022 μM) characteristic of monostable cell survival, to

higher values in accord with the relative increases reported in Figure 3 of Katiyar et al. (2005). The selected $[p53]_0$ values and resulting caspase-3 concentrations are shown in panel A of Figure 15. The accompanying changes in the relative levels of Bax, Bcl-2 and cyt *c* are displayed in the respective panels B-D of the same figure. The comparison of the computational results (filled bars) with those from experiments Katiyar et al. (2005), shown by the crisscrossed bars, shows that there is a good qualitative agreement between the two sets, except for Bcl-2 concentrations at relatively high p53 levels, which seem to deplete faster in computations than in experiments. This discrepancy may be due to the adoption of equations 3-8 and 3-9 for describing the time evolution of Bcl-2 and Bax expression levels as a function of p53 concentration. The threshold p53 concentration for inducing transcriptional activity refers to a relative increase in $[p53]_0$ of approximately two (abscissa in Figure 15), and the computed abrupt decrease in Bcl-2 may be attributed to this change in regime. Additionally, experiments show the average behavior of an ensemble of cells (with a distribution of p53 concentrations), which would be expected to lead to a smoother change in [Bcl-2] compared to that predicted by computations. We examined the effect of exponent in equations 3-8 and 3-9. We can not adopt an exponent smaller than four because the normalized steady-state concentration of caspase-3 is 0.7 for concentration of unity for $[p53]_0$. This is in disagreement with the experimental results (See the vanishingly low concentration of casp3 in Figure 16, panel A for relative $[p53]_0 = 1$). Additionally, the agreement between the theoretical results and experimental results does not improve when the exponent is greater than four.

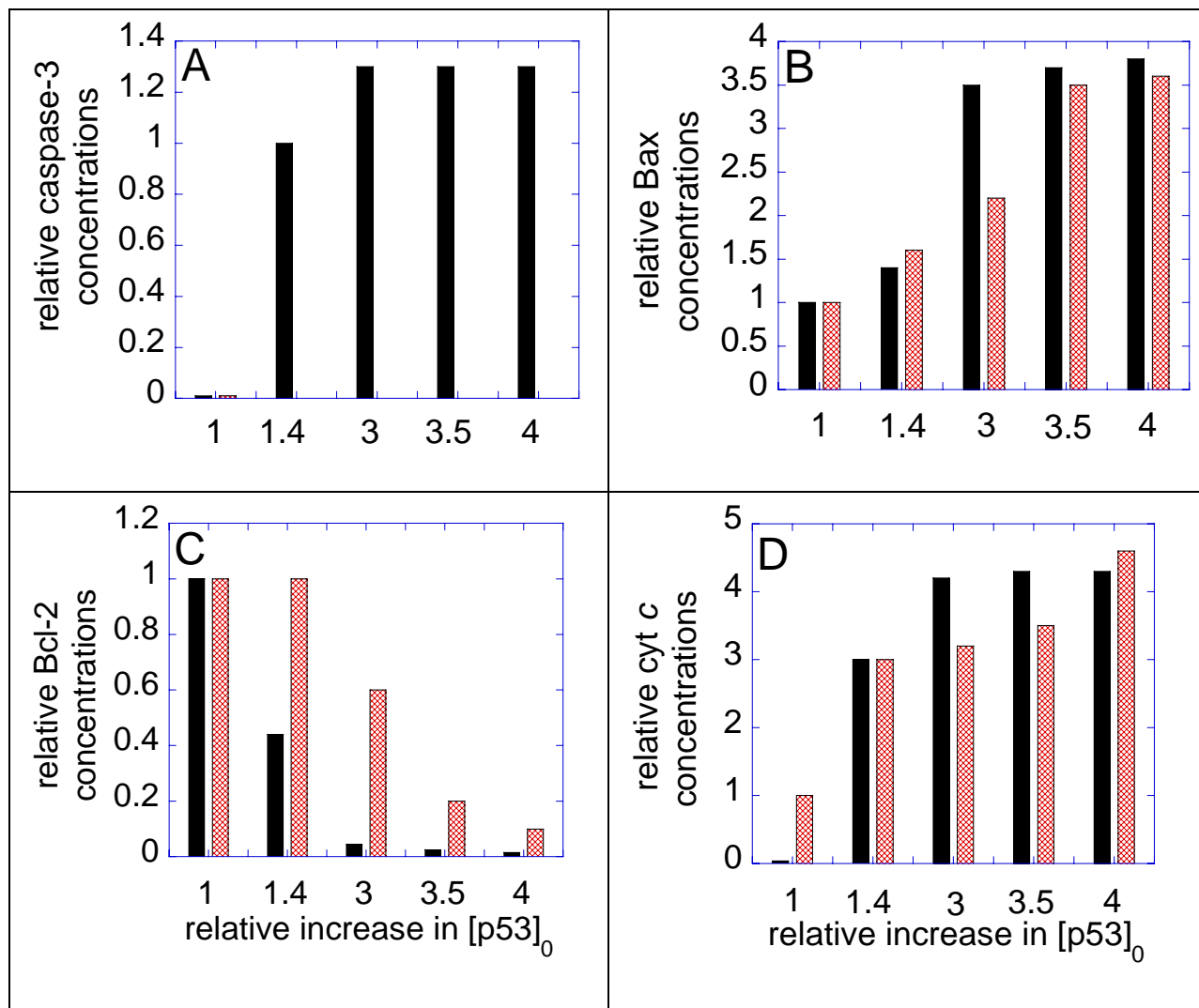


Figure 15. Comparison of the experimental and theoretical changes in casp3, Bax, Bcl-2 and cytochrome *c* concentrations in response to the relative changes in $[p53]$ (that are induced by changes in the flavanoid silymarin concentrations). Panel A displays the caspase-3 levels corresponding to each selected $[p53]$ computed by present simulations using Model 3. Panels B-D display the results from computations (solid bars) and those from experiments (cross-hatched bars) for each choice of relative $[p53]$ shown in panel A.

3.7 SUGGESTED EXPERIMENT TO REVEAL THE MECHANISM OF CASPASE-3 ACTIVATION

The mechanism of regulation in apoptosis is unclear. One hypothesis is that the regulation mechanisms due to positive feedback mechanisms involving casp3 and causing bistability (Bagci et al., 2006; Eissing et al., 2004; Legewie et al. 2006) and the other is switch mechanism in mitochondria (Bentele et al., 2004). One way to understand if the regulation is caused by positive feedback involving casp3 or not, is to do cell-free experiments in the absence of procaspase-3. The extract can then be loaded with wild-type and mutated procaspase-3 that lack the catalytic cysteine residue. If the positive feedback mechanisms are ensuring the control, casp3 would not be activated in the cell-free extract in the presence of mutated procaspase-3 (this is also predicted by the Model 3 by equating rates of catalytic reactions of casp3 to zero). However, if mitochondrial switch mechanisms are alone ensuring all or none behaviour in apoptosis, casp3 would be activated in the presence of mutated casp3.

4.0 COMPETING EFFECTS OF NITRIC OXIDE IN REGULATING APOPTOSIS: INSIGHTS FROM COMPUTATIONAL MODELING

We propose a new mathematical model for simulating the effects of nitric oxide (NO) on apoptosis. The new model integrates mitochondria-dependent apoptotic pathways with NO-related reactions, to provide information on the regulatory effect of the reactive NO species N_2O_3 , non-heme iron nitrosyl species (FeL_nNO), and peroxynitrite ($ONOO^-$). In the absence of NO, the model predicts either cell survival or apoptosis (a bistable behavior) with shifts in the onset time of apoptotic response depending on the strength of extracellular stimuli. Computations shed light on experimentally observed dichotomous effects of NO, demonstrating that the relative concentrations of anti-apoptotic and pro-apoptotic reactive NO species, and their interplay with glutathione, determine the net anti- or pro-apoptotic effects at long time points. Interestingly, transient effects on apoptosis are also observed, the duration of which may reach up to hours, despite the eventual convergence to an anti-apoptotic state. Our computations point to the importance of precise timing of NO production and external stimulation in determining the eventual pro- or anti-apoptotic role of NO.

4.1 NITRIC OXIDE EFFECTS ON APOPTOSIS

Nitric oxide has opposite, competing effects in regulating apoptosis: it exerts an anti-apoptotic effect on hepatocytes (Kim et al., 2004; Vodovotz et al., 2004; Wang et al., 2002), endothelial cells (Bulotta et al., 2001; Ceneviva et al., 1998; Dimmeler et al., 1997b; Dimmeler et al., 1997a; Tzeng et al., 1997) and keratinocytes (Weller et al., 2003), whereas it is pro-apoptotic in the case of macrophages (Albina et al., 1993; Messmer and Brune, 1996; Messmer et al., 1995; Sarih et al., 1993).

The variability and complexity of the effects of NO on ultimate cellular fate may arise from this molecule's ability to react with oxygen, reactive oxygen species, metal ions, small thiol-containing molecules, and proteins. The resulting reactive NO species can either trigger or suppress apoptosis through various mechanisms. Chief among them is the S-nitrosative suppression of caspase activation, subsequent to the generation of FeL_nNO or other species capable of carrying out S-nitrosation reactions (see below) (Li et al., 1997; Vodovotz et al., 2004).

Differences in the levels of NO and its reaction products may also arise from diverse inflammatory settings in which the expression of nitric oxide synthases (NOS) is affected. For example, quiescent endothelial cells express constitutive NOS (eNOS) that directly produce NO molecules and mediate the so-called "direct" effects (Wink et al., 1999). Some inflammatory stimuli, on the other hand, lead to inducible NOS (iNOS) expression that subsequently generates reactive NO species, which in turn mediate "indirect" effects of NO. The simultaneous presence

of oxygen radicals can generate other reactive NO species that mediate further indirect effects of NO (Wink et al., 1999). As another example, hepatocytes and macrophages have different amounts of non-heme iron complexes, which affect the levels of iron-nitrosyl species when NO is produced (Kim et al., 2000). Finally, different intracellular levels of glutathione (GSH) can also modulate the time evolution of NO-related compounds (Hu et al., 2006).

Computational approaches have been used previously to help unravel the complex biology of NO. Biotransport of NO was first modeled by Lancaster (Lancaster, 1994; Lancaster, 1997) followed by other groups (reviewed by Buerk (2001)), recently by Zhang and Edwards (2006). Recently, Hu and coworkers focused on a detailed reaction mechanism of NO (Hu et al., 2006). These models have improved our understanding of the biotransport of NO and the types of chemical reactions that involve NO and related reactive species. Additionally, a number of mathematical models have been proposed for understanding the mechanisms of apoptosis (Aldridge et al., 2006; Bagci et al., 2006; Bentele et al., 2004; Eissing et al., 2004; Fussenegger et al., 2000; Legewie et al., 2006; Rehm et al., 2006; Siehs et al., 2002; Stucki and Simon, 2005). The work of Eissing et al. (2004) is of interest, in particular, which demonstrated the importance of IAP inhibition for imparting bistability in type I cells (Eissing et al., 2004). The studies by Rehm et al. (2006) and Legewie et al. (2006) also showed the same effect in type II cells. These studies have improved our understanding of the robustness of switch mechanisms for regulating apoptosis, but none of these models has addressed the dichotomous effects of NO (Aldridge et al., 2006; Bagci et al., 2006; Bentele et al., 2004; Eissing et al., 2004; Fussenegger et al., 2000; Legewie et al., 2006; Rehm et al., 2006; Siehs et al., 2002; Stucki and Simon, 2005).

Herein, we propose a mathematical model that can potentially shed light on the pro- and anti-apoptotic effects of NO in specific contexts. The model we propose here couples the

apoptotic cascade ((Bagci et al., 2006) and chapter 3 of this thesis) to an extended model of NO reaction pathways initially proposed by Hu et al. (2006). First, we illustrate how identical cells can undergo apoptosis at different time points after being exposed to apoptotic stimuli, in accord with experimental data collected on single cells (Rehm et al., 2002; Tyas et al., 2000). Then, we examine the apoptotic behavior in response to changes in N_2O_3 , FeL_nNO , $ONOO^-$ and GSH levels, in the presence of NO production by iNOS.

4.2 MODELS

Three models are considered in this chapter. **Model 3**, presented in chapter 3, focuses on the pathways involved in mitochondria-dependent apoptosis (Figure 1). **Model 4-A** is an extension of the kinetic model of NO-associated reactions recently proposed by Hu et al. (2006) (Figure 2). Finally, **Model 4-B** is the integration of Models 3 and 4-A, constructed to examine the pro-apoptotic and anti-apoptotic effects of NO.

4.2.1 Generation of NO-related oxidative and nitrosative species $ONOO^-$, N_2O_3 , and FeL_nNO (Model 4-A).

We extended the network originally proposed by Hu et al. (2006) to introduce additional reactions involving NO, as well as additional compounds such as the NO-related species FeL_nNO (L denotes ligands that do not contain heme), NO_2 , and cytochrome *c* oxidase (CcOx). Figure 2 illustrates the extended network of interactions. Table 3 lists the corresponding reactions (indexed as (4-I) – (4-XX)) and rate constants. The reactions (4-XII) and (4-XVIII)

break down the production of N_2O_3 from NO and O_2 into two steps that replace the corresponding reaction (with rate constant k_{12}) used in the model of Hu et al. (2006). Reactions (4-XVI) – (4-XX) are introduced in the present study. The identity of the products is not written when these compounds do not serve as reactants in any of the reactions listed in Table 3.

Table 4 lists the rate laws for these reactions (Eq.s 4-1 – 4-20), which are used in the differential rate equations (Eq.s 4-21 – 4-29) that control the time evolution of the concentration of the individual compounds. Model 4-A contains 16 components. Eleven of them reach steady-state concentrations within a short time interval (~ 20 minutes) after initiation of the simulations for $[\text{GSH}]_0 \leq 10^3 \mu\text{M}$ and within four and half hours for $[\text{GSH}]_0 = 10^4 \mu\text{M}$, whereas five compounds (superoxide dismutase (SOD), glutathione peroxidase (GPX), CO_2 , O_2 , and *cyt c*) retain their equilibrium concentrations. Table 5 lists the initial and equilibrium concentrations different from zero, adopted in Model 4-A, and the corresponding references.

Table 3. Reactions included in Model 4-A

Description of the reaction/interaction	Rate constant (*)	Reference	Reaction index
Production of NO	$k_{1NO} = 1 \mu\text{M/s}$	(Hu et al., 2006) (Beckman and Koppenol, 1996)	(4-I)
Production of O_2^-	$k_{2NO} = 0.1 \mu\text{M/s}$	(Hu et al., 2006) (Antunes et al., 1996)	(4-II)
Production of GSH	$k_{3NO} = 0$	(Hu et al., 2006)	(4-III)
$\text{NO} + \text{O}_2^- \rightarrow \text{ONOO}^-$	$k_{4NO} = 6700 \mu\text{M}^{-1}\text{s}^{-1}$	(Huie and Padmaja, 1993)	(4-IV)
$\text{SOD} + \text{O}_2^- + \text{H}^+ \rightarrow \text{SOD} + \frac{1}{2} \text{O}_2 + \frac{1}{2} \text{H}_2\text{O}_2$	$k_{5NO} = 2400 \mu\text{M}^{-1}\text{s}^{-1}$	(Fielden et al., 1974)	(4-V)
$\text{ONOO}^- + \text{GSH} \rightarrow \text{GSNO} + \text{products}$	$k_{6NO} = 0.00135 \mu\text{M}^{-1}\text{s}^{-1}$	(Koppenol et al., 1992)	(4-VI)
$\text{ONOO}^- + \text{GPX} \rightarrow \text{GPX} + \text{products}$	$k_{7NO} = 2 \mu\text{M}^{-1}\text{s}^{-1}$	(Sies et al., 1997)	(4-VII)
$\text{ONOO}^- + \text{CO}_2 \rightarrow \text{products}$	$k_{8NO} = 0.058 \mu\text{M}^{-1}\text{s}^{-1}$	(Denicola et al., 1996; Squadrito and PRYOR, 1998)	(4-VIII)
$\text{ONOO}^- + \text{cyt } c \rightarrow \text{cyt } c + \text{products}$	$k_{9NO} = 0.025 \mu\text{M}^{-1}\text{s}^{-1}$	(Thomson et al., 1995)	(4-IX)
$2\text{GSNO} + \text{O}_2^- + \text{H}_2\text{O} \rightarrow \text{GSSG} + \text{products}$	$k_{10NO} = 0.0006 \mu\text{M}^{-2}\text{s}^{-1}$	(Jour'dHeuil et al., 1998)	(4-X)
$\text{N}_2\text{O}_3 + \text{GSH} \rightarrow \text{GSNO} + \text{NO}_2^- + \text{H}^+$	$k_{11NO} = 66 \mu\text{M}^{-1}\text{s}^{-1}$	(Keshive et al., 1996)	(4-XI)
$2\text{NO} + \text{O}_2 \rightarrow 2\text{NO}_2$	$k_{12aNO} = 0.000006 \mu\text{M}^{-2}\text{s}^{-1}$	(Czapski and Goldstein, 1995)	(4-XII)

$\text{NO}_2 + \text{NO} \leftrightarrow \text{N}_2\text{O}_3$	$k_{12\text{bNO}^+} = 1100 \mu\text{M}^{-1}\text{s}^{-1}$ $k_{12\text{bNO}^-} = 81000 \text{s}^{-1}$	(Czapski and Goldstein, 1995)	(4-XIII)
$\text{N}_2\text{O}_3 + \text{H}_2\text{O} \rightarrow \text{products}$	$k_{13\text{NO}} = 1600 \text{s}^{-1}$	(Licht et al., 1988; Czapski and Goldstein, 1995)	(4-XIV)
$\text{GSSG} + \text{NADPH} + \text{H}^+ \rightarrow 2\text{GSH} + \text{NADP}^+$	$V_m = 320 \mu\text{M}\text{s}^{-1}$ $K_m = 50 \mu\text{M}$	(Antunes et al., 1996)	(4-XV)
Cu^+ $\text{GSNO} \rightarrow \frac{1}{2} \text{GSSG} + \text{NO}$	$k_{14\text{NO}} = 0.0002 \text{s}^{-1}$	(Gorren et al., 1996; Hofseth et al., 2003)	(4-XVI)
$\text{CcOx} + \text{NO} \rightarrow \text{CcOX.NO}$	$k_{15\text{NO}} = 100 \mu\text{M}^{-1}\text{s}^{-1}$	(Sarti et al., 2003)	(4-XVII)
$\text{FeL}_n + \text{NO} \rightarrow \text{FeL}_n\text{NO}$	$k_{16\text{NO}} = 1.21 \mu\text{M}^{-1}\text{s}^{-1}$	(Pou et al., 1999)	(4-XVIII)
$\text{FeL}_n\text{NO} + \text{GSH} \rightarrow \text{GSNO} + \text{FeL}_n$	$k_{17\text{NO}} = 66 \mu\text{M}^{-1}\text{s}^{-1}$ ^a	(Afshar et al., 2004)	(4-XIX)
$\text{GSH} + \text{O}_2^- \rightarrow \frac{1}{2} \text{GSSG} + \text{products}$	$k_{17\text{bNO}} = 0.0002 \mu\text{M}^{-1}\text{s}^{-1}$	(Jones et al., 2002)	(4-XX)

^a Same as $k_{11\text{NO}}$

Table 4. Rate equations for Model 4-A

Rate laws (Eq.s 4-1 – 4-20) and differential rate equations (Eq.s 4-21 – 4-29)	Equation numbers
$r_{1NO} = k_{1NO}$	(4-1)
$r_{2NO} = k_{2NO}$	(4-2)
$r_{3NO} = k_{3NO}$	(4-3)
$r_{4NO} = k_{4NO}[NO][O_2^-]$	(4-4)
$r_{5NO} = k_{5NO}[SOD][O_2^-]$	(4-5)
$r_{6NO} = k_{6NO}[ONOO^-][GSH]$	(4-6)
$r_{7NO} = k_{7NO}[ONOO^-][GPX]$	(4-7)
$r_{8NO} = k_{8NO}[ONOO^-][CO_2]$	(4-8)
$r_{9NO} = k_{9NO}[ONOO^-][cyt\ c]$	(4-9)
$r_{10NO} = k_{10NO}[GSNO]^2[O_2^-]$	(4-10)
$r_{11NO} = k_{11NO}[N_2O_3][GSH]$	(4-11)
$r_{12aNO} = k_{12aNO}[NO]^2[O_2]$	(4-12)
$r_{12bNO}^+ = k_{12bNO}^+[NO_2][NO]$	(4-13)
$r_{12bNO}^- = k_{12bNO}^-[N_2O_3]$	(4-14)
$r_{13NO} = k_{13NO}[N_2O_3]$	(4-15)
$r_m = V_m[GSSG]/(K_m+[GSSG])$	(4-16)
$r_{14NO} = k_{14NO}[GSNO]$	(4-17)
$r_{15NO} = k_{15NO}[CcOx][NO]$	(4-18)
$r_{16NO} = k_{16NO}[FeL_n][NO]$	(4-19)
$r_{17NO} = k_{17NO}[FeL_nNO][GSH]$	(4-20)

$d[\text{NO}]/dt = r_{1\text{NO}} - r_{4\text{NO}} - 2r_{12\text{aNO}} - r_{12\text{bNO}}^+ + r_{12\text{bNO}}^- + r_{14\text{NO}} - r_{15\text{NO}} - r_{16\text{NO}}$	(4-21)
$d[\text{O}_2^-]/dt = r_{2\text{NO}} - r_{4\text{NO}} - r_{5\text{NO}} - r_{10\text{NO}}$	(4-22)
$d[\text{ONOO}^-]/dt = r_{4\text{NO}} - r_{6\text{NO}} - r_{7\text{NO}} - r_{8\text{NO}} - r_{9\text{NO}}$	(4-23)
$d[\text{GSH}]/dt = r_{3\text{NO}} - r_{6\text{NO}} - r_{11\text{NO}} + 2r_m - r_{17\text{NO}}$	(4-24)
$d[\text{GSNO}]/dt = r_{6\text{NO}} - 2r_{10\text{NO}} + r_{11\text{NO}} - r_{14\text{NO}} + r_{17\text{NO}}$	(4-25)
$d[\text{N}_2\text{O}_3]/dt = -r_{11\text{NO}} + r_{12\text{bNO}}^+ - r_{12\text{bNO}}^- - r_{13\text{NO}}$	(4-26)
$d[\text{NO}_2]/dt = 2r_{12\text{aNO}} - r_{12\text{bNO}}^+ + r_{12\text{bNO}}^-$	(4-27)
$d[\text{CcOx}]/dt = -r_{15\text{NO}}$	(4-28)
$d[\text{FeL}_n]/dt = -r_{16\text{NO}} + r_{17\text{NO}}$	(4-29)

(*) Note that $[\text{FeL}_n\text{NO}] = [\text{FeL}_n]_0 - [\text{FeL}_n]$, and $[\text{GSSG}] = ([\text{GSH}]_0 - [\text{GSH}] - [\text{GSNO}]) / 2$

Table 5. Equilibrium levels and initial concentrations used in Model 4-A

Equilibrium concentrations	References
$[\text{SOD}]_{\infty} = 10 \mu\text{M}$	<i>(Squadrito and Pryor, 1998)</i>
$[\text{GPX}]_{\infty} = 5.8 \mu\text{M}$	<i>(Antunes et al., 1996)</i>
$[\text{CO}_2]_{\infty} = 10^3 \mu\text{M}$	<i>(Radi et al., 2000)</i>
$[\text{O}_2]_{\infty} = 35 \mu\text{M}$	<i>(Beckman and Koppenol, 1996)</i>
$[\text{cyt c}]_{\infty} = 400 \mu\text{M}$	<i>(Antunes et al., 1996)</i>
Initial concentrations	References
$[\text{CcOx}]_0 = 0.1 \mu\text{M}$	<i>(De Visscher et al., 2005)</i>
$[\text{FeL}_n]_0 = 0.05 \mu\text{M}$	<i>(Pourzand et al., 1999)</i>
$[\text{GSH}]_0 = 10^4 \mu\text{M}$ (or otherwise specified)	<i>(Hu et al., 2006)</i>

4.2.2 Effects of NO-related reactions on apoptotic pathways (Model 4-B).

Model 4-B combines Models 3 and 4-A upon inclusion of the additional reactions presented in Table 6. See the orange compounds in Figure 2, which are the species that couple the NO pathways to apoptotic pathways. We note that ONOO^- has a pro-apoptotic effect, while N_2O_3 and FeL_nNO (reactions labeled (4-XXIII) – (4-XXV)) deactivate the caspases, thus inducing anti-apoptotic effects. The associated rate constants and references are given in Table 6. Table 7 provides the rate expressions (Eq.s 4-30 – 4-34) and differential rate equations (Eq.s 4-35 – 4-43) for these reactions and involved compounds, respectively.

The steady-state concentrations $[H^+]_{\infty}$ in reaction (4-V), $[H_2O]_{\infty}$ in reactions (4-X) and (4-XIV), $[NADPH]_{\infty}$ and $[H^+]_{\infty}$ in reaction (4-XV), $[Cu^+]_{\infty}$ in reaction (4-XVI) are incorporated into the corresponding rate constants.

Table 6. Reactions bridging between Models 3 to 4-A (*)

Equilibrium concentrations	Rate Constant	Reference	Reaction index
$ONOO^- + PTPC \rightarrow PTPC_{act} +$ products	k_{18NO}	accounts for $ONOO^-$ induced formation of non-specific pore associated with mitochondrial permeability transition (Vieira et al., 2001)	(4-XXI)
$N_2O_3 + casp8 \rightarrow casp8.NO + FeL_n$	k_{19NO}	(Wink et al., 1994)	(4-XXII)
$FeL_nNO + casp8 \rightarrow casp8.NO + FeL_n$	k_{20NO}	(Kim et al., 2001)	(4-XXIII)
$FeL_nNO + casp9 \rightarrow casp9.NO + FeL_n$	k_{21NO}	(Kim et al., 2001)	(4-XXIV)
$FeL_nNO + casp3 \rightarrow casp3.NO + FeL_n$	k_{22NO}	(Kim et al., 2001)	(4-XXV)

(*) The parameters used in the present study are $k_{18NO} = 1 \mu M^{-1}s^{-1}$ (varying the value between $0.01 \mu M^{-1}s^{-1}$ and $100 \mu M^{-1}s^{-1}$ does not affect the results), $k_{19NO} = 10 \mu M^{-1}s^{-1}$ (Wink et al., 1994), $k_{20NO} = k_{21NO} = k_{22NO} = 66 \mu M^{-1}s^{-1}$ (the same value as k_{11NO}). PTPC is mitochondrial permeability transition pore complex.

Table 7. Modified differential equations from either Model 3 or 4-A

Rate laws (Eq.s 4-30 – 34) and differential rate equations (Eq.s 4-35 – 43)	Equation numbers
$r_{18NO} = k_{18NO}[ONOO^-][PTPC]$	(4-30)
$r_{19NO} = k_{19NO}[N_2O_3][casp8]$	(4-31)
$r_{20NO} = k_{20NO}[FeL_nNO][casp8]$	(4-32)
$r_{21NO} = k_{21NO}[FeL_nNO][casp9]$	(4-33)
$r_{22NO} = k_{22NO}[FeL_nNO][casp3]$	(4-34)
$d[ONOO^-]/dt = r_{4NO} - r_{6NO} - r_{7NO} - r_{8NO} - r_{9NO} - r_{18NO}$	(4-35)
$d[PTPC]/dt = -r_{19NO}$	(4-36)
$d[N_2O_3]/dt = -r_{11NO} + r_{12bNO}^+ - r_{12bNO}^- - r_{13NO} - r_{19NO}$	(4-37)
$d[casp8]/dt = -J_0 + J_0^f + J_{casp8} - r_{19NO} - r_{20NO} (*)$	(4-38)
$d[FeL_nNO]/dt = r_{16NO} - r_{17NO} - r_{20NO} - r_{21NO} - r_{22NO}$	(4-39)
$d[FeL_n]/dt = -r_{16NO} + r_{17NO} + r_{20NO} + r_{21NO} + r_{22NO}$	(4-40)
$d[casp9]/dt = J_4 - J_{4b} - J_5 - J_6 + J_6^f + J_{casp9} - r_{21NO} (*)$	(4-41)
$d[casp3]/dt = J_6^f + J_{6b}^f - J_7 - J_8 + J_8^f - J_9 + J_9^f + J_{casp3} - r_{22NO} (*)$	(4-42)
$d[cyt c]/dt = J_{14} - J_1 + J_{cytc} + k[PTPC_{act}][cyt c_{mit}]$ where $k = 1 \mu M^{-1} s^{-1} (*)$	(4-43)

(*) J refers to fluxes of components, for details see ref (Bageci et al., 2006) and Chapter 3 of this thesis. $PTPC_{act}$

refers to the nonspecific pore at the mitochondria that releases *cyt c*. Note that $[PTPC_{act}] = [PTPC]_0 - [PTPC]$.

4.3 RESULTS AND DISCUSSION

First, we illustrate how different strengths of EC pro-apoptotic signals may result in opposite qualitative responses or different quantitative (time-dependent) responses in the same type of cells (Tyas et al., 2000), using our recently introduced bistable model (Bagci et al., 2006). Then, we examine the differences in the bistable response of diverse NO producing cells, e.g. cells with different concentrations of GSH and FeL_n - and in different settings, i.e., with or without production of superoxide.

4.3.1 Delay in apoptosis induction (Model 3).

Tyas et al. (2000) showed that cells of the same type simultaneously subjected to EC stimuli initiate their apoptotic response at different times. Figure 16 panels A-C illustrate the theoretical time evolutions of casp3 levels in three identical cells subjected to different strengths of EC apoptotic stimuli (represented here by the $[\text{casp8}]_0$) in the absence of NO. For these simulations, we used Model 3 with three different values of $[\text{casp8}]_0$; 10^{-5} μM , 10^{-4} μM , and 1.5×10^{-4} μM in the respective panels A-C, while $[\text{casp3}]_0$ was 10^{-5} μM in all three cases. Panel A shows that low $[\text{casp8}]_0$ leads to the depletion of $[\text{casp3}]$, while $[\text{casp8}]_0$ above a certain threshold (8.35×10^{-5} μM) (panels B and C) lead to increase in $[\text{casp3}]$ and thereby onset of cell death. Furthermore, comparison of panels B and C shows that a relatively lower $[\text{casp8}]_0$ (or weaker EC apoptotic signal) results in a time-delayed initiation of apoptosis, in agreement with the single cell experiments done by Tyas et al. (2000). The sharp increase in $[\text{casp3}]$ to its equilibrium level indeed starts about 30 minutes later in panel B, compared to panel C.

Next, we examined how this onset time varies with $[\text{casp8}]_0$. Figure 16D displays the results. An increase in onset time is predicted with decreasing $[\text{casp8}]_0$ up to $[\text{casp8}]_0 = 8.35 \times 10^{-5} \mu\text{M}$, after which no apoptotic effect is observed. This value ($8.35 \times 10^{-5} \mu\text{M}$) also represents the threshold value for $[\text{casp8}]_0$ to initiate apoptosis. The time delay is found to obey a logarithmic decay with increasing $\Delta[\text{casp8}]_0 \equiv [\text{casp8}]_0 - 8.35 \times 10^{-5} \mu\text{M}$, as indicated by the best fitting curve.

This analysis shows that cells of the same type may undergo apoptosis at different times due to their different EC microenvironments. Hence, the difference in the onset times among cells of the same type in a given cell culture may be explained without recourse to alterations in the underlying network of biochemical reactions (2006).

4.3.2 Nitric oxide associated network (Model 4-A).

The results from our calculations using Model 4-A are shown in Figure 17. Here, we focused on the time evolution of four compounds, GSH, N_2O_3 , FeL_nNO and ONOO^- , displayed in respective panels A-D. The NO species N_2O_3 , FeL_nNO and ONOO^- have been proposed to carry out various indirect effects of NO on cellular pathways, including apoptosis, during inflammation (Wink et al., 1999).

GSH is an anti-oxidant reduced to GSSG by reacting with nitrosative N_2O_3 and FeL_nNO , and with oxidative ONOO^- (Table 3). GSH is depleted to low levels in a switch-like manner due to those reactions (panel A). The depletion of GSH is accompanied by increases in N_2O_3 and FeL_nNO concentrations (panels B-C). On the other hand, this switch-like behavior is not that pronounced in $[\text{ONOO}^-]$ time dependence (panel D). Simulations performed with different initial GSH concentrations (three different curves in each panel) change the steady-state concentrations of all three NO-related compounds that interfere with apoptotic pathways (panels B-D). The

switch-like increase in $[N_2O_3]$ and non-switch-like increase in $[ONOO^-]$ is in agreement with the results of Hu et al. (2006).

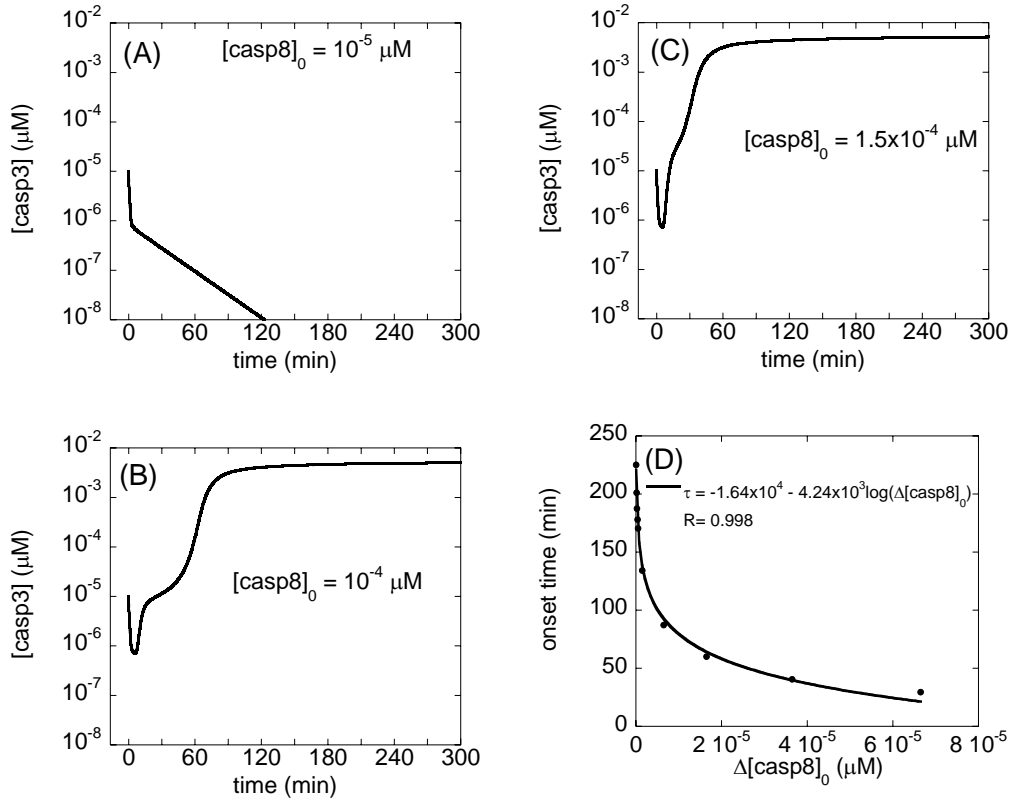


Figure 16. Time evolution of $[casp3]$ predicted by the bistable Model 3 in response to different strengths of apoptotic stimuli, A) in a cell subjected to a weak EC apoptotic signal (reflected by the low concentration $[casp8]_0$); B) in a cell that is subjected to a stronger EC pro-apoptotic signal. Caspase-3 is activated at 60 minutes; C) in a cell that is subjected to a stronger EC pro-apoptotic signal than one in panel B. Caspase-3 is activated at 30 minutes. Panels A and B illustrate two opposite effects induced by different initial concentrations of caspase-8. The threshold concentration $[casp8]_0$ required for the switch from anti-apoptotic to pro-apoptotic response is calculated to be $8.35 \times 10^{-5} \mu M$. Panels B and C illustrate the shift in the onset time of apoptosis depending on $[casp8]_0$. D) Dependence of apoptotic response time on the initial caspase-8 concentration. The ordinate is the onset time of caspase-3 activation, and the abscissa is the initial concentration of caspase-8 in excess of the threshold concentration required for the initiation of apoptosis (evidenced by increase in $[casp3]$, see panels B-C). The onset time of caspase-3 activation exhibits a logarithmic decrease with $\Delta[casp8]_0$ ($[casp8]_0 - 8.35 \times 10^{-5} \mu M$).

4.3.3 Anti-apoptotic and pro-apoptotic effects of NO (Model 4-B).

We analyze here the dynamics of the mitochondria-dependent apoptosis model coupled to anti- and pro-apoptotic pathways associated with NO; see Table 6 for the list of new reactions/interactions/steps that come into play in this model (4-B). As mentioned above, NO-related pathways are coupled to apoptotic pathways through N_2O_3 , FeL_nNO , and $ONOO^-$ that are produced by the reaction of NO with O_2 , FeL_n and O_2^- , respectively. For simplicity, those effects of NO mediated by cGMP (Kim et al., 2001b; Kim et al., 1997) are not included in our mathematical model.

4.3.3.1. Modulating roles of N_2O_3 and GSH in apoptosis

We initially excluded non-heme iron compounds in order to assess the effect of N_2O_3 exclusively. The production rate of superoxide was likewise assumed to be zero. N_2O_3 is produced by reactions (4-XXII) and (4-XIII) in Table 3. NO production and EC stimulation were initiated simultaneously. Figures 18A-C are the counterparts of Figures 16A-C, respectively (same initial conditions, except for the interference of NO pathways through N_2O_3), where the time-dependence of [casp3] (solid curve) and [GSH] are shown. The bistable response to apoptotic stimuli, dependent on [casp8]₀, is shown to be maintained despite the interference of NO pathways through N_2O_3 . The three columns refer to different initial concentrations of GSH, decreasing from [GSH]₀ = 10³ (Panels A-C), to [GSH]₀ = 10² (panels D-F) and [GSH]₀ = 0 (panels G-I). The threshold [casp8]₀ value for casp3 activation was 8.35x10⁻⁵ μM in Figure 16, where NO was not produced at all. This value remains the same for both [GSH]₀ = 10⁴ μM (not shown) and 10³ μM (panels A-C) in the presence of NO, but increases to 9.9 x10⁻⁵ μM when

$[GSH]_0$ is $10^2 \mu M$ (panels D-F) and to $1.26 \times 10^{-4} \mu M$ when $[GSH]_0$ is zero (panels G-I), hence the different (pro-apoptotic) behavior observed in panel H.

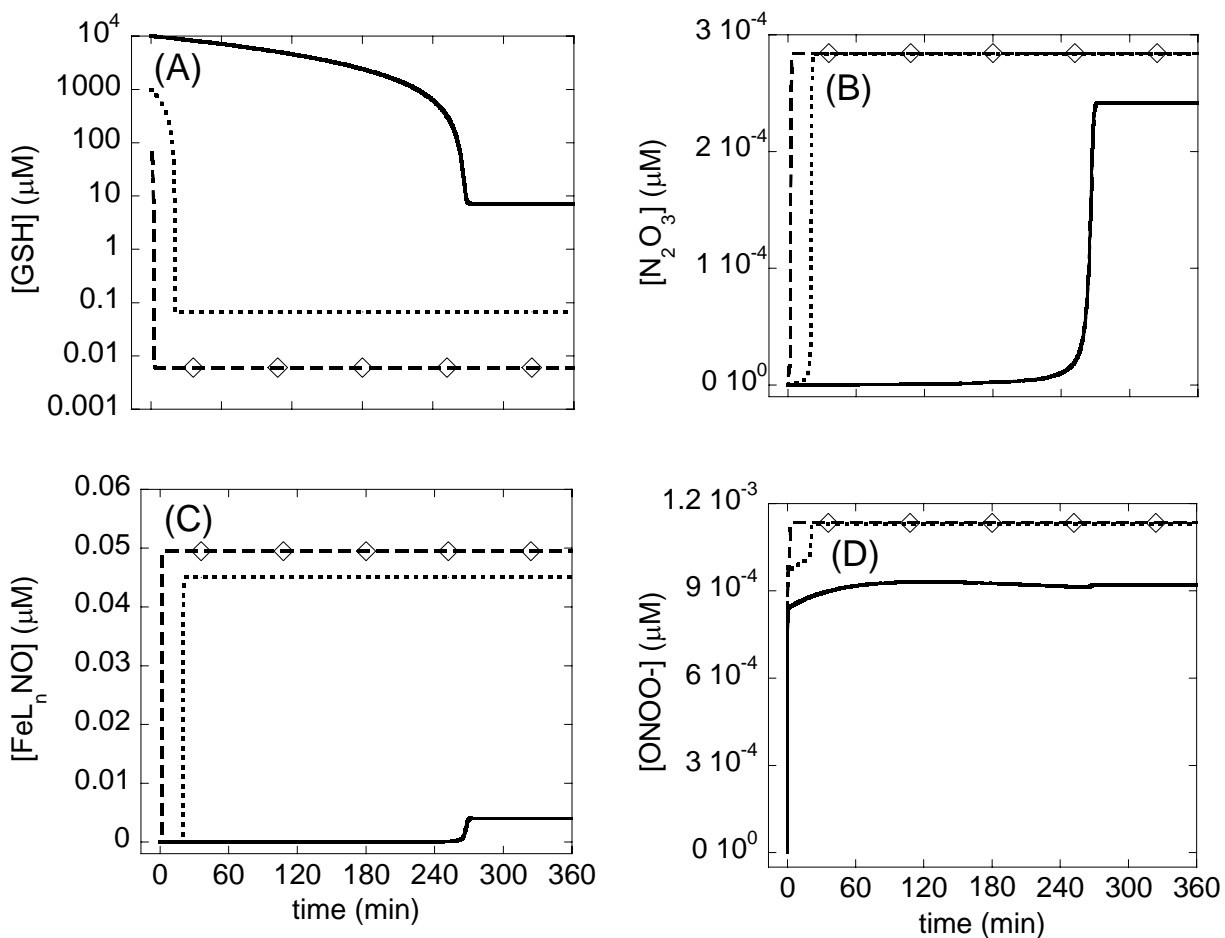


Figure 17. Time evolution of A) GSH, B) N_2O_3 , C) $FeLnNO$, and D) $ONOO^-$ concentrations predicted by Model 4- A. N_2O_3 and $FeLnNO$ increase to high concentrations by a switch-like mechanism induced by a decrease in $[GSH]$ due to conversion of GSH to GSNO and subsequently to GSSG. $[ONOO^-]$ does not follow a similar switch-like increase in its concentration. Solid curve is for $[GSH]_0 = 10^4 \mu M$, dotted curve for $[GSH]_0 = 10^3 \mu M$, and dashed curve with diamonds for $[GSH]_0 = 10^2 \mu M$. The response is thus sharper and earlier in the presence of lower initial concentrations of GSH.

These results suggest that N_2O_3 does not affect the bistable character of the response to EC stimuli, except for modifying the threshold for onset of apoptosis, which is shifted to higher $[casp8]_0$ (i.e. rendered more difficult) with decreasing $[GSH]_0$. However, high initial concentrations of GSH restore the threshold back to $8.35 \times 10^{-5} \mu M$. Therefore, N_2O_3 can serve as an effective modulator of apoptosis provided that the level of GSH in the system is sufficiently low.

4.3.3.2. How does N_2O_3 affect the threshold degradation rates of Bax for transition from bistable to monostable behavior?

In our computational study of apoptotic pathways, we observe a bistable behavior (selecting between cell death and survival) for degradation rates of Bax (μ_{Bax}) lower than a threshold value ($0.11 s^{-1}$), while monostable cell survival was predicted when $\mu_{Bax} > 0.11 s^{-1}$ (Figure 12A). This critical value of μ_{Bax} for the transition from bistability to monostability is called a limit point. We explored how the inclusion of NO reactions affects these findings. The limit point value of the Bax degradation rate for monostable cell survival is found to remain unchanged (at $0.11 s^{-1}$) for the range $10^3 \leq [GSH]_0 \leq 10^4 \mu M$. However, it decreases to $0.098 s^{-1}$ for $[GSH]_0 = 10^2 \mu M$ and $0.096 s^{-1}$ for $[GSH]_0 = 0 \mu M$ in the present model. The model again predicts that N_2O_3 is not influential when the GSH level is sufficiently high in the cell.

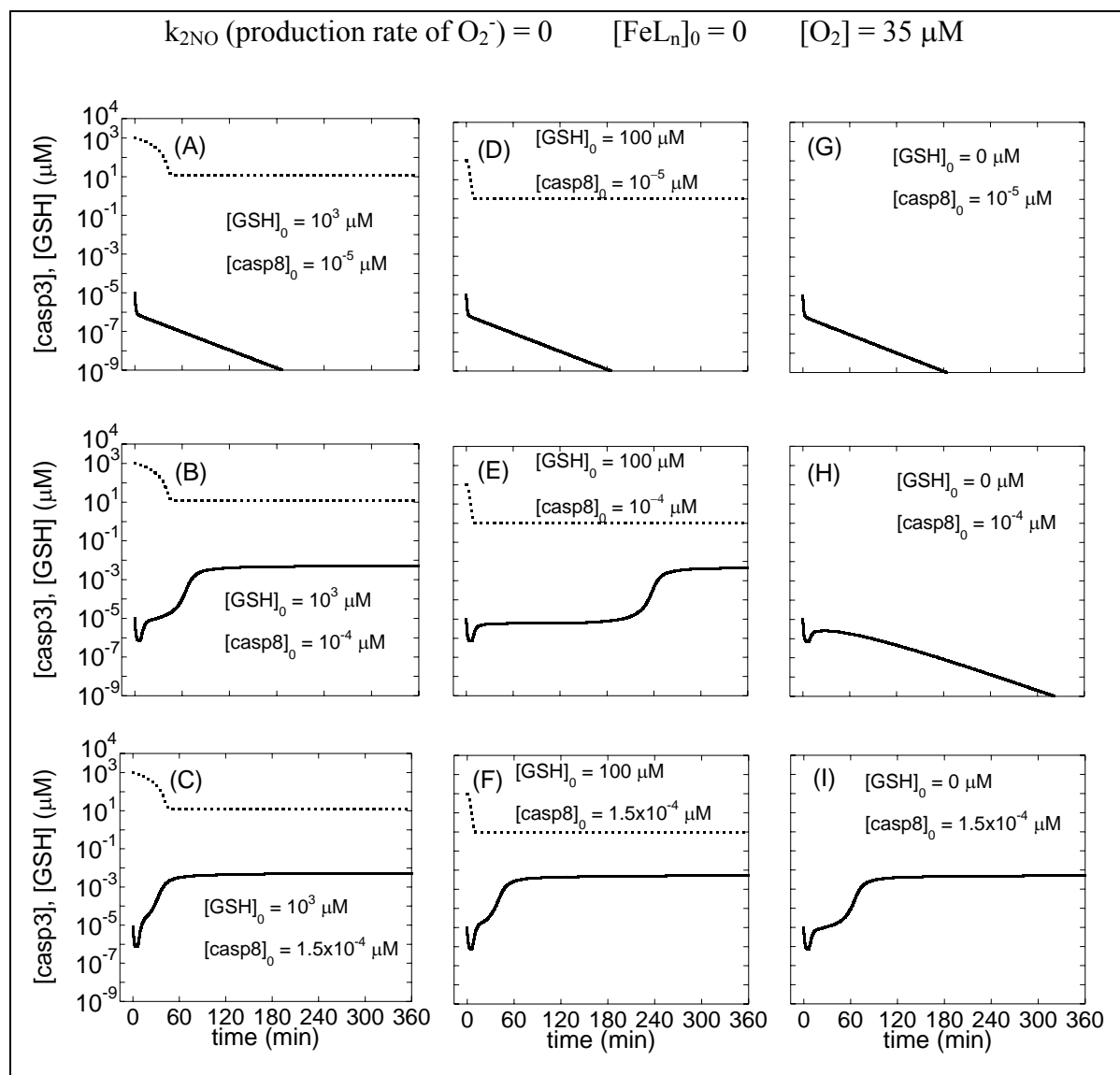


Figure 18. Time evolution of $[GSH]$ and $[casp3]$ predicted by Model 4-B in the presence of N_2O_3 effects. Here, in order to visualize the effect of N_2O_3 exclusively, the reaction (4-XXII) in Table 6 is included in the model while those involving FeL_nNO and $ONOO^-$ (reactions (4-XX,4-XXIII-XXV) are not, assuming FeL_n concentration and rate of formation of superoxide to be zero. The solid curves depict the time evolution of $[casp3]$, and dotted curves refer to $[GSH]$. The three rows of panels are the counterparts of those in Figure 16A-C, with the different columns referring to different initial concentrations of GSH: A-C) $[GSH]_0 = 10^3 \mu M$; D-F) $[GSH]_0 = 10^2 \mu M$; G-I) $[GSH]_0 = 0 \mu M$.

4.3.3.3. Roles of non-heme iron complexes and GSH in apoptotic response.

One of the important anti-apoptotic effects of NO is presumed to occur via its ability to react with non-heme iron complexes (FeL_n) to form FeL_nNO . These species inhibit caspases by S-nitrosating the catalytic cysteine in the active site of these enzymes (Li et al., 1997; Mannick et al., 1999; Rossig et al., 1999).

The results are presented in Figure 19, panels A-F, organized similarly to Figure 18 (i.e. using different $[\text{casp8}]_0$ in each row, and different $[\text{GSH}]_0$ in the two columns). Our calculations suggest that when the FeL_n concentration is higher than $0.03 \mu\text{M}$, there are no longer two stable steady-states at long times: casp3 levels always decrease to zero, even though their time evolutions depend on $[\text{casp8}]_0$ and $[\text{GSH}]_0$. Yet, depending on the level of GSH, both apoptosis and cell survival may be possible. Panels A-C correspond to relatively high $[\text{GSH}]_0$. In panel A, $[\text{casp3}]$ decreases to $10^{-8} \mu\text{M}$ that is less than 1 molecule per cell, hence zero, from $10^{-5} \mu\text{M}$ within the first two hours. However, in panels B and C, $[\text{casp3}]$ increases to nanomolar values and remains at those levels for more than three hours. Caspase-3 may cause enough damage to kill the cell before it is depleted at longer times. We note that lower $[\text{GSH}]_0$ (e.g. $[\text{GSH}]_0 = 10^3 \mu\text{M}$, panels D-F and $[\text{GSH}]_0 < 10^3 \mu\text{M}$, data not shown) do not permit the casp3 concentration to reach such pro-apoptotic levels and monostable cell survival is observed irrespective of $[\text{casp8}]_0$.

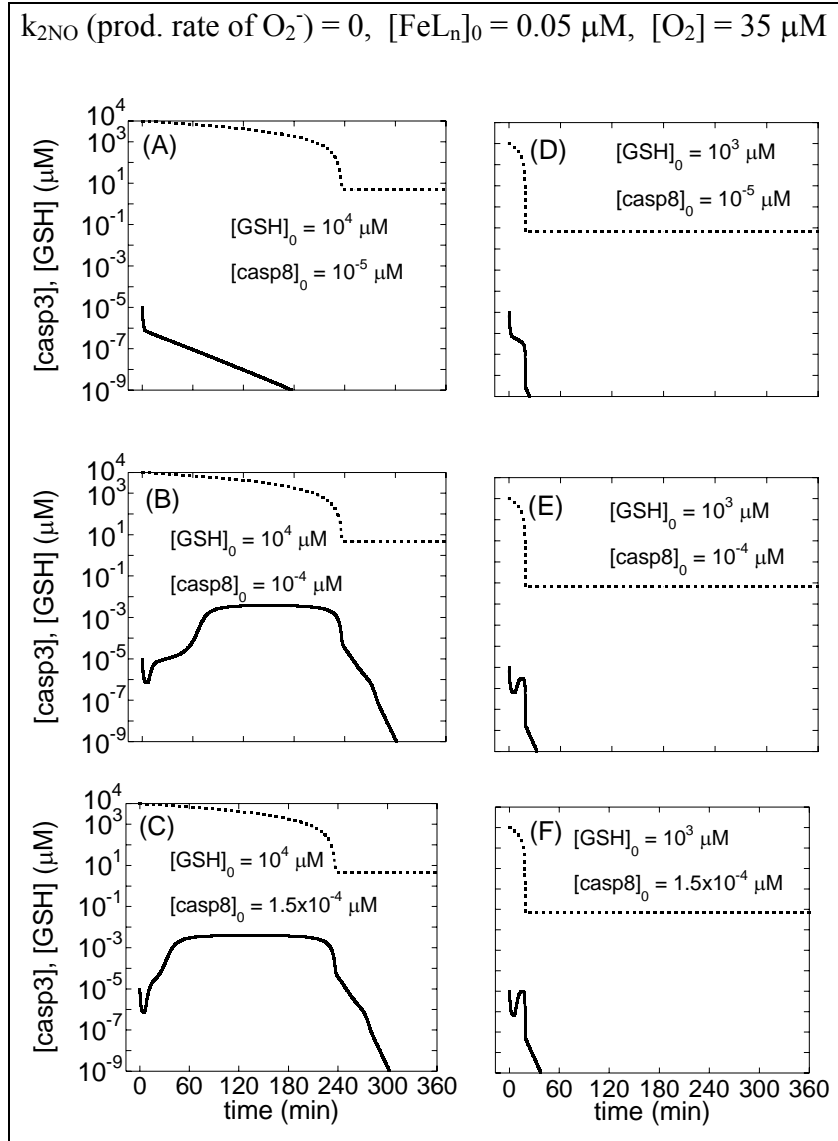


Figure 19. Time evolution of [GSH] and [casp3] predicted by Model 4-B in the presence of N_2O_3 and FeL_nNO . N_2O_3 is present in the model ($[O_2]$ is non-zero) as well as FeL_nNO ($[FeL_n]_0$ is non-zero). Each column is a counterpart of Figure 16A-C with different initial concentrations of GSH. A-C) $[GSH]_0 = 10^4 \mu M$; D-F) $[GSH]_0 = 10^3 \mu M$. Solid curve shows the time evolution of [casp3], and dotted curve that of [GSH].

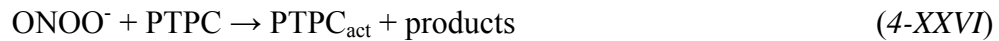
Various cell types subject to different intracellular microenvironments, or even the same cells under different settings (e.g. healthy state vs. inflammation or oxidative stress), may produce or experience different reactive NO intermediates (Stamler, 1994; Vodovotz et al., 2004; Wink et al., 1999). For example, more FeL_nNO may be produced in hepatocytes than in RAW264.7 macrophage-like cells due to the high level of non-heme iron complexes in hepatocytes (Kim et al., 2000). In a previous study, RAW264.7 cells underwent apoptosis in the presence of NO; conversely, no casp3 activation was observed in either hepatocytes or iron loaded RAW 264.7 cells (Kim et al., 2000). The results (Figure 18 and data not shown) suggests that in cells with iron concentrations lower than 0.03 μM (e.g. RAW264.7 cells), both cell survival and apoptosis are possible depending on the strength of apoptotic stimuli (in agreement with our experimental results) (Kim et al., 2000). However, a change in the intracellular environment of the same cell can change the response. Figure 19D-F shows that casp3 is not activated in the presence of non-heme iron ([FeL_n]₀ = 0.05 μM) when [GSH]₀ = 10³ μM and [GSH]₀ < 10³ μM (data not shown). We also checked if casp3 is activated when [casp8]₀ is as high as 0.1 μM when [GSH] = 10³ μM. In this case, caspase-3 concentration increased to 0.0007 μM for approximately 5 minutes, an apoptotic stimulus that is likely insufficient for apoptosis. This prediction is in good agreement with the observation that caspase-3 is not activated in non-heme iron-loaded RAW264.7 cells whose [GSH]₀ does not reach 10⁴ μM (Kim et al., 2000).

4.3.3.4. Roles of ONOO⁻ and GSH in apoptotic response

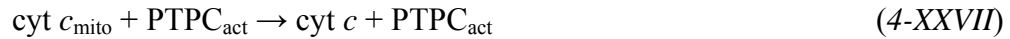
The mechanism by which NO or its reactive species exert pro-apoptotic effects is not well established (Benhar and Stamler, 2005). In the present study, we assume that the pro-apoptotic

effect of NO occurs via formation of ONOO⁻, as has been suggested from a large number of experimental studies both *in vitro* and *in vivo* (Ghafourifar et al., 2005; Radi et al., 2002). Experimental studies suggest that ONOO⁻ may induce the opening of mitochondrial permeability transition pores (MPTPs) and subsequent cyt *c* release from mitochondria (Kim et al., 2001).

The possible mechanisms of cyt *c* release from mitochondria are diverse and controversial (Nakagawa et al., 2005; Newmeyer and Ferguson-Miller, 2003). In our model, we assume that cyt *c* release is mediated by activation of MPTPs, independent of Bax channel formation on mitochondria. The complex that forms the MPTPs is called mitochondrial permeability transition pore complex (PTPC). The complex consists of peripheral benzodiazepine receptor, cyclophilin D, adenine nucleotide translocator (ANT), voltage-dependent anion channel (VDAC), and other proteins (Vieira et al., 2000). ANT is proposed to be converted from a specific transporter to a non-specific pore which then releases cyt *c* into the cytoplasm and subsequently induces apoptosis. It has been suggested that ONOO⁻ acts on PTPC, specifically on ANT, to convert it to a non-specific pore (PTPC_{act}) (Vieira et al., 2001). We represent this process as:



Cytochrome *c* is then released from the pore formed by PTPC_{act}



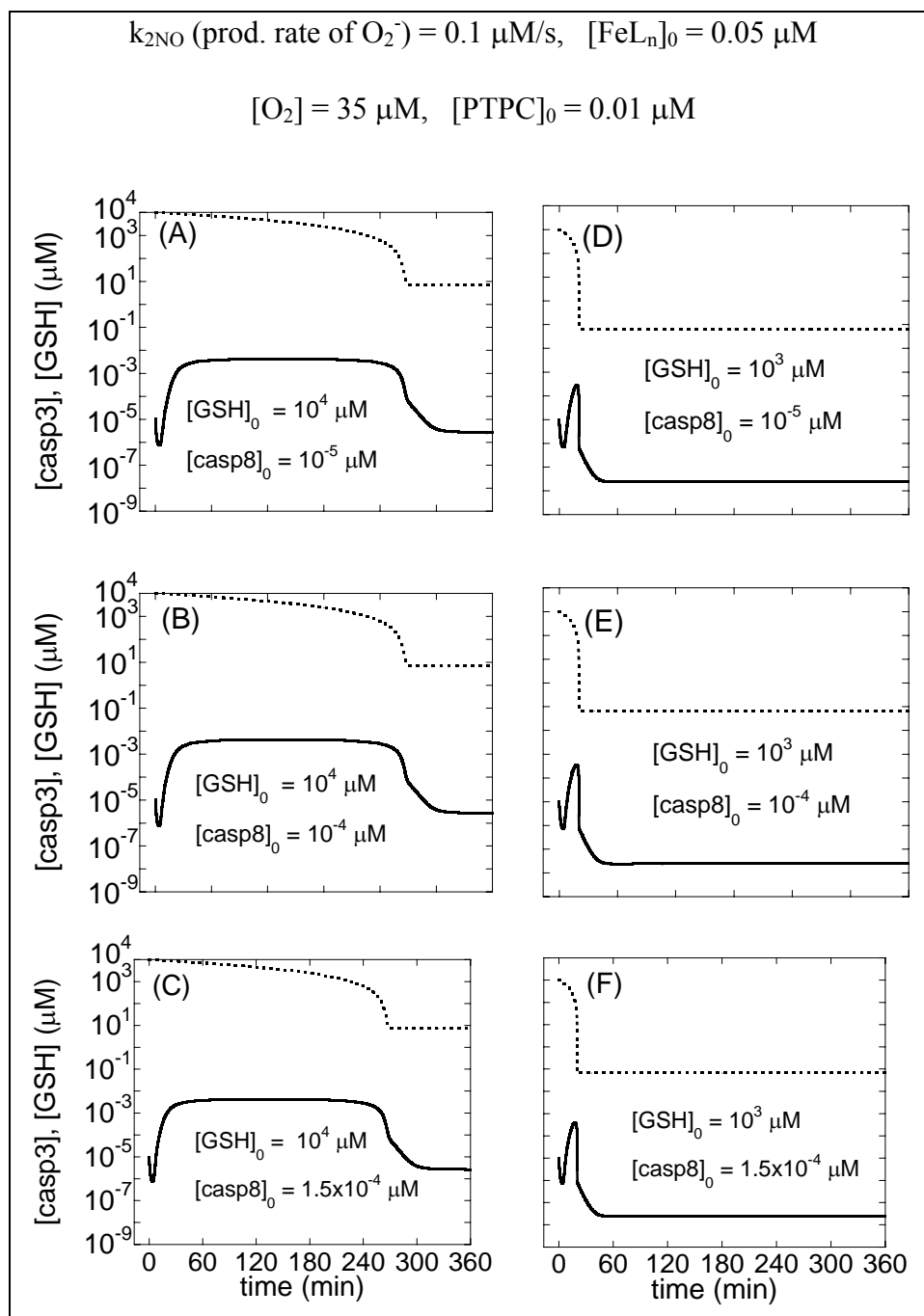


Figure 20. Time evolutions of [GSH] and [casp3] predicted by Model 4-B in the presence of N_2O_3 , FeL_nNO and ONOO^- . The initial concentration of PTPC is $0.01 \mu\text{M}$. Each column is a counterpart of Figure 16A-C and has a different initial concentration for GSH. A-C) $[\text{GSH}]_0 = 10^4 \mu\text{M}$; D-F) $[\text{GSH}]_0 = 10^3 \mu\text{M}$. Solid curve is for time evolution of [casp3], and dashed curve for time evolution of [GSH]. Caspase-3 concentrations at long times are $2.4 \times 10^{-4} \mu\text{M}$ and $2.5 \times 10^{-8} \mu\text{M}$ for panels A-C and D-F, respectively.

The results are shown in Figure 20. The initial concentration of PTPC is assumed to be high ($0.01 \mu\text{M}$). At that value, Model 3 predicts the response to apoptotic stimuli to be monostable apoptosis (Figure 13). We see a similar response in Figure 20A; a low initial value of casp8 ($10^{-5} \mu\text{M}$) results in an increase of [casp3] to nanomolar levels. Casp3 activation was observed with even lower values of [casp8]₀. However, casp3 does not reach nanomolar concentrations when [GSH]₀ = $10^3 \mu\text{M}$ (Figures 20D-F) and [GSH]₀ < $10^3 \mu\text{M}$ (data not shown). Initial concentrations [casp8]₀ higher than $1.5 \times 10^{-4} \mu\text{M}$ did not change this prediction.

These results suggest that in cells with large numbers of MPTPs (probably with high numbers of mitochondria), there are two possible outcomes in the presence of NO and O₂⁻ production: pathological cell death when GSH level is high ($10^4 \mu\text{M}$) and solely cell survival when GSH level is low ([GSH] ≤ $10^3 \mu\text{M}$) in the presence of O₂ and FeL_n. This result stands in contrast with studies in which GSH protects against oxidative stress (high concentrations of O₂⁻ and ONOO⁻) that can cause apoptosis. The reason for this paradoxical prediction is that GSH has both protective and pro-apoptotic effects: it has apoptotic effects due to its reaction with anti-apoptotic N₂O₃ and FeL_n, and protective effects due to its reaction with pro-apoptotic O₂⁻ and ONOO⁻. Simulations (Figure 20) suggest that the pro-apoptotic effect of GSH is stronger than its protective effect using the interactions and parameters adopted in current simulations.

To examine the possibility of an alternative response, we repeated the computations depicted in Figure 20 in the absence of O₂ (so that N₂O₃ is not produced) and FeL_n. We also used initial PTPC concentration of $0.0001 \mu\text{M}$, at which Model 3 predicts bistability (Figure 13). As seen in Figure 21, both cell survival and apoptosis are possible under these conditions, depending on [casp8]₀. Higher [GSH]₀ ($10^4 \mu\text{M}$) results in cell survival (Figure 21B) in contrast to lower [GSH]₀ resulting in apoptosis (Figure 21E) under the same amount of EC stimulus ([casp8]₀ =

$7 \times 10^{-5} \mu\text{M}$). The present analysis thus shows that the protection by GSH against oxidative stress is possible provided that O_2 and FeL_n levels are sufficiently low.

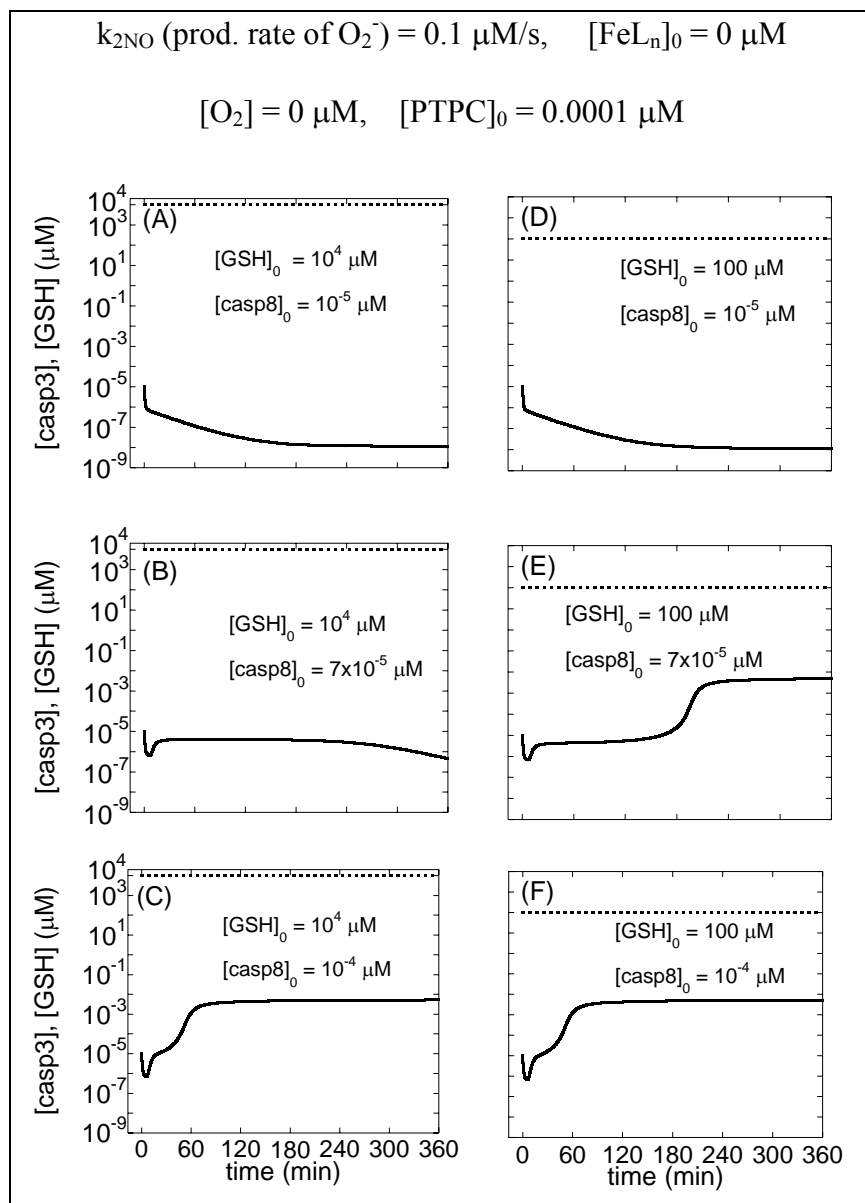


Figure 21. Time evolutions of [GSH] and [casp3] predicted by Model 4-B in the absence of N_2O_3 , FeL_nNO and presence of ONOO^- . The initial concentration of PTPC is $0.0001 \mu\text{M}$. A-C) $[\text{GSH}]_0 = 10^4 \mu\text{M}$; D-F) $[\text{GSH}]_0 = 10^2 \mu\text{M}$. Solid and dashed curves refer to the time evolutions of [casp3] and [GSH], respectively.

5.0 CONCLUSION

5.1 INSIGHTS ON APOPTOSIS FROM MATHEMATICAL MODELING AND SIMULATIONS AND RELEVANT EXPERIMENTAL DATA

In the present study, the cooperative formation of heptameric apoptosome complex is proposed to be an important mechanism for the bistable behavior (survival or apoptosis) of cells in response to apoptotic stimuli.

To gain a better understanding of the role of different components in regulating apoptosis, we examined the effects of Bax, Bcl-2, and MPTP levels on the time evolution of mitochondria-dependent apoptotic events, and show that there are subtle changes from monostable to bistable response, which may also be counteracted, depending on the relative concentrations of these components.

We concentrated on two positive feedback loops in particular, which are suggested to play an important role in ensuring bistability (Angeli et al., 2004). The former is initiated by the cleavage/inhibition of Bcl-2, and the latter by the truncation of Bid to tBid, both by the executioner caspase-3 (Cherry and Adler, 2000; Ferrell and Xiong, 2001; Ferrell, 2002; Xiong and Ferrell, 2003).

Several conclusions with possible biomedical implications are inferred from the present analysis:

- There are critical values for the minimal synthesis rate or maximal degradation rate of Bax, a pro-apoptotic protein, beyond which cells will switch from bistable behavior to a monostable cell survival. This result is in accord with observations suggesting that human prostate cancer cells might use Bax degradation as a survival mechanism (Li and Dou, 2000). Our results are also consistent with the observed decreases in Bax expression levels in primary human breast tumors (Schorr et al., 1999).
- Bcl-2 can counteract the pro-apoptotic effect of Bax to result in monostable cell survival, in line with the over-expression of Bcl-2 in many types of tumors (Reed, 1999) and the known role of Bcl-2 in countering the effects of Bax (Danial and Korsmeyer, 2004).
- The extent of MPTP may result in a diversity of responses, ranging from monostable cell survival, to bistable behavior, or monostable apoptosis. As shown in Fig.13, an increase in mitochondrial permeability transition pore complex concentration ([PTPC]) converts monostable cell survival response into a bistable response. The figure also shows that high [PTPC] can lead to pathological cell death, in accord with the role of MPTPs in pathological cell death suggested by Green and Kroemer (Green and Kroemer, 2004).
- The inhibition of Bax degradation can induce apoptosis. This result is in agreement with the observation of Li and Dou (2000).
- Our model predictions are in *quantitative* agreement with the experimental data reported by Katiyar et al. (2005) where p53 was induced by silymarin which activates casp3. The concentrations of cyt *c* and Bax are shown in both analyses to increase with the increases in p53 levels, while that of Bcl-2 would decrease.

Taken together, our results suggest that there might be a transition from bistable to monostable behavior depending on the apoptotic stimuli and/or concentrations of particular compounds. The changes in synthesis and degradation rates of Bax and Bcl-2 and in the number of MPTPs may have a role in leading to aberrant phenotypes such as cancer, and neurodegenerative disorders (Fadeel et al., 1999).

5.2 SUMMARY OF NO EFFECTS ON APOPTOSIS, AND RELEVANT EXPERIMENTAL DATA

We presented here the results from simulations that incorporate the main chemical interactions of NO with components of the apoptotic interactions network, with the goal of shedding light on the dichotomous effects of NO on apoptosis. Based on previously published studies, we considered N_2O_3 and FeL_nNO to be anti-apoptotic and $ONOO^-$ pro-apoptotic. The results predict that cell survival or apoptosis is determined by a complex interplay among these reactive NO species and GSH. We observed that relative concentrations of anti-apoptotic and pro-apoptotic species determine the anti- or pro-apoptotic effects at long times. Interestingly, transient apoptotic effects were observed under specific conditions (e.g. Figure 19 panels B-C). These intriguing findings point to the importance of the *timing* of NO production and apoptotic stimuli in determining the actual anti- or pro-apoptotic response, even if steady state conditions favor cell survival. Another interesting effect we observed in our simulations was the time shift/delay in the onset of apoptosis in the presence of weak EC stimulus (panel B-D in Figure 16), consistent with the experiments of Tyas et al. (2000).

Our simulations suggest that N_2O_3 and non-heme iron nitrosyl form in a switch-like manner after depletion of GSH. ONOO^- formation, on the other hand, hardly shows any switch-like behavior. We further found that N_2O_3 does not eliminate the bistability between cell survival and apoptosis, but rather increases the threshold $[\text{casp8}]_0$ for onset of apoptosis. However, high initial concentrations of GSH restore the threshold back to its original value. Therefore, we would predict, non-intuitively, that N_2O_3 does not influence cell survival when $[\text{GSH}]_0$ level is high.

On the other hand, our simulations suggest that there are no longer two stable steady states (cell survival and apoptosis) in the presence of non-heme iron at a level higher than a threshold value. Caspase-3 levels always decrease to zero even though their time evolution may depend on $[\text{casp8}]_0$ and $[\text{GSH}]_0$. Yet, despite the steady state conditions that favor cell survival, executioner caspase concentrations can reach and retain apoptotic levels for several hours before they level off, when $[\text{GSH}]_0$ is high. When $[\text{GSH}]_0$ is low, on the other hand, our simulations predict resistance to apoptosis, in agreement with experimental observation (Wink et al., 1999).

In cells with high numbers of MPTPs (probably cells that contain high numbers of mitochondria), our simulations suggest two possibilities in the presence of simultaneous NO and O_2^- production and sufficiently high $[\text{FeL}_n]_0$: pathological cell death when $[\text{GSH}]_0$ is high ($10^4 \mu\text{M}$) or solely cell survival when $[\text{GSH}]_0$ level is low ($[\text{GSH}]_0 \leq 10^3 \mu\text{M}$). On the other hand, GSH is protective against oxidative stress when O_2 and FeL_n levels are low in cells with low numbers of MPTPs.

Recent experimental data by Billiar and coworkers demonstrated that GSH depletion renders hepatocytes sensitive to NO -mediated toxicity (Chen et al., 2005). These experiments also showed that hypoxia causes hepatocytes to be susceptible to cell death by NO (Kim et al.,

2005). These data point to the complexity of NO-related reactions network in agreement with the present computational study. We note that our experimental studies suggested that treatment with NO in the setting of GSH depletion or hypoxia led to death by necrosis; nonetheless, it is still possible that other types of cells than hepatocytes may react to these changes in apoptosis. In our experimental results on hepatocytes (Chen et al., 2005; Kim et al., 2005), the levels of ATP were decreased. This decrease might have prevented apoptosis, which requires ATP, and switched the cellular death of cells to necrosis (Nicotera et al., 1998).

5.3 LIMITATIONS AND FUTURE DIRECTIONS

Our results are subject to several limitations. While we have adopted values for kinetic parameters and concentrations in accord with experimental data whenever available, many of the true intracellular rate constants for the reactions in our simulations are unknown. Given that the observed apoptotic responses are so sensitive to model parameters, detailed knowledge of reaction mechanisms and accurate values of rate constants are needed in modeling reaction networks as complicated as the ones presented here.

Additionally, the hypotheses raised by our simulations remain to be tested by further experiments. Some of the predictions could be tested by iron chelation and/or treatment with superoxide donors in a cell-free system or in single-cell studies, though each of these manipulations may have additional, artifactual effects. The hypothesis of bistability with regards to the apoptotic response can be tested as suggested by Legewie et al. (2006), either in cell free-systems by adding casp3 or in single living cells by microinjecting casp3. The time evolution of casp3 can be monitored by fluorescent casp3 substrates. The time needed for casp3 activation

will increase abruptly as casp3 concentration added will approach threshold value in a bistable system (Figure 16D). Our study does not consider NO-induced cGMP production which regulates many important biological processes along with apoptosis. The present model that combines apoptotic pathways with NO-related reactions can thus be extended to incorporate the effect of NO on apoptosis mediated by cGMP. Such combined experimental and computational studies may potentially help us understand and design therapeutics for diseases associated with apoptosis dysregulation.

APPENDIX A

A.1 SCRIPTS USED IN THE CALCULATIONS

A.1.1 Script used in Figure 4

```
# figure4.ode
# REACTIONS
# 2cc -> c3          k1
# c3 + ccm -> c3 + cc    k2
# ODE'S
c3'=k1*cc^2-muc3*c3
cc'=-2*k1*cc^2+k2*c3*ccm-mucc*cc
ccm'=om-k2*c3*ccm-muccm*ccm
# PARAMETERS
par k1=2,k2=2,om=0.0003,muc3=0.006,mucc=0.006,muccm=0.006
# INITIAL CONDITIONS
init cc=0,c3=0.001
# DISPLAY
@ xlo=0,xhi=4,ylo=0,yhi=2
@ nplot=1,yp=c3
# METHOD
@ meth=cvode,atol=1e-10,tol=1e-11,total=2000,dt=0.1,bounds=1000
done
```

A.1.2 Scripts used in Figure 10

```
# figure10A.ode
# REACTIONS
# om -> Ap
# om -> IAP
# om -> c3z
# om -> c9z
# om -> Bid
# om -> Bcl2
# om -> Bax
# om -> Ccmito
# c8a -> *
# c9a -> *
# c3a -> *
# Ap -> *
# IAP -> *
# c3z -> *
# c9z -> *
# Bcl2 -> *
# Bid -> *
# Bax -> *
# Ccmito -> *
# Bax -> *
# Bax2 -> *
# Cc -> *
# tBid -> *
# tBidBax -> *
# tBidmito -> *
# Cc + Ap <-> CcAp      k1p,k1m
# 7 CcAp <-> Apop      k1bp,k1bm
# Apop + c9z <-> Apopc9z  k2p,k2m
# Apopc9z + c9z <-> Apopc9z2 k3p,k3m
# Apopc9z2 -> Apopc9a2    k3f
# Apopc9a2 <-> Apopc9a + c9a k4p,k4m
# Apopc9a <-> Apop + c9a   k4bp,k4bm
# c9a + IAP <-> IAP9     k5p,k5m
# Apopc9a + IAP <-> IAPA9  k5bp,k5bm
# Apopc9a2 + IAP <-> IAPA29 k5cp,k5cm
# c3z + c9a <-> c93      k6p,k6m
# c93 -> c3a + c9a      k6f
# c3z + Apopc9a2 <-> cA93  k6bp,k6bm
# cA93 -> c3a + Apopc9a2  k6bf
# c3a + IAP <-> IAP3     k7p,k7m
# c8a + Bid <-> c8B     k8p,k8m
```

```

# c8B -> c8a + tBid      k8f
# c3a + Bid <-> c3B      k8p,k8m
# c3B -> c3a + tBid      k8f
# c3a + Bcl2 <-> c3L     k9p,k9m
# c3L -> c3a + B2c       k9f
# tBid -> tBidmito       k11
# tBidmito + Bax -> tBidBax k12a
# tBidBax + Bax -> tBid + Bax2 k12b
# Bcl2 + Bax -> *        k13
# Bax2 + Ccmito -> Cc + Bax2 k14
# REACTION RATES
r1p=k1p*Cc*Ap
r1m=k1m*CcAp
r1bp=k1bp*CcAp^p
r1bm=k1bm*Apop
r2p=k2p*Apop*c9z
r2m=k2m*Apopc9z
r3p=k3p*Apopc9z*c9z
r3m=k3m*Apopc9z2
r3f=k3f*Apopc9z2
r4p=k4p*Apopc9a2
r4m=k4m*Apopc9a*c9a
r4bp=k4bp*Apopc9a
r4bm=k4bm*Apop*c9a
r5p=k5p*c9a*IAP
r5m=k5m*IAP9
r5bp=k5bp*Apopc9a*IAP
r5bm=k5bm*IAPA9
r5cp=k5cp*Apopc9a2*IAP
r5cm=k5cm*IAPA29
r6p=k6p*c3z*c9a
r6m=k6m*c93
r6f=k6f*c93
r6bp=k6p*c3z*Apopc9a2
r6bm=k6m*cA93
r6bf=k6f*cA93
r7p=k7p*c3a*IAP
r7m=k7m*IAP3
r8p=k8p*c3a*Bid
r8m=k8m*c3B
r8f=k8f*c3B
r8pp=k8p*c8a*Bid
r8mp=k8m*c8B
r8fp=k8f*c8B
r9p=k9p*c3a*Bcl2
r9m=k9m*c3L

```

```

r9f=k9f*c3L
r11=k11*tbid
r12a=k12a*tbidmito*bax
r12b=k12b*tbidbax*bax
r13=k13*bcl2*bax
r14=k14*bax2*ccmito
# FLUXES
J1=r1p-r1m
J1b=r1bp-r1bm
J2=r2p-r2m
J3=r3p-r3m
J3f=r3f
J4=r4p-r4m
J4b=r4bp-r4bm
J5=r5p-r5m
J5b=r5bp-r5bm
J5c=r5cp-r5cm
J6=r6p-r6m
J6f=r6f
J6b=r6bp-r6bm
J6bf=r6bf
J7=r7p-r7m
J8=r8p-r8m
J8f=r8f
J8p=r8pp-r8mp
J8fp=r8fp
J9=r9p-r9m
J9f=r9f
j11=r11
j12a=r12a
j12b=r12b
j13=r13
j14=r14
# PRODUCTION AND DEGRADATION RATES
Jp8=-mu*c8a
JAp=0.0001*a1-mu*Ap
JIAP=0.0001*a2-mu*IAP
Jp3=0.0001*a3-mu*c3z
Jp9=0.0001*a4-mu*c9z
jbidp=0.0001*a5-mu*bid
jbcl2p=0.0001*a6*p53thresh^4/(p53^4+p53thresh^4)-mu*bcl2
jbax=0.0001*a7*(1+p53^4/(p53^4+p53thresh^4))-mu*bax
jccmito=0.0001*a8-mu*ccmito
# ODE'S
bax'=jbax-j12a-j12b-j13
Bcl2'=-J9+jbcl2p-j13

```

```

cc'=j14-j1-mu*cc+mptp*ccmito
c3a'=J6f+J6bf-J7-J8+J8f-J9+J9f-mu*c3a
AP'=-J1+JAp
CcAp'=J1-7*J1b
Apop'=J1b-J2+J4b
Apopc9z'=J2-J3
Apopc9z2'=J3-J3f
Apopc9a2'=J3f-J4-J5c-J6b+J6bf
Apopc9a'=J4-J4b-J5b
c9a'=J4+J4b-J5-J6+J6f-mu*c9a
c9z'=-J2-J3+Jp9
IAP'=-J5-J5b-J5c-J7+JIAP
IAP9'=J5
IAPA9'=J5b
IAPA29'=J5c
IAP3'=J7
c3z'=-J6-J6b+Jp3-10*nop*c3z
c93'=J6-J6f
cA93'=J6b-J6bf
c8a'=Jp8-J8p+J8fp
Bid'=-J8-J8p+jbidp
c8B'=J8p-J8fp
c3B'=J8-J8f
c3L'=J9-J9f
tbid'=j8f+j8fp-j11+j12b-mu*tbid+tbid0
tbidbax'=j12a-j12b-mu*tbidbax
ccmito'=jccmito-j14-mptp*ccmito
bax2'=j12b-mu*bax2
tbidmito'=j11-j12a-mu*tbidmito
# PARAMETERS
par MPTP=0
par nop=0
par tbid0=0
par p53=0.0066
par p=4
par k1p=5,k1m=0.5
par k1bp=50000*a9,k1bm=0.5*a9
par k2p=10,k2m=0.5
par k3p=10,k3m=0.5,k3f=0.1
par k4p=5,k4m=0.5
par k4bp=5,k4bm=0.5
par k5p=5*a10,k5m=0.0035*a10
par k5bp=5*a10,k5bm=0.0035*a10
par k5cp=5*a10,k5cm=0.0035*a10
par k6p=10*a11,k6m=0.5*a11,k6f=0.001*a11
par k6bp=10*a11,k6bm=0.5*a11,k6bf=0.1*a11

```

```

par k7p=5*a10,k7m=0.0035*a10
par k8p=10,k8m=0.5,k8f=0.1
par k9p=10,k9m=0.5,k9f=0.1
par k11=10*a12,k12a=10*a12,k12b=10*a12,k13=10*a12,k14=10*a12
par a1=3,a2=0.3,a3=3,a4=3,a5=0.3,a6=0.8,a7=0.3,a8=3,a9=1,a10=1,a11=1,a12=1,a13=3
mu=0.002*a13
par p53thresh=0.004
# INITIAL CONDITIONS
init Ap=.004,c9z=.004,c3z=.004,IAP=.004,Bid=.004,Bcl2=.004,bax=.004
init CcAp=0,Apop=0,Apopc9z=0,Apopc9z2=0,Apopc9a2=0,Apopc9a=0,c9a=0.00,IAP3=0
init IAP9=0,IAPA9=0,IAPA29=0,c93=0,cA93=0,c3a=0.00001,c3B=0,c3L=0
init c8a=0.00001,c8B=0
init cc=0,ccmito=.004
# DISPLAY
@ xhi=10000,ylo=0,yhi=0.001
@ nplot=1,yp=c3a
# METHOD
@ meth=cvode,atol=1e-8,tol=1e-9,total=200000,dt=5,bounds=100000
done
*****

# figure10B.ode
# REACTIONS
# om -> Ap
# om -> IAP
# om -> c3z
# om -> c9z
# om -> Bid
# om -> Bcl2
# om -> Bax
# om -> Ccmito
# c8a -> *
# c9a -> *
# c3a -> *
# Ap -> *
# IAP -> *
# c3z -> *
# c9z -> *
# Bcl2 -> *
# Bid -> *
# Bax -> *
# Ccmito -> *
# Bax -> *
# Bax2 -> *
# Cc -> *
# tBid -> *

```

```

# tBidBax -> *
# tBidmito -> *
# Cc + Ap <-> CcAp      k1p,k1m
# 7 CcAp <-> Apop      k1bp,k1bm
# Apop + c9z <-> Apopc9z  k2p,k2m
# Apopc9z + c9z <-> Apopc9z2 k3p,k3m
# Apopc9z2 -> Apopc9a2    k3f
# Apopc9a2 <-> Apopc9a + c9a k4p,k4m
# Apopc9a <-> Apop + c9a    k4bp,k4bm
# c9a + IAP <-> IAP9      k5p,k5m
# Apopc9a + IAP <-> IAPA9  k5bp,k5bm
# Apopc9a2 + IAP <-> IAPA29 k5cp,k5cm
# c3z + c9a <-> c93      k6p,k6m
# c93 -> c3a + c9a      k6f
# c3z + Apopc9a2 <-> cA93  k6bp,k6bm
# cA93 -> c3a + Apopc9a2  k6bf
# c3a + IAP <-> IAP3     k7p,k7m
# c8a + Bid <-> c8B     k8p,k8m
# c8B -> c8a + tBid     k8f
# c3a + Bid <-> c3B     k8p,k8m
# c3B -> c3a + tBid     k8f
# c3a + Bcl2 <-> c3L    k9p,k9m
# c3L -> c3a + B2c     k9f
# tBid -> tBidmito     k11
# tBidmito + Bax -> tBidBax k12a
# tBidBax + Bax -> tBid + Bax2 k12b
# Bcl2 + Bax -> *      k13
# Bax2 + Ccmito -> Cc + Bax2 k14
# REACTION RATES
r1p=k1p*Cc*Ap
r1m=k1m*CcAp
r1bp=k1bp*CcAp^p
r1bm=k1bm*Apop
r2p=k2p*Apop*c9z
r2m=k2m*Apopc9z
r3p=k3p*Apopc9z*c9z
r3m=k3m*Apopc9z2
r3f=k3f*Apopc9z2
r4p=k4p*Apopc9a2
r4m=k4m*Apopc9a*c9a
r4bp=k4bp*Apopc9a
r4bm=k4bm*Apop*c9a
r5p=k5p*c9a*IAP
r5m=k5m*IAP9
r5bp=k5bp*Apopc9a*IAP
r5bm=k5bm*IAPA9

```

$r5cp=k5cp*Apopc9a2*IAP$
 $r5cm=k5cm*IAPA29$
 $r6p=k6p*c3z*c9a$
 $r6m=k6m*c93$
 $r6f=k6f*c93$
 $r6bp=k6p*c3z*Apopc9a2$
 $r6bm=k6m*cA93$
 $r6bf=k6f*cA93$
 $r7p=k7p*c3a*IAP$
 $r7m=k7m*IAP3$
 $r8p=k8p*c3a*Bid$
 $r8m=k8m*c3B$
 $r8f=k8f*c3B$
 $r8pp=k8p*c8a*Bid$
 $r8mp=k8m*c8B$
 $r8fp=k8f*c8B$
 $r9p=k9p*c3a*Bcl2$
 $r9m=k9m*c3L$
 $r9f=k9f*c3L$
 $r11=k11*tbid$
 $r12a=k12a*tbidmito*bax$
 $r12b=k12b*tbidbax*bax$
 $r13=k13*bcl2*bax$
 $r14=k14*bax2*ccmito$
FLUXES
 $J1=r1p-r1m$
 $J1b=r1bp-r1bm$
 $J2=r2p-r2m$
 $J3=r3p-r3m$
 $J3f=r3f$
 $J4=r4p-r4m$
 $J4b=r4bp-r4bm$
 $J5=r5p-r5m$
 $J5b=r5bp-r5bm$
 $J5c=r5cp-r5cm$
 $J6=r6p-r6m$
 $J6f=r6f$
 $J6b=r6bp-r6bm$
 $J6bf=r6bf$
 $J7=r7p-r7m$
 $J8=r8p-r8m$
 $J8f=r8f$
 $J8p=r8pp-r8mp$
 $J8fp=r8fp$
 $J9=r9p-r9m$
 $J9f=r9f$

```

j11=r11
j12a=r12a
j12b=r12b
j13=r13
j14=r14
# PRODUCTION AND DEGRADATION RATES
Jp8=-mu*c8a
JAp=0.0001*a1-mu*Ap
JIAP=0.0001*a2-mu*IAP
Jp3=0.0001*a3-mu*c3z
Jp9=0.0001*a4-mu*c9z
jbidp=0.0001*a5-mu*bid
jbc12p=0.0001*a6*p53thresh^4/(p53^4+p53thresh^4)-mu*bc12
jbax=0.0001*a7*(1+p53^4/(p53^4+p53thresh^4))-mu*bax
jccmito=0.0001*a8-mu*ccmito
# ODE'S
bax'=jbax-j12a-j12b-j13
Bcl2'=-J9+jbc12p-j13
cc'=j14-j1-mu*cc+mptp*ccmito
c3a'=J6f+J6bf-J7-J8+J8f-J9+J9f-mu*c3a
AP'=-J1+JAp
CcAp'=J1-7*J1b
Apop'=J1b-J2+J4b
Apopc9z'=J2-J3
Apopc9z2'=J3-J3f
Apopc9a2'=J3f-J4-J5c-J6b+J6bf
Apopc9a'=J4-J4b-J5b
c9a'=J4+J4b-J5-J6+J6f-mu*c9a
c9z'=-J2-J3+Jp9
IAP'=-J5-J5b-J5c-J7+JIAP
IAP9'=J5
IAPA9'=J5b
IAPA29'=J5c
IAP3'=J7
c3z'=-J6-J6b+Jp3-10*nop*c3z
c93'=J6-J6f
cA93'=J6b-J6bf
c8a'=Jp8-J8p+J8fp
Bid'=-J8-J8p+jbidp
c8B'=J8p-J8fp
c3B'=J8-J8f
c3L'=J9-J9f
tbid'=j8f+j8fp-j11+j12b-mu*tbid+tbid0
tbidbax'=j12a-j12b-mu*tbidbax
ccmito'=jccmito-j14-mptp*ccmito
bax2'=j12b-mu*bax2

```

```

tbidmito'=j11-j12a-mu*tbidmito
# INITIAL CONDITIONS
init Ap=.004,c9z=.004,c3z=.004,IAP=.004,Bid=.004,Bcl2=.004,bax=.004
init CcAp=0,Apop=0,Apopc9z=0,Apopc9z2=0,Apopc9a2=0,Apopc9a=0,c9a=0.00,IAP3=0
init IAP9=0,IAPA9=0,IAPA29=0,c93=0,cA93=0,c3a=0.00001,c3B=0,c3L=0
init c8a=0.0001,c8B=0
init cc=0,ccmito=.004
# PARAMETERS
par MPTP=0
par nop=0
par tbid0=0
par p53=0.0066
par p=4
par k1p=5,k1m=0.5
par k1bp=50000*a9,k1bm=0.5*a9
par k2p=10,k2m=0.5
par k3p=10,k3m=0.5,k3f=0.1
par k4p=5,k4m=0.5
par k4bp=5,k4bm=0.5
par k5p=5*a10,k5m=0.0035*a10
par k5bp=5*a10,k5bm=0.0035*a10
par k5cp=5*a10,k5cm=0.0035*a10
par k6p=10*a11,k6m=0.5*a11,k6f=0.001*a11
par k6bp=10*a11,k6bm=0.5*a11,k6bf=0.1*a11
par k7p=5*a10,k7m=0.0035*a10
par k8p=10,k8m=0.5,k8f=0.1
par k9p=10,k9m=0.5,k9f=0.1
par k11=10*a12,k12a=10*a12,k12b=10*a12,k13=10*a12,k14=10*a12
par a1=3,a2=0.3,a3=3,a4=3,a5=0.3,a6=0.8,a7=0.3,a8=3,a9=1,a10=1,a11=1,a12=1,a13=3
mu=0.002*a13
par p53thresh=0.004
# display
@ xhi=10000,ylo=0,yhi=0.001
@ nplot=1,yp=c3a
# METHOD
@ meth=cvode,atol=1e-8,tol=1e-9,total=200000,dt=5,bounds=100000
done
*****

# figure10C.ode
# REACTIONS
# om -> Ap
# om -> IAP
# om -> c3z
# om -> c9z

```

```

# om -> Bid
# om -> Bcl2
# om -> Bax
# om -> Ccmito
# c8a -> *
# c9a -> *
# c3a -> *
# Ap -> *
# IAP -> *
# c3z -> *
# c9z -> *
# Bcl2 -> *
# Bid -> *
# Bax -> *
# Ccmito -> *
# Bax -> *
# Bax2 -> *
# Cc -> *
# tBid -> *
# tBidBax -> *
# tBidmito -> *
# Cc + Ap <-> CcAp      k1p,k1m
# 7 CcAp <-> Apop      k1bp,k1bm
# Apop + c9z <-> Apopc9z  k2p,k2m
# Apopc9z + c9z <-> Apopc9z2 k3p,k3m
# Apopc9z2 -> Apopc9a2    k3f
# Apopc9a2 <-> Apopc9a + c9a k4p,k4m
# Apopc9a <-> Apop + c9a    k4bp,k4bm
# c9a + IAP <-> IAP9      k5p,k5m
# Apopc9a + IAP <-> IAPA9  k5bp,k5bm
# Apopc9a2 + IAP <-> IAPA29 k5cp,k5cm
# c3z + c9a <-> c93      k6p,k6m
# c93 -> c3a + c9a      k6f
# c3z + Apopc9a2 <-> cA93  k6bp,k6bm
# cA93 -> c3a + Apopc9a2  k6bf
# c3a + IAP <-> IAP3     k7p,k7m
# c8a + Bid <-> c8B      k8p,k8m
# c8B -> c8a + tBid     k8f
# c3a + Bid <-> c3B      k8p,k8m
# c3B -> c3a + tBid     k8f
# c3a + Bcl2 <-> c3L    k9p,k9m
# c3L -> c3a + B2c     k9f
# tBid -> tBidmito     k11
# tBidmito + Bax -> tBidBax k12a
# tBidBax + Bax -> tBid + Bax2 k12b
# Bcl2 + Bax -> *      k13

```

Bax2 + Ccmito -> Cc + Bax2 k14

REACTION RATES

$r1p = k1p * Cc * Ap$

$r1m = k1m * CcAp$

$r1bp = k1bp * CcAp^p$

$r1bm = k1bm * Apop$

$r2p = k2p * Apop * c9z$

$r2m = k2m * Apopc9z$

$r3p = k3p * Apopc9z * c9z$

$r3m = k3m * Apopc9z^2$

$r3f = k3f * Apopc9z^2$

$r4p = k4p * Apopc9a^2$

$r4m = k4m * Apopc9a * c9a$

$r4bp = k4bp * Apopc9a$

$r4bm = k4bm * Apop * c9a$

$r5p = k5p * c9a * IAP$

$r5m = k5m * IAP^9$

$r5bp = k5bp * Apopc9a * IAP$

$r5bm = k5bm * IAPA^9$

$r5cp = k5cp * Apopc9a^2 * IAP$

$r5cm = k5cm * IAPA^2^9$

$r6p = k6p * c3z * c9a$

$r6m = k6m * c9^3$

$r6f = k6f * c9^3$

$r6bp = k6p * c3z * Apopc9a^2$

$r6bm = k6m * cA^9^3$

$r6bf = k6f * cA^9^3$

$r7p = k7p * c3a * IAP$

$r7m = k7m * IAP^3$

$r8p = k8p * c3a * Bid$

$r8m = k8m * c3B$

$r8f = k8f * c3B$

$r8pp = k8p * c8a * Bid$

$r8mp = k8m * c8B$

$r8fp = k8f * c8B$

$r9p = k9p * c3a * Bcl2$

$r9m = k9m * c3L$

$r9f = k9f * c3L$

$r11 = k11 * tbid$

$r12a = k12a * tbidmito * bax$

$r12b = k12b * tbidbax * bax$

$r13 = k13 * bcl2 * bax$

$r14 = k14 * bax^2 * ccmito$

FLUXES

$J1 = r1p - r1m$

$J1b = r1bp - r1bm$

$J2=r2p-r2m$
 $J3=r3p-r3m$
 $J3f=r3f$
 $J4=r4p-r4m$
 $J4b=r4bp-r4bm$
 $J5=r5p-r5m$
 $J5b=r5bp-r5bm$
 $J5c=r5cp-r5cm$
 $J6=r6p-r6m$
 $J6f=r6f$
 $J6b=r6bp-r6bm$
 $J6bf=r6bf$
 $J7=r7p-r7m$
 $J8=r8p-r8m$
 $J8f=r8f$
 $J8p=r8pp-r8mp$
 $J8fp=r8fp$
 $J9=r9p-r9m$
 $J9f=r9f$
 $j11=r11$
 $j12a=r12a$
 $j12b=r12b$
 $j13=r13$
 $j14=r14$
PRODUCTION AND DEGRADATION RATES
 $Jp8=-\mu*c8a$
 $JAp=0.0001*a1-\mu*Ap$
 $JIAP=0.0001*a2-\mu*IAP$
 $Jp3=0.0001*a3-\mu*c3z$
 $Jp9=0.0001*a4-\mu*c9z$
 $jbidp=0.0001*a5-\mu*bid$
 $jbcl2p=0.0001*a6*p53thresh^4/(p53^4+p53thresh^4)-\mu*bcl2$
 $jbax=0.0001*a7*(1+p53^4/(p53^4+p53thresh^4))-\mu*bax$
 $jccmito=0.0001*a8-\mu*ccmito$
ODE'S
 $bax'=jbax-j12a-j12b-j13$
 $Bcl2'=-J9+jbcl2p-j13$
 $cc'=j14-j1-\mu*cc+mptp*ccmito$
 $c3a'=J6f+J6bf-J7-J8+J8f-J9+J9f-\mu*c3a$
 $AP'=-J1+JAp$
 $CcAp'=J1-7*J1b$
 $Apop'=J1b-J2+J4b$
 $Apopc9z'=J2-J3$
 $Apopc9z2'=J3-J3f$
 $Apopc9a2'=J3f-J4-J5c-J6b+J6bf$
 $Apopc9a'=J4-J4b-J5b$

```

c9a'=J4+J4b-J5-J6+J6f-mu*c9a
c9z'=-J2-J3+Jp9
IAP'=-J5-J5b-J5c-J7+JIAP
IAP9'=J5
IAPA9'=J5b
IAPA29'=J5c
IAP3'=J7
c3z'=-J6-J6b+Jp3-10*nop*c3z
c93'=J6-J6f
cA93'=J6b-J6bf
c8a'=Jp8-J8p+J8fp
Bid'=-J8-J8p+jbidp
c8B'=J8p-J8fp
c3B'=J8-J8f
c3L'=J9-J9f
tbid'=j8f+j8fp-j11+j12b-mu*tbid+tbid0
tbidbax'=j12a-j12b-mu*tbidbax
ccmito'=jccmito-j14-mptp*ccmito
bax2'=j12b-mu*bax2
tbidmito'=j11-j12a-mu*tbidmito
# INITIAL CONDITIONS
init Ap=.004,c9z=.004,c3z=.004,IAP=.004,Bid=.004,Bcl2=.004,bax=.004
init CcAp=0,Apop=0,Apopc9z=0,Apopc9z2=0,Apopc9a2=0,Apopc9a=0,c9a=0.00,IAP3=0
init IAP9=0,IAPA9=0,IAPA29=0,c93=0,cA93=0,c3a=0.00001,c3B=0,c3L=0
init c8a=0.00001,c8B=0
init cc=0,ccmito=.004
# PARAMETERS
par p=1
par MPTP=0
par nop=0
par tbid0=0
par p53=0.0066
par k1p=5,k1m=0.5
par k1bp=50000*a9,k1bm=0.5*a9
par k2p=10,k2m=0.5
par k3p=10,k3m=0.5,k3f=0.1
par k4p=5,k4m=0.5
par k4bp=5,k4bm=0.5
par k5p=5*a10,k5m=0.0035*a10
par k5bp=5*a10,k5bm=0.0035*a10
par k5cp=5*a10,k5cm=0.0035*a10
par k6p=10*a11,k6m=0.5*a11,k6f=0.001*a11
par k6bp=10*a11,k6bm=0.5*a11,k6bf=0.1*a11
par k7p=5*a10,k7m=0.0035*a10
par k8p=10,k8m=0.5,k8f=0.1
par k9p=10,k9m=0.5,k9f=0.1

```

```

par k11=10*a12,k12a=10*a12,k12b=10*a12,k13=10*a12,k14=10*a12
par a1=3,a2=0.3,a3=3,a4=3,a5=0.3,a6=0.8,a7=0.3,a8=3,a9=1,a10=1,a11=1,a12=1,a13=3
mu=0.002*a13
par p53thresh=0.004
# DISPLAY
@ xhi=10000,ylo=0,yhi=0.001
@ nplot=1,yp=c3a
# METHOD
@ meth=cvode,atol=1e-8,tol=1e-9,total=200000,dt=5,bounds=100000
done

```

A.1.3 Scripts used in Figure 11

```

# figure11A.ode
# REACTIONS
# om -> Ap
# om -> IAP
# om -> c3z
# om -> c9z
# om -> Bid
# om -> Bcl2
# om -> Bax
# om -> Ccmito
# c8a -> *
# c9a -> *
# c3a -> *
# Ap -> *
# IAP -> *
# c3z -> *
# c9z -> *
# Bcl2 -> *
# Bid -> *
# Bax -> *
# Ccmito -> *
# Bax -> *
# Bax2 -> *
# Cc -> *
# tBid -> *
# tBidBax -> *
# tBidmito -> *
# Cc + Ap <-> CcAp      k1p,k1m
# 7 CcAp <-> Apop      k1bp,k1bm
# Apop + c9z <-> Apopc9z  k2p,k2m
# Apopc9z + c9z <-> Apopc9z2 k3p,k3m

```

```

# Apopc9z2 -> Apopc9a2      k3f
# Apopc9a2 <-> Apopc9a + c9a k4p,k4m
# Apopc9a <-> Apop + c9a    k4bp,k4bm
# c9a + IAP <-> IAP9      k5p,k5m
# Apopc9a + IAP <-> IAPA9  k5bp,k5bm
# Apopc9a2 + IAP <-> IAPA29 k5cp,k5cm
# c3z + c9a <-> c93      k6p,k6m
# c93 -> c3a + c9a      k6f
# c3z + Apopc9a2 <-> cA93  k6bp,k6bm
# cA93 -> c3a + Apopc9a2  k6bf
# c3a + IAP <-> IAP3     k7p,k7m
# c8a + Bid <-> c8B     k8p,k8m
# c8B -> c8a + tBid     k8f
# c3a + Bid <-> c3B     k8p,k8m
# c3B -> c3a + tBid     k8f
# c3a + Bcl2 <-> c3L    k9p,k9m
# c3L -> c3a + B2c     k9f
# tBid -> tBidmito     k11
# tBidmito + Bax -> tBidBax k12a
# tBidBax + Bax -> tBid + Bax2 k12b
# Bcl2 + Bax -> *      k13
# Bax2 + Ccmito -> Cc + Bax2 k14
# REACTION RATES
r1p=k1p*Cc*Ap
r1m=k1m*CcAp
r1bp=k1bp*CcAp^p
r1bm=k1bm*Apop
r2p=k2p*Apop*c9z
r2m=k2m*Apopc9z
r3p=k3p*Apopc9z*c9z
r3m=k3m*Apopc9z2
r3f=k3f*Apopc9z2
r4p=k4p*Apopc9a2
r4m=k4m*Apopc9a*c9a
r4bp=k4bp*Apopc9a
r4bm=k4bm*Apop*c9a
r5p=k5p*c9a*IAP
r5m=k5m*IAP9
r5bp=k5bp*Apopc9a*IAP
r5bm=k5bm*IAPA9
r5cp=k5cp*Apopc9a2*IAP
r5cm=k5cm*IAPA29
r6p=k6p*c3z*c9a
r6m=k6m*c93
r6f=k6f*c93
r6bp=k6p*c3z*Apopc9a2

```

$r_{6bm} = k_{6m} * c_{A93}$
 $r_{6bf} = k_{6f} * c_{A93}$
 $r_{7p} = k_{7p} * c_{3a} * IAP$
 $r_{7m} = k_{7m} * IAP^3$
 $r_{8p} = k_{8p} * c_{3a} * Bid$
 $r_{8m} = k_{8m} * c_{3B}$
 $r_{8f} = k_{8f} * c_{3B}$
 $r_{8pp} = k_{8p} * c_{8a} * Bid$
 $r_{8mp} = k_{8m} * c_{8B}$
 $r_{8fp} = k_{8f} * c_{8B}$
 $r_{9p} = k_{9p} * c_{3a} * Bcl2$
 $r_{9m} = k_{9m} * c_{3L}$
 $r_{9f} = k_{9f} * c_{3L}$
 $r_{11} = k_{11} * t_{bid}$
 $r_{12a} = k_{12a} * t_{bid} * m_{ito} * b_{ax}$
 $r_{12b} = k_{12b} * t_{bid} * b_{ax} * b_{ax}$
 $r_{13} = k_{13} * b_{cl2} * b_{ax}$
 $r_{14} = k_{14} * b_{ax}^2 * c_{cm_{ito}}$
FLUXES
 $J_1 = r_{1p} - r_{1m}$
 $J_{1b} = r_{1bp} - r_{1bm}$
 $J_2 = r_{2p} - r_{2m}$
 $J_3 = r_{3p} - r_{3m}$
 $J_{3f} = r_{3f}$
 $J_4 = r_{4p} - r_{4m}$
 $J_{4b} = r_{4bp} - r_{4bm}$
 $J_5 = r_{5p} - r_{5m}$
 $J_{5b} = r_{5bp} - r_{5bm}$
 $J_{5c} = r_{5cp} - r_{5cm}$
 $J_6 = r_{6p} - r_{6m}$
 $J_{6f} = r_{6f}$
 $J_{6b} = r_{6bp} - r_{6bm}$
 $J_{6bf} = r_{6bf}$
 $J_7 = r_{7p} - r_{7m}$
 $J_8 = r_{8p} - r_{8m}$
 $J_{8f} = r_{8f}$
 $J_{8p} = r_{8pp} - r_{8mp}$
 $J_{8fp} = r_{8fp}$
 $J_9 = r_{9p} - r_{9m}$
 $J_{9f} = r_{9f}$
 $j_{11} = r_{11}$
 $j_{12a} = r_{12a}$
 $j_{12b} = r_{12b}$
 $j_{13} = r_{13}$
 $j_{14} = r_{14}$
PRODUCTION AND DEGRADATION RATES

```

Jp8=-mu*c8a
JAp=0.0001*a1-mu*Ap
JIAP=0.0001*a2-mu*IAP
Jp3=0.0001*a3-mu*c3z
Jp9=0.0001*a4-mu*c9z
jbidp=0.0001*a5-mu*bid
jbcl2p=0.0001*a6*p53thresh^4/(p53^4+p53thresh^4)-mu*bc12
jbax=0.0001*a7*(1+p53^4/(p53^4+p53thresh^4))-mubax*bax
jccmito=0.0001*a8-mu*ccmito
# ODE'S
bax'=jbax-j12a-j12b-j13
Bcl2'=-J9+jbcl2p-j13
cc'=j14-j1-mu*cc+mptp*ccmito
c3a'=J6f+J6bf-J7-J8+J8f-J9+J9f-mu*c3a
AP'=-J1+JAp
CcAp'=J1-7*J1b
Apop'=J1b-J2+J4b
Apopc9z'=J2-J3
Apopc9z2'=J3-J3f
Apopc9a2'=J3f-J4-J5c-J6b+J6bf
Apopc9a'=J4-J4b-J5b
c9a'=J4+J4b-J5-J6+J6f-mu*c9a
c9z'=-J2-J3+Jp9
IAP'=-J5-J5b-J5c-J7+JIAP
IAP9'=J5
IAPA9'=J5b
IAPA29'=J5c
IAP3'=J7
c3z'=-J6-J6b+Jp3-10*nop*c3z
c93'=J6-J6f
cA93'=J6b-J6bf
c8a'=Jp8-J8p+J8fp
Bid'=-J8-J8p+jbidp
c8B'=J8p-J8fp
c3B'=J8-J8f
c3L'=J9-J9f
tbid'=j8f+j8fp-j11+j12b-mu*tbid+tbid0
tbidbax'=j12a-j12b-mu*tbidbax
ccmito'=jccmito-j14-mptp*ccmito
bax2'=j12b-mu*bax2
tbidmito'=j11-j12a-mu*tbidmito
# PARAMETERS
par mubax=0.001
par MPTP=0
par nop=0
par tbid0=0

```

```

par p53=0.0066
par p=4
par k1p=5,k1m=0.5
par k1bp=50000*a9,k1bm=0.5*a9
par k2p=10,k2m=0.5
par k3p=10,k3m=0.5,k3f=0.1
par k4p=5,k4m=0.5
par k4bp=5,k4bm=0.5
par k5p=5*a10,k5m=0.0035*a10
par k5bp=5*a10,k5bm=0.0035*a10
par k5cp=5*a10,k5cm=0.0035*a10
par k6p=10*a11,k6m=0.5*a11,k6f=0.001*a11
par k6bp=10*a11,k6bm=0.5*a11,k6bf=0.1*a11
par k7p=5*a10,k7m=0.0035*a10
par k8p=10,k8m=0.5,k8f=0.1
par k9p=10,k9m=0.5,k9f=0.1
par k11=10*a12,k12a=10*a12,k12b=10*a12,k13=10*a12,k14=10*a12
par a1=3,a2=0.3,a3=3,a4=3,a5=0.3,a6=0.8,a7=0.3,a8=3,a9=1,a10=1,a11=1,a12=1,a13=3
mu=0.002*a13
par p53thresh=0.004
# INITIAL CONDITIONS
init Ap=.004,c9z=.004,c3z=.004,IAP=.004,Bid=.004,Bcl2=.004,bax=.004
init CcAp=0,Apop=0,Apopc9z=0,Apopc9z2=0,Apopc9a2=0,Apopc9a=0,c9a=0.00
init IAP3=0,IAP9=0,IAPA9=0,IAPA29=0,c93=0,cA93=0,c3a=0.004,c3B=0,c3L=0
init c8a=0.0000,c8B=0
init cc=0,ccmito=.004
# DISPLAY
@ xhi=10000,ylo=0,yhi=0.001
@ nplot=1,yp=c3a
# METHOD
@ meth=cvode,atol=1e-8,tol=1e-9,total=200000,dt=5,bounds=100000
done
*****

# figure11B.ode
# REACTIONS
# om -> Ap
# om -> IAP
# om -> c3z
# om -> c9z
# om -> Bid
# om -> Bcl2
# om -> Bax
# om -> Ccmito
# c8a -> *

```

```

# c9a -> *
# c3a -> *
# Ap -> *
# IAP -> *
# c3z -> *
# c9z -> *
# Bcl2 -> *
# Bid -> *
# Bax -> *
# Ccm1to -> *
# Bax -> *
# Bax2 -> *
# Cc -> *
# tBid -> *
# tBidBax -> *
# tBidmito -> *
# Cc + Ap <-> CcAp      k1p,k1m
# 7 CcAp <-> Apop      k1bp,k1bm
# Apop + c9z <-> Apopc9z  k2p,k2m
# Apopc9z + c9z <-> Apopc9z2 k3p,k3m
# Apopc9z2 -> Apopc9a2    k3f
# Apopc9a2 <-> Apopc9a + c9a k4p,k4m
# Apopc9a <-> Apop + c9a    k4bp,k4bm
# c9a + IAP <-> IAP9      k5p,k5m
# Apopc9a + IAP <-> IAPA9  k5bp,k5bm
# Apopc9a2 + IAP <-> IAPA29 k5cp,k5cm
# c3z + c9a <-> c93      k6p,k6m
# c93 -> c3a + c9a      k6f
# c3z + Apopc9a2 <-> cA93  k6bp,k6bm
# cA93 -> c3a + Apopc9a2  k6bf
# c3a + IAP <-> IAP3     k7p,k7m
# c8a + Bid <-> c8B     k8p,k8m
# c8B -> c8a + tBid     k8f
# c3a + Bid <-> c3B     k8p,k8m
# c3B -> c3a + tBid     k8f
# c3a + Bcl2 <-> c3L    k9p,k9m
# c3L -> c3a + B2c     k9f
# tBid -> tBidmito     k11
# tBidmito + Bax -> tBidBax k12a
# tBidBax + Bax -> tBid + Bax2 k12b
# Bcl2 + Bax -> *      k13
# Bax2 + Ccm1to -> Cc + Bax2 k14
# REACTION RATES
r1p=k1p*Cc*Ap
r1m=k1m*CcAp
r1bp=k1bp*CcAp^p

```

$r1bm = k1bm * Apop$
 $r2p = k2p * Apop * c9z$
 $r2m = k2m * Apopc9z$
 $r3p = k3p * Apopc9z * c9z$
 $r3m = k3m * Apopc9z2$
 $r3f = k3f * Apopc9z2$
 $r4p = k4p * Apopc9a2$
 $r4m = k4m * Apopc9a * c9a$
 $r4bp = k4bp * Apopc9a$
 $r4bm = k4bm * Apop * c9a$
 $r5p = k5p * c9a * IAP$
 $r5m = k5m * IAP9$
 $r5bp = k5bp * Apopc9a * IAP$
 $r5bm = k5bm * IAPA9$
 $r5cp = k5cp * Apopc9a2 * IAP$
 $r5cm = k5cm * IAPA29$
 $r6p = k6p * c3z * c9a$
 $r6m = k6m * c93$
 $r6f = k6f * c93$
 $r6bp = k6p * c3z * Apopc9a2$
 $r6bm = k6m * cA93$
 $r6bf = k6f * cA93$
 $r7p = k7p * c3a * IAP$
 $r7m = k7m * IAP3$
 $r8p = k8p * c3a * Bid$
 $r8m = k8m * c3B$
 $r8f = k8f * c3B$
 $r8pp = k8p * c8a * Bid$
 $r8mp = k8m * c8B$
 $r8fp = k8f * c8B$
 $r9p = k9p * c3a * Bcl2$
 $r9m = k9m * c3L$
 $r9f = k9f * c3L$
 $r11 = k11 * tbid$
 $r12a = k12a * tbidmito * bax$
 $r12b = k12b * tbidbax * bax$
 $r13 = k13 * bcl2 * bax$
 $r14 = k14 * bax2 * ccmto$
FLUXES
 $J1 = r1p - r1m$
 $J1b = r1bp - r1bm$
 $J2 = r2p - r2m$
 $J3 = r3p - r3m$
 $J3f = r3f$
 $J4 = r4p - r4m$
 $J4b = r4bp - r4bm$

$J5=r5p-r5m$
 $J5b=r5bp-r5bm$
 $J5c=r5cp-r5cm$
 $J6=r6p-r6m$
 $J6f=r6f$
 $J6b=r6bp-r6bm$
 $J6bf=r6bf$
 $J7=r7p-r7m$
 $J8=r8p-r8m$
 $J8f=r8f$
 $J8p=r8pp-r8mp$
 $J8fp=r8fp$
 $J9=r9p-r9m$
 $J9f=r9f$
 $j11=r11$
 $j12a=r12a$
 $j12b=r12b$
 $j13=r13$
 $j14=r14$
PRODUCTION AND DEGRADATION RATES
 $Jp8=-\mu*c8a$
 $JAp=0.0001*a1-\mu*Ap$
 $JIAP=0.0001*a2-\mu*IAP$
 $Jp3=0.0001*a3-\mu*c3z$
 $Jp9=0.0001*a4-\mu*c9z$
 $jbidp=0.0001*a5-\mu*bid$
 $jbcl2p=0.0001*a6*p53thresh^4/(p53^4+p53thresh^4)-\mu*bcl2$
 $jbax=0.0001*a7*(1+p53^4/(p53^4+p53thresh^4))-\mu*bax$
 $jccmito=0.0001*a8-\mu*ccmito$
ODE'S
 $bax'=jbax-j12a-j12b-j13$
 $Bcl2'=-J9+jbcl2p-j13$
 $cc'=j14-j1-\mu*cc+mptp*ccmito$
 $c3a'=J6f+J6bf-J7-J8+J8f-J9+J9f-\mu*c3a$
 $AP'=-J1+JAp$
 $CcAp'=J1-7*J1b$
 $Apop'=J1b-J2+J4b$
 $Apopc9z'=J2-J3$
 $Apopc9z2'=J3-J3f$
 $Apopc9a2'=J3f-J4-J5c-J6b+J6bf$
 $Apopc9a'=J4-J4b-J5b$
 $c9a'=J4+J4b-J5-J6+J6f-\mu*c9a$
 $c9z'=-J2-J3+Jp9$
 $IAP'=-J5-J5b-J5c-J7+JIAP$
 $IAP9'=J5$
 $IAPA9'=J5b$

```

IAPA29'=J5c
IAP3'=J7
c3z'=-J6-J6b+Jp3-10*nop*c3z
c93'=J6-J6f
cA93'=J6b-J6bf
c8a'=Jp8-J8p+J8fp
Bid'=-J8-J8p+jbidp
c8B'=J8p-J8fp
c3B'=J8-J8f
c3L'=J9-J9f
tbid'=j8f+j8fp-j11+j12b-mu*tbid+tbid0
tbidbax'=j12a-j12b-mu*tbidbax
ccmito'=jccmito-j14-mptp*ccmito
bax2'=j12b-mu*bax2
tbidmito'=j11-j12a-mu*tbidmito
# PARAMETERS
par mubax=0.2
par MPTP=0
par nop=0
par tbid0=0
par p53=0.0066
par p=4
par k1p=5,k1m=0.5
par k1bp=50000*a9,k1bm=0.5*a9
par k2p=10,k2m=0.5
par k3p=10,k3m=0.5,k3f=0.1
par k4p=5,k4m=0.5
par k4bp=5,k4bm=0.5
par k5p=5*a10,k5m=0.0035*a10
par k5bp=5*a10,k5bm=0.0035*a10
par k5cp=5*a10,k5cm=0.0035*a10
par k6p=10*a11,k6m=0.5*a11,k6f=0.001*a11
par k6bp=10*a11,k6bm=0.5*a11,k6bf=0.1*a11
par k7p=5*a10,k7m=0.0035*a10
par k8p=10,k8m=0.5,k8f=0.1
par k9p=10,k9m=0.5,k9f=0.1
par k11=10*a12,k12a=10*a12,k12b=10*a12,k13=10*a12,k14=10*a12
par a1=3,a2=0.3,a3=3,a4=3,a5=0.3,a6=0.8,a7=0.3,a8=3,a9=1,a10=1,a11=1,a12=1,a13=3
mu=0.002*a13
par p53thresh=0.004
# INITIAL CONDITIONS
init Ap=.004,c9z=.004,c3z=.004,IAP=.004,Bid=.004,Bcl2=.004,bax=.004
init CcAp=0,Apop=0,Apopc9z=0,Apopc9z2=0,Apopc9a2=0,Apopc9a=0,c9a=0.00
init IAP3=0,IAP9=0,IAPA9=0,IAPA29=0,c93=0,cA93=0,c3a=0.1,c3B=0,c3L=0
init c8a=0.1,c8B=0
init cc=0,ccmito=.004

```

```

# DISPLAY
@ xhi=10000,ylo=0,yhi=0.001
@ nplot=1,yp=c3a
# METHOD
@ meth=cvode,atol=1e-8,tol=1e-9,total=200000,dt=5,bounds=100000
done
*****

```

```

# figure11C.ode
# REACTIONS
# om -> Ap
# om -> IAP
# om -> c3z
# om -> c9z
# om -> Bid
# om -> Bcl2
# om -> Bax
# om -> Ccmito
# c8a -> *
# c9a -> *
# c3a -> *
# Ap -> *
# IAP -> *
# c3z -> *
# c9z -> *
# Bcl2 -> *
# Bid -> *
# Bax -> *
# Ccmito -> *
# Bax -> *
# Bax2 -> *
# Cc -> *
# tBid -> *
# tBidBax -> *
# tBidmito -> *
# Cc + Ap <-> CcAp      k1p,k1m
# 7 CcAp <-> Apop      k1bp,k1bm
# Apop + c9z <-> Apopc9z  k2p,k2m
# Apopc9z + c9z <-> Apopc9z2 k3p,k3m
# Apopc9z2 -> Apopc9a2    k3f
# Apopc9a2 <-> Apopc9a + c9a k4p,k4m
# Apopc9a <-> Apop + c9a   k4bp,k4bm
# c9a + IAP <-> IAP9     k5p,k5m
# Apopc9a + IAP <-> IAPA9  k5bp,k5bm
# Apopc9a2 + IAP <-> IAPA29 k5cp,k5cm

```

```

# c3z + c9a <-> c93      k6p,k6m
# c93 -> c3a + c9a      k6f
# c3z + Apopc9a2 <-> cA93  k6bp,k6bm
# cA93 -> c3a + Apopc9a2  k6bf
# c3a + IAP <-> IAP3    k7p,k7m
# c8a + Bid <-> c8B    k8p,k8m
# c8B -> c8a + tBid    k8f
# c3a + Bid <-> c3B    k8p,k8m
# c3B -> c3a + tBid    k8f
# c3a + Bcl2 <-> c3L   k9p,k9m
# c3L -> c3a + B2c    k9f
# tBid -> tBidmito    k11
# tBidmito + Bax -> tBidBax  k12a
# tBidBax + Bax -> tBid + Bax2 k12b
# Bcl2 + Bax -> *      k13
# Bax2 + Ccmito -> Cc + Bax2 k14
# REACTION RATES
r1p=k1p*Cc*Ap
r1m=k1m*CcAp
r1bp=k1bp*CcAp^p
r1bm=k1bm*Apop
r2p=k2p*Apop*c9z
r2m=k2m*Apopc9z
r3p=k3p*Apopc9z*c9z
r3m=k3m*Apopc9z2
r3f=k3f*Apopc9z2
r4p=k4p*Apopc9a2
r4m=k4m*Apopc9a*c9a
r4bp=k4bp*Apopc9a
r4bm=k4bm*Apop*c9a
r5p=k5p*c9a*IAP
r5m=k5m*IAP9
r5bp=k5bp*Apopc9a*IAP
r5bm=k5bm*IAPA9
r5cp=k5cp*Apopc9a2*IAP
r5cm=k5cm*IAPA29
r6p=k6p*c3z*c9a
r6m=k6m*c93
r6f=k6f*c93
r6bp=k6p*c3z*Apopc9a2
r6bm=k6m*cA93
r6bf=k6f*cA93
r7p=k7p*c3a*IAP
r7m=k7m*IAP3
r8p=k8p*c3a*Bid
r8m=k8m*c3B

```

$r8f=k8f*c3B$
 $r8pp=k8p*c8a*Bid$
 $r8mp=k8m*c8B$
 $r8fp=k8f*c8B$
 $r9p=k9p*c3a*Bcl2$
 $r9m=k9m*c3L$
 $r9f=k9f*c3L$
 $r11=k11*tbid$
 $r12a=k12a*tbidmito*bax$
 $r12b=k12b*tbidbax*bax$
 $r13=k13*bcl2*bax$
 $r14=k14*bax2*ccmito$
FLUXES
 $J1=r1p-r1m$
 $J1b=r1bp-r1bm$
 $J2=r2p-r2m$
 $J3=r3p-r3m$
 $J3f=r3f$
 $J4=r4p-r4m$
 $J4b=r4bp-r4bm$
 $J5=r5p-r5m$
 $J5b=r5bp-r5bm$
 $J5c=r5cp-r5cm$
 $J6=r6p-r6m$
 $J6f=r6f$
 $J6b=r6bp-r6bm$
 $J6bf=r6bf$
 $J7=r7p-r7m$
 $J8=r8p-r8m$
 $J8f=r8f$
 $J8p=r8pp-r8mp$
 $J8fp=r8fp$
 $J9=r9p-r9m$
 $J9f=r9f$
 $j11=r11$
 $j12a=r12a$
 $j12b=r12b$
 $j13=r13$
 $j14=r14$
PRODUCTION AND DEGRADATION RATES
 $Jp8=-\mu*c8a$
 $JAp=0.0001*a1-\mu*Ap$
 $JIAP=0.0001*a2-\mu*IAP$
 $Jp3=0.0001*a3-\mu*c3z$
 $Jp9=0.0001*a4-\mu*c9z$
 $jbidp=0.0001*a5-\mu*bid$

```

jbcl2p=0.0001*a6*p53thresh^4/(p53^4+p53thresh^4)-mu*bcl2
jbax=ombax*(1+p53^4/(p53^4+p53thresh^4))-mu*bax
jccmito=0.0001*a8-mu*ccmito
#ODE'S
bax'=jbax-j12a-j12b-j13
Bcl2'=-J9+jbcl2p-j13
cc'=j14-j1-mu*cc+mptp*ccmito
c3a'=J6f+J6bf-J7-J8+J8f-J9+J9f-mu*c3a
AP'=-J1+JAp
CcAp'=J1-7*J1b
Apop'=J1b-J2+J4b
Apopc9z'=J2-J3
Apopc9z2'=J3-J3f
Apopc9a2'=J3f-J4-J5c-J6b+J6bf
Apopc9a'=J4-J4b-J5b
c9a'=J4+J4b-J5-J6+J6f-mu*c9a
c9z'=-J2-J3+Jp9
IAP'=-J5-J5b-J5c-J7+JIAP
IAP9'=J5
IAPA9'=J5b
IAPA29'=J5c
IAP3'=J7
c3z'=-J6-J6b+Jp3-10*nop*c3z
c93'=J6-J6f
cA93'=J6b-J6bf
c8a'=Jp8-J8p+J8fp
Bid'=-J8-J8p+jbidp
c8B'=J8p-J8fp
c3B'=J8-J8f
c3L'=J9-J9f
tbid'=j8f+j8fp-j11+j12b-mu*tbid+tbid0
tbidbax'=j12a-j12b-mu*tbidbax
ccmito'=jccmito-j14-mptp*ccmito
bax2'=j12b-mu*bax2
tbidmito'=j11-j12a-mu*tbidmito
# PARAMETERS
par ombax=0.000024
par MPTP=0
par nop=0
par tbid0=0
par p53=0.0066
par p=4
par k1p=5,k1m=0.5
par k1bp=50000*a9,k1bm=0.5*a9
par k2p=10,k2m=0.5
par k3p=10,k3m=0.5,k3f=0.1

```

```

par k4p=5,k4m=0.5
par k4bp=5,k4bm=0.5
par k5p=5*a10,k5m=0.0035*a10
par k5bp=5*a10,k5bm=0.0035*a10
par k5cp=5*a10,k5cm=0.0035*a10
par k6p=10*a11,k6m=0.5*a11,k6f=0.001*a11
par k6bp=10*a11,k6bm=0.5*a11,k6bf=0.1*a11
par k7p=5*a10,k7m=0.0035*a10
par k8p=10,k8m=0.5,k8f=0.1
par k9p=10,k9m=0.5,k9f=0.1
par k11=10*a12,k12a=10*a12,k12b=10*a12,k13=10*a12,k14=10*a12
par a1=3,a2=0.3,a3=3,a4=3,a5=0.3,a6=0.8,a8=3,a9=1,a10=1,a11=1,a12=1,a13=3
mu=0.002*a13
par p53thresh=0.004
# INITIAL CONDITIONS
init Ap=.004,c9z=.004,c3z=.004,IAP=.004,Bid=.004,Bcl2=.004,bax=.004
init CcAp=0,Apop=0,Apopc9z=0,Apopc9z2=0,Apopc9a2=0,Apopc9a=0,c9a=0.00
init IAP3=0,IAP9=0,IAPA9=0,IAPA29=0,c93=0,cA93=0,c3a=0.004,c3B=0,c3L=0
init c8a=0.00005,c8B=0
init cc=0,ccmito=.004
# DISPLAY
@ xhi=10000,ylo=0,yhi=0.001
@ nplot=1,yp=c3a
# METHOD
@ meth=cvode,atol=1e-8,tol=1e-9,total=200000,dt=5,bounds=100000
done

```

A.1.4 Scripts used in Figure 12

```

# figure12A-point00008.ode
# REACTIONS
# om -> Ap
# om -> IAP
# om -> c3z
# om -> c9z
# om -> Bid
# om -> Bcl2
# om -> Bax
# om -> Ccmito
# c8a -> *
# c9a -> *
# c3a -> *
# Ap -> *
# IAP -> *

```

```

# c3z -> *
# c9z -> *
# Bcl2 -> *
# Bid -> *
# Bax -> *
# Ccmito -> *
# Bax -> *
# Bax2 -> *
# Cc -> *
# tBid -> *
# tBidBax -> *
# tBidmito -> *
# Cc + Ap <-> CcAp      k1p,k1m
# 7 CcAp <-> Apop      k1bp,k1bm
# Apop + c9z <-> Apopc9z  k2p,k2m
# Apopc9z + c9z <-> Apopc9z2 k3p,k3m
# Apopc9z2 -> Apopc9a2    k3f
# Apopc9a2 <-> Apopc9a + c9a k4p,k4m
# Apopc9a <-> Apop + c9a    k4bp,k4bm
# c9a + IAP <-> IAP9      k5p,k5m
# Apopc9a + IAP <-> IAPA9  k5bp,k5bm
# Apopc9a2 + IAP <-> IAPA29 k5cp,k5cm
# c3z + c9a <-> c93      k6p,k6m
# c93 -> c3a + c9a      k6f
# c3z + Apopc9a2 <-> cA93  k6bp,k6bm
# cA93 -> c3a + Apopc9a2  k6bf
# c3a + IAP <-> IAP3     k7p,k7m
# c8a + Bid <-> c8B     k8p,k8m
# c8B -> c8a + tBid     k8f
# c3a + Bid <-> c3B     k8p,k8m
# c3B -> c3a + tBid     k8f
# c3a + Bcl2 <-> c3L    k9p,k9m
# c3L -> c3a + B2c     k9f
# tBid -> tBidmito     k11
# tBidmito + Bax -> tBidBax k12a
# tBidBax + Bax -> tBid + Bax2 k12b
# Bcl2 + Bax -> *      k13
# Bax2 + Ccmito -> Cc + Bax2 k14
# REACTION RATES
r1p=k1p*Cc*Ap
r1m=k1m*CcAp
r1bp=k1bp*CcAp^p
r1bm=k1bm*Apop
r2p=k2p*Apop*c9z
r2m=k2m*Apopc9z
r3p=k3p*Apopc9z*c9z

```

$r3m=k3m*Apopc9z2$
 $r3f=k3f*Apopc9z2$
 $r4p=k4p*Apopc9a2$
 $r4m=k4m*Apopc9a*c9a$
 $r4bp=k4bp*Apopc9a$
 $r4bm=k4bm*Apop*c9a$
 $r5p=k5p*c9a*IAP$
 $r5m=k5m*IAP9$
 $r5bp=k5bp*Apopc9a*IAP$
 $r5bm=k5bm*IAPA9$
 $r5cp=k5cp*Apopc9a2*IAP$
 $r5cm=k5cm*IAPA29$
 $r6p=k6p*c3z*c9a$
 $r6m=k6m*c93$
 $r6f=k6f*c93$
 $r6bp=k6p*c3z*Apopc9a2$
 $r6bm=k6m*cA93$
 $r6bf=k6f*cA93$
 $r7p=k7p*c3a*IAP$
 $r7m=k7m*IAP3$
 $r8p=k8p*c3a*Bid$
 $r8m=k8m*c3B$
 $r8f=k8f*c3B$
 $r8pp=k8p*c8a*Bid$
 $r8mp=k8m*c8B$
 $r8fp=k8f*c8B$
 $r9p=k9p*c3a*Bcl2$
 $r9m=k9m*c3L$
 $r9f=k9f*c3L$
 $r11=k11*tbid$
 $r12a=k12a*tbidmito*bax$
 $r12b=k12b*tbidbax*bax$
 $r13=k13*bcl2*bax$
 $r14=k14*bax2*ccmito$
FLUXES
 $J1=r1p-r1m$
 $J1b=r1bp-r1bm$
 $J2=r2p-r2m$
 $J3=r3p-r3m$
 $J3f=r3f$
 $J4=r4p-r4m$
 $J4b=r4bp-r4bm$
 $J5=r5p-r5m$
 $J5b=r5bp-r5bm$
 $J5c=r5cp-r5cm$
 $J6=r6p-r6m$

$J6f=r6f$
 $J6b=r6bp-r6bm$
 $J6bf=r6bf$
 $J7=r7p-r7m$
 $J8=r8p-r8m$
 $J8f=r8f$
 $J8p=r8pp-r8mp$
 $J8fp=r8fp$
 $J9=r9p-r9m$
 $J9f=r9f$
 $j11=r11$
 $j12a=r12a$
 $j12b=r12b$
 $j13=r13$
 $j14=r14$
PRODUCTION AND DEGRADATION RATES
 $Jp8=-\mu*c8a$
 $JAp=0.0001*a1-\mu*Ap$
 $JIAP=0.0001*a2-\mu*IAP$
 $Jp3=0.0001*a3-\mu*c3z$
 $Jp9=0.0001*a4-\mu*c9z$
 $jbidp=0.0001*a5-\mu*bid$
 $jbcl2p=0.0001*a6*p53thresh^4/(p53^4+p53thresh^4)-\mu*bcl2$
 $jbax=0.0001*a7*(1+p53^4/(p53^4+p53thresh^4))-mubax*bax$
 $jccmito=0.0001*a8-\mu*ccmito$
ODE'S
 $bax'=jbax-j12a-j12b-j13$
 $Bcl2'=-J9+jbcl2p-j13$
 $cc'=j14-j1-\mu*cc+mptp*ccmito$
 $c3a'=J6f+J6bf-J7-J8+J8f-J9+J9f-\mu*c3a$
 $AP'=-J1+JAp$
 $CcAp'=J1-7*J1b$
 $Apop'=J1b-J2+J4b$
 $Apopc9z'=J2-J3$
 $Apopc9z2'=J3-J3f$
 $Apopc9a2'=J3f-J4-J5c-J6b+J6bf$
 $Apopc9a'=J4-J4b-J5b$
 $c9a'=J4+J4b-J5-J6+J6f-\mu*c9a$
 $c9z'=-J2-J3+Jp9$
 $IAP'=-J5-J5b-J5c-J7+JIAP$
 $IAP9'=J5$
 $IAPA9'=J5b$
 $IAPA29'=J5c$
 $IAP3'=J7$
 $c3z'=-J6-J6b+Jp3-10*nop*c3z$
 $c93'=J6-J6f$

```

cA93'=J6b-J6bf
c8a'=Jp8-J8p+J8fp
Bid'=-J8-J8p+jbidp
c8B'=J8p-J8fp
c3B'=J8-J8f
c3L'=J9-J9f
tbid'=j8f+j8fp-j11+j12b-mu*tbid+tbid0
tbidbax'=j12a-j12b-mu*tbidbax
ccmito'=jccmito-j14-mptp*ccmito
bax2'=j12b-mu*bax2
tbidmito'=j11-j12a-mu*tbidmito
# PARAMETERS
par p=4
par mubax=0.001
par MPTP=0
par nop=0
par tbid0=0
par p53=0.0066
par k1p=5,k1m=0.5
par k1bp=50000*a9,k1bm=0.5*a9
par k2p=10,k2m=0.5
par k3p=10,k3m=0.5,k3f=0.1
par k4p=5,k4m=0.5
par k4bp=5,k4bm=0.5
par k5p=5*a10,k5m=0.0035*a10
par k5bp=5*a10,k5bm=0.0035*a10
par k5cp=5*a10,k5cm=0.0035*a10
par k6p=10*a11,k6m=0.5*a11,k6f=0.001*a11
par k6bp=10*a11,k6bm=0.5*a11,k6bf=0.1*a11
par k7p=5*a10,k7m=0.0035*a10
par k8p=10,k8m=0.5,k8f=0.1
par k9p=10,k9m=0.5,k9f=0.1
par k11=10*a12,k12a=10*a12,k12b=10*a12,k13=10*a12,k14=10*a12
par a1=3,a2=0.3,a3=3,a4=3,a5=0.3,a6=0.8,a7=0.3,a8=3,a9=1,a10=1,a11=1,a12=1,a13=3
mu=0.002*a13
par p53thresh=0.004
# INITIAL CONDITIONS
init Ap=.004,c9z=.004,c3z=.004,IAP=.004,Bid=.004,Bcl2=.004,bax=.004
init CcAp=0,Apop=0,Apopc9z=0,Apopc9z2=0,Apopc9a2=0,Apopc9a=0,c9a=0.00
init IAP3=0,IAP9=0,IAPA9=0,IAPA29=0,c93=0,cA93=0,c3a=0.004,c3B=0,c3L=0
init c8a=0.0000,c8B=0
init cc=0,ccmito=.004
# DISPLAY
@ xhi=10000,ylo=0,yhi=0.001
@ nplot=1,yp=c3a
# METHOD

```

@ meth=cvode,atol=1e-8,tol=1e-9,total=200000,dt=5,bounds=100000
done

```
# figure12A-point00032.ode
# REACTIONS
# om -> Ap
# om -> IAP
# om -> c3z
# om -> c9z
# om -> Bid
# om -> Bcl2
# om -> Bax
# om -> Ccmito
# c8a -> *
# c9a -> *
# c3a -> *
# Ap -> *
# IAP -> *
# c3z -> *
# c9z -> *
# Bcl2 -> *
# Bid -> *
# Bax -> *
# Ccmito -> *
# Bax -> *
# Bax2 -> *
# Cc -> *
# tBid -> *
# tBidBax -> *
# tBidmito -> *
# Cc + Ap <-> CcAp      k1p,k1m
# 7 CcAp <-> Apop      k1bp,k1bm
# Apop + c9z <-> Apopc9z  k2p,k2m
# Apopc9z + c9z <-> Apopc9z2 k3p,k3m
# Apopc9z2 -> Apopc9a2      k3f
# Apopc9a2 <-> Apopc9a + c9a k4p,k4m
# Apopc9a <-> Apop + c9a    k4bp,k4bm
# c9a + IAP <-> IAP9      k5p,k5m
# Apopc9a + IAP <-> IAPA9   k5bp,k5bm
# Apopc9a2 + IAP <-> IAPA29 k5cp,k5cm
# c3z + c9a <-> c93      k6p,k6m
# c93 -> c3a + c9a      k6f
# c3z + Apopc9a2 <-> cA93   k6bp,k6bm
# cA93 -> c3a + Apopc9a2   k6bf
```

```

# c3a + IAP <-> IAP3    k7p,k7m
# c8a + Bid <-> c8B      k8p,k8m
# c8B -> c8a + tBid      k8f
# c3a + Bid <-> c3B      k8p,k8m
# c3B -> c3a + tBid      k8f
# c3a + Bcl2 <-> c3L    k9p,k9m
# c3L -> c3a + B2c      k9f
# tBid -> tBidmito      k11
# tBidmito + Bax -> tBidBax k12a
# tBidBax + Bax -> tBid + Bax2 k12b
# Bcl2 + Bax -> *        k13
# Bax2 + Ccmito -> Cc + Bax2 k14
# REACTION RATES
r1p=k1p*Cc*Ap
r1m=k1m*CcAp
r1bp=k1bp*CcAp^p
r1bm=k1bm*Apop
r2p=k2p*Apop*c9z
r2m=k2m*Apopc9z
r3p=k3p*Apopc9z*c9z
r3m=k3m*Apopc9z2
r3f=k3f*Apopc9z2
r4p=k4p*Apopc9a2
r4m=k4m*Apopc9a*c9a
r4bp=k4bp*Apopc9a
r4bm=k4bm*Apop*c9a
r5p=k5p*c9a*IAP
r5m=k5m*IAP9
r5bp=k5bp*Apopc9a*IAP
r5bm=k5bm*IAPA9
r5cp=k5cp*Apopc9a2*IAP
r5cm=k5cm*IAPA29
r6p=k6p*c3z*c9a
r6m=k6m*c93
r6f=k6f*c93
r6bp=k6p*c3z*Apopc9a2
r6bm=k6m*cA93
r6bf=k6f*cA93
r7p=k7p*c3a*IAP
r7m=k7m*IAP3
r8p=k8p*c3a*Bid
r8m=k8m*c3B
r8f=k8f*c3B
r8pp=k8p*c8a*Bid
r8mp=k8m*c8B
r8fp=k8f*c8B

```

```

r9p=k9p*c3a*Bcl2
r9m=k9m*c3L
r9f=k9f*c3L
r11=k11*tbid
r12a=k12a*tbidmito*bax
r12b=k12b*tbidbax*bax
r13=k13*bcl2*bax
r14=k14*bax2*ccmito
# FLUXES
J1=r1p-r1m
J1b=r1bp-r1bm
J2=r2p-r2m
J3=r3p-r3m
J3f=r3f
J4=r4p-r4m
J4b=r4bp-r4bm
J5=r5p-r5m
J5b=r5bp-r5bm
J5c=r5cp-r5cm
J6=r6p-r6m
J6f=r6f
J6b=r6bp-r6bm
J6bf=r6bf
J7=r7p-r7m
J8=r8p-r8m
J8f=r8f
J8p=r8pp-r8mp
J8fp=r8fp
J9=r9p-r9m
J9f=r9f
j11=r11
j12a=r12a
j12b=r12b
j13=r13
j14=r14
# PRODUCTION AND DEGRADATION RATES
Jp8=-mu*c8a
JAp=0.0001*a1-mu*Ap
JIAP=0.0001*a2-mu*IAP
Jp3=0.0001*a3-mu*c3z
Jp9=0.0001*a4-mu*c9z
jbidp=0.0001*a5-mu*bid
jbcl2p=ombcl2*p53thresh^4/(p53^4+p53thresh^4)-mu*bcl2
jbax=0.0001*a7*(1+p53^4/(p53^4+p53thresh^4))-mubax*bax
jccmito=0.0001*a8-mu*ccmito
# ODE'S

```

bax'=jbax-j12a-j12b-j13
 Bcl2'=-J9+jbcl2p-j13
 cc'=j14-j1-mu*cc+mptp*ccmito
 c3a'=J6f+J6bf-J7-J8+J8f-J9+J9f-mu*c3a
 AP'=-J1+JAp
 CcAp'=J1-7*J1b
 Apop'=J1b-J2+J4b
 Apopc9z'=J2-J3
 Apopc9z2'=J3-J3f
 Apopc9a2'=J3f-J4-J5c-J6b+J6bf
 Apopc9a'=J4-J4b-J5b
 c9a'=J4+J4b-J5-J6+J6f-mu*c9a
 c9z'=-J2-J3+Jp9
 IAP'=-J5-J5b-J5c-J7+JIAP
 IAP9'=J5
 IAPA9'=J5b
 IAPA29'=J5c
 IAP3'=J7
 c3z'=-J6-J6b+Jp3-10*nop*c3z
 c93'=J6-J6f
 cA93'=J6b-J6bf
 c8a'=Jp8-J8p+J8fp
 Bid'=-J8-J8p+jbidp
 c8B'=J8p-J8fp
 c3B'=J8-J8f
 c3L'=J9-J9f
 tbid'=j8f+j8fp-j11+j12b-mu*tbid+tbid0
 tbidbax'=j12a-j12b-mu*tbidbax
 ccmito'=jccmito-j14-mptp*ccmito
 bax2'=j12b-mu*bax2
 tbidmito'=j11-j12a-mu*tbidmito
 # PARAMETERS
 par mubax=0.001
 par MPTP=0
 par nop=0
 par tbid0=0
 par p53=0.0066
 par ombcl2=0.00032
 par p=4
 par k1p=5,k1m=0.5
 par k1bp=50000*a9,k1bm=0.5*a9
 par k2p=10,k2m=0.5
 par k3p=10,k3m=0.5,k3f=0.1
 par k4p=5,k4m=0.5
 par k4bp=5,k4bm=0.5
 par k5p=5*a10,k5m=0.0035*a10

```

par k5bp=5*a10,k5bm=0.0035*a10
par k5cp=5*a10,k5cm=0.0035*a10
par k6p=10*a11,k6m=0.5*a11,k6f=0.001*a11
par k6bp=10*a11,k6bm=0.5*a11,k6bf=0.1*a11
par k7p=5*a10,k7m=0.0035*a10
par k8p=10,k8m=0.5,k8f=0.1
par k9p=10,k9m=0.5,k9f=0.1
par k11=10*a12,k12a=10*a12,k12b=10*a12,k13=10*a12,k14=10*a12
par a1=3,a2=0.3,a3=3,a4=3,a5=0.3,a7=0.3,a8=3,a9=1,a10=1,a11=1,a12=1,a13=3
mu=0.002*a13
par p53thresh=0.004
# INITIAL CONDITIONS
init Ap=.004,c9z=.004,c3z=.004,IAP=.004,Bid=.004,Bcl2=.004,bax=.004
init CcAp=0,Apop=0,Apopc9z=0,Apopc9z2=0,Apopc9a2=0,Apopc9a=0,c9a=0.00
init IAP3=0,IAP9=0,IAPA9=0,IAPA29=0,c93=0,cA93=0,c3a=0.1,c3B=0,c3L=0
init c8a=0.0000,c8B=0
init cc=0,ccmito=.004
# DISPLAY
@ xhi=10000,ylo=0,yhi=0.001
@ nplot=1,yp=c3a
# METHOD
@ meth=cvode,atol=1e-8,tol=1e-9,total=200000,dt=5,bounds=100000
done
*****

```

```

# figure12A-point0008.ode
# REACTIONS
# om -> Ap
# om -> IAP
# om -> c3z
# om -> c9z
# om -> Bid
# om -> Bcl2
# om -> Bax
# om -> Ccmito
# c8a -> *
# c9a -> *
# c3a -> *
# Ap -> *
# IAP -> *
# c3z -> *
# c9z -> *
# Bcl2 -> *
# Bid -> *
# Bax -> *

```

```

# Ccmto -> *
# Bax -> *
# Bax2 -> *
# Cc -> *
# tBid -> *
# tBidBax -> *
# tBidmito -> *
# Cc + Ap <-> CcAp      k1p,k1m
# 7 CcAp <-> Apop      k1bp,k1bm
# Apop + c9z <-> Apopc9z  k2p,k2m
# Apopc9z + c9z <-> Apopc9z2 k3p,k3m
# Apopc9z2 -> Apopc9a2    k3f
# Apopc9a2 <-> Apopc9a + c9a k4p,k4m
# Apopc9a <-> Apop + c9a    k4bp,k4bm
# c9a + IAP <-> IAP9      k5p,k5m
# Apopc9a + IAP <-> IAPA9  k5bp,k5bm
# Apopc9a2 + IAP <-> IAPA29 k5cp,k5cm
# c3z + c9a <-> c93      k6p,k6m
# c93 -> c3a + c9a      k6f
# c3z + Apopc9a2 <-> cA93  k6bp,k6bm
# cA93 -> c3a + Apopc9a2  k6bf
# c3a + IAP <-> IAP3     k7p,k7m
# c8a + Bid <-> c8B      k8p,k8m
# c8B -> c8a + tBid     k8f
# c3a + Bid <-> c3B      k8p,k8m
# c3B -> c3a + tBid     k8f
# c3a + Bcl2 <-> c3L     k9p,k9m
# c3L -> c3a + B2c      k9f
# tBid -> tBidmito      k11
# tBidmito + Bax -> tBidBax k12a
# tBidBax + Bax -> tBid + Bax2 k12b
# Bcl2 + Bax -> *      k13
# Bax2 + Ccmto -> Cc + Bax2 k14
# REACTION RATES
r1p=k1p*Cc*Ap
r1m=k1m*CcAp
r1bp=k1bp*CcAp^p
r1bm=k1bm*Apop
r2p=k2p*Apop*c9z
r2m=k2m*Apopc9z
r3p=k3p*Apopc9z*c9z
r3m=k3m*Apopc9z2
r3f=k3f*Apopc9z2
r4p=k4p*Apopc9a2
r4m=k4m*Apopc9a*c9a
r4bp=k4bp*Apopc9a

```

$r4bm = k4bm * Apop * c9a$
 $r5p = k5p * c9a * IAP$
 $r5m = k5m * IAP9$
 $r5bp = k5bp * Apopc9a * IAP$
 $r5bm = k5bm * IAPA9$
 $r5cp = k5cp * Apopc9a2 * IAP$
 $r5cm = k5cm * IAPA29$
 $r6p = k6p * c3z * c9a$
 $r6m = k6m * c93$
 $r6f = k6f * c93$
 $r6bp = k6p * c3z * Apopc9a2$
 $r6bm = k6m * cA93$
 $r6bf = k6f * cA93$
 $r7p = k7p * c3a * IAP$
 $r7m = k7m * IAP3$
 $r8p = k8p * c3a * Bid$
 $r8m = k8m * c3B$
 $r8f = k8f * c3B$
 $r8pp = k8p * c8a * Bid$
 $r8mp = k8m * c8B$
 $r8fp = k8f * c8B$
 $r9p = k9p * c3a * Bcl2$
 $r9m = k9m * c3L$
 $r9f = k9f * c3L$
 $r11 = k11 * tbid$
 $r12a = k12a * tbidmito * bax$
 $r12b = k12b * tbidbax * bax$
 $r13 = k13 * bcl2 * bax$
 $r14 = k14 * bax2 * ccmito$
FLUXES
 $J1 = r1p - r1m$
 $J1b = r1bp - r1bm$
 $J2 = r2p - r2m$
 $J3 = r3p - r3m$
 $J3f = r3f$
 $J4 = r4p - r4m$
 $J4b = r4bp - r4bm$
 $J5 = r5p - r5m$
 $J5b = r5bp - r5bm$
 $J5c = r5cp - r5cm$
 $J6 = r6p - r6m$
 $J6f = r6f$
 $J6b = r6bp - r6bm$
 $J6bf = r6bf$
 $J7 = r7p - r7m$
 $J8 = r8p - r8m$

```

J8f=r8f
J8p=r8pp-r8mp
J8fp=r8fp
J9=r9p-r9m
J9f=r9f
j11=r11
j12a=r12a
j12b=r12b
j13=r13
j14=r14
# PRODUCTION AND DEGRADATION RATES
Jp8=-mu*c8a
JAp=0.0001*a1-mu*Ap
JIAP=0.0001*a2-mu*IAP
Jp3=0.0001*a3-mu*c3z
Jp9=0.0001*a4-mu*c9z
jbidp=0.0001*a5-mu*bid
jbcl2p=ombcl2*p53thresh^4/(p53^4+p53thresh^4)-mu*bcl2
jbax=0.0001*a7*(1+p53^4/(p53^4+p53thresh^4))-mubax*bax
jccmito=0.0001*a8-mu*ccmito
# ODE'S
bax'=jbax-j12a-j12b-j13
Bcl2'=-J9+jbcl2p-j13
cc'=j14-j1-mu*cc+mptp*ccmito
c3a'=J6f+J6bf-J7-J8+J8f-J9+J9f-mu*c3a
AP'=-J1+JAp
CcAp'=J1-7*J1b
Apop'=J1b-J2+J4b
Apopc9z'=J2-J3
Apopc9z2'=J3-J3f
Apopc9a2'=J3f-J4-J5c-J6b+J6bf
Apopc9a'=J4-J4b-J5b
c9a'=J4+J4b-J5-J6+J6f-mu*c9a
c9z'=-J2-J3+Jp9
IAP'=-J5-J5b-J5c-J7+JIAP
IAP9'=J5
IAPA9'=J5b
IAPA29'=J5c
IAP3'=J7
c3z'=-J6-J6b+Jp3-10*nop*c3z
c93'=J6-J6f
cA93'=J6b-J6bf
c8a'=Jp8-J8p+J8fp
Bid'=-J8-J8p+jbidp
c8B'=J8p-J8fp
c3B'=J8-J8f

```

```

c3L'=J9-J9f
tbid'=j8f+j8fp-j11+j12b-mu*tbid+tbid0
tbidbax'=j12a-j12b-mu*tbidbax
ccmito'=jccmito-j14-mptp*ccmito
bax2'=j12b-mu*bax2
tbidmito'=j11-j12a-mu*tbidmito
# PARAMETERS
par mubax=0.001
par MPTP=0
par nop=0
par tbid0=0
par p53=0.0066
par ombcl2=0.0008
par p=4
par k1p=5,k1m=0.5
par k1bp=50000*a9,k1bm=0.5*a9
par k2p=10,k2m=0.5
par k3p=10,k3m=0.5,k3f=0.1
par k4p=5,k4m=0.5
par k4bp=5,k4bm=0.5
par k5p=5*a10,k5m=0.0035*a10
par k5bp=5*a10,k5bm=0.0035*a10
par k5cp=5*a10,k5cm=0.0035*a10
par k6p=10*a11,k6m=0.5*a11,k6f=0.001*a11
par k6bp=10*a11,k6bm=0.5*a11,k6bf=0.1*a11
par k7p=5*a10,k7m=0.0035*a10
par k8p=10,k8m=0.5,k8f=0.1
par k9p=10,k9m=0.5,k9f=0.1
par k11=10*a12,k12a=10*a12,k12b=10*a12,k13=10*a12,k14=10*a12
par a1=3,a2=0.3,a3=3,a4=3,a5=0.3,a7=0.3,a8=3,a9=1,a10=1,a11=1,a12=1,a13=3
mu=0.002*a13
par p53thresh=0.004
# INITIAL CONDITIONS
init Ap=.004,c9z=.004,c3z=.004,IAP=.004,Bid=.004,Bcl2=.004,bax=.004
init CcAp=0,Apop=0,Apopc9z=0,Apopc9z2=0,Apopc9a2=0,Apopc9a=0,c9a=0.00
init IAP3=0,IAP9=0,IAPA9=0,IAPA29=0,c93=0,cA93=0,c3a=0.1,c3B=0,c3L=0
init c8a=0.0000,c8B=0
init cc=0,ccmito=.004
# DISPLAY
@ xhi=10000,ylo=0,yhi=0.001
@ nplot=1,yp=c3a
# METHOD
@ meth=cvode,atol=1e-8,tol=1e-9,total=200000,dt=5,bounds=100000
done
*****

```

```

# figure12B-point00008.ode
# REACTIONS
# om -> Ap
# om -> IAP
# om -> c3z
# om -> c9z
# om -> Bid
# om -> Bcl2
# om -> Bax
# om -> Ccmito
# c8a -> *
# c9a -> *
# c3a -> *
# Ap -> *
# IAP -> *
# c3z -> *
# c9z -> *
# Bcl2 -> *
# Bid -> *
# Bax -> *
# Ccmito -> *
# Bax -> *
# Bax2 -> *
# Cc -> *
# tBid -> *
# tBidBax -> *
# tBidmito -> *
# Cc + Ap <-> CcAp      k1p,k1m
# 7 CcAp <-> Apop      k1bp,k1bm
# Apop + c9z <-> Apopc9z  k2p,k2m
# Apopc9z + c9z <-> Apopc9z2 k3p,k3m
# Apopc9z2 -> Apopc9a2    k3f
# Apopc9a2 <-> Apopc9a + c9a k4p,k4m
# Apopc9a <-> Apop + c9a    k4bp,k4bm
# c9a + IAP <-> IAP9      k5p,k5m
# Apopc9a + IAP <-> IAPA9   k5bp,k5bm
# Apopc9a2 + IAP <-> IAPA29 k5cp,k5cm
# c3z + c9a <-> c93      k6p,k6m
# c93 -> c3a + c9a      k6f
# c3z + Apopc9a2 <-> cA93   k6bp,k6bm
# cA93 -> c3a + Apopc9a2   k6bf
# c3a + IAP <-> IAP3      k7p,k7m
# c8a + Bid <-> c8B      k8p,k8m
# c8B -> c8a + tBid     k8f
# c3a + Bid <-> c3B      k8p,k8m
# c3B -> c3a + tBid     k8f

```

```

# c3a + Bcl2 <-> c3L      k9p,k9m
# c3L -> c3a + B2c      k9f
# tBid -> tBidmito      k11
# tBidmito + Bax -> tBidBax  k12a
# tBidBax + Bax -> tBid + Bax2 k12b
# Bcl2 + Bax -> *      k13
# Bax2 + Ccmito -> Cc + Bax2 k14
# REACTION RATES
r1p=k1p*Cc*Ap
r1m=k1m*CcAp
r1bp=k1bp*CcAp^p
r1bm=k1bm*Apop
r2p=k2p*Apop*c9z
r2m=k2m*Apopc9z
r3p=k3p*Apopc9z*c9z
r3m=k3m*Apopc9z2
r3f=k3f*Apopc9z2
r4p=k4p*Apopc9a2
r4m=k4m*Apopc9a*c9a
r4bp=k4bp*Apopc9a
r4bm=k4bm*Apop*c9a
r5p=k5p*c9a*IAP
r5m=k5m*IAP9
r5bp=k5bp*Apopc9a*IAP
r5bm=k5bm*IAPA9
r5cp=k5cp*Apopc9a2*IAP
r5cm=k5cm*IAPA29
r6p=k6p*c3z*c9a
r6m=k6m*c93
r6f=k6f*c93
r6bp=k6p*c3z*Apopc9a2
r6bm=k6m*cA93
r6bf=k6f*cA93
r7p=k7p*c3a*IAP
r7m=k7m*IAP3
r8p=k8p*c3a*Bid
r8m=k8m*c3B
r8f=k8f*c3B
r8pp=k8p*c8a*Bid
r8mp=k8m*c8B
r8fp=k8f*c8B
r9p=k9p*c3a*Bcl2
r9m=k9m*c3L
r9f=k9f*c3L
r11=k11*tbid
r12a=k12a*tbidmito*bax

```

```

r12b=k12b*tbidbax*bax
r13=k13*bcl2*bax
r14=k14*bax2*ccmito
# FLUXES
J1=r1p-r1m
J1b=r1bp-r1bm
J2=r2p-r2m
J3=r3p-r3m
J3f=r3f
J4=r4p-r4m
J4b=r4bp-r4bm
J5=r5p-r5m
J5b=r5bp-r5bm
J5c=r5cp-r5cm
J6=r6p-r6m
J6f=r6f
J6b=r6bp-r6bm
J6bf=r6bf
J7=r7p-r7m
J8=r8p-r8m
J8f=r8f
J8p=r8pp-r8mp
J8fp=r8fp
J9=r9p-r9m
J9f=r9f
j11=r11
j12a=r12a
j12b=r12b
j13=r13
j14=r14
# PRODUCTION AND DEGRADATION RATES
Jp8=-mu*c8a
JAp=0.0001*a1-mu*Ap
JIAP=0.0001*a2-mu*IAP
Jp3=0.0001*a3-mu*c3z
Jp9=0.0001*a4-mu*c9z
jbidp=0.0001*a5-mu*bid
jbcl2p=0.0001*a6*p53thresh^4/(p53^4+p53thresh^4)-mu*bcl2
jbax=ombax*(1+p53^4/(p53^4+p53thresh^4))-mu*bax
jccmito=0.0001*a8-mu*ccmito
# ODE'S
bax'=jbax-j12a-j12b-j13
Bcl2'=-J9+jbcl2p-j13
cc'=j14-j1-mu*cc+mptp*ccmito
c3a'=J6f+J6bf-J7-J8+J8f-J9+J9f-mu*c3a
AP'=-J1+JAp

```

CcAp'=J1-7*J1b
Apop'=J1b-J2+J4b
Apopc9z'=J2-J3
Apopc9z2'=J3-J3f
Apopc9a2'=J3f-J4-J5c-J6b+J6bf
Apopc9a'=J4-J4b-J5b
c9a'=J4+J4b-J5-J6+J6f-mu*c9a
c9z'=-J2-J3+Jp9
IAP'=-J5-J5b-J5c-J7+JIAP
IAP9'=J5
IAPA9'=J5b
IAPA29'=J5c
IAP3'=J7
c3z'=-J6-J6b+Jp3-10*nop*c3z
c93'=J6-J6f
cA93'=J6b-J6bf
c8a'=Jp8-J8p+J8fp
Bid'=-J8-J8p+jbidp
c8B'=J8p-J8fp
c3B'=J8-J8f
c3L'=J9-J9f
tbid'=j8f+j8fp-j11+j12b-mu*tbid+tbid0
tbidbax'=j12a-j12b-mu*tbidbax
ccmito'=jccmito-j14-mptp*ccmito
bax2'=j12b-mu*bax2
tbidmito'=j11-j12a-mu*tbidmito
PARAMETERS
par ombax=0.000024
par MPTP=0
par nop=0
par tbid0=0
par p53=0.0066
par p=4
par k1p=5,k1m=0.5
par k1bp=50000*a9,k1bm=0.5*a9
par k2p=10,k2m=0.5
par k3p=10,k3m=0.5,k3f=0.1
par k4p=5,k4m=0.5
par k4bp=5,k4bm=0.5
par k5p=5*a10,k5m=0.0035*a10
par k5bp=5*a10,k5bm=0.0035*a10
par k5cp=5*a10,k5cm=0.0035*a10
par k6p=10*a11,k6m=0.5*a11,k6f=0.001*a11
par k6bp=10*a11,k6bm=0.5*a11,k6bf=0.1*a11
par k7p=5*a10,k7m=0.0035*a10
par k8p=10,k8m=0.5,k8f=0.1

```

par k9p=10,k9m=0.5,k9f=0.1
par k11=10*a12,k12a=10*a12,k12b=10*a12,k13=10*a12,k14=10*a12
par a1=3,a2=0.3,a3=3,a4=3,a5=0.3,a6=0.8,a8=3,a9=1,a10=1,a11=1,a12=1,a13=3
mu=0.002*a13
par p53thresh=0.004
# INITIAL CONDITIONS
init Ap=.004,c9z=.004,c3z=.004,IAP=.004,Bid=.004,Bcl2=.004,bax=.004
init CcAp=0,Apop=0,Apopc9z=0,Apopc9z2=0,Apopc9a2=0,Apopc9a=0,c9a=0.00
init IAP3=0,IAP9=0,IAPA9=0,IAPA29=0,c93=0,cA93=0,c3a=0.004,c3B=0,c3L=0
init c8a=0.00005,c8B=0
init cc=0,ccmito=.004
# DISPLAY
@ xhi=10000,ylo=0,yhi=0.001
@ nplot=1,yp=c3a
# METHOD
@ meth=cvode,atol=1e-8,tol=1e-9,total=200000,dt=5,bounds=100000
done
*****

# figure12B-point00032.ode
# REACTIONS
# om -> Ap
# om -> IAP
# om -> c3z
# om -> c9z
# om -> Bid
# om -> Bcl2
# om -> Bax
# om -> Ccmito
# c8a -> *
# c9a -> *
# c3a -> *
# Ap -> *
# IAP -> *
# c3z -> *
# c9z -> *
# Bcl2 -> *
# Bid -> *
# Bax -> *
# Ccmito -> *
# Bax -> *
# Bax2 -> *
# Cc -> *
# tBid -> *
# tBidBax -> *
# tBidmito -> *

```

```

# Cc + Ap <-> CcAp      k1p,k1m
# 7 CcAp <-> Apop      k1bp,k1bm
# Apop + c9z <-> Apopc9z  k2p,k2m
# Apopc9z + c9z <-> Apopc9z2 k3p,k3m
# Apopc9z2 -> Apopc9a2    k3f
# Apopc9a2 <-> Apopc9a + c9a k4p,k4m
# Apopc9a <-> Apop + c9a    k4bp,k4bm
# c9a + IAP <-> IAP9     k5p,k5m
# Apopc9a + IAP <-> IAPA9  k5bp,k5bm
# Apopc9a2 + IAP <-> IAPA29 k5cp,k5cm
# c3z + c9a <-> c93      k6p,k6m
# c93 -> c3a + c9a      k6f
# c3z + Apopc9a2 <-> cA93  k6bp,k6bm
# cA93 -> c3a + Apopc9a2  k6bf
# c3a + IAP <-> IAP3     k7p,k7m
# c8a + Bid <-> c8B     k8p,k8m
# c8B -> c8a + tBid     k8f
# c3a + Bid <-> c3B     k8p,k8m
# c3B -> c3a + tBid     k8f
# c3a + Bcl2 <-> c3L    k9p,k9m
# c3L -> c3a + B2c     k9f
# tBid -> tBidmito     k11
# tBidmito + Bax -> tBidBax k12a
# tBidBax + Bax -> tBid + Bax2 k12b
# Bcl2 + Bax -> *      k13
# Bax2 + Ccmito -> Cc + Bax2 k14
# REACTION RATES
r1p=k1p*Cc*Ap
r1m=k1m*CcAp
r1bp=k1bp*CcAp^p
r1bm=k1bm*Apop
r2p=k2p*Apop*c9z
r2m=k2m*Apopc9z
r3p=k3p*Apopc9z*c9z
r3m=k3m*Apopc9z2
r3f=k3f*Apopc9z2
r4p=k4p*Apopc9a2
r4m=k4m*Apopc9a*c9a
r4bp=k4bp*Apopc9a
r4bm=k4bm*Apop*c9a
r5p=k5p*c9a*IAP
r5m=k5m*IAP9
r5bp=k5bp*Apopc9a*IAP
r5bm=k5bm*IAPA9
r5cp=k5cp*Apopc9a2*IAP
r5cm=k5cm*IAPA29

```

$r6p=k6p*c3z*c9a$
 $r6m=k6m*c93$
 $r6f=k6f*c93$
 $r6bp=k6p*c3z*Apopc9a2$
 $r6bm=k6m*cA93$
 $r6bf=k6f*cA93$
 $r7p=k7p*c3a*IAP$
 $r7m=k7m*IAP3$
 $r8p=k8p*c3a*Bid$
 $r8m=k8m*c3B$
 $r8f=k8f*c3B$
 $r8pp=k8p*c8a*Bid$
 $r8mp=k8m*c8B$
 $r8fp=k8f*c8B$
 $r9p=k9p*c3a*Bcl2$
 $r9m=k9m*c3L$
 $r9f=k9f*c3L$
 $r11=k11*tbid$
 $r12a=k12a*tbidmito*bax$
 $r12b=k12b*tbidbax*bax$
 $r13=k13*bcl2*bax$
 $r14=k14*bax2*ccmito$
FLUXES
 $J1=r1p-r1m$
 $J1b=r1bp-r1bm$
 $J2=r2p-r2m$
 $J3=r3p-r3m$
 $J3f=r3f$
 $J4=r4p-r4m$
 $J4b=r4bp-r4bm$
 $J5=r5p-r5m$
 $J5b=r5bp-r5bm$
 $J5c=r5cp-r5cm$
 $J6=r6p-r6m$
 $J6f=r6f$
 $J6b=r6bp-r6bm$
 $J6bf=r6bf$
 $J7=r7p-r7m$
 $J8=r8p-r8m$
 $J8f=r8f$
 $J8p=r8pp-r8mp$
 $J8fp=r8fp$
 $J9=r9p-r9m$
 $J9f=r9f$
 $j11=r11$
 $j12a=r12a$

```

j12b=r12b
j13=r13
j14=r14
# PRODUCTION AND DEGRADATION RATES
Jp8=-mu*c8a
JAp=0.0001*a1-mu*Ap
JIAP=0.0001*a2-mu*IAP
Jp3=0.0001*a3-mu*c3z
Jp9=0.0001*a4-mu*c9z
jbidp=0.0001*a5-mu*bid
jbcl2p=ombcl2*p53thresh^4/(p53^4+p53thresh^4)-mu*bcl2
jbax=ombax*(1+p53^4/(p53^4+p53thresh^4))-mu*bax
jccmito=0.0001*a8-mu*ccmito
# ODE'S
bax'=jbax-j12a-j12b-j13
Bcl2'=-J9+jbcl2p-j13
cc'=j14-j1-mu*cc+mptp*ccmito
c3a'=J6f+J6bf-J7-J8+J8f-J9+J9f-mu*c3a
AP'=-J1+JAp
CcAp'=J1-7*J1b
Apop'=J1b-J2+J4b
Apopc9z'=J2-J3
Apopc9z2'=J3-J3f
Apopc9a2'=J3f-J4-J5c-J6b+J6bf
Apopc9a'=J4-J4b-J5b
c9a'=J4+J4b-J5-J6+J6f-mu*c9a
c9z'=-J2-J3+Jp9
IAP'=-J5-J5b-J5c-J7+JIAP
IAP9'=J5
IAPA9'=J5b
IAPA29'=J5c
IAP3'=J7
c3z'=-J6-J6b+Jp3-10*nop*c3z
c93'=J6-J6f
cA93'=J6b-J6bf
c8a'=Jp8-J8p+J8fp
Bid'=-J8-J8p+jbidp
c8B'=J8p-J8fp
c3B'=J8-J8f
c3L'=J9-J9f
tbid'=j8f+j8fp-j11+j12b-mu*tbid+tbid0
tbidbax'=j12a-j12b-mu*tbidbax
ccmito'=jccmito-j14-mptp*ccmito
bax2'=j12b-mu*bax2
tbidmito'=j11-j12a-mu*tbidmito
# PARAMETERS

```

```

par ombax=0.000024
par MPTP=0
par nop=0
par tbid0=0
par p53=0.0066
par ombcl2=0.00032
par p=4
par k1p=5,k1m=0.5
par k1bp=50000*a9,k1bm=0.5*a9
par k2p=10,k2m=0.5
par k3p=10,k3m=0.5,k3f=0.1
par k4p=5,k4m=0.5
par k4bp=5,k4bm=0.5
par k5p=5*a10,k5m=0.0035*a10
par k5bp=5*a10,k5bm=0.0035*a10
par k5cp=5*a10,k5cm=0.0035*a10
par k6p=10*a11,k6m=0.5*a11,k6f=0.001*a11
par k6bp=10*a11,k6bm=0.5*a11,k6bf=0.1*a11
par k7p=5*a10,k7m=0.0035*a10
par k8p=10,k8m=0.5,k8f=0.1
par k9p=10,k9m=0.5,k9f=0.1
par k11=10*a12,k12a=10*a12,k12b=10*a12,k13=10*a12,k14=10*a12
par a1=3,a2=0.3,a3=3,a4=3,a5=0.3,a8=3,a9=1,a10=1,a11=1,a12=1,a13=3
mu=0.002*a13
par p53thresh=0.004
# INITIAL CONDITIONS
init Ap=.004,c9z=.004,c3z=.004,IAP=.004,Bid=.004,Bcl2=.004,bax=.004
init CcAp=0,Apop=0,Apopc9z=0,Apopc9z2=0,Apopc9a2=0,Apopc9a=0,c9a=0.00
init IAP3=0,IAP9=0,IAPA9=0,IAPA29=0,c93=0,cA93=0,c3a=0.004,c3B=0,c3L=0
init c8a=0.00005,c8B=0
init cc=0,ccmito=.004
# DISPLAY
@ xhi=10000,ylo=0,yhi=0.001
@ nplot=1,yp=c3a
# METHOD
@ meth=cvode,atol=1e-8,tol=1e-9,total=200000,dt=5,bounds=100000
done
*****

# figure12B-point0008.ode
# REACTIONS
# om -> Ap
# om -> IAP
# om -> c3z
# om -> c9z
# om -> Bid

```

```

# om -> Bcl2
# om -> Bax
# om -> Ccmito
# c8a -> *
# c9a -> *
# c3a -> *
# Ap -> *
# IAP -> *
# c3z -> *
# c9z -> *
# Bcl2 -> *
# Bid -> *
# Bax -> *
# Ccmito -> *
# Bax -> *
# Bax2 -> *
# Cc -> *
# tBid -> *
# tBidBax -> *
# tBidmito -> *
# Cc + Ap <-> CcAp      k1p,k1m
# 7 CcAp <-> Apop      k1bp,k1bm
# Apop + c9z <-> Apopc9z  k2p,k2m
# Apopc9z + c9z <-> Apopc9z2 k3p,k3m
# Apopc9z2 -> Apopc9a2      k3f
# Apopc9a2 <-> Apopc9a + c9a k4p,k4m
# Apopc9a <-> Apop + c9a    k4bp,k4bm
# c9a + IAP <-> IAP9      k5p,k5m
# Apopc9a + IAP <-> IAPA9   k5bp,k5bm
# Apopc9a2 + IAP <-> IAPA29 k5cp,k5cm
# c3z + c9a <-> c93      k6p,k6m
# c93 -> c3a + c9a      k6f
# c3z + Apopc9a2 <-> cA93   k6bp,k6bm
# cA93 -> c3a + Apopc9a2   k6bf
# c3a + IAP <-> IAP3      k7p,k7m
# c8a + Bid <-> c8B      k8p,k8m
# c8B -> c8a + tBid      k8f
# c3a + Bid <-> c3B      k8p,k8m
# c3B -> c3a + tBid      k8f
# c3a + Bcl2 <-> c3L     k9p,k9m
# c3L -> c3a + B2c      k9f
# tBid -> tBidmito      k11
# tBidmito + Bax -> tBidBax k12a
# tBidBax + Bax -> tBid + Bax2 k12b
# Bcl2 + Bax -> *      k13
# Bax2 + Ccmito -> Cc + Bax2 k14

```

```

# REACTION RATES
r1p=k1p*Cc*Ap
r1m=k1m*CcAp
r1bp=k1bp*CcAp^p
r1bm=k1bm*Apop
r2p=k2p*Apop*c9z
r2m=k2m*Apopc9z
r3p=k3p*Apopc9z*c9z
r3m=k3m*Apopc9z2
r3f=k3f*Apopc9z2
r4p=k4p*Apopc9a2
r4m=k4m*Apopc9a*c9a
r4bp=k4bp*Apopc9a
r4bm=k4bm*Apop*c9a
r5p=k5p*c9a*IAP
r5m=k5m*IAP9
r5bp=k5bp*Apopc9a*IAP
r5bm=k5bm*IAPA9
r5cp=k5cp*Apopc9a2*IAP
r5cm=k5cm*IAPA29
r6p=k6p*c3z*c9a
r6m=k6m*c93
r6f=k6f*c93
r6bp=k6p*c3z*Apopc9a2
r6bm=k6m*cA93
r6bf=k6f*cA93
r7p=k7p*c3a*IAP
r7m=k7m*IAP3
r8p=k8p*c3a*Bid
r8m=k8m*c3B
r8f=k8f*c3B
r8pp=k8p*c8a*Bid
r8mp=k8m*c8B
r8fp=k8f*c8B
r9p=k9p*c3a*Bcl2
r9m=k9m*c3L
r9f=k9f*c3L
r11=k11*tbid
r12a=k12a*tbidmito*bax
r12b=k12b*tbidbax*bax
r13=k13*bcl2*bax
r14=k14*bax2*ccmito
# FLUXES
J1=r1p-r1m
J1b=r1bp-r1bm
J2=r2p-r2m

```

```

J3=r3p-r3m
J3f=r3f
J4=r4p-r4m
J4b=r4bp-r4bm
J5=r5p-r5m
J5b=r5bp-r5bm
J5c=r5cp-r5cm
J6=r6p-r6m
J6f=r6f
J6b=r6bp-r6bm
J6bf=r6bf
J7=r7p-r7m
J8=r8p-r8m
J8f=r8f
J8p=r8pp-r8mp
J8fp=r8fp
J9=r9p-r9m
J9f=r9f
j11=r11
j12a=r12a
j12b=r12b
j13=r13
j14=r14
# PRODUCTION AND DEGRADATION RATES
Jp8=-mu*c8a
JAp=0.0001*a1-mu*Ap
JIAP=0.0001*a2-mu*IAP
Jp3=0.0001*a3-mu*c3z
Jp9=0.0001*a4-mu*c9z
jbidp=0.0001*a5-mu*bid
jbcl2p=ombcl2*p53thresh^4/(p53^4+p53thresh^4)-mu*bcl2
jbax=ombax*(1+p53^4/(p53^4+p53thresh^4))-mu*bax
jccmito=0.0001*a8-mu*ccmito
# ODE'S
bax'=jbax-j12a-j12b-j13
Bcl2'=-J9+jbcl2p-j13
cc'=j14-j1-mu*cc+mtp*ccmito
c3a'=J6f+J6bf-J7-J8+J8f-J9+J9f-mu*c3a
AP'=-J1+JAp
CcAp'=J1-7*J1b
Apop'=J1b-J2+J4b
Apopc9z'=J2-J3
Apopc9z2'=J3-J3f
Apopc9a2'=J3f-J4-J5c-J6b+J6bf
Apopc9a'=J4-J4b-J5b
c9a'=J4+J4b-J5-J6+J6f-mu*c9a

```

```

c9z'=-J2-J3+Jp9
IAP'=-J5-J5b-J5c-J7+JIAP
IAP9'=J5
IAPA9'=J5b
IAPA29'=J5c
IAP3'=J7
c3z'=-J6-J6b+Jp3-10*nop*c3z
c93'=J6-J6f
cA93'=J6b-J6bf
c8a'=Jp8-J8p+J8fp
Bid'=-J8-J8p+jbidp
c8B'=J8p-J8fp
c3B'=J8-J8f
c3L'=J9-J9f
tbid'=j8f+j8fp-j11+j12b-mu*tbid+tbid0
tbidbax'=j12a-j12b-mu*tbidbax
ccmito'=jccmito-j14-mptp*ccmito
bax2'=j12b-mu*bax2
tbidmito'=j11-j12a-mu*tbidmito
# PARAMETERS
par ombax=0.000024
par MPTP=0
par nop=0
par tbid0=0
par p53=0.0066
par ombcl2=0.0008
par p=4
par k1p=5,k1m=0.5
par k1bp=50000*a9,k1bm=0.5*a9
par k2p=10,k2m=0.5
par k3p=10,k3m=0.5,k3f=0.1
par k4p=5,k4m=0.5
par k4bp=5,k4bm=0.5
par k5p=5*a10,k5m=0.0035*a10
par k5bp=5*a10,k5bm=0.0035*a10
par k5cp=5*a10,k5cm=0.0035*a10
par k6p=10*a11,k6m=0.5*a11,k6f=0.001*a11
par k6bp=10*a11,k6bm=0.5*a11,k6bf=0.1*a11
par k7p=5*a10,k7m=0.0035*a10
par k8p=10,k8m=0.5,k8f=0.1
par k9p=10,k9m=0.5,k9f=0.1
par k11=10*a12,k12a=10*a12,k12b=10*a12,k13=10*a12,k14=10*a12
par a1=3,a2=0.3,a3=3,a4=3,a5=0.3,a8=3,a9=1,a10=1,a11=1,a12=1,a13=3
mu=0.002*a13
par p53thresh=0.004
# INITIAL CONDITIONS

```

```

init Ap=.004,c9z=.004,c3z=.004,IAP=.004,Bid=.004,Bcl2=.004,bax=.004
init CcAp=0,Apop=0,Apopc9z=0,Apopc9z2=0,Apopc9a2=0,Apopc9a=0,c9a=0.00
init IAP3=0,IAP9=0,IAPA9=0,IAPA29=0,c93=0,cA93=0,c3a=0.04,c3B=0,c3L=0
init c8a=0.00005,c8B=0
init cc=0,ccmito=.004
# DISPLAY
@ xhi=10000,ylo=0,yhi=0.001
@ nplot=1,yp=c3a
# METHOD
@ meth=cvode,atol=1e-8,tol=1e-9,total=200000,dt=5,bounds=100000
done

```

A.1.5 Script used in Figure 13

```

# figure13.ode
# REACTIONS
# om -> Ap
# om -> IAP
# om -> c3z
# om -> c9z
# om -> Bid
# om -> Bcl2
# om -> Bax
# om -> Ccmito
# c8a -> *
# c9a -> *
# c3a -> *
# Ap -> *
# IAP -> *
# c3z -> *
# c9z -> *
# Bcl2 -> *
# Bid -> *
# Bax -> *
# Ccmito -> *
# Bax -> *
# Bax2 -> *
# Cc -> *
# tBid -> *
# tBidBax -> *
# tBidmito -> *
# Cc + Ap <-> CcAp      k1p,k1m
# 7 CcAp <-> Apop      k1bp,k1bm
# Apop + c9z <-> Apopc9z  k2p,k2m

```

```

# Apopc9z + c9z <-> Apopc9z2 k3p,k3m
# Apopc9z2 -> Apopc9a2 k3f
# Apopc9a2 <-> Apopc9a + c9a k4p,k4m
# Apopc9a <-> Apop + c9a k4bp,k4bm
# c9a + IAP <-> IAP9 k5p,k5m
# Apopc9a + IAP <-> IAPA9 k5bp,k5bm
# Apopc9a2 + IAP <-> IAPA29 k5cp,k5cm
# c3z + c9a <-> c93 k6p,k6m
# c93 -> c3a + c9a k6f
# c3z + Apopc9a2 <-> cA93 k6bp,k6bm
# cA93 -> c3a + Apopc9a2 k6bf
# c3a + IAP <-> IAP3 k7p,k7m
# c8a + Bid <-> c8B k8p,k8m
# c8B -> c8a + tBid k8f
# c3a + Bid <-> c3B k8p,k8m
# c3B -> c3a + tBid k8f
# c3a + Bcl2 <-> c3L k9p,k9m
# c3L -> c3a + B2c k9f
# tBid -> tBidmito k11
# tBidmito + Bax -> tBidBax k12a
# tBidBax + Bax -> tBid + Bax2 k12b
# Bcl2 + Bax -> * k13
# Bax2 + Ccmito -> Cc + Bax2 k14
# REACTION RATES
r1p=k1p*Cc*Ap
r1m=k1m*CcAp
r1bp=k1bp*CcAp^p
r1bm=k1bm*Apop
r2p=k2p*Apop*c9z
r2m=k2m*Apopc9z
r3p=k3p*Apopc9z*c9z
r3m=k3m*Apopc9z2
r3f=k3f*Apopc9z2
r4p=k4p*Apopc9a2
r4m=k4m*Apopc9a*c9a
r4bp=k4bp*Apopc9a
r4bm=k4bm*Apop*c9a
r5p=k5p*c9a*IAP
r5m=k5m*IAP9
r5bp=k5bp*Apopc9a*IAP
r5bm=k5bm*IAPA9
r5cp=k5cp*Apopc9a2*IAP
r5cm=k5cm*IAPA29
r6p=k6p*c3z*c9a
r6m=k6m*c93
r6f=k6f*c93

```

r6bp=k6p*c3z*Apopc9a2
 r6bm=k6m*cA93
 r6bf=k6f*cA93
 r7p=k7p*c3a*IAP
 r7m=k7m*IAP3
 r8p=k8p*c3a*Bid
 r8m=k8m*c3B
 r8f=k8f*c3B
 r8pp=k8p*c8a*Bid
 r8mp=k8m*c8B
 r8fp=k8f*c8B
 r9p=k9p*c3a*Bcl2
 r9m=k9m*c3L
 r9f=k9f*c3L
 r11=k11*tbid
 r12a=k12a*tbidmito*bax
 r12b=k12b*tbidbax*bax
 r13=k13*bcl2*bax
 r14=k14*bax2*ccmito
 # FLUXES
 J1=r1p-r1m
 J1b=r1bp-r1bm
 J2=r2p-r2m
 J3=r3p-r3m
 J3f=r3f
 J4=r4p-r4m
 J4b=r4bp-r4bm
 J5=r5p-r5m
 J5b=r5bp-r5bm
 J5c=r5cp-r5cm
 J6=r6p-r6m
 J6f=r6f
 J6b=r6bp-r6bm
 J6bf=r6bf
 J7=r7p-r7m
 J8=r8p-r8m
 J8f=r8f
 J8p=r8pp-r8mp
 J8fp=r8fp
 J9=r9p-r9m
 J9f=r9f
 j11=r11
 j12a=r12a
 j12b=r12b
 j13=r13
 j14=r14

```

# PRODUCTION AND DEGRADATION RATES
Jp8=-mu*c8a
JAp=0.0001*a1-mu*Ap
JIAP=0.0001*a2-mu*IAP
Jp3=0.0001*a3-mu*c3z
Jp9=0.0001*a4-mu*c9z
jbidp=0.0001*a5-mu*bid
jbcl2p=0.0001*a6*p53thresh^4/(p53^4+p53thresh^4)-mu*bc12
jbax=0.0001*a7*(1+p53^4/(p53^4+p53thresh^4))-mu*bax
jccmito=0.0001*a8-mu*ccmito
# ODE'S
bax'=jbax-j12a-j12b-j13
Bcl2'=-J9+jbcl2p-j13
cc'=j14-j1-mu*cc+mptp*ccmito
c3a'=J6f+J6bf-J7-J8+J8f-J9+J9f-mu*c3a
AP'=-J1+JAp
CcAp'=J1-7*J1b
Apop'=J1b-J2+J4b
Apopc9z'=J2-J3
Apopc9z2'=J3-J3f
Apopc9a2'=J3f-J4-J5c-J6b+J6bf
Apopc9a'=J4-J4b-J5b
c9a'=J4+J4b-J5-J6+J6f-mu*c9a
c9z'=-J2-J3+Jp9
IAP'=-J5-J5b-J5c-J7+JIAP
IAP9'=J5
IAPA9'=J5b
IAPA29'=J5c
IAP3'=J7
c3z'=-J6-J6b+Jp3-10*nop*c3z
c93'=J6-J6f
cA93'=J6b-J6bf
c8a'=Jp8-J8p+J8fp
Bid'=-J8-J8p+jbidp
c8B'=J8p-J8fp
c3B'=J8-J8f
c3L'=J9-J9f
tbid'=j8f+j8fp-j11+j12b-mu*tbid+tbid0
tbidbax'=j12a-j12b-mu*tbidbax
ccmito'=jccmito-j14-mptp*ccmito
bax2'=j12b-mu*bax2
tbidmito'=j11-j12a-mu*tbidmito
# PARAMETERS
par MPTP=0.01
par nop=0
par tbid0=0

```

```

par p53=0.0022
par p=4
par k1p=5,k1m=0.5
par k1bp=50000*a9,k1bm=0.5*a9
par k2p=10,k2m=0.5
par k3p=10,k3m=0.5,k3f=0.1
par k4p=5,k4m=0.5
par k4bp=5,k4bm=0.5
par k5p=5*a10,k5m=0.0035*a10
par k5bp=5*a10,k5bm=0.0035*a10
par k5cp=5*a10,k5cm=0.0035*a10
par k6p=10*a11,k6m=0.5*a11,k6f=0.001*a11
par k6bp=10*a11,k6bm=0.5*a11,k6bf=0.1*a11
par k7p=5*a10,k7m=0.0035*a10
par k8p=10,k8m=0.5,k8f=0.1
par k9p=10,k9m=0.5,k9f=0.1
par k11=10*a12,k12a=10*a12,k12b=10*a12,k13=10*a12,k14=10*a12
par a1=3,a2=0.3,a3=3,a4=3,a5=0.3,a6=0.8,a7=0.3,a8=3,a9=1,a10=1,a11=1,a12=1,a13=3
mu=0.002*a13
par p53thresh=0.004
# INITIAL CONDITIONS
init Ap=.004,c9z=.004,c3z=.004,IAP=.004,Bid=.004,Bcl2=.004,bax=.004
init CcAp=0,Apop=0,Apopc9z=0,Apopc9z2=0,Apopc9a2=0,Apopc9a=0,c9a=0.00
init IAP3=0,IAP9=0,IAPA9=0,IAPA29=0,c93=0,cA93=0,c3a=0.04,c3B=0,c3L=0
init c8a=0.0000,c8B=0
init cc=0,ccmito=.004
# DISPLAY
@ xhi=10000,ylo=0,yhi=0.001
@ nplot=1,yp=c3a
# METHOD
@ meth=cvode,atol=1e-8,tol=1e-9,total=200000,dt=5,bounds=100000
done

```

A.1.6 Scripts used in Figure 14

```

# figure14-point00032-withinh.ode
#REACTIONS
# om -> Ap
# om -> IAP
# om -> c3z
# om -> c9z
# om -> Bid
# om -> Bcl2
# om -> Bax

```

```

# om -> Ccmito
# c8a -> *
# c9a -> *
# c3a -> *
# Ap -> *
# IAP -> *
# c3z -> *
# c9z -> *
# Bcl2 -> *
# Bid -> *
# Bax -> *
# Ccmito -> *
# Bax -> *
# Bax2 -> *
# Cc -> *
# tBid -> *
# tBidBax -> *
# tBidmito -> *
# Cc + Ap <-> CcAp      k1p,k1m
# 7 CcAp <-> Apop      k1bp,k1bm
# Apop + c9z <-> Apopc9z  k2p,k2m
# Apopc9z + c9z <-> Apopc9z2 k3p,k3m
# Apopc9z2 -> Apopc9a2    k3f
# Apopc9a2 <-> Apopc9a + c9a k4p,k4m
# Apopc9a <-> Apop + c9a    k4bp,k4bm
# c9a + IAP <-> IAP9      k5p,k5m
# Apopc9a + IAP <-> IAPA9   k5bp,k5bm
# Apopc9a2 + IAP <-> IAPA29 k5cp,k5cm
# c3z + c9a <-> c93      k6p,k6m
# c93 -> c3a + c9a      k6f
# c3z + Apopc9a2 <-> cA93   k6bp,k6bm
# cA93 -> c3a + Apopc9a2   k6bf
# c3a + IAP <-> IAP3      k7p,k7m
# c8a + Bid <-> c8B      k8p,k8m
# c8B -> c8a + tBid     k8f
# c3a + Bid <-> c3B      k8p,k8m
# c3B -> c3a + tBid     k8f
# c3a + Bcl2 <-> c3L     k9p,k9m
# c3L -> c3a + B2c      k9f
# tBid -> tBidmito      k11
# tBidmito + Bax -> tBidBax k12a
# tBidBax + Bax -> tBid + Bax2 k12b
# Bcl2 + Bax -> *      k13
# Bax2 + Ccmito -> Cc + Bax2 k14
# FUNCTION
mubax(t)=if(t<1200)then(0.1-t*5*10^(-5))else(0.04)

```

```

# REACTION RATES
r1p=k1p*Cc*Ap
r1m=k1m*CcAp
r1bp=k1bp*CcAp^p
r1bm=k1bm*Apop
r2p=k2p*Apop*c9z
r2m=k2m*Apopc9z
r3p=k3p*Apopc9z*c9z
r3m=k3m*Apopc9z2
r3f=k3f*Apopc9z2
r4p=k4p*Apopc9a2
r4m=k4m*Apopc9a*c9a
r4bp=k4bp*Apopc9a
r4bm=k4bm*Apop*c9a
r5p=k5p*c9a*IAP
r5m=k5m*IAP9
r5bp=k5bp*Apopc9a*IAP
r5bm=k5bm*IAPA9
r5cp=k5cp*Apopc9a2*IAP
r5cm=k5cm*IAPA29
r6p=k6p*c3z*c9a
r6m=k6m*c93
r6f=k6f*c93
r6bp=k6p*c3z*Apopc9a2
r6bm=k6m*cA93
r6bf=k6f*cA93
r7p=k7p*c3a*IAP
r7m=k7m*IAP3
r8p=k8p*c3a*Bid
r8m=k8m*c3B
r8f=k8f*c3B
r8pp=k8p*c8a*Bid
r8mp=k8m*c8B
r8fp=k8f*c8B
r9p=k9p*c3a*Bcl2
r9m=k9m*c3L
r9f=k9f*c3L
r11=k11*tbid
r12a=k12a*tbidmito*bax
r12b=k12b*tbidbax*bax
r13=k13*bcl2*bax
r14=k14*bax2*ccmito
# FLUXES
J1=r1p-r1m
J1b=r1bp-r1bm
J2=r2p-r2m

```

$J3=r3p-r3m$
 $J3f=r3f$
 $J4=r4p-r4m$
 $J4b=r4bp-r4bm$
 $J5=r5p-r5m$
 $J5b=r5bp-r5bm$
 $J5c=r5cp-r5cm$
 $J6=r6p-r6m$
 $J6f=r6f$
 $J6b=r6bp-r6bm$
 $J6bf=r6bf$
 $J7=r7p-r7m$
 $J8=r8p-r8m$
 $J8f=r8f$
 $J8p=r8pp-r8mp$
 $J8fp=r8fp$
 $J9=r9p-r9m$
 $J9f=r9f$
 $j11=r11$
 $j12a=r12a$
 $j12b=r12b$
 $j13=r13$
 $j14=r14$
PRODUCTION AND DEGRADATION RATES
 $Jp8=-\mu*c8a$
 $JAp=0.0001*a1-\mu*Ap$
 $JIAP=0.0001*a2-\mu*IAP$
 $Jp3=0.0001*a3-\mu*c3z$
 $Jp9=0.0001*a4-\mu*c9z$
 $jbidp=0.0001*a5-\mu*bid$
 $jbcl2p=ombcl2*p53thresh^4/(p53^4+p53thresh^4)-\mu*bcl2$
 $jbax=0.0001*a7*(1+p53^4/(p53^4+p53thresh^4))-mubax(t)*bax$
 $jccmito=0.0001*a8-\mu*ccmito$
ODE'S
 $bax'=jbax-j12a-j12b-j13$
 $Bcl2'=-J9+jbcl2p-j13$
 $cc'=j14-j1-\mu*cc+mtp*ccmito$
 $c3a'=J6f+J6bf-J7-J8+J8f-J9+J9f-\mu*c3a$
 $AP'=-J1+JAp$
 $CcAp'=J1-7*J1b$
 $Apop'=J1b-J2+J4b$
 $Apopc9z'=J2-J3$
 $Apopc9z2'=J3-J3f$
 $Apopc9a2'=J3f-J4-J5c-J6b+J6bf$
 $Apopc9a'=J4-J4b-J5b$
 $c9a'=J4+J4b-J5-J6+J6f-\mu*c9a$

```

c9z'=-J2-J3+Jp9
IAP'=-J5-J5b-J5c-J7+JIAP
IAP9'=J5
IAPA9'=J5b
IAPA29'=J5c
IAP3'=J7
c3z'=-J6-J6b+Jp3-10*nop*c3z
c93'=J6-J6f
cA93'=J6b-J6bf
c8a'=Jp8-J8p+J8fp
Bid'=-J8-J8p+jbidp
c8B'=J8p-J8fp
c3B'=J8-J8f
c3L'=J9-J9f
tbid'=j8f+j8fp-j11+j12b-mu*tbid+tbid0
tbidbax'=j12a-j12b-mu*tbidbax
ccmito'=jccmito-j14-mptp*ccmito
bax2'=j12b-mu*bax2
tbidmito'=j11-j12a-mu*tbidmito
# PARAMETERS
par MPTP=0
par nop=0
par tbid0=0
par p53=0.0066
par ombcl2=0.00032
par p=4
par k1p=5,k1m=0.5
par k1bp=50000*a9,k1bm=0.5*a9
par k2p=10,k2m=0.5
par k3p=10,k3m=0.5,k3f=0.1
par k4p=5,k4m=0.5
par k4bp=5,k4bm=0.5
par k5p=5*a10,k5m=0.0035*a10
par k5bp=5*a10,k5bm=0.0035*a10
par k5cp=5*a10,k5cm=0.0035*a10
par k6p=10*a11,k6m=0.5*a11,k6f=0.001*a11
par k6bp=10*a11,k6bm=0.5*a11,k6bf=0.1*a11
par k7p=5*a10,k7m=0.0035*a10
par k8p=10,k8m=0.5,k8f=0.1
par k9p=10,k9m=0.5,k9f=0.1
par k11=10*a12,k12a=10*a12,k12b=10*a12,k13=10*a12,k14=10*a12
par a1=3,a2=0.3,a3=3,a4=3,a5=0.3,a7=0.3,a8=3,a9=1,a10=1,a11=1,a12=1,a13=3
mu=0.002*a13
par p53thresh=0.004
# INITIAL CONDITIONS
init Ap=.004,c9z=.004,c3z=.004,IAP=.004,Bid=.004,Bcl2=.004,bax=.004

```

```

init CcAp=0,Apop=0,Apopc9z=0,Apopc9z2=0,Apopc9a2=0,Apopc9a=0,c9a=0.00
init IAP3=0,IAP9=0,IAPA9=0,IAPA29=0,c93=0,cA93=0,c3a=0.1,c3B=0,c3L=0
init c8a=0.1,c8B=0
init cc=0,ccmito=.004
# DISPLAY
@ xhi=10000,ylo=0,yhi=0.001
@ nplot=2,yp=c3a,yp2=Cc
# METHOD
@ meth=cvode,atol=1e-8,tol=1e-9,total=200000,dt=5,bounds=100000
done
*****

# figure14-point00032-withoutinh.ode
# REACTIONS
# om -> Ap
# om -> IAP
# om -> c3z
# om -> c9z
# om -> Bid
# om -> Bcl2
# om -> Bax
# om -> Ccmito
# c8a -> *
# c9a -> *
# c3a -> *
# Ap -> *
# IAP -> *
# c3z -> *
# c9z -> *
# Bcl2 -> *
# Bid -> *
# Bax -> *
# Ccmito -> *
# Bax -> *
# Bax2 -> *
# Cc -> *
# tBid -> *
# tBidBax -> *
# tBidmito -> *
# Cc + Ap <-> CcAp      k1p,k1m
# 7 CcAp <-> Apop      k1bp,k1bm
# Apop + c9z <-> Apopc9z  k2p,k2m
# Apopc9z + c9z <-> Apopc9z2 k3p,k3m
# Apopc9z2 -> Apopc9a2    k3f
# Apopc9a2 <-> Apopc9a + c9a k4p,k4m
# Apopc9a <-> Apop + c9a   k4bp,k4bm

```

```

# c9a + IAP <-> IAP9    k5p,k5m
# Apopc9a + IAP <-> IAPA9  k5bp,k5bm
# Apopc9a2 + IAP <-> IAPA29 k5cp,k5cm
# c3z + c9a <-> c93      k6p,k6m
# c93 -> c3a + c9a      k6f
# c3z + Apopc9a2 <-> cA93  k6bp,k6bm
# cA93 -> c3a + Apopc9a2  k6bf
# c3a + IAP <-> IAP3     k7p,k7m
# c8a + Bid <-> c8B      k8p,k8m
# c8B -> c8a + tBid     k8f
# c3a + Bid <-> c3B      k8p,k8m
# c3B -> c3a + tBid     k8f
# c3a + Bcl2 <-> c3L    k9p,k9m
# c3L -> c3a + B2c     k9f
# tBid -> tBidmito     k11
# tBidmito + Bax -> tBidBax k12a
# tBidBax + Bax -> tBid + Bax2 k12b
# Bcl2 + Bax -> *      k13
# Bax2 + Ccmito -> Cc + Bax2 k14
# REACTION RATES
r1p=k1p*Cc*Ap
r1m=k1m*CcAp
r1bp=k1bp*CcAp^p
r1bm=k1bm*Apop
r2p=k2p*Apop*c9z
r2m=k2m*Apopc9z
r3p=k3p*Apopc9z*c9z
r3m=k3m*Apopc9z2
r3f=k3f*Apopc9z2
r4p=k4p*Apopc9a2
r4m=k4m*Apopc9a*c9a
r4bp=k4bp*Apopc9a
r4bm=k4bm*Apop*c9a
r5p=k5p*c9a*IAP
r5m=k5m*IAP9
r5bp=k5bp*Apopc9a*IAP
r5bm=k5bm*IAPA9
r5cp=k5cp*Apopc9a2*IAP
r5cm=k5cm*IAPA29
r6p=k6p*c3z*c9a
r6m=k6m*c93
r6f=k6f*c93
r6bp=k6p*c3z*Apopc9a2
r6bm=k6m*cA93
r6bf=k6f*cA93
r7p=k7p*c3a*IAP

```

```

r7m=k7m*IAP3
r8p=k8p*c3a*Bid
r8m=k8m*c3B
r8f=k8f*c3B
r8pp=k8p*c8a*Bid
r8mp=k8m*c8B
r8fp=k8f*c8B
r9p=k9p*c3a*Bcl2
r9m=k9m*c3L
r9f=k9f*c3L
r11=k11*tbid
r12a=k12a*tbidmito*bax
r12b=k12b*tbidbax*bax
r13=k13*bcl2*bax
r14=k14*bax2*ccmito
# FLUXES
J1=r1p-r1m
J1b=r1bp-r1bm
J2=r2p-r2m
J3=r3p-r3m
J3f=r3f
J4=r4p-r4m
J4b=r4bp-r4bm
J5=r5p-r5m
J5b=r5bp-r5bm
J5c=r5cp-r5cm
J6=r6p-r6m
J6f=r6f
J6b=r6bp-r6bm
J6bf=r6bf
J7=r7p-r7m
J8=r8p-r8m
J8f=r8f
J8p=r8pp-r8mp
J8fp=r8fp
J9=r9p-r9m
J9f=r9f
j11=r11
j12a=r12a
j12b=r12b
j13=r13
j14=r14
# PRODUCTION AND DEGRADATION RATES
Jp8=-mu*c8a
JAp=0.0001*a1-mu*Ap
JIAP=0.0001*a2-mu*IAP

```

```

Jp3=0.0001*a3-mu*c3z
Jp9=0.0001*a4-mu*c9z
jbidp=0.0001*a5-mu*bid
jbcl2p=ombcl2*p53thresh^4/(p53^4+p53thresh^4)-mu*bcl2
jbax=0.0001*a7*(1+p53^4/(p53^4+p53thresh^4))-mubax*bax
jccmito=0.0001*a8-mu*ccmito
# ODE'S
bax'=jbax-j12a-j12b-j13
Bcl2'=-J9+jbcl2p-j13
cc'=j14-j1-mu*cc+mptp*ccmito
c3a'=J6f+J6bf-J7-J8+J8f-J9+J9f-mu*c3a
AP'=-J1+JAp
CcAp'=J1-7*J1b
Apop'=J1b-J2+J4b
Apopc9z'=J2-J3
Apopc9z2'=J3-J3f
Apopc9a2'=J3f-J4-J5c-J6b+J6bf
Apopc9a'=J4-J4b-J5b
c9a'=J4+J4b-J5-J6+J6f-mu*c9a
c9z'=-J2-J3+Jp9
IAP'=-J5-J5b-J5c-J7+JIAP
IAP9'=J5
IAPA9'=J5b
IAPA29'=J5c
IAP3'=J7
c3z'=-J6-J6b+Jp3-10*nop*c3z
c93'=J6-J6f
cA93'=J6b-J6bf
c8a'=Jp8-J8p+J8fp
Bid'=-J8-J8p+jbidp
c8B'=J8p-J8fp
c3B'=J8-J8f
c3L'=J9-J9f
tbid'=j8f+j8fp-j11+j12b-mu*tbid+tbid0
tbidbax'=j12a-j12b-mu*tbidbax
ccmito'=jccmito-j14-mptp*ccmito
bax2'=j12b-mu*bax2
tbidmito'=j11-j12a-mu*tbidmito
# PARAMETERS
par mubax=0.1
par MPTP=0
par nop=0
par tbid0=0
par p53=0.0066
par ombcl2=0.00032
par p=4

```

```

par k1p=5,k1m=0.5
par k1bp=50000*a9,k1bm=0.5*a9
par k2p=10,k2m=0.5
par k3p=10,k3m=0.5,k3f=0.1
par k4p=5,k4m=0.5
par k4bp=5,k4bm=0.5
par k5p=5*a10,k5m=0.0035*a10
par k5bp=5*a10,k5bm=0.0035*a10
par k5cp=5*a10,k5cm=0.0035*a10
par k6p=10*a11,k6m=0.5*a11,k6f=0.001*a11
par k6bp=10*a11,k6bm=0.5*a11,k6bf=0.1*a11
par k7p=5*a10,k7m=0.0035*a10
par k8p=10,k8m=0.5,k8f=0.1
par k9p=10,k9m=0.5,k9f=0.1
par k11=10*a12,k12a=10*a12,k12b=10*a12,k13=10*a12,k14=10*a12
par a1=3,a2=0.3,a3=3,a4=3,a5=0.3,a7=0.3,a8=3,a9=1,a10=1,a11=1,a12=1,a13=3
mu=0.002*a13
par p53thresh=0.004
# INITIAL CONDITIONS
init Ap=.004,c9z=.004,c3z=.004,IAP=.004,Bid=.004,Bcl2=.004,bax=.004
init CcAp=0,Apop=0,Apopc9z=0,Apopc9z2=0,Apopc9a2=0,Apopc9a=0,c9a=0.00
init IAP3=0,IAP9=0,IAPA9=0,IAPA29=0,c93=0,cA93=0,c3a=0.1,c3B=0,c3L=0
init c8a=0.1,c8B=0
init cc=0,ccmito=.004
# DISPLAY
@ xhi=10000,ylo=0,yhi=0.001
@ nplot=2,yp=c3a,yp2=Cc
# METHOD
@ meth=cvode,atol=1e-8,tol=1e-9,total=200000,dt=5,bounds=100000
done

```

A.1.7 Scripts used in Figure 15

```

# figure15-p53-0022.ode
# REACTIONS
# om -> Ap
# om -> IAP
# om -> c3z
# om -> c9z
# om -> Bid
# om -> Bcl2
# om -> Bax
# om -> Ccmito
# c8a -> *

```

```

# c9a -> *
# c3a -> *
# Ap -> *
# IAP -> *
# c3z -> *
# c9z -> *
# Bcl2 -> *
# Bid -> *
# Bax -> *
# Ccmto -> *
# Bax -> *
# Bax2 -> *
# Cc -> *
# tBid -> *
# tBidBax -> *
# tBidmito -> *
# Cc + Ap <-> CcAp      k1p,k1m
# 7 CcAp <-> Apop      k1bp,k1bm
# Apop + c9z <-> Apopc9z  k2p,k2m
# Apopc9z + c9z <-> Apopc9z2 k3p,k3m
# Apopc9z2 -> Apopc9a2    k3f
# Apopc9a2 <-> Apopc9a + c9a k4p,k4m
# Apopc9a <-> Apop + c9a    k4bp,k4bm
# c9a + IAP <-> IAP9      k5p,k5m
# Apopc9a + IAP <-> IAPA9  k5bp,k5bm
# Apopc9a2 + IAP <-> IAPA29 k5cp,k5cm
# c3z + c9a <-> c93      k6p,k6m
# c93 -> c3a + c9a      k6f
# c3z + Apopc9a2 <-> cA93  k6bp,k6bm
# cA93 -> c3a + Apopc9a2  k6bf
# c3a + IAP <-> IAP3     k7p,k7m
# c8a + Bid <-> c8B     k8p,k8m
# c8B -> c8a + tBid     k8f
# c3a + Bid <-> c3B     k8p,k8m
# c3B -> c3a + tBid     k8f
# c3a + Bcl2 <-> c3L    k9p,k9m
# c3L -> c3a + B2c     k9f
# tBid -> tBidmito     k11
# tBidmito + Bax -> tBidBax k12a
# tBidBax + Bax -> tBid + Bax2 k12b
# Bcl2 + Bax -> *      k13
# Bax2 + Ccmto -> Cc + Bax2 k14
# REACTION RATES
r1p=k1p*Cc*Ap
r1m=k1m*CcAp
r1bp=k1bp*CcAp^p

```

$r1bm = k1bm * Apop$
 $r2p = k2p * Apop * c9z$
 $r2m = k2m * Apopc9z$
 $r3p = k3p * Apopc9z * c9z$
 $r3m = k3m * Apopc9z2$
 $r3f = k3f * Apopc9z2$
 $r4p = k4p * Apopc9a2$
 $r4m = k4m * Apopc9a * c9a$
 $r4bp = k4bp * Apopc9a$
 $r4bm = k4bm * Apop * c9a$
 $r5p = k5p * c9a * IAP$
 $r5m = k5m * IAP9$
 $r5bp = k5bp * Apopc9a * IAP$
 $r5bm = k5bm * IAPA9$
 $r5cp = k5cp * Apopc9a2 * IAP$
 $r5cm = k5cm * IAPA29$
 $r6p = k6p * c3z * c9a$
 $r6m = k6m * c93$
 $r6f = k6f * c93$
 $r6bp = k6p * c3z * Apopc9a2$
 $r6bm = k6m * cA93$
 $r6bf = k6f * cA93$
 $r7p = k7p * c3a * IAP$
 $r7m = k7m * IAP3$
 $r8p = k8p * c3a * Bid$
 $r8m = k8m * c3B$
 $r8f = k8f * c3B$
 $r8pp = k8p * c8a * Bid$
 $r8mp = k8m * c8B$
 $r8fp = k8f * c8B$
 $r9p = k9p * c3a * Bcl2$
 $r9m = k9m * c3L$
 $r9f = k9f * c3L$
 $r11 = k11 * tbid$
 $r12a = k12a * tbidmito * bax$
 $r12b = k12b * tbidbax * bax$
 $r13 = k13 * bcl2 * bax$
 $r14 = k14 * bax2 * ccmto$
FLUXES
 $J1 = r1p - r1m$
 $J1b = r1bp - r1bm$
 $J2 = r2p - r2m$
 $J3 = r3p - r3m$
 $J3f = r3f$
 $J4 = r4p - r4m$
 $J4b = r4bp - r4bm$

$J5=r5p-r5m$
 $J5b=r5bp-r5bm$
 $J5c=r5cp-r5cm$
 $J6=r6p-r6m$
 $J6f=r6f$
 $J6b=r6bp-r6bm$
 $J6bf=r6bf$
 $J7=r7p-r7m$
 $J8=r8p-r8m$
 $J8f=r8f$
 $J8p=r8pp-r8mp$
 $J8fp=r8fp$
 $J9=r9p-r9m$
 $J9f=r9f$
 $j11=r11$
 $j12a=r12a$
 $j12b=r12b$
 $j13=r13$
 $j14=r14$
PRODUCTION AND DEGRADATION RATES
 $Jp8=-\mu*c8a$
 $JAp=0.0001*a1-\mu*Ap$
 $JIAP=0.0001*a2-\mu*IAP$
 $Jp3=0.0001*a3-\mu*c3z$
 $Jp9=0.0001*a4-\mu*c9z$
 $jbidp=0.0001*a5-\mu*bid$
 $jbcl2p=0.0001*a6*p53thresh^4/(p53^4+p53thresh^4)-\mu*bcl2$
 $jbax=0.0001*a7*(1+p53^4/(p53^4+p53thresh^4))-\mu*bax$
 $jccmito=0.0001*a8-\mu*ccmito$
ODE'S
 $bax'=jbax-j12a-j12b-j13$
 $Bcl2'=-J9+jbcl2p-j13$
 $cc'=j14-j1-\mu*cc+mptp*ccmito$
 $c3a'=J6f+J6bf-J7-J8+J8f-J9+J9f-\mu*c3a$
 $AP'=-J1+JAp$
 $CcAp'=J1-7*J1b$
 $Apop'=J1b-J2+J4b$
 $Apopc9z'=J2-J3$
 $Apopc9z2'=J3-J3f$
 $Apopc9a2'=J3f-J4-J5c-J6b+J6bf$
 $Apopc9a'=J4-J4b-J5b$
 $c9a'=J4+J4b-J5-J6+J6f-\mu*c9a$
 $c9z'=-J2-J3+Jp9$
 $IAP'=-J5-J5b-J5c-J7+JIAP$
 $IAP9'=J5$
 $IAPA9'=J5b$

```

IAPA29'=J5c
IAP3'=J7
c3z'=-J6-J6b+Jp3-10*nop*c3z
c93'=J6-J6f
cA93'=J6b-J6bf
c8a'=Jp8-J8p+J8fp
Bid'=-J8-J8p+jbidp
c8B'=J8p-J8fp
c3B'=J8-J8f
c3L'=J9-J9f
tbid'=j8f+j8fp-j11+j12b-mu*tbid+tbid0
tbidbax'=j12a-j12b-mu*tbidbax
ccmito'=jccmito-j14-mptp*ccmito
bax2'=j12b-mu*bax2
tbidmito'=j11-j12a-mu*tbidmito
# PARAMETERS
par MPTP=0
par nop=0
par tbid0=0
par p53=0.0022
par p=4
par k1p=5,k1m=0.5
par k1bp=50000*a9,k1bm=0.5*a9
par k2p=10,k2m=0.5
par k3p=10,k3m=0.5,k3f=0.1
par k4p=5,k4m=0.5
par k4bp=5,k4bm=0.5
par k5p=5*a10,k5m=0.0035*a10
par k5bp=5*a10,k5bm=0.0035*a10
par k5cp=5*a10,k5cm=0.0035*a10
par k6p=10*a11,k6m=0.5*a11,k6f=0.001*a11
par k6bp=10*a11,k6bm=0.5*a11,k6bf=0.1*a11
par k7p=5*a10,k7m=0.0035*a10
par k8p=10,k8m=0.5,k8f=0.1
par k9p=10,k9m=0.5,k9f=0.1
par k11=10*a12,k12a=10*a12,k12b=10*a12,k13=10*a12,k14=10*a12
par a1=3,a2=0.3,a3=3,a4=3,a5=0.3,a6=0.8,a7=0.3,a8=3,a9=1,a10=1,a11=1,a12=1,a13=3
mu=0.002*a13
par p53thresh=0.004
# INITIAL CONDITIONS
init Ap=.004,c9z=.004,c3z=.004,IAP=.004,Bid=.004,Bcl2=.004,bax=.004
init CcAp=0,Apop=0,Apopc9z=0,Apopc9z2=0,Apopc9a2=0,Apopc9a=0,c9a=0.00,IAP3=0
init IAP9=0,IAPA9=0,IAPA29=0,c93=0,cA93=0,c3a=0.04,c3B=0,c3L=0
init c8a=0.0001,c8B=0
init cc=0,ccmito=.004
# DISPLAY

```

```

@ xhi=10000,ylo=0,yhi=0.001
@ nplot=1,yp=c3a
# METHOD
@ meth=cvode,atol=1e-8,tol=1e-9,total=200000,dt=5,bounds=100000
done
*****

# figure15-p53-00308.ode
# REACTIONS
# om -> Ap
# om -> IAP
# om -> c3z
# om -> c9z
# om -> Bid
# om -> Bcl2
# om -> Bax
# om -> Ccmito
# c8a -> *
# c9a -> *
# c3a -> *
# Ap -> *
# IAP -> *
# c3z -> *
# c9z -> *
# Bcl2 -> *
# Bid -> *
# Bax -> *
# Ccmito -> *
# Bax -> *
# Bax2 -> *
# Cc -> *
# tBid -> *
# tBidBax -> *
# tBidmito -> *
# Cc + Ap <-> CcAp      k1p,k1m
# 7 CcAp <-> Apop      k1bp,k1bm
# Apop + c9z <-> Apopc9z  k2p,k2m
# Apopc9z + c9z <-> Apopc9z2 k3p,k3m
# Apopc9z2 -> Apopc9a2    k3f
# Apopc9a2 <-> Apopc9a + c9a k4p,k4m
# Apopc9a <-> Apop + c9a    k4bp,k4bm
# c9a + IAP <-> IAP9      k5p,k5m
# Apopc9a + IAP <-> IAPA9  k5bp,k5bm
# Apopc9a2 + IAP <-> IAPA29 k5cp,k5cm
# c3z + c9a <-> c93      k6p,k6m
# c93 -> c3a + c9a      k6f

```

```

# c3z + Apopc9a2 <-> cA93    k6bp,k6bm
# cA93 -> c3a + Apopc9a2    k6bf
# c3a + IAP <-> IAP3    k7p,k7m
# c8a + Bid <-> c8B    k8p,k8m
# c8B -> c8a + tBid    k8f
# c3a + Bid <-> c3B    k8p,k8m
# c3B -> c3a + tBid    k8f
# c3a + Bcl2 <-> c3L    k9p,k9m
# c3L -> c3a + B2c    k9f
# tBid -> tBidmito    k11
# tBidmito + Bax -> tBidBax    k12a
# tBidBax + Bax -> tBid + Bax2    k12b
# Bcl2 + Bax -> *    k13
# Bax2 + Ccmito -> Cc + Bax2    k14
# REACTION RATES
r1p=k1p*Cc*Ap
r1m=k1m*CcAp
r1bp=k1bp*CcAp^p
r1bm=k1bm*Apop
r2p=k2p*Apop*c9z
r2m=k2m*Apopc9z
r3p=k3p*Apopc9z*c9z
r3m=k3m*Apopc9z2
r3f=k3f*Apopc9z2
r4p=k4p*Apopc9a2
r4m=k4m*Apopc9a*c9a
r4bp=k4bp*Apopc9a
r4bm=k4bm*Apop*c9a
r5p=k5p*c9a*IAP
r5m=k5m*IAP9
r5bp=k5bp*Apopc9a*IAP
r5bm=k5bm*IAPA9
r5cp=k5cp*Apopc9a2*IAP
r5cm=k5cm*IAPA29
r6p=k6p*c3z*c9a
r6m=k6m*c93
r6f=k6f*c93
r6bp=k6p*c3z*Apopc9a2
r6bm=k6m*cA93
r6bf=k6f*cA93
r7p=k7p*c3a*IAP
r7m=k7m*IAP3
r8p=k8p*c3a*Bid
r8m=k8m*c3B
r8f=k8f*c3B
r8pp=k8p*c8a*Bid

```

$r8mp = k8m * c8B$
 $r8fp = k8f * c8B$
 $r9p = k9p * c3a * Bcl2$
 $r9m = k9m * c3L$
 $r9f = k9f * c3L$
 $r11 = k11 * tbid$
 $r12a = k12a * tbidmito * bax$
 $r12b = k12b * tbidbax * bax$
 $r13 = k13 * bcl2 * bax$
 $r14 = k14 * bax^2 * ccmito$
FLUXES
 $J1 = r1p - r1m$
 $J1b = r1bp - r1bm$
 $J2 = r2p - r2m$
 $J3 = r3p - r3m$
 $J3f = r3f$
 $J4 = r4p - r4m$
 $J4b = r4bp - r4bm$
 $J5 = r5p - r5m$
 $J5b = r5bp - r5bm$
 $J5c = r5cp - r5cm$
 $J6 = r6p - r6m$
 $J6f = r6f$
 $J6b = r6bp - r6bm$
 $J6bf = r6bf$
 $J7 = r7p - r7m$
 $J8 = r8p - r8m$
 $J8f = r8f$
 $J8p = r8pp - r8mp$
 $J8fp = r8fp$
 $J9 = r9p - r9m$
 $J9f = r9f$
 $j11 = r11$
 $j12a = r12a$
 $j12b = r12b$
 $j13 = r13$
 $j14 = r14$
PRODUCTION AND DEGRADATION RATES
 $Jp8 = -\mu * c8a$
 $JAp = 0.0001 * a1 - \mu * Ap$
 $JIAP = 0.0001 * a2 - \mu * IAP$
 $Jp3 = 0.0001 * a3 - \mu * c3z$
 $Jp9 = 0.0001 * a4 - \mu * c9z$
 $jbidp = 0.0001 * a5 - \mu * bid$
 $jbcl2p = 0.0001 * a6 * p53thresh^4 / (p53^4 + p53thresh^4) - \mu * bcl2$
 $jbax = 0.0001 * a7 * (1 + p53^4 / (p53^4 + p53thresh^4)) - \mu * bax$

```

jccmito=0.0001*a8-mu*cemito
# ODE'S
bax'=jbax-j12a-j12b-j13
Bcl2'=-J9+jbcl2p-j13
cc'=j14-j1-mu*cc+mptp*cemito
c3a'=J6f+J6bf-J7-J8+J8f-J9+J9f-mu*c3a
AP'=-J1+JAp
CcAp'=J1-7*J1b
Apop'=J1b-J2+J4b
Apopc9z'=J2-J3
Apopc9z2'=J3-J3f
Apopc9a2'=J3f-J4-J5c-J6b+J6bf
Apopc9a'=J4-J4b-J5b
c9a'=J4+J4b-J5-J6+J6f-mu*c9a
c9z'=-J2-J3+Jp9
IAP'=-J5-J5b-J5c-J7+JIAP
IAP9'=J5
IAPA9'=J5b
IAPA29'=J5c
IAP3'=J7
c3z'=-J6-J6b+Jp3-10*nop*c3z
c93'=J6-J6f
cA93'=J6b-J6bf
c8a'=Jp8-J8p+J8fp
Bid'=-J8-J8p+jbidp
c8B'=J8p-J8fp
c3B'=J8-J8f
c3L'=J9-J9f
tbid'=j8f+j8fp-j11+j12b-mu*tbid+tbid0
tbidbax'=j12a-j12b-mu*tbidbax
cemito'=jccmito-j14-mptp*cemito
bax2'=j12b-mu*bax2
tbidmito'=j11-j12a-mu*tbidmito
# PARAMETERS
par MPTP=0
par nop=0
par tbid0=0
par p53=0.00308
par p=4
par k1p=5,k1m=0.5
par k1bp=50000*a9,k1bm=0.5*a9
par k2p=10,k2m=0.5
par k3p=10,k3m=0.5,k3f=0.1
par k4p=5,k4m=0.5
par k4bp=5,k4bm=0.5
par k5p=5*a10,k5m=0.0035*a10

```

```

par k5bp=5*a10,k5bm=0.0035*a10
par k5cp=5*a10,k5cm=0.0035*a10
par k6p=10*a11,k6m=0.5*a11,k6f=0.001*a11
par k6bp=10*a11,k6bm=0.5*a11,k6bf=0.1*a11
par k7p=5*a10,k7m=0.0035*a10
par k8p=10,k8m=0.5,k8f=0.1
par k9p=10,k9m=0.5,k9f=0.1
par k11=10*a12,k12a=10*a12,k12b=10*a12,k13=10*a12,k14=10*a12
par a1=3,a2=0.3,a3=3,a4=3,a5=0.3,a6=0.8,a7=0.3,a8=3,a9=1,a10=1,a11=1,a12=1,a13=3
mu=0.002*a13
par p53thresh=0.004
# INITIAL CONDITIONS
init Ap=.004,c9z=.004,c3z=.004,IAP=.004,Bid=.004,Bcl2=.004,bax=.004
init CcAp=0,Apop=0,Apopc9z=0,Apopc9z2=0,Apopc9a2=0,Apopc9a=0,c9a=0.00,IAP3=0
init IAP9=0,IAPA9=0,IAPA29=0,c93=0,cA93=0,c3a=0.04,c3B=0,c3L=0
init c8a=0.0001,c8B=0
init cc=0,ccmito=.004
# DISPLAY
@ xhi=10000,ylo=0,yhi=0.001
@ nplot=1,yp=c3a
# METHOD
@ meth=cvode,atol=1e-8,tol=1e-9,total=200000,dt=5,bounds=100000
done
*****

# figure15-p53-0088.ode
# REACTIONS
# om -> Ap
# om -> IAP
# om -> c3z
# om -> c9z
# om -> Bid
# om -> Bcl2
# om -> Bax
# om -> Ccmito
# c8a -> *
# c9a -> *
# c3a -> *
# Ap -> *
# IAP -> *
# c3z -> *
# c9z -> *
# Bcl2 -> *
# Bid -> *
# Bax -> *
# Ccmito -> *

```

```

# Bax -> *
# Bax2 -> *
# Cc -> *
# tBid -> *
# tBidBax -> *
# tBidmito -> *
# Cc + Ap <-> CcAp      k1p,k1m
# 7 CcAp <-> Apop      k1bp,k1bm
# Apop + c9z <-> Apopc9z  k2p,k2m
# Apopc9z + c9z <-> Apopc9z2 k3p,k3m
# Apopc9z2 -> Apopc9a2    k3f
# Apopc9a2 <-> Apopc9a + c9a k4p,k4m
# Apopc9a <-> Apop + c9a    k4bp,k4bm
# c9a + IAP <-> IAP9      k5p,k5m
# Apopc9a + IAP <-> IAPA9   k5bp,k5bm
# Apopc9a2 + IAP <-> IAPA29 k5cp,k5cm
# c3z + c9a <-> c93      k6p,k6m
# c93 -> c3a + c9a      k6f
# c3z + Apopc9a2 <-> cA93   k6bp,k6bm
# cA93 -> c3a + Apopc9a2   k6bf
# c3a + IAP <-> IAP3      k7p,k7m
# c8a + Bid <-> c8B      k8p,k8m
# c8B -> c8a + tBid      k8f
# c3a + Bid <-> c3B      k8p,k8m
# c3B -> c3a + tBid      k8f
# c3a + Bcl2 <-> c3L     k9p,k9m
# c3L -> c3a + B2c      k9f
# tBid -> tBidmito      k11
# tBidmito + Bax -> tBidBax k12a
# tBidBax + Bax -> tBid + Bax2 k12b
# Bcl2 + Bax -> *      k13
# Bax2 + Ccmito -> Cc + Bax2 k14
# REACTION RATES
r1p=k1p*Cc*Ap
r1m=k1m*CcAp
r1bp=k1bp*CcAp^p
r1bm=k1bm*Apop
r2p=k2p*Apop*c9z
r2m=k2m*Apopc9z
r3p=k3p*Apopc9z*c9z
r3m=k3m*Apopc9z2
r3f=k3f*Apopc9z2
r4p=k4p*Apopc9a2
r4m=k4m*Apopc9a*c9a
r4bp=k4bp*Apopc9a
r4bm=k4bm*Apop*c9a

```

$r5p=k5p*c9a*IAP$
 $r5m=k5m*IAP9$
 $r5bp=k5bp*Apopc9a*IAP$
 $r5bm=k5bm*IAPA9$
 $r5cp=k5cp*Apopc9a2*IAP$
 $r5cm=k5cm*IAPA29$
 $r6p=k6p*c3z*c9a$
 $r6m=k6m*c93$
 $r6f=k6f*c93$
 $r6bp=k6p*c3z*Apopc9a2$
 $r6bm=k6m*cA93$
 $r6bf=k6f*cA93$
 $r7p=k7p*c3a*IAP$
 $r7m=k7m*IAP3$
 $r8p=k8p*c3a*Bid$
 $r8m=k8m*c3B$
 $r8f=k8f*c3B$
 $r8pp=k8p*c8a*Bid$
 $r8mp=k8m*c8B$
 $r8fp=k8f*c8B$
 $r9p=k9p*c3a*Bcl2$
 $r9m=k9m*c3L$
 $r9f=k9f*c3L$
 $r11=k11*tbid$
 $r12a=k12a*tbidmito*bax$
 $r12b=k12b*tbidbax*bax$
 $r13=k13*bcl2*bax$
 $r14=k14*bax2*ccmito$
FLUXES
 $J1=r1p-r1m$
 $J1b=r1bp-r1bm$
 $J2=r2p-r2m$
 $J3=r3p-r3m$
 $J3f=r3f$
 $J4=r4p-r4m$
 $J4b=r4bp-r4bm$
 $J5=r5p-r5m$
 $J5b=r5bp-r5bm$
 $J5c=r5cp-r5cm$
 $J6=r6p-r6m$
 $J6f=r6f$
 $J6b=r6bp-r6bm$
 $J6bf=r6bf$
 $J7=r7p-r7m$
 $J8=r8p-r8m$
 $J8f=r8f$

$J8p=r8pp-r8mp$
 $J8fp=r8fp$
 $J9=r9p-r9m$
 $J9f=r9f$
 $j11=r11$
 $j12a=r12a$
 $j12b=r12b$
 $j13=r13$
 $j14=r14$
PRODUCTION AND DEGRADATION RATES
 $Jp8=-\mu*c8a$
 $JAp=0.0001*a1-\mu*Ap$
 $JIAP=0.0001*a2-\mu*IAP$
 $Jp3=0.0001*a3-\mu*c3z$
 $Jp9=0.0001*a4-\mu*c9z$
 $jbidp=0.0001*a5-\mu*bid$
 $jbcl2p=0.0001*a6*p53thresh^4/(p53^4+p53thresh^4)-\mu*bcl2$
 $jbax=0.0001*a7*(1+p53^4/(p53^4+p53thresh^4))-\mu*bax$
 $jccmito=0.0001*a8-\mu*ccmito$
ODE'S
 $bax'=jbax-j12a-j12b-j13$
 $Bcl2'=-J9+jbcl2p-j13$
 $cc'=j14-j1-\mu*cc+mtp*ccmito$
 $c3a'=J6f+J6bf-J7-J8+J8f-J9+J9f-\mu*c3a$
 $AP'=-J1+JAp$
 $CcAp'=J1-7*J1b$
 $Apop'=J1b-J2+J4b$
 $Apopc9z'=J2-J3$
 $Apopc9z2'=J3-J3f$
 $Apopc9a2'=J3f-J4-J5c-J6b+J6bf$
 $Apopc9a'=J4-J4b-J5b$
 $c9a'=J4+J4b-J5-J6+J6f-\mu*c9a$
 $c9z'=-J2-J3+Jp9$
 $IAP'=-J5-J5b-J5c-J7+JIAP$
 $IAP9'=J5$
 $IAPA9'=J5b$
 $IAPA29'=J5c$
 $IAP3'=J7$
 $c3z'=-J6-J6b+Jp3-10*nop*c3z$
 $c93'=J6-J6f$
 $cA93'=J6b-J6bf$
 $c8a'=Jp8-J8p+J8fp$
 $Bid'=-J8-J8p+jbidp$
 $c8B'=J8p-J8fp$
 $c3B'=J8-J8f$
 $c3L'=J9-J9f$

```

tbid'=j8f+j8fp-j11+j12b-mu*tbid+tbid0
tbidbax'=j12a-j12b-mu*tbidbax
ccmito'=jccmito-j14-mptp*ccmito
bax2'=j12b-mu*bax2
tbidmito'=j11-j12a-mu*tbidmito
# PARAMETERS
par MPTP=0
par nop=0
par tbid0=0
par p53=0.0088
par p=4
par k1p=5,k1m=0.5
par k1bp=50000*a9,k1bm=0.5*a9
par k2p=10,k2m=0.5
par k3p=10,k3m=0.5,k3f=0.1
par k4p=5,k4m=0.5
par k4bp=5,k4bm=0.5
par k5p=5*a10,k5m=0.0035*a10
par k5bp=5*a10,k5bm=0.0035*a10
par k5cp=5*a10,k5cm=0.0035*a10
par k6p=10*a11,k6m=0.5*a11,k6f=0.001*a11
par k6bp=10*a11,k6bm=0.5*a11,k6bf=0.1*a11
par k7p=5*a10,k7m=0.0035*a10
par k8p=10,k8m=0.5,k8f=0.1
par k9p=10,k9m=0.5,k9f=0.1
par k11=10*a12,k12a=10*a12,k12b=10*a12,k13=10*a12,k14=10*a12
par a1=3,a2=0.3,a3=3,a4=3,a5=0.3,a6=0.8,a7=0.3,a8=3,a9=1,a10=1,a11=1,a12=1,a13=3
mu=0.002*a13
par p53thresh=0.004
# INITIAL CONDITIONS
init Ap=.004,c9z=.004,c3z=.004,IAP=.004,Bid=.004,Bcl2=.004,bax=.004
init CcAp=0,Apop=0,Apopc9z=0,Apopc9z2=0,Apopc9a2=0,Apopc9a=0,c9a=0.00,IAP3=0
init IAP9=0,IAPA9=0,IAPA29=0,c93=0,cA93=0,c3a=0.04,c3B=0,c3L=0
init c8a=0.0001,c8B=0
init cc=0,ccmito=.004
# DISPLAY
@ xhi=10000,ylo=0,yhi=0.001
@ nplot=1,yp=c3a
# METHOD
@ meth=cvode,atol=1e-8,tol=1e-9,total=200000,dt=5,bounds=100000
done

```

A.1.8 Scripts used in Figure 16

```
# figure16A.ode
# REACTIONS
# om -> Ap
# om -> IAP
# om -> c3z
# om -> c9z
# om -> Bid
# om -> Bcl2
# om -> Bax
# om -> Ccmito
# c8a -> *
# c9a -> *
# c3a -> *
# Ap -> *
# IAP -> *
# c3z -> *
# c9z -> *
# Bcl2 -> *
# Bid -> *
# Bax -> *
# Ccmito -> *
# Bax -> *
# Bax2 -> *
# Cc -> *
# tBid -> *
# tBidBax -> *
# tBidmito -> *
# Cc + Ap <-> CcAp      k1p,k1m
# 7 CcAp <-> Apop      k1bp,k1bm
# Apop + c9z <-> Apopc9z  k2p,k2m
# Apopc9z + c9z <-> Apopc9z2 k3p,k3m
# Apopc9z2 -> Apopc9a2    k3f
# Apopc9a2 <-> Apopc9a + c9a k4p,k4m
# Apopc9a <-> Apop + c9a   k4bp,k4bm
# c9a + IAP <-> IAP9     k5p,k5m
# Apopc9a + IAP <-> IAPA9  k5bp,k5bm
# Apopc9a2 + IAP <-> IAPA29 k5cp,k5cm
# c3z + c9a <-> c93      k6p,k6m
# c93 -> c3a + c9a      k6f
# c3z + Apopc9a2 <-> cA93  k6bp,k6bm
# cA93 -> c3a + Apopc9a2  k6bf
# c3a + IAP <-> IAP3     k7p,k7m
# c8a + Bid <-> c8B     k8p,k8m
```

```

# c8B -> c8a + tBid      k8f
# c3a + Bid <-> c3B      k8p,k8m
# c3B -> c3a + tBid      k8f
# c3a + Bcl2 <-> c3L     k9p,k9m
# c3L -> c3a + B2c       k9f
# tBid -> tBidmito       k11
# tBidmito + Bax -> tBidBax k12a
# tBidBax + Bax -> tBid + Bax2 k12b
# Bcl2 + Bax -> *        k13
# Bax2 + Ccmito -> Cc + Bax2 k14
# REACTION RATES
r1p=k1p*Cc*Ap
r1m=k1m*CcAp
r1bp=k1bp*CcAp^p
r1bm=k1bm*Apop
r2p=k2p*Apop*c9z
r2m=k2m*Apopc9z
r3p=k3p*Apopc9z*c9z
r3m=k3m*Apopc9z2
r3f=k3f*Apopc9z2
r4p=k4p*Apopc9a2
r4m=k4m*Apopc9a*c9a
r4bp=k4bp*Apopc9a
r4bm=k4bm*Apop*c9a
r5p=k5p*c9a*IAP
r5m=k5m*IAP9
r5bp=k5bp*Apopc9a*IAP
r5bm=k5bm*IAPA9
r5cp=k5cp*Apopc9a2*IAP
r5cm=k5cm*IAPA29
r6p=k6p*c3z*c9a
r6m=k6m*c93
r6f=k6f*c93
r6bp=k6p*c3z*Apopc9a2
r6bm=k6m*cA93
r6bf=k6f*cA93
r7p=k7p*c3a*IAP
r7m=k7m*IAP3
r8p=k8p*c3a*Bid
r8m=k8m*c3B
r8f=k8f*c3B
r8pp=k8p*c8a*Bid
r8mp=k8m*c8B
r8fp=k8f*c8B
r9p=k9p*c3a*Bcl2
r9m=k9m*c3L

```

```

r9f=k9f*c3L
r11=k11*tbid
r12a=k12a*tbidmito*bax
r12b=k12b*tbidbax*bax
r13=k13*bcl2*bax
r14=k14*bax2*ccmito
# FLUXES
J1=r1p-r1m
J1b=r1bp-r1bm
J2=r2p-r2m
J3=r3p-r3m
J3f=r3f
J4=r4p-r4m
J4b=r4bp-r4bm
J5=r5p-r5m
J5b=r5bp-r5bm
J5c=r5cp-r5cm
J6=r6p-r6m
J6f=r6f
J6b=r6bp-r6bm
J6bf=r6bf
J7=r7p-r7m
J8=r8p-r8m
J8f=r8f
J8p=r8pp-r8mp
J8fp=r8fp
J9=r9p-r9m
J9f=r9f
j11=r11
j12a=r12a
j12b=r12b
j13=r13
j14=r14
# PRODUCTION AND DEGRADATION RATES
Jp8=-mu*c8a
JAp=0.0001*a1-mu*Ap
JIAP=0.0001*a2-mu*IAP
Jp3=0.0001*a3-mu*c3z
Jp9=0.0001*a4-mu*c9z
jbidp=0.0001*a5-mu*bid
jbcl2p=0.0001*a6*p53thresh^4/(p53^4+p53thresh^4)-mu*bcl2
jbax=0.0001*a7*(1+p53^4/(p53^4+p53thresh^4))-mu*bax
jccmito=0.0001*a8-mu*ccmito
# ODE'S
bax'=jbax-j12a-j12b-j13
Bcl2'=-J9+jbcl2p-j13

```

```

cc'=j14-j1-mu*cc+mptp*ccmito
c3a'=J6f+J6bf-J7-J8+J8f-J9+J9f-mu*c3a
AP'=-J1+JAp
CcAp'=J1-7*J1b
Apop'=J1b-J2+J4b
Apopc9z'=J2-J3
Apopc9z2'=J3-J3f
Apopc9a2'=J3f-J4-J5c-J6b+J6bf
Apopc9a'=J4-J4b-J5b
c9a'=J4+J4b-J5-J6+J6f-mu*c9a
c9z'=-J2-J3+Jp9
IAP'=-J5-J5b-J5c-J7+JIAP
IAP9'=J5
IAPA9'=J5b
IAPA29'=J5c
IAP3'=J7
c3z'=-J6-J6b+Jp3-10*nop*c3z
c93'=J6-J6f
cA93'=J6b-J6bf
c8a'=Jp8-J8p+J8fp
Bid'=-J8-J8p+jbidp
c8B'=J8p-J8fp
c3B'=J8-J8f
c3L'=J9-J9f
tbid'=j8f+j8fp-j11+j12b-mu*tbid+tbid0
tbidbax'=j12a-j12b-mu*tbidbax
ccmito'=jccmito-j14-mptp*ccmito
bax2'=j12b-mu*bax2
tbidmito'=j11-j12a-mu*tbidmito
# PARAMETERS
par MPTP=0
par nop=0
par tbid0=0
par p53=0.0066
par p=4
par k1p=5,k1m=0.5
par k1bp=50000*a9,k1bm=0.5*a9
par k2p=10,k2m=0.5
par k3p=10,k3m=0.5,k3f=0.1
par k4p=5,k4m=0.5
par k4bp=5,k4bm=0.5
par k5p=5*a10,k5m=0.0035*a10
par k5bp=5*a10,k5bm=0.0035*a10
par k5cp=5*a10,k5cm=0.0035*a10
par k6p=10*a11,k6m=0.5*a11,k6f=0.001*a11
par k6bp=10*a11,k6bm=0.5*a11,k6bf=0.1*a11

```

```

par k7p=5*a10,k7m=0.0035*a10
par k8p=10,k8m=0.5,k8f=0.1
par k9p=10,k9m=0.5,k9f=0.1
par k11=10*a12,k12a=10*a12,k12b=10*a12,k13=10*a12,k14=10*a12
par a1=3,a2=0.3,a3=3,a4=3,a5=0.3,a6=0.8,a7=0.3,a8=3,a9=1,a10=1,a11=1,a12=1,a13=3
mu=0.002*a13
par p53thresh=0.004
# INITIAL CONDITIONS
init Ap=.004,c9z=.004,c3z=.004,IAP=.004,Bid=.004,Bcl2=.004,bax=.004
init CcAp=0,Apop=0,Apopc9z=0,Apopc9z2=0,Apopc9a2=0,Apopc9a=0,c9a=0.00
init IAP3=0,IAP9=0,IAPA9=0,IAPA29=0,c93=0,cA93=0,c3a=0.00001,c3B=0,c3L=0
init c8a=0.00001,c8B=0
init cc=0,ccmito=.004
# DISPLAY
@ xhi=10000,ylo=0,yhi=0.001
@ nplot=1,yp=c3a
# METHOD
@ meth=cvode,atol=1e-8,tol=1e-9,total=18000,dt=5,bounds=100000
done
*****

# figure16B.ode
# REACTIONS
# om -> Ap
# om -> IAP
# om -> c3z
# om -> c9z
# om -> Bid
# om -> Bcl2
# om -> Bax
# om -> Ccmito
# c8a -> *
# c9a -> *
# c3a -> *
# Ap -> *
# IAP -> *
# c3z -> *
# c9z -> *
# Bcl2 -> *
# Bid -> *
# Bax -> *
# Ccmito -> *
# Bax -> *
# Bax2 -> *
# Cc -> *
# tBid -> *

```

```

# tBidBax -> *
# tBidmito -> *
# Cc + Ap <-> CcAp      k1p,k1m
# 7 CcAp <-> Apop      k1bp,k1bm
# Apop + c9z <-> Apopc9z  k2p,k2m
# Apopc9z + c9z <-> Apopc9z2 k3p,k3m
# Apopc9z2 -> Apopc9a2    k3f
# Apopc9a2 <-> Apopc9a + c9a k4p,k4m
# Apopc9a <-> Apop + c9a    k4bp,k4bm
# c9a + IAP <-> IAP9      k5p,k5m
# Apopc9a + IAP <-> IAPA9  k5bp,k5bm
# Apopc9a2 + IAP <-> IAPA29 k5cp,k5cm
# c3z + c9a <-> c93      k6p,k6m
# c93 -> c3a + c9a      k6f
# c3z + Apopc9a2 <-> cA93  k6bp,k6bm
# cA93 -> c3a + Apopc9a2  k6bf
# c3a + IAP <-> IAP3     k7p,k7m
# c8a + Bid <-> c8B     k8p,k8m
# c8B -> c8a + tBid     k8f
# c3a + Bid <-> c3B     k8p,k8m
# c3B -> c3a + tBid     k8f
# c3a + Bcl2 <-> c3L   k9p,k9m
# c3L -> c3a + B2c     k9f
# tBid -> tBidmito     k11
# tBidmito + Bax -> tBidBax k12a
# tBidBax + Bax -> tBid + Bax2 k12b
# Bcl2 + Bax -> *      k13
# Bax2 + Ccmito -> Cc + Bax2 k14
# REACTION RATES
r1p=k1p*Cc*Ap
r1m=k1m*CcAp
r1bp=k1bp*CcAp^p
r1bm=k1bm*Apop
r2p=k2p*Apop*c9z
r2m=k2m*Apopc9z
r3p=k3p*Apopc9z*c9z
r3m=k3m*Apopc9z2
r3f=k3f*Apopc9z2
r4p=k4p*Apopc9a2
r4m=k4m*Apopc9a*c9a
r4bp=k4bp*Apopc9a
r4bm=k4bm*Apop*c9a
r5p=k5p*c9a*IAP
r5m=k5m*IAP9
r5bp=k5bp*Apopc9a*IAP
r5bm=k5bm*IAPA9

```

$r5cp=k5cp*Apopc9a2*IAP$
 $r5cm=k5cm*IAPA29$
 $r6p=k6p*c3z*c9a$
 $r6m=k6m*c93$
 $r6f=k6f*c93$
 $r6bp=k6p*c3z*Apopc9a2$
 $r6bm=k6m*cA93$
 $r6bf=k6f*cA93$
 $r7p=k7p*c3a*IAP$
 $r7m=k7m*IAP3$
 $r8p=k8p*c3a*Bid$
 $r8m=k8m*c3B$
 $r8f=k8f*c3B$
 $r8pp=k8p*c8a*Bid$
 $r8mp=k8m*c8B$
 $r8fp=k8f*c8B$
 $r9p=k9p*c3a*Bcl2$
 $r9m=k9m*c3L$
 $r9f=k9f*c3L$
 $r11=k11*tbid$
 $r12a=k12a*tbidmito*bax$
 $r12b=k12b*tbidbax*bax$
 $r13=k13*bcl2*bax$
 $r14=k14*bax2*ccmito$
FLUXES
 $J1=r1p-r1m$
 $J1b=r1bp-r1bm$
 $J2=r2p-r2m$
 $J3=r3p-r3m$
 $J3f=r3f$
 $J4=r4p-r4m$
 $J4b=r4bp-r4bm$
 $J5=r5p-r5m$
 $J5b=r5bp-r5bm$
 $J5c=r5cp-r5cm$
 $J6=r6p-r6m$
 $J6f=r6f$
 $J6b=r6bp-r6bm$
 $J6bf=r6bf$
 $J7=r7p-r7m$
 $J8=r8p-r8m$
 $J8f=r8f$
 $J8p=r8pp-r8mp$
 $J8fp=r8fp$
 $J9=r9p-r9m$
 $J9f=r9f$

```

j11=r11
j12a=r12a
j12b=r12b
j13=r13
j14=r14
# PRODUCTION AND DEGRADATION RATES
Jp8=-mu*c8a
JAp=0.0001*a1-mu*Ap
JIAP=0.0001*a2-mu*IAP
Jp3=0.0001*a3-mu*c3z
Jp9=0.0001*a4-mu*c9z
jbidp=0.0001*a5-mu*bid
jbc12p=0.0001*a6*p53thresh^4/(p53^4+p53thresh^4)-mu*bc12
jbax=0.0001*a7*(1+p53^4/(p53^4+p53thresh^4))-mu*bax
jccmito=0.0001*a8-mu*ccmito
# ODE'S
bax'=jbax-j12a-j12b-j13
Bcl2'=-J9+jbc12p-j13
cc'=j14-j1-mu*cc+mptp*ccmito
c3a'=J6f+J6bf-J7-J8+J8f-J9+J9f-mu*c3a
AP'=-J1+JAp
CcAp'=J1-7*J1b
Apop'=J1b-J2+J4b
Apopc9z'=J2-J3
Apopc9z2'=J3-J3f
Apopc9a2'=J3f-J4-J5c-J6b+J6bf
Apopc9a'=J4-J4b-J5b
c9a'=J4+J4b-J5-J6+J6f-mu*c9a
c9z'=-J2-J3+Jp9
IAP'=-J5-J5b-J5c-J7+JIAP
IAP9'=J5
IAPA9'=J5b
IAPA29'=J5c
IAP3'=J7
c3z'=-J6-J6b+Jp3-10*nop*c3z
c93'=J6-J6f
cA93'=J6b-J6bf
c8a'=Jp8-J8p+J8fp
Bid'=-J8-J8p+jbidp
c8B'=J8p-J8fp
c3B'=J8-J8f
c3L'=J9-J9f
tbid'=j8f+j8fp-j11+j12b-mu*tbid+tbid0
tbidbax'=j12a-j12b-mu*tbidbax
ccmito'=jccmito-j14-mptp*ccmito
bax2'=j12b-mu*bax2

```

```

tbidmito'=j11-j12a-mu*tbidmito
# PARAMETERS
par MPTP=0
par nop=0
par tbid0=0
par p53=0.0066
par p=4
par k1p=5,k1m=0.5
par k1bp=50000*a9,k1bm=0.5*a9
par k2p=10,k2m=0.5
par k3p=10,k3m=0.5,k3f=0.1
par k4p=5,k4m=0.5
par k4bp=5,k4bm=0.5
par k5p=5*a10,k5m=0.0035*a10
par k5bp=5*a10,k5bm=0.0035*a10
par k5cp=5*a10,k5cm=0.0035*a10
par k6p=10*a11,k6m=0.5*a11,k6f=0.001*a11
par k6bp=10*a11,k6bm=0.5*a11,k6bf=0.1*a11
par k7p=5*a10,k7m=0.0035*a10
par k8p=10,k8m=0.5,k8f=0.1
par k9p=10,k9m=0.5,k9f=0.1
par k11=10*a12,k12a=10*a12,k12b=10*a12,k13=10*a12,k14=10*a12
par a1=3,a2=0.3,a3=3,a4=3,a5=0.3,a6=0.8,a7=0.3,a8=3,a9=1,a10=1,a11=1,a12=1,a13=3
mu=0.002*a13
par p53thresh=0.004
# INITIAL CONDITIONS
init Ap=.004,c9z=.004,c3z=.004,IAP=.004,Bid=.004,Bcl2=.004,bax=.004
init CcAp=0,Apop=0,Apopc9z=0,Apopc9z2=0,Apopc9a2=0,Apopc9a=0,c9a=0.00
init IAP3=0,IAP9=0,IAPA9=0,IAPA29=0,c93=0,cA93=0,c3a=0.00001,c3B=0,c3L=0
init c8a=0.0001,c8B=0
init cc=0,ccmito=.004
# DISPLAY
@ xhi=10000,ylo=0,yhi=0.001
@ nplot=1,yp=c3a
# METHOD
@ meth=cvode,atol=1e-8,tol=1e-9,total=18000,dt=5,bounds=100000
done
*****

# figure16C.ode
# REACTIONS
# om -> Ap
# om -> IAP
# om -> c3z
# om -> c9z
# om -> Bid

```

```

# om -> Bcl2
# om -> Bax
# om -> Ccmito
# c8a -> *
# c9a -> *
# c3a -> *
# Ap -> *
# IAP -> *
# c3z -> *
# c9z -> *
# Bcl2 -> *
# Bid -> *
# Bax -> *
# Ccmito -> *
# Bax -> *
# Bax2 -> *
# Cc -> *
# tBid -> *
# tBidBax -> *
# tBidmito -> *
# Cc + Ap <-> CcAp      k1p,k1m
# 7 CcAp <-> Apop      k1bp,k1bm
# Apop + c9z <-> Apopc9z  k2p,k2m
# Apopc9z + c9z <-> Apopc9z2 k3p,k3m
# Apopc9z2 -> Apopc9a2    k3f
# Apopc9a2 <-> Apopc9a + c9a k4p,k4m
# Apopc9a <-> Apop + c9a    k4bp,k4bm
# c9a + IAP <-> IAP9      k5p,k5m
# Apopc9a + IAP <-> IAPA9  k5bp,k5bm
# Apopc9a2 + IAP <-> IAPA29 k5cp,k5cm
# c3z + c9a <-> c93      k6p,k6m
# c93 -> c3a + c9a      k6f
# c3z + Apopc9a2 <-> cA93  k6bp,k6bm
# cA93 -> c3a + Apopc9a2  k6bf
# c3a + IAP <-> IAP3     k7p,k7m
# c8a + Bid <-> c8B      k8p,k8m
# c8B -> c8a + tBid     k8f
# c3a + Bid <-> c3B      k8p,k8m
# c3B -> c3a + tBid     k8f
# c3a + Bcl2 <-> c3L    k9p,k9m
# c3L -> c3a + B2c      k9f
# tBid -> tBidmito      k11
# tBidmito + Bax -> tBidBax k12a
# tBidBax + Bax -> tBid + Bax2 k12b
# Bcl2 + Bax -> *      k13
# Bax2 + Ccmito -> Cc + Bax2 k14

```

```

# REACTION RATES
r1p=k1p*Cc*Ap
r1m=k1m*CcAp
r1bp=k1bp*CcAp^p
r1bm=k1bm*Apop
r2p=k2p*Apop*c9z
r2m=k2m*Apopc9z
r3p=k3p*Apopc9z*c9z
r3m=k3m*Apopc9z2
r3f=k3f*Apopc9z2
r4p=k4p*Apopc9a2
r4m=k4m*Apopc9a*c9a
r4bp=k4bp*Apopc9a
r4bm=k4bm*Apop*c9a
r5p=k5p*c9a*IAP
r5m=k5m*IAP9
r5bp=k5bp*Apopc9a*IAP
r5bm=k5bm*IAPA9
r5cp=k5cp*Apopc9a2*IAP
r5cm=k5cm*IAPA29
r6p=k6p*c3z*c9a
r6m=k6m*c93
r6f=k6f*c93
r6bp=k6p*c3z*Apopc9a2
r6bm=k6m*cA93
r6bf=k6f*cA93
r7p=k7p*c3a*IAP
r7m=k7m*IAP3
r8p=k8p*c3a*Bid
r8m=k8m*c3B
r8f=k8f*c3B
r8pp=k8p*c8a*Bid
r8mp=k8m*c8B
r8fp=k8f*c8B
r9p=k9p*c3a*Bcl2
r9m=k9m*c3L
r9f=k9f*c3L
r11=k11*tbid
r12a=k12a*tbidmito*bax
r12b=k12b*tbidbax*bax
r13=k13*bcl2*bax
r14=k14*bax2*ccmito
# FLUXES
J1=r1p-r1m
J1b=r1bp-r1bm
J2=r2p-r2m

```

$J3=r3p-r3m$
 $J3f=r3f$
 $J4=r4p-r4m$
 $J4b=r4bp-r4bm$
 $J5=r5p-r5m$
 $J5b=r5bp-r5bm$
 $J5c=r5cp-r5cm$
 $J6=r6p-r6m$
 $J6f=r6f$
 $J6b=r6bp-r6bm$
 $J6bf=r6bf$
 $J7=r7p-r7m$
 $J8=r8p-r8m$
 $J8f=r8f$
 $J8p=r8pp-r8mp$
 $J8fp=r8fp$
 $J9=r9p-r9m$
 $J9f=r9f$
 $j11=r11$
 $j12a=r12a$
 $j12b=r12b$
 $j13=r13$
 $j14=r14$
PRODUCTION AND DEGRADATION RATES
 $Jp8=-\mu*c8a$
 $JAp=0.0001*a1-\mu*Ap$
 $JIAP=0.0001*a2-\mu*IAP$
 $Jp3=0.0001*a3-\mu*c3z$
 $Jp9=0.0001*a4-\mu*c9z$
 $jbidp=0.0001*a5-\mu*bid$
 $jbcl2p=0.0001*a6*p53thresh^4/(p53^4+p53thresh^4)-\mu*bcl2$
 $jbax=0.0001*a7*(1+p53^4/(p53^4+p53thresh^4))-\mu*bax$
 $jccmito=0.0001*a8-\mu*ccmito$
ODE'S
 $bax'=jbax-j12a-j12b-j13$
 $Bcl2'=-J9+jbcl2p-j13$
 $cc'=j14-j1-\mu*cc+mptp*ccmito$
 $c3a'=J6f+J6bf-J7-J8+J8f-J9+J9f-\mu*c3a$
 $AP'=-J1+JAp$
 $CcAp'=J1-7*J1b$
 $Apop'=J1b-J2+J4b$
 $Apopc9z'=J2-J3$
 $Apopc9z2'=J3-J3f$
 $Apopc9a2'=J3f-J4-J5c-J6b+J6bf$
 $Apopc9a'=J4-J4b-J5b$
 $c9a'=J4+J4b-J5-J6+J6f-\mu*c9a$

```

c9z'=-J2-J3+Jp9
IAP'=-J5-J5b-J5c-J7+JIAP
IAP9'=J5
IAPA9'=J5b
IAPA29'=J5c
IAP3'=J7
c3z'=-J6-J6b+Jp3-10*nop*c3z
c93'=J6-J6f
cA93'=J6b-J6bf
c8a'=Jp8-J8p+J8fp
Bid'=-J8-J8p+jbidp
c8B'=J8p-J8fp
c3B'=J8-J8f
c3L'=J9-J9f
tbid'=j8f+j8fp-j11+j12b-mu*tbid+tbid0
tbidbax'=j12a-j12b-mu*tbidbax
ccmito'=jccmito-j14-mptp*ccmito
bax2'=j12b-mu*bax2
tbidmito'=j11-j12a-mu*tbidmito
# PARAMETERS
par MPTP=0
par nop=0
par tbid0=0
par p53=0.0066
par p=4
par k1p=5,k1m=0.5
par k1bp=50000*a9,k1bm=0.5*a9
par k2p=10,k2m=0.5
par k3p=10,k3m=0.5,k3f=0.1
par k4p=5,k4m=0.5
par k4bp=5,k4bm=0.5
par k5p=5*a10,k5m=0.0035*a10
par k5bp=5*a10,k5bm=0.0035*a10
par k5cp=5*a10,k5cm=0.0035*a10
par k6p=10*a11,k6m=0.5*a11,k6f=0.001*a11
par k6bp=10*a11,k6bm=0.5*a11,k6bf=0.1*a11
par k7p=5*a10,k7m=0.0035*a10
par k8p=10,k8m=0.5,k8f=0.1
par k9p=10,k9m=0.5,k9f=0.1
par k11=10*a12,k12a=10*a12,k12b=10*a12,k13=10*a12,k14=10*a12
par a1=3,a2=0.3,a3=3,a4=3,a5=0.3,a6=0.8,a7=0.3,a8=3,a9=1,a10=1,a11=1,a12=1,a13=3
mu=0.002*a13
par p53thresh=0.004
# INITIAL CONDITIONS
init Ap=.004,c9z=.004,c3z=.004,IAP=.004,Bid=.004,Bcl2=.004,bax=.004
init CcAp=0,Apop=0,Apopc9z=0,Apopc9z2=0,Apopc9a2=0,Apopc9a=0,c9a=0.00

```

```

init IAP3=0,IAP9=0,IAPA9=0,IAPA29=0,c93=0,cA93=0,c3a=0.00001,c3B=0,c3L=0
init c8a=0.00015,c8B=0
init cc=0,ccmito=.004
# DISPLAY
@ xhi=10000,ylo=0,yhi=0.001
@ nplot=1,yp=c3a
# METHOD
@ meth=cvode,atol=1e-8,tol=1e-9,total=18000,dt=5,bounds=100000
done

```

A.1.9 Scripts used in Figure 17

```

# figure17-GSH100.ode
# REACTIONS
# * -> NO                k1NO
# * -> O2m                k2NO
# * -> GSH                k3NO
# NO + O2m -> ONOOm      k4NO
# SOD + O2m + Hp -> SOD + 1/2O2 + 1/2 H2O2 k5NO
# ONOOm + GSH -> GSNO + products      k6NO
# ONOOm + GPX -> GPX + products      k7NO
# ONOOm + CO2 -> products            k8NO
# ONOOm + Cc -> Cc + products        k9NO
# 2GSNO + O2m + H2O -> GSSG + products k10NO
# N2O3 + GSH -> GSNO + products      k11NO
# 2NO + O2 -> 2NO2                k12aNO
# N2O3 + H2O -> products            k13NO
# GSSG + NADPH +Hp -> 2GSH + NADPp    Vm,Km
# NO2 + NO <-> N2O3                k12bNOp,k12bNOm
# GSNO (Cu+) -> 1/2GSSG + NO        k14NO
# CcOx + NO -> CcOX.NO              k15NO
# FeL + NO -> FeLNO                 k16NO
# FeLNO + GSH -> GSNO + FeL         k17NO
# GSH + O2m -> 1/2 GSSG + products   k17NOb
# REACTION RATES
r1NO=k1NO
r2NO=k2NO
r3NO=k3NO
r4NO=k4NO*NO*O2m
r5NO=k5NO*SOD*O2m
r6NO=k6NO*ONOOm*GSH
r7NO=k7NO*ONOOm*GPX
r8NO=k8NO*ONOOm*CO2
r9NO=k9NO*ONOOm*Cc

```

```

r10NO=k10NO*GSNO^2*O2m
r11NO=k11NO*N2O3*GSH
r12aNO=k12aNO*NO*NO*O2
r12bNOp=k12bNOp*NO2*NO
r12bNOm=k12bNOm*N2O3
r13NO=k13NO*N2O3
rm=Vm*GSSG(GSH,GSNO)/(Km+GSSG(GSH,GSNO))
r14NO=k14NO*GSNO
r15NO=k15NO*CcOx*NO
r16NO=k16NO*FeL*NO
r17NO=k17NO*FeLNO(FeL)*GSH
r17NOb=k17NOb*GSH*O2m
# ODE'S
N2O3'=-r11NO-r13NO+r12bNOp-r12bNOm
GSH'=r3NO-r6NO-r11NO+2*rm-r17NO-r17NOb
NO'=r1NO-r4NO-2*r12aNO-r12bNOp+r12bNOm+r14NO-r15NO-r16NO
O2m'=r2NO-r4NO-r5NO-r10NO-r17NOb
ONOOm'=r4NO-r6NO-r7NO-r8NO-r9NO
GSNO'=r6NO-2*r10NO+r11NO-r14NO+r17NO
NO2'=2*r12aNO-r12bNOp+r12bNOm
CcOX'=-r15NO
FeL'=-r16NO+r17NO
# EXPRESSIONS
GSSG(GSH,GSNO)=(100-GSH-GSNO)/2
FeLNO(FeL)=0.05-FeL
aux FeLNOstf=FeLNO(FeL)
# PARAMETERS
# k1NO is varied, i used a bigger number (1)
par k1NO=1
# k2NO is varied
par k2NO=0.1
# k3NO is varied
par k3NO=0
par O2=35
par Cc=400
# SOD is between 1 and 10
par SOD=10
par GPX=5.8
# CO2 is between 1000 and 25000
par CO2=1000
par Km=50
par k4NO=6700
par k5NO=2400
par k6NO=0.00135
par k7NO=2
par k8NO=0.058

```

```

par k9NO=0.025
par k10NO=0.0006
par k11NO=66
par k12aNO=0.000006
par k13NO=1600
par Vm=320
par k12bNOp=1100
par k12bNOm=81000
par k14NO=0.0002
par k15NO=100
par k16NO=1.21
#the same value as k11NO is used for k17NO as a first guess
par k17NO=66
par k17NOb=0.0002
# INITIAL CONDITIONS
init CcOx=0.1
init FeL=0.05
init GSH=100
# DISPLAY
@ xhi=10000,ylo=0,yhi=0.001
@ nplot=3,yp=FeLNOstf,yp2=N2O3,yp3=GSH
# METHOD
@ meth=cvode,atol=1e-8,tol=1e-9,total=60000,dt=5,bounds=1000000000
done
*****

# figure17-GSH1000.ode
# REACTIONS
# * -> NO                k1NO
# * -> O2m               k2NO
# * -> GSH               k3NO
# NO + O2m -> ONOOm      k4NO
# SOD + O2m + Hp -> SOD + 1/2O2 + 1/2 H2O2 k5NO
# ONOOm + GSH -> GSNO + products      k6NO
# ONOOm + GPX -> GPX + products      k7NO
# ONOOm + CO2 -> products      k8NO
# ONOOm + Cc -> Cc + products      k9NO
# 2GSNO + O2m + H2O -> GSSG + products k10NO
# N2O3 + GSH -> GSNO + products      k11NO
# 2NO + O2 -> 2NO2      k12aNO
# N2O3 + H2O -> products      k13NO
# GSSG + NADPH +Hp -> 2GSH + NADPp    Vm,Km
# NO2 + NO <-> N2O3      k12bNOp,k12bNOm
# GSNO (Cu+) -> 1/2GSSG + NO      k14NO
# CcOx + NO -> CcOX.NO      k15NO
# FeL + NO -> FeLNO      k16NO

```

```

# FeLNO + GSH -> GSNO + FeL          k17NO
# GSH + O2m -> 1/2 GSSG + products    k17NOb
# REACTION RATES
r1NO=k1NO
r2NO=k2NO
r3NO=k3NO
r4NO=k4NO*NO*O2m
r5NO=k5NO*SOD*O2m
r6NO=k6NO*ONOOm*GSH
r7NO=k7NO*ONOOm*GPX
r8NO=k8NO*ONOOm*CO2
r9NO=k9NO*ONOOm*Cc
r10NO=k10NO*GSNO^2*O2m
r11NO=k11NO*N2O3*GSH
r12aNO=k12aNO*NO*NO*O2
r12bNOp=k12bNOp*NO2*NO
r12bNOM=k12bNOM*N2O3
r13NO=k13NO*N2O3
rm=Vm*GSSG(GSH,GSNO)/(Km+GSSG(GSH,GSNO))
r14NO=k14NO*GSNO
r15NO=k15NO*CcOx*NO
r16NO=k16NO*FeL*NO
r17NO=k17NO*FeLNO(FeL)*GSH
r17NOb=k17NOb*GSH*O2m
# ODE'S
N2O3'=-r11NO-r13NO+r12bNOp-r12bNOM
GSH'=r3NO-r6NO-r11NO+2*rm-r17NO-r17NOb
NO'=r1NO-r4NO-2*r12aNO-r12bNOp+r12bNOM+r14NO-r15NO-r16NO
O2m'=r2NO-r4NO-r5NO-r10NO-r17NOb
ONOOm'=r4NO-r6NO-r7NO-r8NO-r9NO
GSNO'=r6NO-2*r10NO+r11NO-r14NO+r17NO
NO2'=2*r12aNO-r12bNOp+r12bNOM
CcOX'=-r15NO
FeL'=-r16NO+r17NO
# EXPRESSIONS
GSSG(GSH,GSNO)=(1000-GSH-GSNO)/2
FeLNO(FeL)=0.05-FeL
aux FeLNOstf=FeLNO(FeL)
# PARAMETERS
# k1NO is varied, i used a bigger number (1)
par k1NO=1
# k2NO is varied
par k2NO=0.1
# k3NO is varied
par k3NO=0
par O2=35

```

```

par Cc=400
# SOD is between 1 and 10
par SOD=10
par GPX=5.8
# CO2 is between 1000 and 25000
par CO2=1000
par Km=50
par k4NO=6700
par k5NO=2400
par k6NO=0.00135
par k7NO=2
par k8NO=0.058
par k9NO=0.025
par k10NO=0.0006
par k11NO=66
par k12aNO=0.000006
par k13NO=1600
par Vm=320
par k12bNOp=1100
par k12bNOm=81000
par k14NO=0.0002
par k15NO=100
par k16NO=1.21
#the same value as k11NO is used for k17NO as a first guess
par k17NO=66
par k17NOb=0.0002
# INITIAL CONDITIONS
init CcOx=0.1
init FeL=0.05
init GSH=1000
# DISPLAY
@ xhi=10000,ylo=0,yhi=0.001
@ nplot=3,yp=FeLNOstf,yp2=N2O3,yp3=GSH
# METHOD
@ meth=cvode,atol=1e-8,tol=1e-9,total=60000,dt=5,bounds=1000000000
done
*****

# figure17-GSH10000.ode
# REACTIONS
# * -> NO          k1NO
# * -> O2m         k2NO
# * -> GSH         k3NO
# NO + O2m -> ONOOm          k4NO
# SOD + O2m + Hp -> SOD + 1/2O2 + 1/2 H2O2 k5NO
# ONOOm + GSH -> GSNO + products          k6NO

```

```

# ONOOm + GPX -> GPX + products      k7NO
# ONOOm + CO2 -> products              k8NO
# ONOOm + Cc -> Cc + products          k9NO
# 2GSNO + O2m + H2O -> GSSG + products k10NO
# N2O3 + GSH -> GSNO + products       k11NO
# 2NO + O2 -> 2NO2                    k12aNO
# N2O3 + H2O -> products              k13NO
# GSSG + NADPH +Hp -> 2GSH + NADPp    Vm,Km
# NO2 + NO <-> N2O3                  k12bNOp,k12bNOm
# GSNO (Cu+) -> 1/2GSSG + NO          k14NO
# CcOx + NO -> CcOX.NO                k15NO
# FeL + NO -> FeLNO                   k16NO
# FeLNO + GSH -> GSNO + FeL           k17NO
# GSH + O2m -> 1/2 GSSG + products    k17NOb
# REACTION RATES
r1NO=k1NO
r2NO=k2NO
r3NO=k3NO
r4NO=k4NO*NO*O2m
r5NO=k5NO*SOD*O2m
r6NO=k6NO*ONOOm*GSH
r7NO=k7NO*ONOOm*GPX
r8NO=k8NO*ONOOm*CO2
r9NO=k9NO*ONOOm*Cc
r10NO=k10NO*GSNO^2*O2m
r11NO=k11NO*N2O3*GSH
r12aNO=k12aNO*NO*NO*O2
r12bNOp=k12bNOp*NO2*NO
r12bNOm=k12bNOm*N2O3
r13NO=k13NO*N2O3
rm=Vm*GSSG(GSH,GSNO)/(Km+GSSG(GSH,GSNO))
r14NO=k14NO*GSNO
r15NO=k15NO*CcOx*NO
r16NO=k16NO*FeL*NO
r17NO=k17NO*FeLNO(FeL)*GSH
r17NOb=k17NOb*GSH*O2m
# ODE'S
N2O3'=-r11NO-r13NO+r12bNOp-r12bNOm
GSH'=r3NO-r6NO-r11NO+2*rm-r17NO-r17NOb
NO'=r1NO-r4NO-2*r12aNO-r12bNOp+r12bNOm+r14NO-r15NO-r16NO
O2m'=r2NO-r4NO-r5NO-r10NO-r17NOb
ONOOm'=r4NO-r6NO-r7NO-r8NO-r9NO
GSNO'=r6NO-2*r10NO+r11NO-r14NO+r17NO
NO2'=2*r12aNO-r12bNOp+r12bNOm
CcOX'=-r15NO
FeL'=-r16NO+r17NO

```

```

# EXPRESSIONS
GSSG(GSH,GSNO)=(10000-GSH-GSNO)/2
FeLNO(FeL)=0.05-FeL
aux FeLNOstf=FeLNO(FeL)
# PARAMETERS
# k1NO is varied, i used a bigger number (1)
par k1NO=1
# k2NO is varied
par k2NO=0.1
# k3NO is varied
par k3NO=0
par O2=35
par Cc=400
# SOD is between 1 and 10
par SOD=10
par GPX=5.8
# CO2 is between 1000 and 25000
par CO2=1000
par Km=50
par k4NO=6700
par k5NO=2400
par k6NO=0.00135
par k7NO=2
par k8NO=0.058
par k9NO=0.025
par k10NO=0.0006
par k11NO=66
par k12aNO=0.000006
par k13NO=1600
par Vm=320
par k12bNOp=1100
par k12bNOM=81000
par k14NO=0.0002
par k15NO=100
par k16NO=1.21
#the same value as k11NO is used for k17NO as a first guess
par k17NO=66
par k17NOb=0.0002
# INITIAL CONDITIONS
init CcOx=0.1
init FeL=0.05
init GSH=10000
# DISPLAY
@ xhi=10000,ylo=0,yhi=0.001
@ nplot=3,yp=FeLNOstf,yp2=N2O3,yp3=GSH
# METHOD

```

```
@ meth=cvode,atol=1e-8,tol=1e-9,total=60000,dt=5,bounds=1000000000
done
```

A.1.10 Script used in Figure 18A

```
# figure18A.ode
##### figure16A.ode START #####
# REACTIONS
# om -> Ap
# om -> IAP
# om -> c3z
# om -> c9z
# om -> Bid
# om -> Bcl2
# om -> Bax
# om -> Ccmito
# c8a -> *
# c9a -> *
# c3a -> *
# Ap -> *
# IAP -> *
# c3z -> *
# c9z -> *
# Bcl2 -> *
# Bid -> *
# Bax -> *
# Ccmito -> *
# Bax -> *
# Bax2 -> *
# Cc -> *
# tBid -> *
# tBidBax -> *
# tBidmito -> *
# Cc + Ap <-> CcAp      k1p,k1m
# 7 CcAp <-> Apop      k1bp,k1bm
# Apop + c9z <-> Apopc9z  k2p,k2m
# Apopc9z + c9z <-> Apopc9z2 k3p,k3m
# Apopc9z2 -> Apopc9a2    k3f
# Apopc9a2 <-> Apopc9a + c9a k4p,k4m
# Apopc9a <-> Apop + c9a    k4bp,k4bm
# c9a + IAP <-> IAP9      k5p,k5m
# Apopc9a + IAP <-> IAPA9   k5bp,k5bm
# Apopc9a2 + IAP <-> IAPA29 k5cp,k5cm
# c3z + c9a <-> c93      k6p,k6m
```

```

# c93 -> c3a + c9a      k6f
# c3z + Apopc9a2 <-> cA93  k6bp,k6bm
# cA93 -> c3a + Apopc9a2  k6bf
# c3a + IAP <-> IAP3      k7p,k7m
# c8a + Bid <-> c8B       k8p,k8m
# c8B -> c8a + tBid       k8f
# c3a + Bid <-> c3B       k8p,k8m
# c3B -> c3a + tBid       k8f
# c3a + Bcl2 <-> c3L      k9p,k9m
# c3L -> c3a + B2c        k9f
# tBid -> tBidmito        k11
# tBidmito + Bax -> tBidBax k12a
# tBidBax + Bax -> tBid + Bax2 k12b
# Bcl2 + Bax -> *         k13
# Bax2 + Ccmito -> Cc + Bax2 k14
par nop=0
par tbid0=0
par p53=0.0066
# REACTION RATES
r1p=k1p*Cc*Ap
r1m=k1m*CcAp
r1bp=k1bp*CcAp^p
r1bm=k1bm*Apop
r2p=k2p*Apop*c9z
r2m=k2m*Apopc9z
r3p=k3p*Apopc9z*c9z
r3m=k3m*Apopc9z2
r3f=k3f*Apopc9z2
r4p=k4p*Apopc9a2
r4m=k4m*Apopc9a*c9a
r4bp=k4bp*Apopc9a
r4bm=k4bm*Apop*c9a
r5p=k5p*c9a*IAP
r5m=k5m*IAP9
r5bp=k5bp*Apopc9a*IAP
r5bm=k5bm*IAPA9
r5cp=k5cp*Apopc9a2*IAP
r5cm=k5cm*IAPA29
r6p=k6p*c3z*c9a
r6m=k6m*c93
r6f=k6f*c93
r6bp=k6p*c3z*Apopc9a2
r6bm=k6m*cA93
r6bf=k6f*cA93
r7p=k7p*c3a*IAP
r7m=k7m*IAP3

```

$r8p = k8p * c3a * Bid$
 $r8m = k8m * c3B$
 $r8f = k8f * c3B$
 $r8pp = k8p * c8a * Bid$
 $r8mp = k8m * c8B$
 $r8fp = k8f * c8B$
 $r9p = k9p * c3a * Bcl2$
 $r9m = k9m * c3L$
 $r9f = k9f * c3L$
 $r11 = k11 * tbid$
 $r12a = k12a * tbidmito * bax$
 $r12b = k12b * tbidbax * bax$
 $r13 = k13 * bcl2 * bax$
 $r14 = k14 * bax2 * ccmito$
FLUXES
 $J1 = r1p - r1m$
 $J1b = r1bp - r1bm$
 $J2 = r2p - r2m$
 $J3 = r3p - r3m$
 $J3f = r3f$
 $J4 = r4p - r4m$
 $J4b = r4bp - r4bm$
 $J5 = r5p - r5m$
 $J5b = r5bp - r5bm$
 $J5c = r5cp - r5cm$
 $J6 = r6p - r6m$
 $J6f = r6f$
 $J6b = r6bp - r6bm$
 $J6bf = r6bf$
 $J7 = r7p - r7m$
 $J8 = r8p - r8m$
 $J8f = r8f$
 $J8p = r8pp - r8mp$
 $J8fp = r8fp$
 $J9 = r9p - r9m$
 $J9f = r9f$
 $j11 = r11$
 $j12a = r12a$
 $j12b = r12b$
 $j13 = r13$
 $j14 = r14$
PRODUCTION AND DEGRADATION RATES
 $Jp8 = -\mu * c8a$
 $JAp = 0.0001 * a1 - \mu * Ap$
 $JIAP = 0.0001 * a2 - \mu * IAP$
 $Jp3 = 0.0001 * a3 - \mu * c3z$

```

Jp9=0.0001*a4-mu*c9z
jbidp=0.0001*a5-mu*bid
jbc12p=0.0001*a6*p53thresh^4/(p53^4+p53thresh^4)-mu*bcl2
jbax=0.0001*a7*(1+p53^4/(p53^4+p53thresh^4))-mu*bax
jccmito=0.0001*a8-mu*ccmito
# ODE'S
bax'=jbax-j12a-j12b-j13
Bcl2'=-J9+jbc12p-j13
cc'=j14-j1-mu*cc+mptp(MPTPcl)*ccmito
c3a'=J6f+J6bf-J7-J8+J8f-J9+J9f-mu*c3a-r22NO
AP'=-J1+JAp
CcAp'=J1-7*J1b
Apop'=J1b-J2+J4b
Apopc9z'=J2-J3
Apopc9z2'=J3-J3f
Apopc9a2'=J3f-J4-J5c-J6b+J6bf
Apopc9a'=J4-J4b-J5b
c9a'=J4+J4b-J5-J6+J6f-mu*c9a-r21NO
c9z'=-J2-J3+Jp9
IAP'=-J5-J5b-J5c-J7+JIAP
IAP9'=J5
IAPA9'=J5b
IAPA29'=J5c
IAP3'=J7
c3z'=-J6-J6b+Jp3-10*nop*c3z
c93'=J6-J6f
cA93'=J6b-J6bf
c8a'=Jp8-J8p+J8fp-r19NO-r20NO
Bid'=-J8-J8p+jbidp
c8B'=J8p-J8fp
c3B'=J8-J8f
c3L'=J9-J9f
tbid'=j8f+j8fp-j11+j12b-mu*tbid+tbid0
tbidbax'=j12a-j12b-mu*tbidbax
ccmito'=jccmito-j14-mptp(MPTPcl)*ccmito
bax2'=j12b-mu*bax2
tbidmito'=j11-j12a-mu*tbidmito
par p=4
init Ap=.004,c9z=.004,c3z=.004,IAP=.004,Bid=.004,Bcl2=.004,bax=.004
init CcAp=0,Apop=0,Apopc9z=0,Apopc9z2=0,Apopc9a2=0,Apopc9a=0,c9a=0.00
init IAP3=0,IAP9=0,IAPA9=0,IAPA29=0,c93=0,cA93=0,c3a=0.00001,c3B=0,c3L=0
init c8a=0.00001,c8B=0
init cc=0,ccmito=.004
par k1p=5,k1m=0.5
par k1bp=50000*a9,k1bm=0.5*a9
par k2p=10,k2m=0.5

```

```

par k3p=10,k3m=0.5,k3f=0.1
par k4p=5,k4m=0.5
par k4bp=5,k4bm=0.5
par k5p=5*a10,k5m=0.0035*a10
par k5bp=5*a10,k5bm=0.0035*a10
par k5cp=5*a10,k5cm=0.0035*a10
par k6p=10*a11,k6m=0.5*a11,k6f=0.001*a11
par k6bp=10*a11,k6bm=0.5*a11,k6bf=0.1*a11
par k7p=5*a10,k7m=0.0035*a10
par k8p=10,k8m=0.5,k8f=0.1
par k9p=10,k9m=0.5,k9f=0.1
par k11=10*a12,k12a=10*a12,k12b=10*a12,k13=10*a12,k14=10*a12
par a1=3,a2=0.3,a3=3,a4=3,a5=0.3,a6=0.8,a7=0.3,a8=3,a9=1,a10=1,a11=1,a12=1,a13=3
mu=0.002*a13
par p53thresh=0.004
##### figure16A.ode FINISH #####
##### figure17-GSH10000.ode START #####
# REACTIONS
# * -> NO                k1NO
# * -> O2m                k2NO
# * -> GSH                k3NO
# NO + O2m -> ONOOm      k4NO
# SOD + O2m + Hp -> SOD + 1/2O2 + 1/2 H2O2 k5NO
# ONOOm + GSH -> GSNO + products      k6NO
# ONOOm + GPX -> GPX + products      k7NO
# ONOOm + CO2 -> products      k8NO
# ONOOm + Cc -> Cc + products      k9NO
# 2GSNO + O2m + H2O -> GSSG + products k10NO
# N2O3 + GSH -> GSNO + products      k11NO
# 2NO + O2 -> 2NO2      k12aNO
# N2O3 + H2O -> products      k13NO
# GSSG + NADPH + Hp -> 2GSH + NADPp    Vm,Km
# NO2 + NO <-> N2O3      k12bNOp,k12bNOm
# GSNO (Cu+) -> 1/2GSSG + NO      k14NO
# CcOx + NO -> CcOX.NO      k15NO
# FeL + NO -> FeLNO      k16NO
# FeLNO + GSH -> GSNO + FeL      k17NO
# REACTION RATES
r1NO=k1NO
r2NO=k2NO
r3NO=k3NO
r4NO=k4NO*NO*O2m
r5NO=k5NO*SOD*O2m
r6NO=k6NO*ONOOm*GSH
r7NO=k7NO*ONOOm*GPX
r8NO=k8NO*ONOOm*CO2

```

```

r9NO=k9NO*ONOOm*Cc
r10NO=k10NO*GSNO^2*O2m
r11NO=k11NO*N2O3*GSH
r12aNO=k12aNO*NO*NO*O2
r12bNOp=k12bNOp*NO2*NO
r12bNOm=k12bNOm*N2O3
r13NO=k13NO*N2O3
rm=Vm*GSSG(GSH,GSNO)/(Km+GSSG(GSH,GSNO))
r14NO=k14NO*GSNO
r15NO=k15NO*CCox*NO
r16NO=k16NO*FeL*NO
r17NO=k17NO*FeLNO(FeL)*GSH
# ODE'S
N2O3'=-r11NO-r13NO+r12bNOp-r12bNOm-r19NO
GSH'=r3NO-r6NO-r11NO+2*rm-r17NO
NO'=r1NO-r4NO-2*r12aNO-r12bNOp+r12bNOm+r14NO-r15NO-r16NO
O2m'=r2NO-r4NO-r5NO-r10NO
ONOOm'=r4NO-r6NO-r7NO-r8NO-r9NO-r18NO
GSNO'=r6NO-2*r10NO+r11NO-r14NO+r17NO
GSSG(GSH,GSNO)=(10000-GSH-GSNO)/2
NO2'=2*r12aNO-r12bNOp+r12bNOm
CCox'=-r15NO
FeL'=-r16NO+r17NO+r20NO+r21NO+r22NO
FeLNO(FeL)=0.-FeL
aux FeLNOstf=FeLNO(FeL)
# k1NO is varied, i used a bigger number (1)
par k1NO=1
# k2NO is varied
par k2NO=0.
# k3NO is varied
par k3NO=0
par O2=35
#par Cc=400
# SOD is between 1 and 10
par SOD=10
par GPX=5.8
# CO2 is between 1000 and 25000
par CO2=1000
par Km=50
par k4NO=6700
par k5NO=2400
par k6NO=0.00135
par k7NO=2
par k8NO=0.058
par k9NO=0.025
par k10NO=0.0006

```

```

par k11NO=66
par k12aNO=0.000006
par k13NO=1600
par Vm=320
par k12bNOp=1100
par k12bNOm=81000
par k14NO=0.0002
par k15NO=100
init CcOx=0.1
par k16NO=1.21
init FeL=0.
#the same value as k11NO is used for k17NO as a first guess
par k17NO=66
init GSH=10000
##### figure17-GSH10000.ode FINISH #####
##### coupling START #####
# REACTIONS
# ONOOm + MPTPcl -> MPTP          k18NO
# N2O3 + c8a -> c8aNO + products k19NO
# FeLNO + c8a -> c8aNO + FeL      k20NO
# FeLNO + c9a -> c9aNO + FeL      k21NO
# FeLNO + c3a -> c3aNO + FeL      k22NO
# REACTION RATES
r18NO=k18NO*ONOOm*MPTPcl
r19NO=k19NO*N2O3*c8a
r20NO=k20NO*FeLNO(FeL)*c8a
r21NO=k21NO*FeLNO(FeL)*c9a
r22NO=k22NO*FeLNO(FeL)*c3a
# ODE'S
MPTPcl'=-r18NO
MPTP(MPTPcl)=0.01-MPTPcl
init MPTPcl=0.01
# assume black box
par k18NO=1
par k19NO=10
#the same value as k11NO is used for k20NO,k21NO,k22NO as a first guess
par k20NO=66
par k21NO=66
par k22NO=66
##### coupling FINISH #####
@ xhi=10000,ylo=0,yhi=0.001
@ meth=cvode,atol=1e-8,tol=1e-9,total=60000,dt=5,bounds=1000000000
@ nplot=2,yp=c3a,yp2=gsh
done

```

A.1.11 Script used in Figure 19A

```
# figure19A.ode
##### figure16A.ode START #####
# REACTIONS
# om -> Ap
# om -> IAP
# om -> c3z
# om -> c9z
# om -> Bid
# om -> Bcl2
# om -> Bax
# om -> Ccmito
# c8a -> *
# c9a -> *
# c3a -> *
# Ap -> *
# IAP -> *
# c3z -> *
# c9z -> *
# Bcl2 -> *
# Bid -> *
# Bax -> *
# Ccmito -> *
# Bax -> *
# Bax2 -> *
# Cc -> *
# tBid -> *
# tBidBax -> *
# tBidmito -> *
# Cc + Ap <-> CcAp      k1p,k1m
# 7 CcAp <-> Apop      k1bp,k1bm
# Apop + c9z <-> Apopc9z  k2p,k2m
# Apopc9z + c9z <-> Apopc9z2 k3p,k3m
# Apopc9z2 -> Apopc9a2      k3f
# Apopc9a2 <-> Apopc9a + c9a k4p,k4m
# Apopc9a <-> Apop + c9a    k4bp,k4bm
# c9a + IAP <-> IAP9      k5p,k5m
# Apopc9a + IAP <-> IAPA9  k5bp,k5bm
# Apopc9a2 + IAP <-> IAPA29 k5cp,k5cm
# c3z + c9a <-> c93      k6p,k6m
# c93 -> c3a + c9a      k6f
# c3z + Apopc9a2 <-> cA93  k6bp,k6bm
# cA93 -> c3a + Apopc9a2  k6bf
# c3a + IAP <-> IAP3     k7p,k7m
```

```

# c8a + Bid <-> c8B      k8p,k8m
# c8B -> c8a + tBid      k8f
# c3a + Bid <-> c3B      k8p,k8m
# c3B -> c3a + tBid      k8f
# c3a + Bcl2 <-> c3L     k9p,k9m
# c3L -> c3a + B2c       k9f
# tBid -> tBidmito       k11
# tBidmito + Bax -> tBidBax k12a
# tBidBax + Bax -> tBid + Bax2 k12b
# Bcl2 + Bax -> *        k13
# Bax2 + Ccmito -> Cc + Bax2 k14
par nop=0
par tbid0=0
par p53=0.0066
# REACTION RATES
r1p=k1p*Cc*Ap
r1m=k1m*CcAp
r1bp=k1bp*CcAp^p
r1bm=k1bm*Apop
r2p=k2p*Apop*c9z
r2m=k2m*Apopc9z
r3p=k3p*Apopc9z*c9z
r3m=k3m*Apopc9z2
r3f=k3f*Apopc9z2
r4p=k4p*Apopc9a2
r4m=k4m*Apopc9a*c9a
r4bp=k4bp*Apopc9a
r4bm=k4bm*Apop*c9a
r5p=k5p*c9a*IAP
r5m=k5m*IAP9
r5bp=k5bp*Apopc9a*IAP
r5bm=k5bm*IAPA9
r5cp=k5cp*Apopc9a2*IAP
r5cm=k5cm*IAPA29
r6p=k6p*c3z*c9a
r6m=k6m*c93
r6f=k6f*c93
r6bp=k6p*c3z*Apopc9a2
r6bm=k6m*cA93
r6bf=k6f*cA93
r7p=k7p*c3a*IAP
r7m=k7m*IAP3
r8p=k8p*c3a*Bid
r8m=k8m*c3B
r8f=k8f*c3B
r8pp=k8p*c8a*Bid

```

```

r8mp=k8m*c8B
r8fp=k8f*c8B
r9p=k9p*c3a*Bcl2
r9m=k9m*c3L
r9f=k9f*c3L
r11=k11*tbid
r12a=k12a*tbidmito*bax
r12b=k12b*tbidbax*bax
r13=k13*bcl2*bax
r14=k14*bax2*ccmito
# FLUXES
J1=r1p-r1m
J1b=r1bp-r1bm
J2=r2p-r2m
J3=r3p-r3m
J3f=r3f
J4=r4p-r4m
J4b=r4bp-r4bm
J5=r5p-r5m
J5b=r5bp-r5bm
J5c=r5cp-r5cm
J6=r6p-r6m
J6f=r6f
J6b=r6bp-r6bm
J6bf=r6bf
J7=r7p-r7m
J8=r8p-r8m
J8f=r8f
J8p=r8pp-r8mp
J8fp=r8fp
J9=r9p-r9m
J9f=r9f
j11=r11
j12a=r12a
j12b=r12b
j13=r13
j14=r14
# PRODUCTION AND DEGRADATION RATES
Jp8=-mu*c8a
JAp=0.0001*a1-mu*Ap
JIAP=0.0001*a2-mu*IAP
Jp3=0.0001*a3-mu*c3z
Jp9=0.0001*a4-mu*c9z
jbidp=0.0001*a5-mu*bid
jbc12p=0.0001*a6*p53thresh^4/(p53^4+p53thresh^4)-mu*bcl2
jbax=0.0001*a7*(1+p53^4/(p53^4+p53thresh^4))-mu*bax

```

```

jccmito=0.0001*a8-mu*ccmito
# ODE'S
bax'=jbax-j12a-j12b-j13
Bcl2'=-J9+jbcl2p-j13
cc'=j14-j1-mu*cc+mptp(MPTPcl)*ccmito
c3a'=J6f+J6bf-J7-J8+J8f-J9+J9f-mu*c3a-r22NO
AP'=-J1+JAp
CcAp'=J1-7*J1b
Apop'=J1b-J2+J4b
Apopc9z'=J2-J3
Apopc9z2'=J3-J3f
Apopc9a2'=J3f-J4-J5c-J6b+J6bf
Apopc9a'=J4-J4b-J5b
c9a'=J4+J4b-J5-J6+J6f-mu*c9a-r21NO
c9z'=-J2-J3+Jp9
IAP'=-J5-J5b-J5c-J7+JIAP
IAP9'=J5
IAPA9'=J5b
IAPA29'=J5c
IAP3'=J7
c3z'=-J6-J6b+Jp3-10*nop*c3z
c93'=J6-J6f
cA93'=J6b-J6bf
c8a'=Jp8-J8p+J8fp-r19NO-r20NO
Bid'=-J8-J8p+jbidp
c8B'=J8p-J8fp
c3B'=J8-J8f
c3L'=J9-J9f
tbid'=j8f+j8fp-j11+j12b-mu*tbid+tbid0
tbidbax'=j12a-j12b-mu*tbidbax
ccmito'=jccmito-j14-mptp(MPTPcl)*ccmito
bax2'=j12b-mu*bax2
tbidmito'=j11-j12a-mu*tbidmito
par p=4
init Ap=.004,c9z=.004,c3z=.004,IAP=.004,Bid=.004,Bcl2=.004,bax=.004
init CcAp=0,Apop=0,Apopc9z=0,Apopc9z2=0,Apopc9a2=0,Apopc9a=0,c9a=0.00
init IAP3=0,IAP9=0,IAPA9=0,IAPA29=0,c93=0,cA93=0,c3a=0.00001,c3B=0,c3L=0
init c8a=0.00001,c8B=0
init cc=0,ccmito=.004
par k1p=5,k1m=0.5
par k1bp=50000*a9,k1bm=0.5*a9
par k2p=10,k2m=0.5
par k3p=10,k3m=0.5,k3f=0.1
par k4p=5,k4m=0.5
par k4bp=5,k4bm=0.5
par k5p=5*a10,k5m=0.0035*a10

```

```

par k5bp=5*a10,k5bm=0.0035*a10
par k5cp=5*a10,k5cm=0.0035*a10
par k6p=10*a11,k6m=0.5*a11,k6f=0.001*a11
par k6bp=10*a11,k6bm=0.5*a11,k6bf=0.1*a11
par k7p=5*a10,k7m=0.0035*a10
par k8p=10,k8m=0.5,k8f=0.1
par k9p=10,k9m=0.5,k9f=0.1
par k11=10*a12,k12a=10*a12,k12b=10*a12,k13=10*a12,k14=10*a12
par a1=3,a2=0.3,a3=3,a4=3,a5=0.3,a6=0.8,a7=0.3,a8=3,a9=1,a10=1,a11=1,a12=1,a13=3
mu=0.002*a13
par p53thresh=0.004
##### figure16A.ode FINISH #####
##### figure17-GSH10000.ode START #####
# REACTIONS
# * -> NO                k1NO
# * -> O2m                k2NO
# * -> GSH                k3NO
# NO + O2m -> ONOOm      k4NO
# SOD + O2m + Hp -> SOD + 1/2O2 + 1/2 H2O2 k5NO
# ONOOm + GSH -> GSNO + products      k6NO
# ONOOm + GPX -> GPX + products      k7NO
# ONOOm + CO2 -> products      k8NO
# ONOOm + Cc -> Cc + products      k9NO
# 2GSNO + O2m + H2O -> GSSG + products k10NO
# N2O3 + GSH -> GSNO + products      k11NO
# 2NO + O2 -> 2NO2      k12aNO
# N2O3 + H2O -> products      k13NO
# GSSG + NADPH +Hp -> 2GSH + NADPp    Vm,Km
# NO2 + NO <-> N2O3      k12bNOp,k12bNOm
# GSNO (Cu+) -> 1/2GSSG + NO      k14NO
# CcOx + NO -> CcOX.NO      k15NO
# FeL + NO -> FeLNO      k16NO
# FeLNO + GSH -> GSNO + FeL      k17NO
# REACTION RATES
r1NO=k1NO
r2NO=k2NO
r3NO=k3NO
r4NO=k4NO*NO*O2m
r5NO=k5NO*SOD*O2m
r6NO=k6NO*ONOOm*GSH
r7NO=k7NO*ONOOm*GPX
r8NO=k8NO*ONOOm*CO2
r9NO=k9NO*ONOOm*Cc
r10NO=k10NO*GSNO^2*O2m
r11NO=k11NO*N2O3*GSH
r12aNO=k12aNO*NO*NO*O2

```

```

r12bNOp=k12bNOp*NO2*NO
r12bNOm=k12bNOm*N2O3
r13NO=k13NO*N2O3
rm=Vm*GSSG(GSH,GSNO)/(Km+GSSG(GSH,GSNO))
r14NO=k14NO*GSNO
r15NO=k15NO*CCOx*NO
r16NO=k16NO*FeL*NO
r17NO=k17NO*FeLNO(FeL)*GSH
# ODE'S
N2O3'=-r11NO-r13NO+r12bNOp-r12bNOm-r19NO
GSH'=r3NO-r6NO-r11NO+2*rm-r17NO
NO'=r1NO-r4NO-2*r12aNO-r12bNOp+r12bNOm+r14NO-r15NO-r16NO
O2m'=r2NO-r4NO-r5NO-r10NO
ONOOm'=r4NO-r6NO-r7NO-r8NO-r9NO-r18NO
GSNO'=r6NO-2*r10NO+r11NO-r14NO+r17NO
GSSG(GSH,GSNO)=(10000-GSH-GSNO)/2
NO2'=2*r12aNO-r12bNOp+r12bNOm
CCOX'=-r15NO
FeL'=-r16NO+r17NO+r20NO+r21NO+r22NO
FeLNO(FeL)=0.05-FeL
aux FeLNOstf=FeLNO(FeL)
# k1NO is varied, i used a bigger number (1)
par k1NO=1
# k2NO is varied
par k2NO=0.
# k3NO is varied
par k3NO=0
par O2=35
#par Cc=400
# SOD is between 1 and 10
par SOD=10
par GPX=5.8
# CO2 is between 1000 and 25000
par CO2=1000
par Km=50
par k4NO=6700
par k5NO=2400
par k6NO=0.00135
par k7NO=2
par k8NO=0.058
par k9NO=0.025
par k10NO=0.0006
par k11NO=66
par k12aNO=0.000006
par k13NO=1600
par Vm=320

```

```

par k12bNOp=1100
par k12bNOm=81000
par k14NO=0.0002
par k15NO=100
init CcOx=0.1
par k16NO=1.21
init FeL=0.05
#the same value as k11NO is used for k17NO as a first guess
par k17NO=66
init GSH=10000
##### figure17-GSH10000.ode FINISH #####
##### coupling START #####
# REACTIONS
# ONOOm + MPTPcl -> MPTP          k18NO
# N2O3 + c8a -> c8aNO + products k19NO
# FeLNO + c8a -> c8aNO + FeL      k20NO
# FeLNO + c9a -> c9aNO + FeL      k21NO
# FeLNO + c3a -> c3aNO + FeL      k22NO
# REACTION RATES
r18NO=k18NO*ONOOm*MPTPcl
r19NO=k19NO*N2O3*c8a
r20NO=k20NO*FeLNO(FeL)*c8a
r21NO=k21NO*FeLNO(FeL)*c9a
r22NO=k22NO*FeLNO(FeL)*c3a
# ODE
MPTPcl'=-r18NO
MPTP(MPTPcl)=0.01-MPTPcl
init MPTPcl=0.01
# assume black box
par k18NO=1
par k19NO=10
#the same value as k11NO is used for k20NO,k21NO,k22NO as a first guess
par k20NO=66
par k21NO=66
par k22NO=66
##### coupling FINISH #####
@ xhi=10000,ylo=0,yhi=0.001
@ meth=cvode,atol=1e-8,tol=1e-9,total=60000,dt=5,bounds=1000000000
@ nplot=2,yp=c3a,yp2=gsh
done

```

A.1.12 Script used in Figure 20A

```
# figure20A.ode
```

```

##### figure16A.ode START #####
# om -> Ap
# om -> IAP
# om -> c3z
# om -> c9z
# om -> Bid
# om -> Bcl2
# om -> Bax
# om -> Ccmto
# c8a -> *
# c9a -> *
# c3a -> *
# Ap -> *
# IAP -> *
# c3z -> *
# c9z -> *
# Bcl2 -> *
# Bid -> *
# Bax -> *
# Ccmto -> *
# Bax -> *
# Bax2 -> *
# Cc -> *
# tBid -> *
# tBidBax -> *
# tBidmito -> *
# Cc + Ap <-> CcAp      k1p,k1m
# 7 CcAp <-> Apop      k1bp,k1bm
# Apop + c9z <-> Apopc9z  k2p,k2m
# Apopc9z + c9z <-> Apopc9z2 k3p,k3m
# Apopc9z2 -> Apopc9a2      k3f
# Apopc9a2 <-> Apopc9a + c9a k4p,k4m
# Apopc9a <-> Apop + c9a    k4bp,k4bm
# c9a + IAP <-> IAP9      k5p,k5m
# Apopc9a + IAP <-> IAPA9   k5bp,k5bm
# Apopc9a2 + IAP <-> IAPA29 k5cp,k5cm
# c3z + c9a <-> c93      k6p,k6m
# c93 -> c3a + c9a      k6f
# c3z + Apopc9a2 <-> cA93   k6bp,k6bm
# cA93 -> c3a + Apopc9a2   k6bf
# c3a + IAP <-> IAP3      k7p,k7m
# c8a + Bid <-> c8B      k8p,k8m
# c8B -> c8a + tBid      k8f
# c3a + Bid <-> c3B      k8p,k8m
# c3B -> c3a + tBid      k8f
# c3a + Bcl2 <-> c3L     k9p,k9m

```

```

# c3L -> c3a + B2c      k9f
# tBid -> tBidmito      k11
# tBidmito + Bax -> tBidBax  k12a
# tBidBax + Bax -> tBid + Bax2 k12b
# Bcl2 + Bax -> *        k13
# Bax2 + Ccmito -> Cc + Bax2 k14
par nop=0
par tbid0=0
par p53=0.0066
# REACTION RATES
r1p=k1p*Cc*Ap
r1m=k1m*CcAp
r1bp=k1bp*CcAp^p
r1bm=k1bm*Apop
r2p=k2p*Apop*c9z
r2m=k2m*Apopc9z
r3p=k3p*Apopc9z*c9z
r3m=k3m*Apopc9z2
r3f=k3f*Apopc9z2
r4p=k4p*Apopc9a2
r4m=k4m*Apopc9a*c9a
r4bp=k4bp*Apopc9a
r4bm=k4bm*Apop*c9a
r5p=k5p*c9a*IAP
r5m=k5m*IAP9
r5bp=k5bp*Apopc9a*IAP
r5bm=k5bm*IAPA9
r5cp=k5cp*Apopc9a2*IAP
r5cm=k5cm*IAPA29
r6p=k6p*c3z*c9a
r6m=k6m*c93
r6f=k6f*c93
r6bp=k6p*c3z*Apopc9a2
r6bm=k6m*cA93
r6bf=k6f*cA93
r7p=k7p*c3a*IAP
r7m=k7m*IAP3
r8p=k8p*c3a*Bid
r8m=k8m*c3B
r8f=k8f*c3B
r8pp=k8p*c8a*Bid
r8mp=k8m*c8B
r8fp=k8f*c8B
r9p=k9p*c3a*Bcl2
r9m=k9m*c3L
r9f=k9f*c3L

```

```

r11=k11*tbid
r12a=k12a*tbidmito*bax
r12b=k12b*tbidbax*bax
r13=k13*bcl2*bax
r14=k14*bax2*ccmito
# FLUXES
J1=r1p-r1m
J1b=r1bp-r1bm
J2=r2p-r2m
J3=r3p-r3m
J3f=r3f
J4=r4p-r4m
J4b=r4bp-r4bm
J5=r5p-r5m
J5b=r5bp-r5bm
J5c=r5cp-r5cm
J6=r6p-r6m
J6f=r6f
J6b=r6bp-r6bm
J6bf=r6bf
J7=r7p-r7m
J8=r8p-r8m
J8f=r8f
J8p=r8pp-r8mp
J8fp=r8fp
J9=r9p-r9m
J9f=r9f
j11=r11
j12a=r12a
j12b=r12b
j13=r13
j14=r14
# PRODUCTION AND DEGRADATION RATES
Jp8=-mu*c8a
JAp=0.0001*a1-mu*Ap
JIAP=0.0001*a2-mu*IAP
Jp3=0.0001*a3-mu*c3z
Jp9=0.0001*a4-mu*c9z
jbidp=0.0001*a5-mu*bid
jbcl2p=0.0001*a6*p53thresh^4/(p53^4+p53thresh^4)-mu*bcl2
jbax=0.0001*a7*(1+p53^4/(p53^4+p53thresh^4))-mu*bax
jccmito=0.0001*a8-mu*ccmito
# ODE'S
bax'=jbax-j12a-j12b-j13
Bcl2'=-J9+jbcl2p-j13
cc'=j14-j1-mu*cc+mptp(MPTPcl)*ccmito

```

$c3a' = J6f + J6bf - J7 - J8 + J8f - J9 + J9f - \mu * c3a - r22NO$
 $AP' = -J1 + JAp$
 $CcAp' = J1 - 7 * J1b$
 $Apop' = J1b - J2 + J4b$
 $Apopc9z' = J2 - J3$
 $Apopc9z2' = J3 - J3f$
 $Apopc9a2' = J3f - J4 - J5c - J6b + J6bf$
 $Apopc9a' = J4 - J4b - J5b$
 $c9a' = J4 + J4b - J5 - J6 + J6f - \mu * c9a - r21NO$
 $c9z' = -J2 - J3 + Jp9$
 $IAP' = -J5 - J5b - J5c - J7 + JIAP$
 $IAP9' = J5$
 $IAPA9' = J5b$
 $IAPA29' = J5c$
 $IAP3' = J7$
 $c3z' = -J6 - J6b + Jp3 - 10 * nop * c3z$
 $c93' = J6 - J6f$
 $cA93' = J6b - J6bf$
 $c8a' = Jp8 - J8p + J8fp - r19NO - r20NO$
 $Bid' = -J8 - J8p + jbidp$
 $c8B' = J8p - J8fp$
 $c3B' = J8 - J8f$
 $c3L' = J9 - J9f$
 $tbid' = j8f + j8fp - j11 + j12b - \mu * tbid + tbid0$
 $tbidbax' = j12a - j12b - \mu * tbidbax$
 $ccmito' = jccmito - j14 - mptp(MPTPcl) * ccmito$
 $bax2' = j12b - \mu * bax2$
 $tbidmito' = j11 - j12a - \mu * tbidmito$
par p=4
init Ap=.004,c9z=.004,c3z=.004,IAP=.004,Bid=.004,Bcl2=.004,bax=.004
init CcAp=0,Apop=0,Apopc9z=0,Apopc9z2=0,Apopc9a2=0,Apopc9a=0,c9a=0.00
init IAP3=0,IAP9=0,IAPA9=0,IAPA29=0,c93=0,cA93=0,c3a=0.00001,c3B=0,c3L=0
init c8a=0.00001,c8B=0
init cc=0,ccmito=.004
par k1p=5,k1m=0.5
par k1bp=50000*a9,k1bm=0.5*a9
par k2p=10,k2m=0.5
par k3p=10,k3m=0.5,k3f=0.1
par k4p=5,k4m=0.5
par k4bp=5,k4bm=0.5
par k5p=5*a10,k5m=0.0035*a10
par k5bp=5*a10,k5bm=0.0035*a10
par k5cp=5*a10,k5cm=0.0035*a10
par k6p=10*a11,k6m=0.5*a11,k6f=0.001*a11
par k6bp=10*a11,k6bm=0.5*a11,k6bf=0.1*a11
par k7p=5*a10,k7m=0.0035*a10

```

par k8p=10,k8m=0.5,k8f=0.1
par k9p=10,k9m=0.5,k9f=0.1
par k11=10*a12,k12a=10*a12,k12b=10*a12,k13=10*a12,k14=10*a12
par a1=3,a2=0.3,a3=3,a4=3,a5=0.3,a6=0.8,a7=0.3,a8=3,a9=1,a10=1,a11=1,a12=1,a13=3
mu=0.002*a13
par p53thresh=0.004
##### figure16A.ode FINISH #####
##### figure17-GSH10000.ode START #####
# REACTIONS
# * -> NO                k1NO
# * -> O2m                k2NO
# * -> GSH                k3NO
# NO + O2m -> ONOOm      k4NO
# SOD + O2m + Hp -> SOD + 1/2O2 + 1/2 H2O2 k5NO
# ONOOm + GSH -> GSNO + products      k6NO
# ONOOm + GPX -> GPX + products      k7NO
# ONOOm + CO2 -> products      k8NO
# ONOOm + Cc -> Cc + products      k9NO
# 2GSNO + O2m + H2O -> GSSG + products k10NO
# N2O3 + GSH -> GSNO + products      k11NO
# 2NO + O2 -> 2NO2      k12aNO
# N2O3 + H2O -> products      k13NO
# GSSG + NADPH +Hp -> 2GSH + NADPp    Vm,Km
# NO2 + NO <-> N2O3      k12bNOp,k12bNOm
# GSNO (Cu+) -> 1/2GSSG + NO      k14NO
# CcOx + NO -> CcOX.NO      k15NO
# FeL + NO -> FeLNO      k16NO
# FeLNO + GSH -> GSNO + FeL      k17NO
# GSH + O2m -> 1/2 GSSG + products      k17NOb
# REACTION RATES
r1NO=k1NO
r2NO=k2NO
r3NO=k3NO
r4NO=k4NO*NO*O2m
r5NO=k5NO*SOD*O2m
r6NO=k6NO*ONOOm*GSH
r7NO=k7NO*ONOOm*GPX
r8NO=k8NO*ONOOm*CO2
r9NO=k9NO*ONOOm*Cc
r10NO=k10NO*GSNO^2*O2m
r11NO=k11NO*N2O3*GSH
r12aNO=k12aNO*NO*NO*O2
r12bNOp=k12bNOp*NO2*NO
r12bNOm=k12bNOm*N2O3
r13NO=k13NO*N2O3
rm=Vm*GSSG(GSH,GSNO)/(Km+GSSG(GSH,GSNO))

```

```

r14NO=k14NO*GSNO
r15NO=k15NO*CcOx*NO
r16NO=k16NO*FeL*NO
r17NO=k17NO*FeLNO(FeL)*GSH
r17NOb=k17NOb*GSH*O2m
# ODE'S
N2O3'=-r11NO-r13NO+r12bNOp-r12bNOM-r19NO
GSH'=r3NO-r6NO-r11NO+2*rm-r17NO-r17NOb
NO'=r1NO-r4NO-2*r12aNO-r12bNOp+r12bNOM+r14NO-r15NO-r16NO
O2m'=r2NO-r4NO-r5NO-r10NO-r17NOb
ONOOm'=r4NO-r6NO-r7NO-r8NO-r9NO-r18NO
GSNO'=r6NO-2*r10NO+r11NO-r14NO+r17NO
GSSG(GSH,GSNO)=(10000-GSH-GSNO)/2
NO2'=2*r12aNO-r12bNOp+r12bNOM
CcOX'=-r15NO
FeL'=-r16NO+r17NO+r20NO+r21NO+r22NO
FeLNO(FeL)=0.05-FeL
aux FeLNOstf=FeLNO(FeL)
# k1NO is varied, i used a bigger number (1)
par k1NO=1
# k2NO is varied
par k2NO=0.1
# k3NO is varied
par k3NO=0
par O2=35
#par Cc=400
# SOD is between 1 and 10
par SOD=10
par GPX=5.8
# CO2 is between 1000 and 25000
par CO2=1000
par Km=50
par k4NO=6700
par k5NO=2400
par k6NO=0.00135
par k7NO=2
par k8NO=0.058
par k9NO=0.025
par k10NO=0.0006
par k11NO=66
par k12aNO=0.000006
par k13NO=1600
par Vm=320
par k12bNOp=1100
par k12bNOM=81000
par k14NO=0.0002

```

```

par k15NO=100
init CcOx=0.1
par k16NO=1.21
init FeL=0.05
#the same value as k11NO is used for k17NO as a first guess
par k17NO=66
par k17NOB=0.0002
init GSH=10000
##### figure17-GSH10000.ode FINISH #####
##### coupling START #####
# REACTIONS
# ONOom + MPTPcl -> MPTP          k18NO
# N2O3 + c8a -> c8aNO + products k19NO
# FeLNO + c8a -> c8aNO + FeL     k20NO
# FeLNO + c9a -> c9aNO + FeL     k21NO
# FeLNO + c3a -> c3aNO + FeL     k22NO
# REACTION RATES
r18NO=k18NO*ONOOm*MPTPcl
r19NO=k19NO*N2O3*c8a
r20NO=k20NO*FeLNO(FeL)*c8a
r21NO=k21NO*FeLNO(FeL)*c9a
r22NO=k22NO*FeLNO(FeL)*c3a
# ODE
MPTPcl'=-r18NO
MPTP(MPTPcl)=0.01-MPTPcl
init MPTPcl=0.01
# assume black box
par k18NO=1
par k19NO=10
#the same value as k11NO is used for k20NO,k21NO,k22NO as a first guess
par k20NO=66
par k21NO=66
par k22NO=66
##### coupling FINISH #####
@ xhi=10000,ylo=0,yhi=0.001
@ meth=cvode,atol=1e-8,tol=1e-9,total=60000,dt=5,bounds=1000000000
@ nplot=2,yp=c3a,yp2=gsh
done

```

A.1.13 Script used in Figure 21A

```

# figure21A.ode
##### figure16A.ode START #####
# REACTIONS

```

```

# om -> Ap
# om -> IAP
# om -> c3z
# om -> c9z
# om -> Bid
# om -> Bcl2
# om -> Bax
# om -> Ccmito
# c8a -> *
# c9a -> *
# c3a -> *
# Ap -> *
# IAP -> *
# c3z -> *
# c9z -> *
# Bcl2 -> *
# Bid -> *
# Bax -> *
# Ccmito -> *
# Bax -> *
# Bax2 -> *
# Cc -> *
# tBid -> *
# tBidBax -> *
# tBidmito -> *
# Cc + Ap <-> CcAp      k1p,k1m
# 7 CcAp <-> Apop      k1bp,k1bm
# Apop + c9z <-> Apopc9z  k2p,k2m
# Apopc9z + c9z <-> Apopc9z2 k3p,k3m
# Apopc9z2 -> Apopc9a2    k3f
# Apopc9a2 <-> Apopc9a + c9a k4p,k4m
# Apopc9a <-> Apop + c9a    k4bp,k4bm
# c9a + IAP <-> IAP9      k5p,k5m
# Apopc9a + IAP <-> IAPA9   k5bp,k5bm
# Apopc9a2 + IAP <-> IAPA29 k5cp,k5cm
# c3z + c9a <-> c93      k6p,k6m
# c93 -> c3a + c9a      k6f
# c3z + Apopc9a2 <-> cA93   k6bp,k6bm
# cA93 -> c3a + Apopc9a2   k6bf
# c3a + IAP <-> IAP3      k7p,k7m
# c8a + Bid <-> c8B      k8p,k8m
# c8B -> c8a + tBid      k8f
# c3a + Bid <-> c3B      k8p,k8m
# c3B -> c3a + tBid      k8f
# c3a + Bcl2 <-> c3L     k9p,k9m
# c3L -> c3a + B2c      k9f

```

```

# tBid -> tBidmito      k11
# tBidmito + Bax -> tBidBax  k12a
# tBidBax + Bax -> tBid + Bax2 k12b
# Bcl2 + Bax -> *          k13
# Bax2 + Ccmito -> Cc + Bax2 k14
par nop=0
par tbid0=0
par p53=0.0066
# REACTION RATES
r1p=k1p*Cc*Ap
r1m=k1m*CcAp
r1bp=k1bp*CcAp^p
r1bm=k1bm*Apop
r2p=k2p*Apop*c9z
r2m=k2m*Apopc9z
r3p=k3p*Apopc9z*c9z
r3m=k3m*Apopc9z2
r3f=k3f*Apopc9z2
r4p=k4p*Apopc9a2
r4m=k4m*Apopc9a*c9a
r4bp=k4bp*Apopc9a
r4bm=k4bm*Apop*c9a
r5p=k5p*c9a*IAP
r5m=k5m*IAP9
r5bp=k5bp*Apopc9a*IAP
r5bm=k5bm*IAPA9
r5cp=k5cp*Apopc9a2*IAP
r5cm=k5cm*IAPA29
r6p=k6p*c3z*c9a
r6m=k6m*c93
r6f=k6f*c93
r6bp=k6p*c3z*Apopc9a2
r6bm=k6m*cA93
r6bf=k6f*cA93
r7p=k7p*c3a*IAP
r7m=k7m*IAP3
r8p=k8p*c3a*Bid
r8m=k8m*c3B
r8f=k8f*c3B
r8pp=k8p*c8a*Bid
r8mp=k8m*c8B
r8fp=k8f*c8B
r9p=k9p*c3a*Bcl2
r9m=k9m*c3L
r9f=k9f*c3L
r11=k11*tbid

```

```

r12a=k12a*tbidmito*bax
r12b=k12b*tbidbax*bax
r13=k13*bcl2*bax
r14=k14*bax2*ccmito
# FLUXES
J1=r1p-r1m
J1b=r1bp-r1bm
J2=r2p-r2m
J3=r3p-r3m
J3f=r3f
J4=r4p-r4m
J4b=r4bp-r4bm
J5=r5p-r5m
J5b=r5bp-r5bm
J5c=r5cp-r5cm
J6=r6p-r6m
J6f=r6f
J6b=r6bp-r6bm
J6bf=r6bf
J7=r7p-r7m
J8=r8p-r8m
J8f=r8f
J8p=r8pp-r8mp
J8fp=r8fp
J9=r9p-r9m
J9f=r9f
j11=r11
j12a=r12a
j12b=r12b
j13=r13
j14=r14
# PRODUCTION AND DEGRADATION RATES
Jp8=-mu*c8a
JAp=0.0001*a1-mu*Ap
JIAP=0.0001*a2-mu*IAP
Jp3=0.0001*a3-mu*c3z
Jp9=0.0001*a4-mu*c9z
jbidp=0.0001*a5-mu*bid
jbc12p=0.0001*a6*p53thresh^4/(p53^4+p53thresh^4)-mu*bcl2
jbax=0.0001*a7*(1+p53^4/(p53^4+p53thresh^4))-mu*bax
jccmito=0.0001*a8-mu*ccmito
# ODE'S
bax'=jbax-j12a-j12b-j13
Bcl2'=-J9+jbc12p-j13
cc'=j14-j1-mu*cc+mptp(MPTPcl)*ccmito
c3a'=J6f+J6bf-J7-J8+J8f-J9+J9f-mu*c3a-r22NO

```

$AP' = -J1 + JAp$
 $CcAp' = J1 - 7 * J1b$
 $Apop' = J1b - J2 + J4b$
 $Apopc9z' = J2 - J3$
 $Apopc9z2' = J3 - J3f$
 $Apopc9a2' = J3f - J4 - J5c - J6b + J6bf$
 $Apopc9a' = J4 - J4b - J5b$
 $c9a' = J4 + J4b - J5 - J6 + J6f - \mu * c9a - r21NO$
 $c9z' = -J2 - J3 + Jp9$
 $IAP' = -J5 - J5b - J5c - J7 + JIAP$
 $IAP9' = J5$
 $IAPA9' = J5b$
 $IAPA29' = J5c$
 $IAP3' = J7$
 $c3z' = -J6 - J6b + Jp3 - 10 * nop * c3z$
 $c93' = J6 - J6f$
 $cA93' = J6b - J6bf$
 $c8a' = Jp8 - J8p + J8fp - r19NO - r20NO$
 $Bid' = -J8 - J8p + jbidp$
 $c8B' = J8p - J8fp$
 $c3B' = J8 - J8f$
 $c3L' = J9 - J9f$
 $tbid' = j8f + j8fp - j11 + j12b - \mu * tbid + tbid0$
 $tbidbax' = j12a - j12b - \mu * tbidbax$
 $ccmito' = jccmito - j14 - mptp(MPTPcl) * ccmito$
 $bax2' = j12b - \mu * bax2$
 $tbidmito' = j11 - j12a - \mu * tbidmito$
 $par p = 4$
 $init Ap = .004, c9z = .004, c3z = .004, IAP = .004, Bid = .004, Bcl2 = .004, bax = .004$
 $init CcAp = 0, Apop = 0, Apopc9z = 0, Apopc9z2 = 0, Apopc9a2 = 0, Apopc9a = 0, c9a = 0.00$
 $init IAP3 = 0, IAP9 = 0, IAPA9 = 0, IAPA29 = 0, c93 = 0, cA93 = 0, c3a = 0.00001, c3B = 0, c3L = 0$
 $init c8a = 0.00007, c8B = 0$
 $init cc = 0, ccmito = .004$
 $par k1p = 5, k1m = 0.5$
 $par k1bp = 50000 * a9, k1bm = 0.5 * a9$
 $par k2p = 10, k2m = 0.5$
 $par k3p = 10, k3m = 0.5, k3f = 0.1$
 $par k4p = 5, k4m = 0.5$
 $par k4bp = 5, k4bm = 0.5$
 $par k5p = 5 * a10, k5m = 0.0035 * a10$
 $par k5bp = 5 * a10, k5bm = 0.0035 * a10$
 $par k5cp = 5 * a10, k5cm = 0.0035 * a10$
 $par k6p = 10 * a11, k6m = 0.5 * a11, k6f = 0.001 * a11$
 $par k6bp = 10 * a11, k6bm = 0.5 * a11, k6bf = 0.1 * a11$
 $par k7p = 5 * a10, k7m = 0.0035 * a10$
 $par k8p = 10, k8m = 0.5, k8f = 0.1$

```

par k9p=10,k9m=0.5,k9f=0.1
par k11=10*a12,k12a=10*a12,k12b=10*a12,k13=10*a12,k14=10*a12
par a1=3,a2=0.3,a3=3,a4=3,a5=0.3,a6=0.8,a7=0.3,a8=3,a9=1,a10=1,a11=1,a12=1,a13=3
mu=0.002*a13
par p53thresh=0.004
##### figure16A.ode FINISH #####
##### figure17-GSH10000.ode START #####
# REACTIONS
# * -> NO                k1NO
# * -> O2m                k2NO
# * -> GSH                k3NO
# NO + O2m -> ONOOm      k4NO
# SOD + O2m + Hp -> SOD + 1/2O2 + 1/2 H2O2 k5NO
# ONOOm + GSH -> GSNO + products      k6NO
# ONOOm + GPX -> GPX + products      k7NO
# ONOOm + CO2 -> products            k8NO
# ONOOm + Cc -> Cc + products        k9NO
# 2GSNO + O2m + H2O -> GSSG + products k10NO
# N2O3 + GSH -> GSNO + products      k11NO
# 2NO + O2 -> 2NO2                k12aNO
# N2O3 + H2O -> products          k13NO
# GSSG + NADPH +Hp -> 2GSH + NADPp    Vm,Km
# NO2 + NO <-> N2O3                k12bNOp,k12bNOm
# GSNO (Cu+) -> 1/2GSSG + NO        k14NO
# CcOx + NO -> CcOX.NO              k15NO
# FeL + NO -> FeLNO                 k16NO
# FeLNO + GSH -> GSNO + FeL        k17NO
# GSH + O2m -> 1/2 GSSG + products  k17NOb
# REACTION RATES
r1NO=k1NO
r2NO=k2NO
r3NO=k3NO
r4NO=k4NO*NO*O2m
r5NO=k5NO*SOD*O2m
r6NO=k6NO*ONOOm*GSH
r7NO=k7NO*ONOOm*GPX
r8NO=k8NO*ONOOm*CO2
r9NO=k9NO*ONOOm*Cc
r10NO=k10NO*GSNO^2*O2m
r11NO=k11NO*N2O3*GSH
r12aNO=k12aNO*NO*NO*O2
r12bNOp=k12bNOp*NO2*NO
r12bNOm=k12bNOm*N2O3
r13NO=k13NO*N2O3
rm=Vm*GSSG(GSH,GSNO)/(Km+GSSG(GSH,GSNO))
r14NO=k14NO*GSNO

```

```

r15NO=k15NO*CcOx*NO
r16NO=k16NO*FeL*NO
r17NO=k17NO*FeLNO(FeL)*GSH
r17NOb=k17NOb*GSH*O2m
# ODE'S
N2O3'=-r11NO-r13NO+r12bNOp-r12bNOm-r19NO
GSH'=r3NO-r6NO-r11NO+2*rm-r17NO-r17NOb
NO'=r1NO-r4NO-2*r12aNO-r12bNOp+r12bNOm+r14NO-r15NO-r16NO
O2m'=r2NO-r4NO-r5NO-r10NO-r17NOb
ONOOm'=r4NO-r6NO-r7NO-r8NO-r9NO-r18NO
GSNO'=r6NO-2*r10NO+r11NO-r14NO+r17NO
GSSG(GSH,GSNO)=(100-GSH-GSNO)/2
NO2'=2*r12aNO-r12bNOp+r12bNOm
CcOX'=-r15NO
FeL'=-r16NO+r17NO+r20NO+r21NO+r22NO
FeLNO(FeL)=0.0-FeL
aux FeLNOstf=FeLNO(FeL)
# k1NO is varied, i used a bigger number (1)
par k1NO=1
# k2NO is varied
par k2NO=0.1
# k3NO is varied
par k3NO=0
par O2=0
#par Cc=400
# SOD is between 1 and 10
par SOD=10
par GPX=5.8
# CO2 is between 1000 and 25000
par CO2=1000
par Km=50
par k4NO=6700
par k5NO=2400
par k6NO=0.00135
par k7NO=2
par k8NO=0.058
par k9NO=0.025
par k10NO=0.0006
par k11NO=66
par k12aNO=0.000006
par k13NO=1600
par Vm=320
par k12bNOp=1100
par k12bNOm=81000
par k14NO=0.0002
par k15NO=100

```

```

init CcOx=0.1
par k16NO=1.21
init FeL=0.0
#the same value as k11NO is used for k17NO as a first guess
par k17NO=66
par k17NOb=0.0002
init GSH=100
##### figure17-GSH10000.ode FINISH #####
##### coupling START #####
# REACTIONS
# ONOom + MPTPcl -> MPTP          k18NO
# N2O3 + c8a -> c8aNO + products k19NO
# FeLNO + c8a -> c8aNO + FeL      k20NO
# FeLNO + c9a -> c9aNO + FeL      k21NO
# FeLNO + c3a -> c3aNO + FeL      k22NO
# REACTION RATES
r18NO=k18NO*ONOOm*MPTPcl
r19NO=k19NO*N2O3*c8a
r20NO=k20NO*FeLNO(FeL)*c8a
r21NO=k21NO*FeLNO(FeL)*c9a
r22NO=k22NO*FeLNO(FeL)*c3a
# ODE
MPTPcl'=-r18NO
MPTP(MPTPcl)=0.0001-MPTPcl
init MPTPcl=0.0001
# assume black box
par k18NO=1
par k19NO=10
#the same value as k11NO is used for k20NO,k21NO,k22NO as a first guess
par k20NO=66
par k21NO=66
par k22NO=66
##### coupling FINISH #####
@ xhi=10000,ylo=0,yhi=0.001
@ meth=cvode,atol=1e-8,tol=1e-9,total=60000,dt=5,bounds=1000000000
@ nplot=2,yp=c3a,yp2=gsh
done

```

BIBLIOGRAPHY

- Acehan, D., Jiang, X. J., Morgan, D. G., Heuser, J. E., Wang, X. D., and Akey, C. W. (2002). Three-dimensional structure of the apoptosome: Implications for assembly, procaspase-9 binding, and activation. *Mol. Cell.* *9*, 423-432.
- Afshar, R. K., Patra, A. K., Olmstead, M. M., and Mascharak, P. K. (2004). Syntheses, structures, and reactivities of {Fe-NO}(6) nitrosyls derived from polypyridine-carboxamide ligands: Photoactive NO-donors and reagents for S-nitrosylation of alkyl thiols. *Inorg. Chem.* *43*, 5736-5743.
- Albina, J. E., Cui, S., Mateo, R. B., and Reichner, J. S. (1993). Nitric oxide-mediated apoptosis in murine peritoneal macrophages. *J. Immunol.* *150*, 5080-5085.
- Aldridge, B. B., Haller, G., Sorger, P. K., and Lauffenburger, D. A. (2006). Direct Lyapunov exponent analysis enables parametric study of transient signalling governing cell behaviour. *Syst. Biol. (Stevenage)* *153*, 425-432.
- Angeli, D., Ferrell, J. E., and Sontag, E. D. (2004). Detection of multistability, bifurcations, and hysteresis in a large class of biological positive-feed back systems. *Proc. Natl. Acad. Sci. U S A.* *101*, 1822-1827.
- Antonsson, B., Conti, F., Ciavatta, A., Montessuit, S., Lewis, S., Martinou, I., Bernasconi, L., Bernard, A., Mermoud, J. J., Mazzei, G., Maundrell, K., Gambale, F., Sadoul, R., and Martinou, J.C. (1997). Inhibition of Bax channel-forming activity by Bcl-2. *Science* *277*, 370-372.
- Antunes, F., Salvador, A., Marinho, H. S., Alves, R., and Pinto, R. E. (1996). Lipid peroxidation in mitochondrial inner membranes. 1. An integrative kinetic model. *Free Radic. Biol. and Med.* *21*, 917-943.
- Asthaigiri, A. R. and Lauffenburger, D. A. (2001). A computational study of feedback effects on signal dynamics in a mitogen-activated protein kinase (MAPK) pathway model. *Biotechnol. Prog.* *17*, 227-239.
- Bagci, E. Z., Vodovotz, Y., Billiar, T. R., Ermentrout, G. B., and Bahar, I. (2006). Bistability in apoptosis: Roles of Bax, Bcl-2, and Mitochondrial Permeability Transition Pores. *Biophys. J.* *90*, 1546-1559.

- Bagci, E. Z., Vodovotz, Y., Billiar, T. R., Ermentrout, G. B., and Bahar, I. (2007). Competing effects of nitric oxide in regulating apoptosis: Insights from computational modeling. (submitted)
- Beckman, J. S. and Koppenol, W. H. (1996). Nitric oxide, superoxide, and peroxynitrite: The good, the bad, and the ugly. *Am. J. Physiol., Cell Physiol.* *40*, C1424-C1437.
- Benhar, M. and Stamler, J. S. (2005). A central role for S-nitrosylation in apoptosis. *Nat. Cell Biol.* *7*, 645-646.
- Bentele, M., Lavrik, I., Ulrich, M., Stosser, S., Heermann, D. W., Kalthoff, H., Krammer, P. H., and Eils, R. (2004). Mathematical modeling reveals threshold mechanism in CD95-induced apoptosis. *J. Cell Biol.* *166*, 839-851.
- Bouillet, P., Cory, S., Zhang, L. C., Strasser, A., and Adams, J. M. (2001). Degenerative disorders caused by Bcl-2 deficiency prevented by loss of its BH3-only antagonist Bim. *Dev. Cell* *1*, 645-653.
- Buerk, D. G. (2001). Can we model nitric oxide biotransport? A survey of mathematical models for a simple diatomic molecule with surprisingly complex biological activities. *Annu. Rev. Biomed. Eng.* *3*, 109-143.
- Bulotta, S., Barsacchi, R., Rotiroti, D., Borgese, N., and Clementi, E. (2001). Activation of the endothelial nitric-oxide synthase by tumor necrosis factor-alpha. A novel feedback mechanism regulating cell death. *J. Biol. Chem.* *276*, 6529-6536.
- Cary, S. P. L., Winger, J. A., and Marletta, M. A. (2005). Tonic and acute nitric oxide signaling through soluble guanylate cyclase is mediated by nonheme nitric oxide, ATP, and GTP. *Proc. Natl. Acad. Sci. U S A.* *102*, 13064-13069.
- Ceneviva, G. D., Tzeng, E., Hoyt, D. G., Yee, E., Gallagher, A., Engelhardt, J. F., Kim, Y. M., Billiar, T. R., Watkins, S. A., and Pitt, B. R. (1998). Nitric oxide inhibits lipopolysaccharide-induced apoptosis in pulmonary artery endothelial cells. *Am. J. Physiol* *275*, L717-L728.
- Chawla-Sarkar, M., Bae, S. I., Reu, F. J., Jacobs, B. S., Lindner, D. J., and Borden, E. C. (2004). Downregulation of Bcl-2, FLIP or IAPs (XIAP and survivin) by siRNAs sensitizes resistant melanoma cells to Apo2L/TRAIL-induced apoptosis. *Cell Death Differ.* *11*, 915-923.
- Chen, K. C., Csikasz-Nagy, A., Gyorffy, B., Val, J., Novak, B., and Tyson, J. J. (2000). Kinetic analysis of a molecular model of the budding yeast cell cycle. *Mol. Biol. Cell.* *11*, 369-391.
- Cherry, J. L. and Adler, F. R. (2000). How to make a Biological Switch. *J. Theor. Biol.* *203*, 117-133.

- Craciun, G., Tang, Y., and Feinberg, M. (2006). Understanding bistability in complex enzyme-driven reaction networks. *Proc. Natl. Acad. Sci. U S A.* *103*, 8697-8702.
- Czapski, G. and Goldstein, S. (1995). The role of the reactions of NO with superoxide and oxygen in biological systems – A kinetic approach. *Free Radic. Biol. Med.* *19*, 785-794.
- Danial, N. N. and Korsmeyer, S. J. (2004). Cell death: Critical control points. *Cell* *116*, 205-219.
- De Visscher, G., Rooker, S., Jorens, P., Verlooy, J., Borgers, M., Reneman, R. S., Van Rossem, K., and Flameng, W. (2005). Pentobarbital fails to reduce cerebral oxygen consumption early after non-hemorrhagic closed head injury in rats. *J. Neurotrauma* *22*, 793-806.
- Denicola, A., Freeman, B. A., Trujillo, M., and Radi, R. (1996). Peroxynitrite reaction with carbon dioxide/bicarbonate: Kinetics and influence on peroxynitrite-mediated oxidations. *Arch. Biochem. Biophys.* *333*, 49-58.
- Deveraux, Q. L., Takahashi, R., Salvesen, G. S., and Reed, J. C. (1997). X-linked IAP is a direct inhibitor of cell-death proteases. *Nature* *388*, 300-304.
- Dimmeler, S., Haendeler, J., Nehls, M., and Zeiher, A. M. (1997a). Suppression of apoptosis by nitric oxide via inhibition of interleukin-1 β -converting enzyme (ICE)-like and cysteine protease protein (CPP)-32-like proteases. *J. Exp. Med.* *185*, 601-607.
- Dimmeler, S., Rippmann, V., Weiland, U., Haendeler, J., and Zeiher, A. M. (1997b). Angiotensin II induces apoptosis of human endothelial cells. Protective effect of nitric oxide. *Circ. Res.* *81*, 970-976.
- Eissing, T., Allgower, F., and Bullinger, E. (2005). Robustness properties of apoptosis models with respect to parameter variations and stochastic influences. *Syst. Biol.* *152*, 221-228.
- Eissing, T., Conzelmann, H., Gilles, E. D., Allgower, F., Bullinger, E., and Scheurich, P. (2004). Bistability analyses of a caspase activation model for receptor-induced apoptosis. *J. Biol. Chem.* *279*, 36892-36897.
- Eissing, T., Waldherr, S., Allgower, F., Scheurich, P., Bullinger, E. (2007). Response to Bistability in apoptosis: Roles of Bax, Bcl-2, and mitochondrial permeability transition pores. *Biophys. J.* in press.
- Enari, M., Sakahira, H., Yokoyama, H., Okawa, K., Iwamatsu, A., and Nagata, S. (1998). A caspase-activated DNase that degrades DNA during apoptosis, and its inhibitor ICAD. *Nature* *391*, 43-50.
- Ermentrout, B. (2002). Simulating, analyzing, and animating dynamical systems. A guide to XPPAUT for researchers and students., J.J.Dongarra, ed. (Philedelphia: SIAM).
- Fadeel, B., Orrenius, S., and Zhivotovsky, B. (1999). Apoptosis in human disease: A new skin for the old ceremony? *Biochem. Biophys. Res. Commun.* *266*, 699-717.

- Ferrell, J. E. (2002). Self-perpetuating states in signal transduction: positive feedback, double-negative feedback and bistability. *Curr. Opin. Cell Biol.* *14*, 140-148.
- Ferrell, J. E. and Xiong, W. (2001). Bistability in cell signaling: How to make continuous processes discontinuous, and reversible processes irreversible. *Chaos* *11*, 227-236.
- Fersht, A. (2002). *Structure and mechanism in protein science. A guide to enzyme catalysis and protein folding.* (New York: W. H. Freeman and Company).
- Fielden, E. M., Roberts, P. B., Bray, R. C., Lowe, D. J., Mautner, G. N., Rotilio, G., and Calabrese, L. (1974). The mechanism of action of superdismutase from pulse radiolysis and electron paramagnetic resonance. *Biochem. J.* *139*, 49-60.
- Fussenegger, M., Bailey, J. E., and Varner, J. (2000). A mathematical model of caspase function in apoptosis. *Nature Biotechnol.* *18*, 768-774.
- Ghafourifar, P., Asbury, M. L., Joshi, S. S., and Kincaid, E. D. (2005). Determination of mitochondrial nitric oxide synthase activity. *Meth. Enzymol.* *396*, 424-444.
- Gorren, A. C. F., Schrammel, A., Schmidt, K., and Mayer, B. (1996). Decomposition of S-nitrosoglutathione in the presence of copper ions and glutathione. *Arch. Biochem. Biophys.* *330*, 219-228.
- Green, D. R. and Kroemer, G. (2004). The pathophysiology of mitochondrial cell death. *Science* *305*, 626-629.
- Grisham, M. B., Jourdeuil, D., and Wink, D.A. (1999). Nitric oxide. I. Physiological chemistry of nitric oxide and its metabolites: implications in inflammation. *Am. J. Physiol* *276*, G315-G321.
- Halestrap, A. P. and Brenner, C. (2003). The Adenine Nucleotide Translocase: A central component of the mitochondrial permeability transition pore and key player in cell death. *Curr. Med. Chem.* *10*, 1507-1525.
- Hill, T. L. (1985). *Cooperativity Theory in Biochemistry. Steady-State and Equilibrium Systems.* (New York, N.Y.: Springer-Verlag).
- Hofseth, L. J., Saito, S., Hussain, S. P., Espey, M. G., Miranda, K. M., Araki, Y., Jhappan, C., Higashimoto, Y., He, P. J., Linke, S. P., Quezado, M. M., Zurer, I., Rotter, V., Wink, D. A., Appella, E., and Harris, C. C. (2003). Nitric oxide-induced cellular stress and p53 activation in chronic inflammation. *Proc. Natl. Acad. Sci. U S A.* *100*, 143-148.
- Hon, W. M., Lee, K. H., and Khoo, H. E. (2002). Nitric oxide in liver diseases: friend, foe, or just passerby? *Ann. N. Y. Acad. Sci.* *962*, 275-295.
- Hu, T. M., Hayton, W. L., and Mallary (2006). Kinetic modeling of nitric-oxide-associated reaction network. *Pharm. Res.* *23*, 1702-1711.

- Huie, R. E. and Padmaja, A. S. (1993). The reaction of NO with superoxide. *Free Radic. Res. Commun.* *18*, 195-199.
- Jiang, X. and Wang, X. (2004). Cytochrome *c*- mediated apoptosis. *Annu. Rev. Biochem.* *73*, 87-106.
- Joers, A., Jaks, V., Kase, J., and Maimets, T. (2004). p53-dependent transcription can exhibit both on/off and graded response after genotoxic stress. *Oncogene* *23*, 6175-6185.
- Jones, C. M., Lawrence, A., Wardman, P., and Burkitt, M.J. (2002). Electron paramagnetic resonance spin trapping investigation into the kinetics of glutathione oxidation by the superoxide radical: Re-evaluation of the rate constant. *Free Radic. Biol. Med.* *32*, 982-990.
- Jourd'Heuil, D., Mai, C. T., Laroux, F. S., Wink, D. A., and Grisham, M. B. (1998). The reaction of S-nitrosoglutathione with superoxide. *Biochem. Biophys. Res. Commun.* *244*, 525-530.
- Karpinich, N. O., Tafani, M., Rothman, R. J., Russo, M. A., and Farber, J. L. (2002). The course of etoposide-induced apoptosis from damage to DNA and p53 activation to mitochondrial release of cytochrome *c*. *J. Biol. Chem.* *277*, 16547-16552.
- Katiyar, S. K., Roy, A. M., and Baliga, M. S. (2005). Silymarin induces apoptosis primarily through a p53-dependent pathway involving Bcl-2/Bax, cytochrome *c* release, and caspase activation. *Mol. Cancer Ther.* *4*, 207-216.
- Keshive, M., Singh, S., Wishnok, J. S., Tannenbaum, S. R., and Deen, W. M. (1996). Kinetics of S-nitrosation of thiols in nitric oxide solutions. *Chem. Res. Toxicol.* *9*, 988-993.
- Kholodenko, B. N. (2006). Cell-signalling dynamics in time and space. *Nat. Rev. Mol. Cell Biol.* *7*, 165-176.
- Kim, P. K., Zamora, R., Petrosko, P., and Billiar, T. R. (2001). The regulatory role of nitric oxide in apoptosis. *Int. Immunopharmacol.* *1*, 1421-1441.
- Kim, P. K. M., Zuckerbraun, B. S., Otterbein, L. E., Vodovotz, Y., and Billiar, T. R. (2004). 'Til death do us part: nitric oxide and mechanisms of hepatotoxicity. *Biol. Chem.* *365*, 11-15.
- Kim, Y. M., Chung, H. T., Kim, S. S., Han, J. A., Yoo, Y. M., Kim, K. M., Lee, G. H., Yun, H. Y., Green, A., Li, J., Simmons, R. L., and Billiar, T. R. (1999). Nitric oxide protects PC12 cells from serum deprivation-induced apoptosis by cGMP-dependent inhibition of caspase signaling. *J. Neurosci.* *19*, 6740-6747.
- Kim, Y. M., Chung, H. T., Simmons, R. L., and Billiar, T. R. (2000). Cellular non-heme iron content is a determinant of nitric oxide- mediated apoptosis, necrosis, and caspase inhibition. *J. Biol. Chem.* *275*, 10954-10961.

- Kim, Y. M., Kim, T. H., Seol, D. W., Talanian, R. V., and Billiar, T. R. (1998). Nitric Oxide suppression of apoptosis occurs in association with an inhibition of Bcl-2 cleavage and cytochrome *c* release. *J. Biol. Chem.* 273, 31437-31441.
- Kim, Y. M., Talanian, R. V., and Billiar, T. R. (1997). Nitric oxide inhibits apoptosis by preventing increases in caspase-3-like activity via two distinct mechanisms. *J. Biol. Chem.* 272, 31138-31148.
- King, J. R. B. (2000). *Cancer Biology*. (Harlow, UK: Pearson Education).
- Kitano, H. (2002). Systems biology: A brief overview. *Science* 295, 1662-1664.
- Kitano, H. (2006). Computational cellular dynamics: a network-physics integral. *Nat. Rev. Mol. Cell Biol.* 7, 163.
- Kitano, H., Funahashi, A., Matsuoka, Y., and Oda, K. (2005). Using process diagrams for the graphical representation of biological networks. *Nat. Biotechnol.* 23, 961-966.
- Koppenol, W.H., Moreno, J. J., Pryor, W. A., Ischiropoulos, H., and Beckman, J.S. (1992). Peroxynitrite, a cloaked oxidant formed by nitric oxide and superoxide. *Chem. Res. Toxicol.* 5, 834-842.
- Lancaster, J. R. (1994). Simulation of the diffusion and reaction of endogenously produced nitric oxide. *Proc. Natl. Acad. Sci. U S A.* 91, 8137-8141.
- Lancaster, J. R. (1997). A tutorial on the diffusibility and reactivity of free nitric oxide. *Nitric Oxide* 1, 18-30.
- Legewie, S., Bluthgen, N., and Herzel, H. (2006). Mathematical modeling identifies inhibitors of apoptosis as mediators of positive feedback and bistability. *PLoS Comput. Biol.* 2, 1061-1073.
- Li, B. and Dou, Q. P. (2000). Bax degradation by the ubiquitin/proteasome-dependent pathway: involvement in tumor survival and progression. *Proc. Natl. Acad. Sci. U S A.* 97, 3850-3855.
- Li, J., Billiar, T. R., Talanian, R. V., and Kim, Y. M. (1997). Nitric oxide reversibly inhibits seven members of the caspase family via S-nitrosylation. *Biochem. Biophys. Res. Commun.* 240, 419-424.
- Licht, W. R., Tannenbaum, S. R., and Deen, W. M. (1988). Use of ascorbic acid to inhibit nitrosation: kinetic and mass transfer coefficients for an in vitro system. *Carcinogenesis* 9, 365-372.

- Luo, X., Budihardjo, I., Zou, H., Slaughter, C., and Wang, X. D. (1998). Bid, a Bcl2 interacting protein, mediates cytochrome c release from mitochondria in response to activation of cell surface death receptors. *Cell* 94, 481-490.
- Lutter, M., Perkins, G. A., and Wang, X. D. (2001). The pro-apoptotic Bcl-2 family member tBid localizes to mitochondrial contact sites. *BMC Cell Biol.* 2, 22-30.
- Ma, L., and Iglesias, P. A. (2002). Quantifying robustness of biochemical network models. *BMC Bioinformatics.* 3, 38.
- Mannick, J. B., Hausladen, A., Liu, L. M., Hess, D. T., Zeng, M., Miao, Q. X., Kane, L.S., Gow, A. J., and Stamler, J. S. (1999). Fas-induced caspase denitrosylation. *Science* 284, 651-654.
- Manoharan, A., Kiefer, T., Leist, S., Schrader, K., Urban, C., Walter, D., Maurer, U., Borner, C. (2006). Identification of a 'genuine' mammalian homolog of nematodal CED-4: Is the hunt over or do we need better guns? *Cell Death Differ.* 13, 1310-1317.
- Messmer, U. K. and Brune, B. (1996). Nitric oxide-induced apoptosis: p53-dependent and p53-independent signalling pathways. *Biochem. J.* 319 (Pt 1), 299-305.
- Messmer, U. K., Lapetina, E. G., and Brune, B. (1995). Nitric oxide-induced apoptosis in RAW 264.7 macrophages is antagonized by protein kinase C- and protein kinase A-activating compounds. *Mol. Pharmacol.* 47, 757-765.
- Nagata, S. (1997). Apoptosis by death factor. *Cell* 88, 355-365.
- Nair, V. D., Yuen, T., Olanow, C. W., and Sealfon, S. C. (2004). Early single cell bifurcation of pro- and antiapoptotic states during oxidative stress. *J. Biol. Chem* 279, 27494-27501.
- Nakagawa, T., Shimizu, S., Watanabe, T., Yamaguchi, O., Otsu, K., Yamagata, H., Inohara, H., Kubo, T., and Tsujimoto, Y. (2005). Cyclophilin D-dependent mitochondrial permeability transition regulates some necrotic but not apoptotic cell death. *Nature* 434, 652-658.
- Newmeyer, D. D. and Ferguson-Miller, S. (2003). Mitochondria: Releasing power for life and unleashing the machineries of death. *Cell* 112, 481-490.
- Oltvai, Z. N., Millman, C. L., and Korsmeyer, S. J. (1993). Bcl-2 heterodimerizes in vivo with a conserved homolog, Bax, that accelerates programmed cell death. *Cell* 74, 609-619.
- Ozbudak, E. M., Thattai, M., Lim, H. N., Shraiman, B. I., and van Oudenaarden, A. (2004). Multistability in the lactose utilization network of *Escherichia coli*. *Nature* 427, 737-740.
- Pou, S., Tsai, P., Porasuphatana, S., Halpern, H. J., Chandramouli, G. V. R., Barth, E. D., and Rosen, G. M. (1999). Spin trapping of nitric oxide by ferro-chelates: kinetic and in vivo pharmacokinetic studies. *Biochim Biophys Acta* 1427, 216-226.

- Pourzand, C., Watkin, R. D., Brown, J. E., and Tyrrell, R. M. (1999). Ultraviolet A radiation induces immediate release of iron in human primary skin fibroblasts: The role of ferritin. *Proc. Natl. Acad. Sci. U S A.* 96, 6751-6756.
- Radi, R., Cassina, A., and Hodara, R. (2002). Nitric oxide and peroxynitrite interactions with mitochondria. *Biol. Chem.* 383, 401-409.
- Radi, R., Denicola, A., Ferrer-Sueta, G., and Rubbo, H. (2000). The biological chemistry of peroxynitrite. In *Nitric Oxide: Biology and Pathobiology*, L.J. Ignarro, ed. (San Diego: Academic), pp. 57-82.
- Reed, J. C. (1999). Dysregulation of apoptosis in cancer. *J. Clin. Oncol.* 17, 2941-2953.
- Reed, J. C. (2002). Apoptosis-based therapies. *Nat. Rev. Drug Discov.* 1, 111-121.
- Rehm, M., Dussmann, H., Janicke, R. U., Tavares, J. M., Kogel, D., and Prehn, J. H. M. (2002). Single-cell fluorescence resonance energy transfer analysis demonstrates that caspase activation during apoptosis is a rapid process - Role of caspase-3. *J. Biol. Chem.* 277, 24506-24514.
- Rehm, M., Huber, H. J., Dussmann, H., and Prehn, J. H. M. (2006). Systems analysis of effector caspase activation and its control by X-linked inhibitor of apoptosis protein. *EMBO J.* 25, 4338-4349.
- Riedl, S. J., Li, W., Chao, Y., Schwarzenbacher, R., and Shi, Y. (2005). Structure of the apoptotic protease-activating factor 1 bound to ADP. *Nature* 434, 926-933.
- Rodriguez, J. and Lazebnik, Y. (1999). Caspase-9 and Apaf-1 form an active enzyme. *Genes Dev.* 13, 3179-3184.
- Rossig, L., Fichtlscherer, B., Breitschopf, K., Haendeler, J., Zeiher, A. M., Mulsch, A., and Dimmeler, S. (1999). Nitric oxide inhibits caspase-3 by S-nitrosation in vivo. *J. Biol. Chem.* 274, 6823-6826.
- Salvesen, G. S. (2002). Caspases and apoptosis. In *Proteases in Biology and Medicine Assays in Biochemistry*, pp. 9-19.
- Salvesen, G. S. and Dixit, V. M. (1999). Caspase activation: The induced-proximity model. *Proc. Natl. Acad. Sci. U S A.* 96, 10964-10967.
- Sanfilippo, C. M. and Blaho, J. A. (2003). The facts of death. *Int. Rev. Immunol.* 22, 327-340.
- Sarih, M., Souvannavong, V., and Adam, A. (1993). Nitric oxide synthase induces macrophage death by apoptosis. *Biochem. Biophys. Res. Commun.* 191, 503-508.

- Sarti, P., Arese, M., Bacchi, A., Barone, M.C., Forte, E., Mastronicola, D., Brunori, M., and Giuffre, A. (2003). Nitric oxide and mitochondrial complex IV. *IUBMB Life* 55, 605-611.
- Schorr, K., Li, M., Krajewski, S., Reed, J. C., and Furth, P. A. (1999). Bcl-2 gene family and related proteins in mammary gland involution and breast cancer. *J. Mammary Gland Biol.* 4, 153-164.
- Shiozaki, E. N., Chai, J. J., Rigotti, D. J., Riedl, S. J., Li, P. W., Srinivasula, S. M., Alnemri, E. S., Fairman, R., and Shi, Y. G. (2003). Mechanism of XIAP-mediated inhibition of caspase-9. *Mol. Cell.* 11, 519-527.
- Siehs, C., Oberbauer, R., Mayer, G., Lukas, A., and Mayer, B. (2002). Discrete simulation of regulatory homo- and heterodimerization in the apoptosis effector phase. *Bioinformatics* 18, 67-76.
- Sies, H., Sharov, V. S., Klotz, L. O., and Briviba, K. (1997). Glutathione peroxidase protects against peroxynitrite-mediated oxidations - A new function for selenoproteins as peroxynitrite reductase. *J. Biol. Chem.* 272, 27812-27817.
- Slee, E. A., Keogh, S. A., and Martin, S. J. (2000). Cleavage of Bid during cytotoxic drug and UV radiation-induced apoptosis occurs downstream of the point of Bcl-2 action and is catalysed by caspase-3: a potential feedback loop for amplification of apoptosis-associated mitochondrial cytochrome *c* release. *Cell Death Differ.* 7, 556-565.
- Spencer, J. P. E., Wong, J., Jenner, A., Aruoma, O. I., Cross, C. E., and Halliwell, B. (1996). Base modification and strand breakage in isolated calf thymus DNA and in DNA from human skin epidermal keratinocytes exposed to peroxynitrite or 3-morpholinosydnonimine. *Chem. Res. Toxicol.* 9, 1152-1158.
- Squadrito, G. L. and Pryor, W. A. (1998). Oxidative chemistry of nitric oxide: The roles of superoxide, peroxynitrite, and carbon dioxide. *Free Radic. Biol. Med.* 25, 392-403.
- Stamler, J.S. (1994). Redox signaling – nitrosylation and related target interactions of nitric oxide. *Cell* 78, 931-936.
- Stucki, J. W. and Simon, H. U. (2005). Mathematical modeling of caspase-3 activation and degradation. *J. Theor. Biol.* 234, 123-131.
- Thomson, L., Trujillo, M., Telleri, R., and Radi, R. (1995). Kinetics of cytochrome *c*(2+) oxidation by peroxynitrite – Implications for superoxide measurements in nitric oxide-producing biological systems. *Arch. Biochem. Biophys.* 319, 491-497.
- Tyas, L., Brophy, V. A., Pope, A., Rivett, A. J., and Tavaré, J. M. (2000). Rapid caspase-3 activation during apoptosis revealed using fluorescence-resonance energy transfer. *EMBO Rep.* 1, 266-270.

- Tzeng, E., Kim, Y. M., Pitt, B. R., Lizonova, A., Kovesdi, I., and Billiar, T. R. (1997). Adenoviral transfer of the inducible nitric oxide synthase gene blocks endothelial cell apoptosis. *Surgery* 122, 255-263.
- Vieira, H. L. A., Belzacq, A. S., Haouzi, D., Bernassola, F., Cohen, I., Jacotot, E., Ferri, K. F., El Hamel, C., Bartle, L. M., Melino, G., Brenner, C., Goldmacher, V., and Kroemer, G. (2001). The adenine nucleotide translocator: a target of nitric oxide, peroxynitrite, and 4-hydroxynonenal. *Oncogene* 20, 4305-4316.
- Vieira, H. L. A., Haouzi, D., El Hamel, C., Jacotot, E., Belzacq, A. S., Brenner, C., and Kroemer, G. (2000). Permeabilization of the mitochondrial inner membrane during apoptosis: impact of the adenine nucleotide translocator. *Cell Death Differ.* 7, 1146-1154.
- Vodovotz, Y., Kim, P. K. M., Bagci, E. Z., Ermentrout, G. B., Chow, C. C., Bahar, I., and Billiar, T. R. (2004). Inflammatory modulation of hepatocyte apoptosis by nitric oxide: In vivo, in vitro and in silico studies. *Curr. Mol. Med.* 4, 753-762. *Ann. N. Y. Acad. Sci.*
- Wang, Y. N., Vodovotz, Y., Kim, P. K. M., Zamora, R., and Billiar, T.R. (2002). Mechanisms of hepatoprotection by nitric oxide. *Ann. N. Y. ACAD. SCI.* 962, 415-422.
- Wei, M. C., Zong, W. X., Cheng, E. H. Y., Lindsten, T., Panoutsakopoulou, V., Ross, A. J., Roth, K. A., MacCregor, G. R., Thompson, C. B., and Korsmeyer, S. J. (2001). Proapoptotic Bax and Bak: A requisite gateway to mitochondrial dysfunction and death. *Science* 292, 727-730.
- Weinberg, R. A. (2006). *The Biology of Cancer*. (New York: Garland Science, Taylor & Francis Group).
- Weller, M. (1998). Predicting response to cancer chemotherapy: the role of p53. *Cell Tissue Res.* 292, 435-445.
- Weller, R., Schwentker, A., Billiar, T. R., and Vodovotz, Y. (2003). Autologous nitric oxide protects mouse and human keratinocytes from ultraviolet B radiation-induced apoptosis. *Am. J. Physiol.* 284, C1140-C1148.
- Wink, D. A., Feelisch, M., Vodovotz, Y., Fukuto, J., and Grisham, M. B. (1999). The Chemical Biology of Nitric Oxide. In *Reactive Oxygen Species in Biological Systems: An Interdisciplinary approach*, C.A.Colton and D.L.Gilbert, eds. (New York: Kluwer Academic / Plenum Publishing), pp. 245-291.
- Wink, D.A., Nims, R. W., Darbyshire, J. F., Christodoulou, D., Hanbauer, I., Cox, G. W., Laval, F., Laval, J., Cook, J. A., Krishna, M. C., Degraff, W. G., and Mitchell, J. B. (1994). Reaction kinetics for nitrosation of cysteine and glutathione in aerobic nitric oxide solutions at neutral pH – Insights into the fate and physiological effects of intermediates generated in the NO/O₂⁻ reaction. *Chem. Res. Toxicol.* 7, 519-525.

- Wolter, K. G., Hsu, Y. T., Smith, C. L., Nechushtan, A., Xi, X. G., and Youle, R. J. (1997). Movement of Bax from the cytosol to mitochondria during apoptosis. *J. Cell Biol.* *139*, 1281-1292.
- Xiong, W. and Ferrell, J. E. (2003). A positive-feedback-based bistable 'memory module' that governs a cell fate decision. *Nature* *426*, 460-465.
- Yang, Y. L. and Yu, X. D. (2003). Regulation of apoptosis: the ubiquitous way. *FASEB J.* *17*, 790-799.
- Yi, X. L., Yin, X. M., and Dong, Z. (2003). Inhibition of Bid-induced apoptosis by Bcl-2 - tBid insertion, Bax translocation, and Bax/Bak oligomerization suppressed. *J. Biol. Chem.* *278*, 16992-16999.
- Yin, X. M., Wang, K., Gross, A., Zhao, Y., Zinkel, S., Klocke, B., Roth, K. A., and Korsmeyer, S. J. (1999). Bid-deficient mice are resistant to Fas-induced hepatocellular apoptosis. *Nature* *400*, 886-891.
- Zangemeister-Wittke, U., Leech, S. H., Olie, R. A., Simoes-Wust, A. P., Gautschi, O., Luedke, G. H., Natt, F., Haner, R., Martin, P., Hall, J., Nalin, C.M., and Stahel, R. A. (2000). A novel bispecific antisense oligonucleotide inhibiting both Bcl-2 and Bcl-xL expression efficiently induces apoptosis in tumor cells. *Clin. Cancer Res.* *6*, 2547-2555.
- Zhang, W. and Edwards, A. (2006). A model of nitric oxide tubulo-vascular cross-talk in a renal outer medullary cross-section. *Am. J. Physiol. Renal. Physiol.* *in press*.